

University of Liège
Faculty of Medicine
GIGA Neuroscience

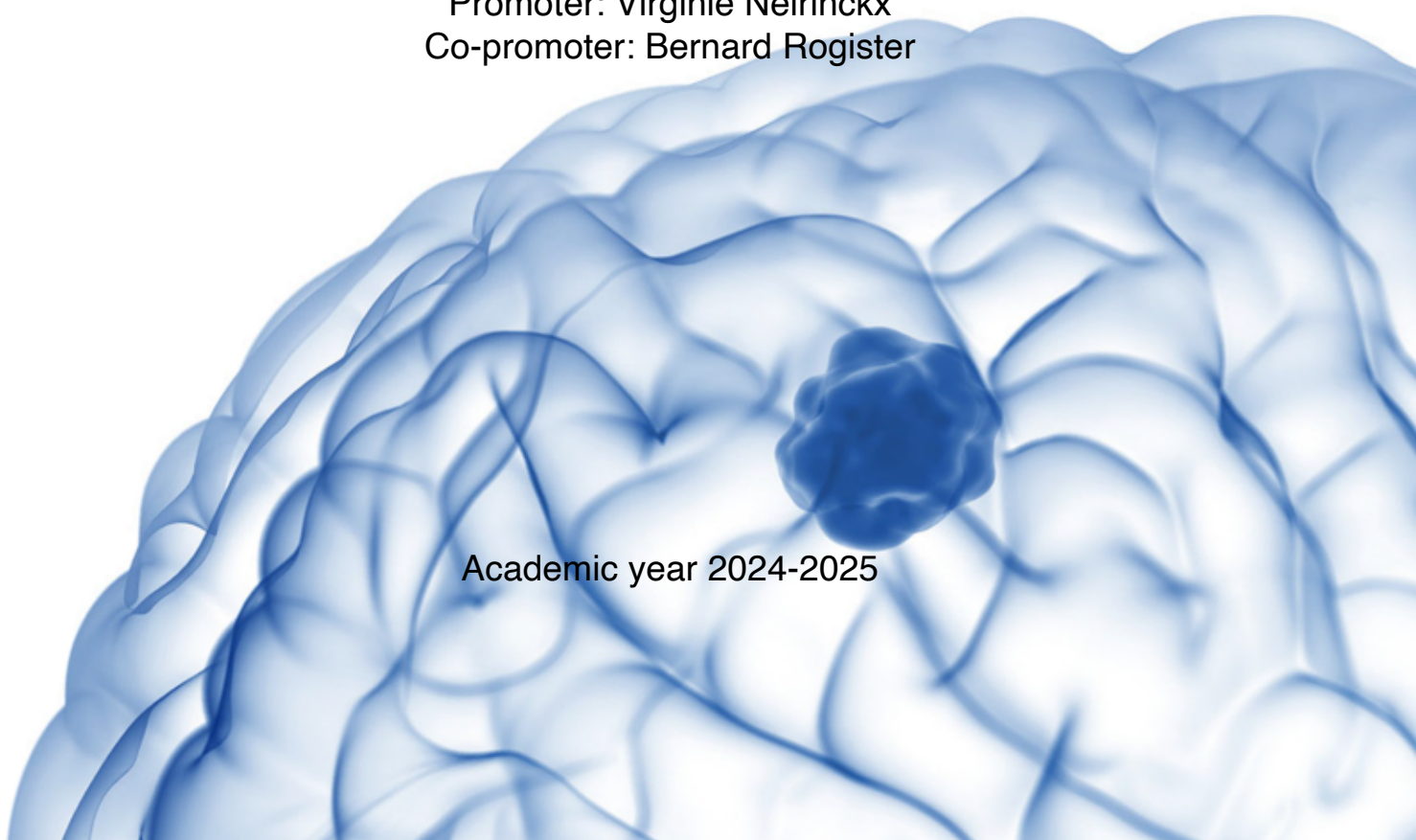
Multilevel investigation of the atypical chemokine receptor 3 (ACKR3) expression and function in glioblastoma

Damla Isci

Thesis submitted to fulfill the requirements for the degree of
Philosophiae Doctor in Biomedical and Pharmaceutical Sciences

Promoter: Virginie Neirinckx
Co-promoter: Bernard Rogister

Academic year 2024-2025



University of Liège
Faculty of Medicine
GIGA Neuroscience



Multilevel investigation of the atypical chemokine receptor 3 (ACKR3) expression and function in glioblastoma

Damla Isci

Thesis submitted to fulfill the requirements for the degree of
Philosophiae Doctor in Biomedical and Pharmaceutical Sciences

Promoter: Virginie Neirinckx
Co-promoter: Bernard Rogister

Academic year 2023-2024

“Most people believe in intelligence, I don’t;
It’s effort that separates us from each other, I
believe in work.”

- Aziz Sancar

ACKNOWLEDGMENTS

Je souhaite à exprimer ma profonde gratitude à mon co-promoteur de thèse, **Bernard Rogister**, pour son encadrement tout au long de ce travail. Sa disponibilité malgré un emploi du temps chargé, et son soutien ont été déterminants dans l'aboutissement de ce travail. Son expertise et sa passion pour la recherche ont enrichi mes réflexions et m'ont guidé avec rigueur. Je vous remercie pour votre confiance et pour avoir été à l'écoute, chaque matin à 7h devant la machine à café. Je n'aurais jamais pensé dire ça un jour, mais vos « Quoi de neuf, miss » vont me manquer.

♥ Je tiens à exprimer toute ma reconnaissance à ma promotrice, **Virginie Neirinckx**, sans qui cette thèse n'aurait jamais vu le jour. Virginie, au fil de ces quatre années passées dans ce laboratoire, tu es devenue bien plus qu'une simple directrice de thèse. Tu es devenue une guide, une alliée, une personne sur qui j'ai pu compter à chaque étape difficile de ce long parcours. Tu m'as non seulement guidé avec une expertise inégalée, mais tu m'as également transmis une passion pour la recherche. J'ai énormément appris à tes côtés, non seulement sur le plan scientifique, mais aussi sur le plan personnel. Je ressens un immense respect pour ton savoir et pour ta maîtrise du sujet. J'ai grandi dans ce laboratoire et c'est en grande partie grâce à toi. Je te remercie du fond du cœur pour tout ce que tu as fait pour moi, pour ta confiance, ton soutien, ta patience et ta bienveillance tout au long de cette aventure. Ton influence s'étendra bien au-delà de cette expérience et je serai toujours reconnaissante pour le rôle que tu as joué dans mon développement. Travailler avec toi a été une belle expérience et ton absence se fera sentir à chaque étape de mon parcours à venir. Ma Vi, tu vas énormément me manquer ♥.

Ensuite, je tiens également à remercier les membres de comité de Thèse, **Akeila Bellahcène**, **Alain Colige**, **Julien Hanson**, **Félix Scholtes** mais également les membres externes, **Andréas Bikfalvi** et **Charles Nicaise**. Merci d'avoir accepté de faire partie de mon jury.

I also thank my colleagues at LIH, **Andy Chevigné**, **Martyna Szpakowska**, **May Wantz**, **Giulia D'Uonno**, **Max Meyrath** for following my project but also **Anna Golebiewska**, **Petr Nazarov**, **Bakhtiyor Nosirov** for agreeing to collaborate with us on the chemokine paper.

Merci à **Catherine Sadzot** car vous m'avez, entre autres, donné l'envie de poursuivre un doctorat. Un grand merci à **Judit** pour ton aide précieuse lors des expériences durant mes premier mois de thèse, et merci aussi à **Maxime** pour tes conseils avisés et pour le panel du FACS.

Merci au **Télévie**, merci au **FNRS**, merci là a **Fondation Léon Frédéricq** pour tous les financements.

Ensuite, je voudrais remercier toutes ces personnes formidables que j'ai rencontrées:

Tout d'abord, un immense merci à **Odile**, ma toute première collègue. Merci pour tes conseils de labo précieux et pour toutes nos pauses café.

Ensuite, je ne peux pas continuer sans adresser un immense merci à mon gang des **A+ (Mon bouton d'or et Jo, le gars sûr)**. Vous avez illuminé mes journées avec vos rires et votre bonne humeur. Merci pour tous les litres de café partagés, même si honnêtement, je pense que c'est assez sinon je vais finir par me ***** dessus ! Merci pour tous les dinosaures quand vous étiez sages. Merci pour ces petites séances de Padel et sans oublier le HIIT. Ces petits moments resteront gravés dans ma mémoire et je ne vous oublierai jamais. Vous êtes des collègues formidables. Sans vous, cette aventure n'aurait certainement pas été aussi drôle et amusante. Bouton d'or, merci d'avoir repris mon pauvre ACKR3. Prends-en soin, et essaye enfin de lui trouver un foutu rôle dans le GBM, je compte vraiment sur toi ! Et Jo, n'abandonne pas trop Kup quand tu es en business. Je suis tellement reconnaissante de vous avoir eu à mes côtés ! Ne m'oubliez pas... On se revois dans quelques années pour nos retrouvailles annuelles à la Truffe Noire à Bruxelles. Portez-vous bien les copains !

Un grand merci à **Arnaud S**. Ce fut un plaisir de partager une année en binôme pour étudier B7-H3. J'espère sincèrement que travailler avec moi n'a pas été trop pénible. Merci pour les discussions enrichissantes pendant les longues périodes d'incubation (Bien sûr que je parle de cette fameuse expérience de FACS spectrale). Ne laisse personne douter de tes compétences. Tu es un bon scientifique, et je suis convaincue que tu continueras à réaliser de bonnes choses dans ton domaine.

Merci aussi à l'autre **Arnaud L**. Yo, merci de m'avoir confié ton projet AAV et de m'avoir accordé une confiance totale. Ce petit bout de chemin parcouru ensemble était chouette !

Merci aussi à tous les autres doctorants de l'équipe Rogister ; **Marc Antoine, Kim, Célia, Louise** (oui, je ne t'oublie pas même à l'autre bout du monde) et **Julie**. Un grand merci aussi à **Laetitia** et **Thérèse**. Merci pour votre aide dans les expériences. Tenez le coup et prenez soin de vous les petits gars !

Merci également à tous les **membres et techniciens** du **GIGA-Neurosciences**, ainsi qu'au département de **Neurochirurgie** du CHU de Liège.

Merci à toi aussi **Lari**. Merci pour avoir pris en charge toute la paperasse parfois fastidieuse, et surtout merci pour tous les cahiers de note BLEUS. Ne changes pas et surtout garde toujours ton beau sourire !

Merci à la plateforme d'imagerie et de cyrtométrie en flux. Un grand merci à **Raafat** et **Céline** pour leur aide précieuse avec toutes les manip FACS. Merci également à la plateforme des vecteurs viraux. Merci **Manu**, **Alex** et **François** pour toutes ces productions virales et ces accueils chaleureux au L2.

Merci ma **Puce** de toujours croire en moi et de me soutenir sans cesse. Vie sur toi.

Aileme en derin teşekkürlerimi sunmak istiyorum. Sevgili **Annem**, **Babam**, **Abim** ve kıymetli eşim **Ayhan**, sizin bana verdiğiniz büyük destek için minnettarım. Her zaman bana olan inancınız ve zor zamanlarımda yanımda olmanız benim için çok değerliydi. Bana kattığınız eğitim, sevgi ve destek için sonsuz teşekkürler. Sizleri çok seviyorum ve hayatımda sizlerden daha değerli bir şey olmadığını biliyorum. İyi ki varsınız, siz olmadan hayatımın nasıl olacağını düşünemiyorum. Rabbim sizleri başımdan eksik etmesin. Her şey için teşekkür ederim.

Pour finir, j'espère avoir laissé une belle trace dans vos cœurs et dans ce laboratoire. Et lorsque vous êtes tristes, qu'une expérience ne fonctionne pas, ou que vous traversez une période difficile pour quelque raison que ce soit, souvenez-vous de moi qui vous murmure à l'oreille : « **RIEN N'EST PLUS IMPORTANT QUE TOI** ».

Damla ♥

ABSTRACT

Glioblastoma (GBM) is the most common and aggressive primary malignant brain tumor of the Central Nervous System (CNS), and it accounts for approximately 55% of glioma in adults. Despite the standard care of therapy associating maximal safe surgery and concomitant radio-chemotherapy with temozolomide, the median survival after diagnosis is about 16 months. Moreover, the progression of the disease is characterized by systematic relapses explained by the huge infiltrating nature through surrounding tissue, both intra-tumoral and inter-patient heterogeneity and GBM cells plasticity.

Chemokines constitute a subpopulation of chemotactic proteins secreted by various types of cells in different tissues. They are important regulator of development, immune responses, and tissue repair. In normal tissues, chemokines and chemokines receptors are expressed a wide range of cell subtypes. In GBM, they are described to play diverse roles such as angiogenesis or tumor progression and abilities to resist to treatment. Our previous reports demonstrate that a population of GBM stem cells can migrate and invade the ventricles via the CXCR4/CXCL12 chemokine signaling pathway. Furthermore, we demonstrated that these SVZ-nested cells are radioresistant.

ACKR3, the atypical chemokine receptor 3, is the second receptor for the chemokine CXCL12, binding it with a 10-fold higher affinity than CXCR4, the first described receptor for CXCL12. ACKR3 is expressed in various immune cells, neurons and endothelial cells and plays a crucial role in cardiovascular and neuronal development as well as in the migration and homing of hematopoietic progenitor cells. Unlike CXCR4, which signals via G protein, ACKR3 activity relies on β -arrestin recruitment.

The main goal of this study was to investigate the role of ACKR3 in GBM, focusing on its expression pattern. We demonstrate that unlike to CXCR4, ACKR3 expression is low in patient-derived GBM stem-like cells but distributed in diverse cell types within GBM patient tissues. We showed also that overexpression of ACKR3 did not change GBM cell proliferation or invasion, suggesting its minor role(s) in GBM cells.

Aside of the experimental work, we implemented *in silico* analyses of chemokines and receptor expression in patient-derived tissue data, that globally converge to our preliminary conclusions. Since the ACKR3 receptor is observed in different cells of the GBM microenvironment, we consider imperative to study the function of this receptor in a complete immunocompetent tumor microenvironment, by considering not only the tumor cells but also the cells surrounding them.

The second objective of this thesis was to develop a new method to detect and track specifically SVZ-GBM nested cells in a xenograft model. This approach is based on

color conversion mediated by an AAV injected intracerebroventricularly. We designed a model consisting of the implantation of patient-derived GBM stem cells, initially red, turning green when they invade the SVZ, where they are transduced by an AAV. These cells were genetically modified to contain floxed dsRED/STOP cassette upstream of eGFP gene. After intracerebroventricular injection of a recombinant AAV expressing CRE recombinase, the floxed cassette is excised allowing the cells to express eGFP. These results confirm the effectiveness of this method and open the way to new research on the role of the SVZ in GBM biology.

ABBREVIATIONS

α -KG: α -ketoglutarate
+7/-10: the gain on chromosome 7 and loss on chromosome 10
1p/19q code1: deletion of the short arm of chromosome 1 and the long arm of chromosome 19
2-HG: 2-hydroxyglutarate
5-ALA: 5-aminolevulinic acid
AADC: aromatic L-amino acid decarboxylase
AAVs: adeno-associated viruses
AC-like: astrocyte-like
ACKR3: atypical chemokine receptor 3
ACKRs: atypical chemokine receptors
ALT: alternative lengthening of telomere
AM: adrenomedullin
ANGPTL: angiopoietin-like protein
ATRX: α -thalassemia/mental retardation X-linked
AurA: Serine/threonine Aurora A mitotic kinase
BBB: disruption of the blood-brain barrier
BDM: blood derived macrophages/monocytes
CALCR: calcitonin receptor
CNA: copy number alterations
CDKN2A/B HG: Homozygous deletion of CDKN2A/B
CDKN2A/B: Cyclin dependent kinase inhibitor 2A and B
CIMP: CpG island methylator
CNS: Central Nervous System
CSF: cerebrospinal fluid
CT: cellular tumor
CXCR4: the chemokine receptor 4
DC: dendritic cells
DDC: dopa decarboxylase
DLBCL: diffuse large B-cell lymphoma
DR5: death receptor 5
ECM: the extracellular matrix
EGFR: epithelial growth factor receptor
EGFRamp: *EGFR* amplification
EGFRvIII: EGFR variant III
EMT: epithelial mesenchymal transition
FDA: Food and Drug Administration
GAFs: glioma-associated fibroblasts
GBM: glioblastoma
GDP: guanosine diphosphate
GFAP: glial fibrillary acidic protein
GPCRs: G protein-coupled receptors
GRKs: G protein-coupled kinases
GSC: GBM stem like cells
GTP: guanosine triphosphate
HIV: human immunodeficiency virus
HSV-tk: herpes simplex virus thymidine kinase gene
IDH-mut: IDH-mutant tumors
IDH-WT: IDH-wild type

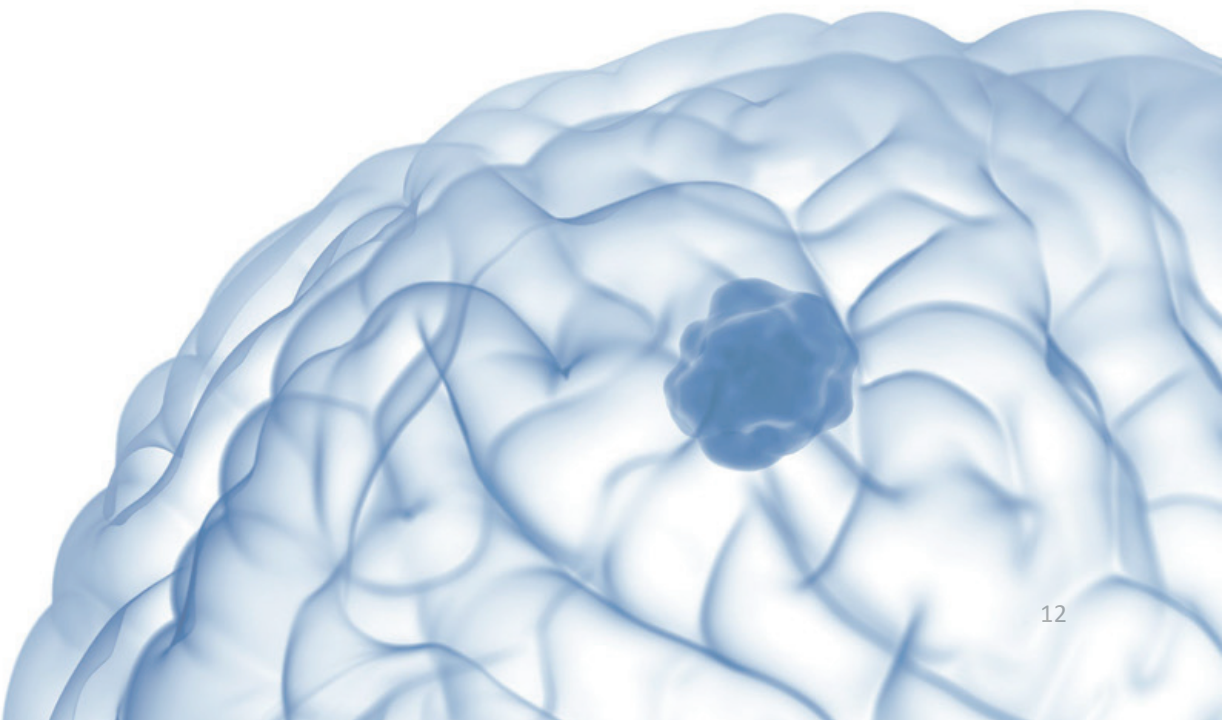
IDH: isocitrate dehydrogenase
IDR: inherited retinal dystrophy
IFN- β : interferon-beta
IT: Infiltrating Tumor
ITR: inverted terminal repeats
IvyGAP: Ivy Glioblastoma Atlas Project
LE: Leading edge
LRP1: LDL-associated protein receptor
MCAM: Melanoma Cell Adhesion Molecule
MDSC: myeloid suppressor cells
MES-like: mesenchymal-like
MG: microglia
MGMT: DNA repair enzyme O6-methylguanine-DNA methyltransferase
MIF: macrophage migration inhibitory factor
MKP1: the nuclear MAP kinase phosphatase 1
MMPs: matrix metalloproteinases
MRI: magnetic resonance imaging
MVP: Microvascular Proliferation
NHEJ: non-homologous end joining
NK: natural killer
NPC-like: neural progenitor cell-like
NSCLC: non-small cell lung cancer
O6-MeG: O⁶-methylguanine (O6-MeG).
OPC-like: oligodendrocyte progenitor cell-like
OS: overall survival
OSM: oncostatin M
PAN: Pseudopalisading cells Around Necrosis
PFS: progression-free survival
R132H: substitution from arginine to histidine on the position 132
rAAVs: recombinant adeno-associated virus
RPE65: retinal pigment epithelium-specific protein 65-kD
SMA: spinal muscular atrophy
SMN1: human survival motor neuron
SVZ: subventricular zone
TAMs: tumor-associated macrophages
TCGA: the Cancer Genome Atlas
TERT: telomerase reverse transcriptase
TFPI-2: tissue factor pathway inhibitor-2
TGF β -1: Transforming Growth Factor β -1
TILs: tumor-infiltrating lymphocytes
TME: tumor microenvironment
TMZ: temozolomide
TRAIL: TNF-Related Apoptosis-Inducing Ligand
Treg: regulatory T lymphocytes
TTFs: tumor treatment fields
vCCL2: bind the virus-encoded CC chemokine
VEGFA: vascular endothelial growth factor A
WHO: world health organization
WNT5A: wingless-related integration site family member 5A

INDEX

ACKNOWLEDGMENTS	3
ABSTRACT	6
ABREVIATIONS	8
INDEX.....	10
PART 1: INTRODUCTION	13
1. Gliomas – general overview	13
1.1. Histomolecular classification of gliomas	13
2. WHO grade 4, IDH WT glioblastoma	17
2.1. Epidemiology.....	17
2.2. Etiology.....	18
2.3. Clinical aspects – symptoms and diagnosis	18
2.4. Therapeutic aspects – Standard-of-care	20
2.5. Therapeutic aspects – Second-line treatments	22
2.6. GBM recurrence and underlying mechanisms	23
2.6.1. GBM cell invasiveness and interactions with host brain cells.....	23
2.6.2. The blood-brain-barrier (BBB): a barrier to effective drug penetration	23
2.6.3. GBM stem cells	24
2.6.4. Heterogeneity and plasticity.....	25
2.6.5. The tumor microenvironment (TME) in glioblastoma	26
2.6.6. The role of the subventricular zone	29
2.6.7. Background of the host lab	31
3. Chemokines and chemokine receptors.....	34
3.1. Chemokines	35
3.2. Chemokine receptors	35
3.2.1. CXCR4, the classical receptor for CXCL12	36
3.2.2. ACKR3, the atypical receptor for CXCL12.....	37
3.3. The ACKR3 receptor – roles in physiopathology	41
3.3.1. ACKR3 function during embryonic development.....	41
3.3.2. ACKR3 role in cancer	42
3.4. ACKR3 in glioblastoma – State of the art.....	45
PART 2: OBJECTIVES	48

PART 3: IN SILICO ANALYSIS OF CHEMOKINES AND CHEMOKINE RECEPTOR EXPRESSION IN GLIOMA	51
I. Patient-Oriented Perspective on Chemokine Receptor Expression and Function in Glioma (Isci et al. 2021)51	
II. Patient-based multilevel transcriptome exploration highlights relevant chemokines and chemokine receptor axes in glioblastoma" (D'Uonnolo, Isci et al. 2024).....	65
PART 4: ANALYSIS OF ACKR3 AND ITS ROLE IN GBM	74
I. Heterogeneous expression of the atypical chemokine receptor ACKR3 in glioblastoma patient-derived tissue samples and cell cultures. (Isci et al. 2024)	74
II. TME data on ACKR3.....	78
PART 5: APPROACHES OF GBM TARGETING VIA VIRUSES.....	86
I. Development of an intraventricular Adeno-Associated Virus-based labelling strategy for glioblastoma cells nested in the subventricular zone. (Lombard, Isci et al. 2024)	86
II. Nanobody-based retargeting of an oncolytic herpesvirus for eliminating CXCR4+ GBM cells: A proof of principle (Sanchez Gil et al. 2022)	96
PART 6: CONCLUSION AND PERSPECTIVES	98
REFERENCES	105

PART 1: INTRODUCTION



PART 1: INTRODUCTION

1. Gliomas – general overview

Tumors of the central nervous system (CNS) constitute the fifth most prevalent cancer type, and gliomas are the most common primary CNS tumors¹. The overall annual incidence rate of brain/CNS tumors in the United States between 2016 and 2020 stood at 24.83 per 100,000, with gliomas representing 26.3% of cases¹. These tumors share histological characteristics with normal glial cells and are typically named based on these similarities². Gliomas can vary widely in their aggressiveness, with grades ranging from low-grade (WHO grade 1-2) to high-grade (WHO grade 3-4). In adult, most gliomas occur in the supratentorial brain structures (frontal, temporal, parietal and occipital lobes combined)¹.

1.1. Histomolecular classification of gliomas

The glioma classification system has dramatically changed over the past decade. Historically, neuropathologists relied on histopathology as the "gold standard" for the diagnosis and classification of gliomas³. Tumors were classified from WHO grade 1 to 4, following a decision tree based on characteristics of increasing malignancy, including degree of cellular atypia, mitotic index, and for certain specific tumor types (e.g. GBM), necrosis and microvascular proliferation^{3,4}. Astrocytomas present hypercellularity and nuclear atypia (enlarged, irregularly/elongated shaped and hyperchromatic) (Fig. 1a). Oligodendrogliomas are characterized by different size of round cells, uniform nuclei, coarse chromatin, and few cytoplasm (Fig. 1b). And glioblastomas (WHO grade IV) exhibit microvascular proliferation (Fig. 1c) and/or necrosis (Fig. 1d)⁵.

Recent advances in molecular biology have supported a deeper understanding of molecular alterations in gliomas, which led to the revision of diagnostic criteria, the identification of prognostic biomarkers and the implementation of targeted therapies^{5,6}. This progress is notably reflected in the versions of the 2016 and 2021 WHO

classification of CNS tumors, which integrate evolving molecular knowledge, allowing better precision for the diagnosis and management of gliomas⁶⁻⁸. The most important molecular alterations are listed below (Fig. 2).

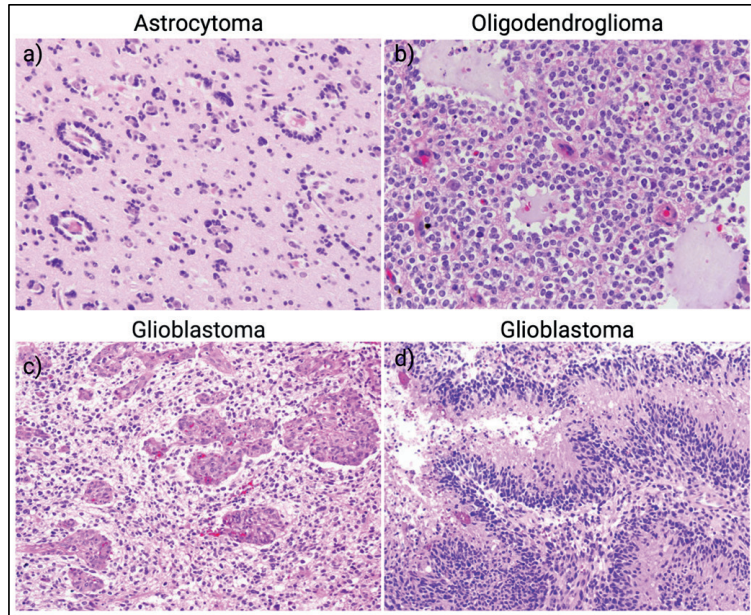


Figure 1 : a) Astrocytoma showing nuclear atypia (enlarged, irregularly/elongated shaped and hyperchromatic). b) Oligodendroglioma with round regular nuclei, coarse chromatin, and clear perinuclear halos. Glioblastomas with typical features, such as (c) microvascular proliferation and (d) pseudopalisading necrosis (Adapted from Ferris et al. 2017) (Created with BioRender.com)

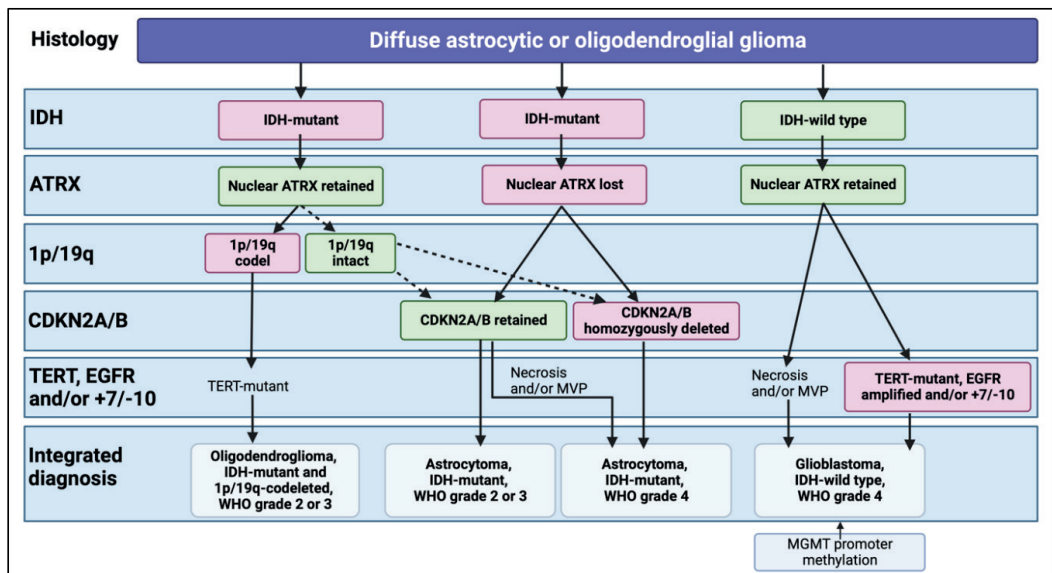


Figure 2 : WHO CNS5 2016/2021 classification-based decision tree for glioma diagnosis, illustrating the integration of molecular criteria. (Adapted from Weller et al. 2021) (Created with BioRender.com)

- **Isocitrate dehydrogenase 1 and 2 (IDH 1/2)**

The isocitrate dehydrogenase (*IDH*) mutation status represents a key feature allowing the categorization of gliomas⁹, essentially separating IDH-mutant (IDH-mut) tumors, such as oligodendrogliomas and astrocytomas, from IDH-wild type (IDH-WT) glioblastoma (Fig. 2). In 2008, Parsons' team performed mutational analysis of the glioblastoma DNA samples which led to the identification of somatic mutations in the *IDH1* gene¹⁰. The most frequent mutation affects *IDH1*, with a change of the arginine to a histidine at the position 132 (R132H). Rarer mutations in *IDH2* rather affect the position 172 with a substitution of arginine to a lysine¹¹. The IDH enzyme is an oxidoreductase that catalyzes oxidative decarboxylation of isocitrate to produce α -ketoglutarate (α -KG) and the reduction of NAD^+ to $\text{NADH} + \text{H}^+$ ^{12,13}. The mutations lead to a deficient catalytic activity and the production of an oncometabolite, 2-hydroxyglutarate (2-HG)^{12,14}. 2-HG inhibits crucial histone demethylases, leading to DNA methylation and repression of multiple genes^{12,13}. Moreover, the IDH1 mutation cause CpG island methylator (CIMP) phenotype by remodeling the epigenome (modifying methylation patterns, changing transcriptional programs and altering the differentiation state)¹⁵.

- **Alpha-thalassemia/mental retardation X-linked (ATRX)**

α -thalassemia/mental retardation X-linked (ATRX) is a chromatin remodeling protein involved in maintaining genomic stability, DNA repair processes and telomere preservation¹⁶. The loss of ATRX is a second-level molecular marker for glioma classification (Fig. 2). Functionally, ATRX loss impairs DNA repair by non-homologous end joining (NHEJ) and promotes alternative lengthening of telomeres (ALT) activity, leading to genetic instability^{17,18}.

- **1p/19q co deletion**

The deletion of the short arm of chromosome 1 and the long arm of chromosome 19 (1p/19q code) distinguishes oligodendrogliomas from astrocytomas, which are 1p/19q intact¹⁹ (Fig. 2). Several studies have highlighted the fact that 1p/19q codeletion was associated with increased sensitivity to chemotherapy, favoring a better prognosis²⁰⁻

²². This could be explained by the crucial role of 1p/19q codeletion in the regulation of immune cell infiltration and expression of multiple immune checkpoint genes²³.

- **Cyclin-dependent inhibitor 2A and B (CDKN2A/B)**

The cyclin-dependent kinase inhibitor 2A and B (*CDKN2A/B*) genes encode the p14, p16, and p15 proteins, respectively. Under physiological conditions, these proteins play a crucial role in regulating the cell cycle and angiogenesis²⁴. Homozygous deletion of *CDKN2A/B* (*CDKN2A/B* HG) leads to a direct oncogenic effect through the loss of cell cycle control and angiogenesis and, characterizes astrocytomas of higher grades (Fig. 2).

- **Telomerase reverse transcriptase (TERT)**

Another key genomic alteration involves the *TERT* promoter²⁵. Cancer cells divide endlessly, and telomerase reverse transcriptase is an essential enzyme that allows this escape from senescence²⁶. Mutations in the *TERT* promoter induce the TERT protein overexpression, resulting in telomere elongation²⁶. These mutations are found in IDH WT glioblastomas, as well as in IDH-mut, 1p/19q codeleted oligodendrogliomas^{26,27} (Fig. 2).

- **Epithelial growth factor receptor (EGFR)**

The consideration of molecular alterations targeting epithelial growth factor receptor (EGFR) are also an important biomarker for the diagnosis of gliomas²⁸. IDH WT Glioblastoma is often associated with *EGFR* amplification (EGFRamp) or mutation. A common mutant of EGFR is known as variant III (EGFRvIII)²⁹. Currently, experimental therapeutic approaches aimed at targeting EGFRvIII are under validation, including CAR-T cell therapy, therapeutic vaccines, antibodies, and bispecific T cell engagement strategies^{29–33}. The combination of EGFRamp and/or EGFRvIII with other alterations is highly specific of WHO grade 4 IDH WT glioblastoma (Fig. 2)^{28,34}.

- **Copy number variation on chromosomes 7 and 10**

The gain on chromosome 7 combined with loss on chromosome 10 (+7/-10) is considered as a key molecular signature for WHO grade 4, IDH WT glioblastomas^{28,35} (Fig. 2).

In GBM, gains of genetic material are slightly more frequent than losses. The most common gains occur on chromosome 7, which involve the amplification of EGFR gene, a critical oncogene. EGFR amplification drives tumor progression by enhancing cell proliferation, migration and resistance to therapies. On the other hand, the most frequent loss occurs on chromosome 10, leading to the deletion of PTEN, a key tumor suppressor gene³⁶.

2. WHO grade 4, IDH WT glioblastoma

2.1. Epidemiology

Glioblastoma (GBM) is the most aggressive form (grade 4) of gliomas and represents the most common primary tumor of the CNS, constituting 14.2% of all brain tumors and 50.9% of malignant tumors (Fig. 3). GBM is mostly diagnosed in adults, with a median age of 66 years. In the United States, between 2016 and 2020, the incidence of glioblastoma was higher in men (4.09 per 100,000 inhabitants) than in women (2.55 per 100,000 inhabitants). GBM has the lowest median survival of only 8 months from diagnosis¹ (Fig. 4). In contrast, the median survival for patients with oligodendroglioma reaches 205 months. ¹In Belgium, a recent study demonstrated that between 2017 and 2019, the median overall survival of GBM was 9.3 months, significantly shorter compared to astrocytoma (25.9 months)³⁷.

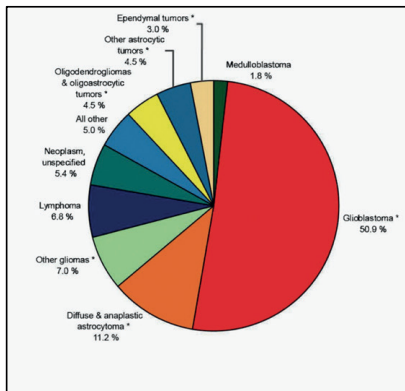


Figure 3: Distribution of malignant primary brain and other CNS tumors (between 2016-2020) (Adapted from Ostrom et al. 2023).

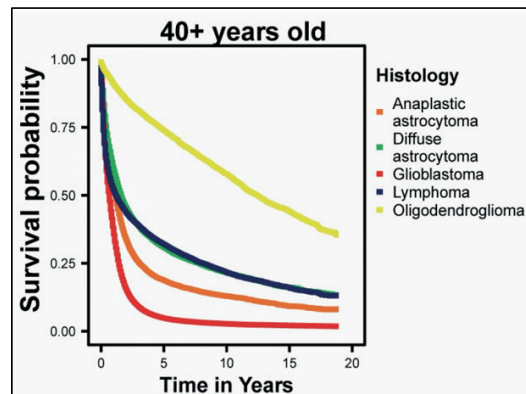


Figure 4: Kaplan-Meier survival curves between 2016-2020 in the United States, for the five most common pathologies within 40+ years group. (Adapted from Ostrom et al. 2023).

2.2. Etiology

GBM is considered as a sporadic disease, and most patients do not present any risk factors for tumor development at the time of diagnosis³⁸. Even so, the head exposure to ionizing radiation constitutes the most significant environmental risk factor for GBM³⁹⁻⁴¹. Some familial cancer syndromes (e.g., Lynch syndrome, Li-Fraumeni syndrome, tuberous sclerosis and Neurofibromatosis type 1) are also associated with an increasing risk of GBM⁴². Notably, a history of allergies or atopic diseases is associated with a reduced risk of developing GBM⁴³. Respiratory allergies appear to lower the risk of GBM by 30%, and eczema was associated with a 30%-reduced risk of developing glioma overall^{43,44}. Another study shows that regular aspirin use was associated with a reduced risk of GBM⁴⁵. Aside from these considerations, there is currently no proven evidence that GBM is related to environmental factors including, smoking, mobile phone use, exposure to low frequency electromagnetic fields, hormones, dietary factors, height and body mass index and others⁴⁶.

2.3. Clinical aspects – symptoms and diagnosis

The clinical signs of GBM are generally linked to the function of the brain area that is affected⁴⁷. At diagnosis, GBM patients present different symptoms including,

neurological symptoms, with headache, motor dysfunction and, aphasia being the most common^{47,48}. However, other symptoms may include intracranial hypertension, and some patients even develop epileptic seizures⁴⁸.

The appearance of abnormal neurological symptoms suggestive of a brain tumor is usually monitored using magnetic resonance imaging (MRI)⁴⁹. Classically, the MRI of GBM patients is characterized by (1) an infiltrative lesion showing contrast enhancement at the margins on T1-weighted images, due to disruption of the blood-brain barrier (BBB), (2) a hypo-signal in the center of the lesion on T2-weighted images which marks necrosis, and (3) hyper-signal on T2-weighted fluid-attenuated inversion recovery (FLAIR) images, highlighting peritumoral edema⁵⁰ (Fig. 5).

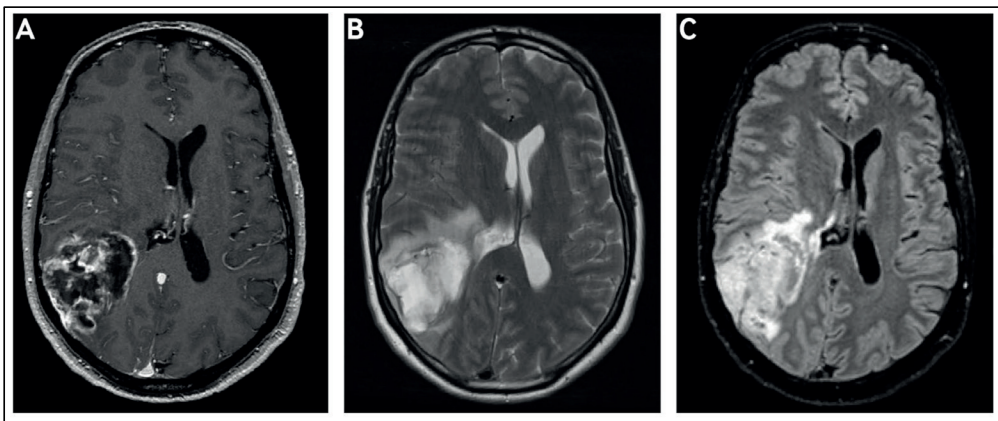


Figure 5 : Axial MRI head scan with (A) gadolinium enhanced T1-weighted, (B) T2-weighted, and (C) FLAIR sequences demonstrating a right parietal glioblastoma (Adapted from Mckinnon et al. 2021.).

Following the diagnosis of GBM, histological analysis is typically performed on tissue obtained from a tumor biopsy or resection⁵¹. GBM is characterized by high cell density and significant variability, comprising astrocytic cells with pronounced nuclear abnormalities⁵². There is observable strong cell division activity, and the presence of necrosis and/or microvascular proliferation is common⁵². Immunostainings reveals that the tumor is positive for glial fibrillary acidic protein (GFAP) and OLIG2, with high mitotic activity indicated by Ki67 positivity^{49,50}.

As mentioned above, certain molecular markers are routinely used to refine GBM diagnosis⁵². GBM is characterized by IDH WT status (indicating the absence of IDHmut in immunostaining), retention of nuclear ATRX staining, and often exhibits nuclear

accumulation of the p53 protein⁵². Additionally, key molecular alterations include mutations in genes that regulate receptor tyrosine kinases (RTKs) and downstream signaling pathways (RAS/PI3K), as well as TP53 and RB signaling pathways⁵². Finally, mutations in the *TERT* promoter, as well as alterations in the EGFR gene (EGFR_{amp} and EGFR_{vIII}), along with specific chromosomal losses/gains (+7/-10), are common parameters that help guide GBM diagnosis⁵².

2.4. Therapeutic aspects – Standard-of-care

The standard treatment for GBM involves maximal safe surgical resection to eliminate as many cancer cells as possible, followed by concomitant radiotherapy and TMZ chemotherapy⁵¹.

Resection surgery facilitates the macroscopic removal of the tumor, allowing for biopsies that aid in genetic and histological analyses, thereby confirming and refining the diagnosis^{53 54}. The primary objective of this procedure is to maximize cytoreduction while preserving the patient's neurological functions. Despite technical advances, such as the neuronavigation and the judicious use of fluorescence techniques (e.g., 5-aminolevulinic acid), which allow more extensive and secure resection, tumor cells infiltrating the brain parenchyma nevertheless persist⁵³.

The introduction of tumor cell fluorescence derived from 5-aminolevulinic acid (5-ALA) has improved contrast enhancement, leading to more “complete” tumor resections⁵⁵. Metabolically active tumor cells convert 5-ALA into protoporphyrin, which fluoresces red/violet when exposed to blue light⁵⁶(Fig. 6). Following the clinical trials conducted by Stummer et al. in 2006, 5-ALA was approved by the Food and Drug Administration (FDA) as an intraoperative imaging agent in suspected cases of high-grade glioma⁵⁷. By enhancing the rate of macroscopic complete tumor resection, 5-ALA significantly improves both progression-free survival and overall survival for patients⁵⁷⁻⁵⁹.

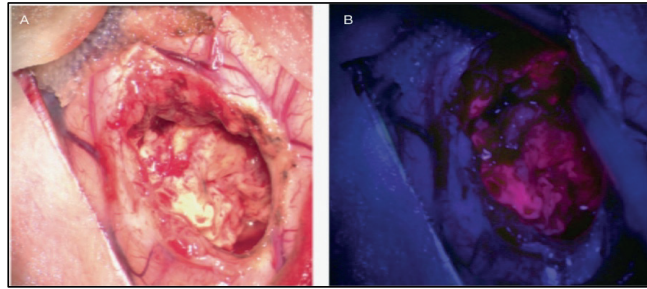


Figure 6 : 5-ALA derived fluorescence-guided GBM surgery (A) surgical resection cavity visualization with white light (B) surgical resection cavity under blue light (635nm) with red and violet fluorescence representing tumor cells, compared to normal brain appearing in blue. (Adapted from Hadjipanayis CG et al. 2021).

Since 2005, the debulking resection is followed by adjuvant radiotherapy and chemotherapy, as the standard of care. At the time, Roger Stupp’s team indeed highlighted the benefit of combining temozolomide (TMZ) with radiotherapy, which significantly improved prognosis for GBM patients. In their study, the median survival for patients treated with radiotherapy plus TMZ was 14.6 months, compared for those receiving radiotherapy alone⁶⁰ (Fig. 7).

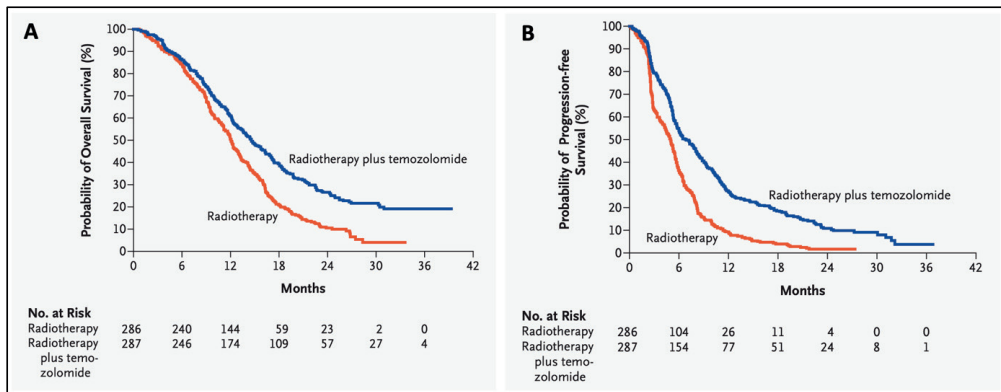


Figure 7 : Kaplan–Meier curves of overall survival (A) and progression-free survival (B) among patients treated with radiotherapy plus temozolomide (blue) compared with patients treated with radiotherapy alone (red) (Adapted from Stupp et al. 2005).

TMZ is an alkylating agent that adds methyl groups to purine bases, mainly on O⁶-guanines, generating O⁶-methylguanine (O6-MeG). This modification disrupts proper DNA replication, leading to double-strand breaks and ultimately cell death⁶¹. The DNA repair enzyme O6-methylguanine-DNA methyltransferase (MGMT) can remove O6-MeG induced by alkylating chemotherapy, thereby suppressing cytotoxicity and resulting in chemoresistance. Methylation of the *MGMT* promoter at CpG sites leads

to protein silencing and a responsiveness to TMZ⁶². In 2009, the group of Roger Stupp indeed showed that MGMT methylation status identifies patients most likely to respond to TMZ⁶³.

In addition to standard treatment, supportive medications are prescribed to improve the quality of life for GBM patients⁴⁷. Corticosteroids (e.g. dexamethasone) are used to reduce peritumoral edema and help to relieve headaches, nausea and vomiting associated with intracranial hypertension⁴⁷. Antiepileptics medications, such as levetiracetam, may also be prescribed for patients experiencing seizures⁶⁴.

2.5. Therapeutic aspects – Second-line treatments

Tumor treatment fields (TTFs) are a novel therapeutic modality involving low-intensity alternating electric fields applied directly at the tumor site, through electrodes placed on the skin. These electric fields disrupt cell division in rapidly dividing cells (tumor cells), leading to cellular death by apoptosis⁶⁵. In 2012, patients with recurrent GBM were treated with the NovoTTF-100A device; however, no improvement in overall survival was observed⁶⁶. In 2015, the same team conducted a new clinical study to evaluate the effectiveness and safety of TTFs combined with TMZ in GBM patients. They showed that the addition of TTFs to TMZ chemotherapy significantly prolonged progression-free survival and overall survival⁶⁷. Antiangiogenic treatments can also be used for GBM patients. Two different clinical studies evaluated the effect of the bevacizumab, a monoclonal antibody against vascular endothelial growth factor A (VEGFA), in combination to standard therapy in GBM patients. While the quality of life and health-related performance status were improved in the bevacizumab group, there were no significant differences in overall survival^{68,69}. The addition of bevacizumab to TMZ/radiotherapy also led to more significant adverse effects in patients. Furthermore, advances in the molecular deciphering of GBM have opened the door to targeted therapies as potential adjunct treatments⁷. For instance, vemurafenib is a BRAF inhibitor, has demonstrated clinical efficacy in patients with brain metastases from BRAF V600E mutant melanoma and has been tested in patients with diffuse malignant glioma harboring the same mutation⁷⁰. In this trial, only one patient exhibited a partial response, while others achieved disease stabilization, sometimes lasting over a year⁷¹.

2.6. GBM recurrence and underlying mechanisms

Despite these standard treatments, the aggressive and invasive nature of GBM leads to disease progression, making relapses inevitable for most patients⁷². The majority of tumor recurrences occur within 2 cm of the initial tumor site, although some may arise at greater distances^{72–74}. Recurrent tumors tend to be more aggressive than primary tumors, and are generally less responsive to treatment⁷². A recent study investigated the molecular determinant of GBM evolution by comparing paired primary and recurrent longitudinal samples, and show that genetic alterations, tumor cell heterogeneity and malignant phenotype change over time and upon treatment⁷⁵.

2.6.1. GBM cell invasiveness and interactions with host brain cells

GBM cells are highly invasive, making them a significant obstacle to treatment as they can evade surgical intervention⁷⁶. Although GBM rarely metastasizes outside the brain, local invasion occurs along blood vessels, white matter tracts, and the subarachnoid space⁷⁷. GBM cells have the ability to remodel their cytoskeleton and the extracellular matrix, facilitating their invasion into surrounding tissues⁷⁷. Recently, Venkataramani et al. showed that GBM cells receive synaptic input from neurons, contributing to brain invasion and disease progression. Their findings indicate that GBM cell invasion is similar to neuronal progenitor migration, characterized by synaptic communication between neurons and migrating tumor cells⁷⁸. In that line, it has been demonstrated in the GLASS consortium study revealed that, at recurrence, IDH-WT GBM tumors exhibit increased expression of “neuronal signaling” programs⁷⁵.

2.6.2. The blood-brain-barrier (BBB): a barrier to effective drug penetration

The blood-brain-barrier (BBB) serves as a protective brain barrier that compartmentalizes the brain from the blood, regulating ionic composition, nutrients and oxygen supply, while preventing the entry of macromolecules and potentially neurotoxic substances typically found in the blood⁷⁹. Although the BBB integrity may be compromised in certain tumor regions^{80–82}, the poor prognosis of GBM is, at least

in part, due to the challenge of effective drug delivery across this barrier⁸³. In the last decades, several studies have focused on developing new strategies to improve the delivery of therapeutic agents. In 2023, Roger Stupp's team proposed a novel approach involving low-intensity pulsed ultrasound combined with intravenous microbubbles (LIPU-MB) to open the BBB and enhance paclitaxel delivery to the peritumoral brain in patients with recurrent GBM⁸⁴. The objective of this phase I clinical trial was to determine the maximum tolerated dose during the first cycle of sonication associated with paclitaxel chemotherapy, with an assessment of safety in treated patients. In 2024, a phase II study was conducted to evaluate the BBB opening via MRI and assess therapeutic efficacy. Results indicated that among the 12 patients who received carboplatin immediately before sonication, the progression-free survival was 3.1 months, with a one-year overall survival rate of 58%, and a median survival of 14 months following surgery⁸⁵.

2.6.3. GBM stem cells

In line with the concept of cancer stem cells, which emerged and developed throughout the 20th century, GBM stem cells (GSC) were defined in the early 2000's as pluripotent cells capable of self-renew, exhibiting a high rate of proliferation and multilineage differentiation capacity. Upon secondary transplantation, GSC initiate a new tumor that recapitulates the cellular heterogeneity of the parental tumor (Fig. 8)^{86,87}. *In situ*, GSC predominantly reside in hypoxic niches of the brain, where they display resistance to conventional treatment^{88–90}. The identification of GSC often relies on the expression of various 'stem cell' membrane markers such as CD133, CD15, CD44 or intracellular markers such as Sox2 and Nestin⁹¹, although these markers are not entirely specific. Finally, several studies have demonstrated that GSC are the primary drivers of tumor development and play a pivotal role in establishing intra-tumoral heterogeneity^{92–94}.

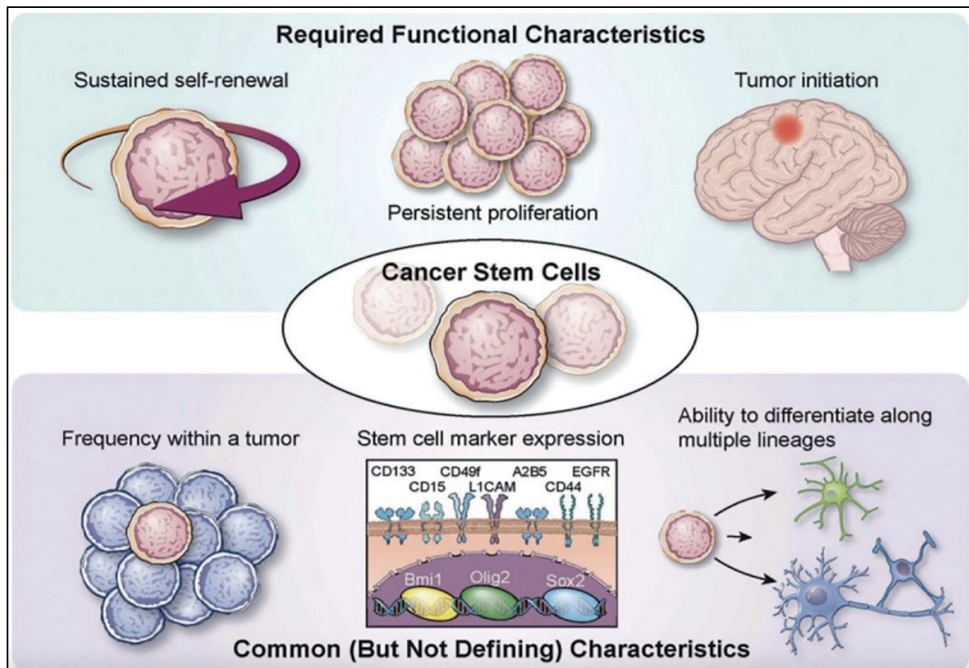


Figure 8 : Schematic criteria of GSCs. GSCs are defined by various functional characteristics including self-renewal, high proliferation rate, and tumor initiation upon secondary transplantation. GSCs share also common characteristics including frequency within a tumor, stem cell marker expression, and potential for differentiation. (Adapted from Lathia et al. 2015).

2.6.4. Heterogeneity and plasticity

The identification of “stem-like” cells in GBM tumors has raised the idea that not all cells in a tumor are identical and have further led to the detailed investigation of intra- and intertumoral heterogeneity, that has increasingly been considered as a major factor contributing to treatment failure. In 2008, the pioneering study of the Cancer Genome Atlas (TCGA) project analyzed the genomic profile of hundreds of GBM patients and revealed a significant genetic and epigenetic inter-tumor heterogeneity, across tumors⁹⁵. This study allowed the identification of frequently mutated genes (*TP53*, *EGFR*, *NF1* and *PTEN*). Three critical signaling pathways have also been highlighted as being frequently altered in GBM (p53, Rb and RTK/RAS/PI3K)⁹⁵. Two years later, a study made it possible to classify GBM into different molecular subtypes based on genomic and transcriptomic profiles⁹⁶. Verhaak et al. addressed transcriptomic heterogeneity and defined four GBM subtypes, namely proneural, neural, classic and mesenchymal⁹⁶. Their study demonstrated that the effectiveness

of standard treatment varied across subtypes, as it drastically reduced mortality in the classical and mesenchymal subtypes, but moderately in the neural subtypes while no change was associated with the proneural subtypes⁹⁶. Along with the rise of single-cell RNA sequencing technologies, Patel et al. were the first to shed light on the intra-tumor heterogeneity, showing the coexistence of different cell types within GBM, at the individual level. They demonstrated that GBM was composed of various cell subtypes with particular transcriptional signatures, and several cells with intermediate/mixed signatures. They showed that tumor cells were either in a stem-like or a differentiated state, exhibit variable proliferation capacities, and express differing levels of quiescence marker⁹⁷. Then, in 2019, Neftel et al. demonstrated cellular state transitions based on four single-cell transcriptomic signatures: astrocyte-like (AC), neural progenitor cell-like (NPC), oligodendrocyte progenitor cell-like (OPC) and mesenchymal-like (MES)⁹⁸. Importantly, multiple cellular states coexist within each GBM tumor. Altogether, GBM is characterized by extensive cellular heterogeneity and plasticity, which means that GBM cells are in a constant dynamic process, undergo changes in cell states and adapt depending on the disease development and microenvironmental signals^{99,100}.

2.6.5. The tumor microenvironment (TME) in glioblastoma

The GBM tumor microenvironment (TME) is a complex network that not only includes tumoral cells (under various states) but also other non-malignant cells such as, microglia, tumor-associated macrophages (TAMs), tumor-infiltrating lymphocytes (TILs), myeloid suppressor cells (MDSC), astrocytes, endothelial cells, pericytes and fibroblasts¹⁰¹ (Fig. 9). The TME is a dynamic system where permanent communications and interactions take place between these cell populations to ensure growth, invasion and immune escape leading to therapeutic resistance. The communication of GBM cells with their environment is especially mediated by secreted factors (e.g. chemokines and growth factors), via the transfer of extracellular vesicles, or using interconnecting microtubes¹⁰¹.

The extracellular matrix (ECM) is a key component of TME. It includes proteins like collagen, fibronectin and laminins that provide a physical and biochemical support for surrounding cells¹⁰². Alterations in ECM composition and stiffness, often mediated by matrix metalloproteinases (MMPs), promote GBM cell invasion through surround tissue and contribute to tumor progression^{103,104}. Cancer-associated fibroblasts (CAFs) actively participate to this ECM remodeling the ECM, further supporting GBM progression^{105,106}.

The GBM TME is globally characterized by an immunosuppressive activity that promotes the survival and proliferation of tumor cells by decreasing the immune response. This is reinforced by the major abundance in immunosuppressive macrophages, MDSC and regulatory T lymphocytes (Treg)^{107–109}. TAMs (especially M2-like) represent the major component of the GBM TME. Blood-derived TAMs significantly infiltrate gliomas, upregulate immunosuppressive cytokines and exhibit a different metabolism compared to microglial TAMs¹¹⁰. In contrast, TILs represent a small proportion in the GBM environment¹¹¹. Typically, GBM TME is considered as “cold” environment with a weak adaptative immune response, in which glioma cells express different immune checkpoint molecules that impede immune cell activation¹¹². In addition to their low abundance, many factors (PD-1 and CTLA-4) contribute to the depletion or exhaustion of TILs present in the TME making them nonfunctional¹¹³. Of note, CAFs also appear to play role in GBM immune suppression¹⁰⁶.

Adding up on the aforementioned GBM malignant cell heterogeneity, Martinez-Large et al. have shown that GBM immune infiltrate is also very different across patients and within individual tumors over time¹¹⁴. In the same line, White et al. presents a multicenter study exploring TME subtypes in GBM and their potential role in predicting immunotherapy response. They revealed three distinct subtypes (TME^{High}, TME^{Med} and TME^{Low}) based on immune and endothelial cell abundance. The study shows that TME^{Low} patients, with low immune infiltration, may benefit from a combination therapy targeting EGFR inhibition. In contrast TME^{Med} and TME^{high} subtypes, with higher immune cell density, suggest potential responses to immunomodulatory therapies¹¹⁵. Finally, many reports showed that increased T cells infiltration in GBM TME was

associated with prolonged survival¹¹⁶. However, unlike in other solid tumors, no surprising and major advances have been observed in terms of immunotherapy for GBM^{117,118}. The idea of countering glioma-associated immunosuppression has been extensively studied in clinical trials with the aim of generating anti-tumor responses. Many clinical trials have been conducted, testing vaccines^{119–124}, CAR-T cell therapies^{125–129}, and treatments with immune checkpoint inhibitors for GBM^{130–133}, but all these studies have so far failed at the step of clinical translation.

Moreover, the GBM TME is also characterized by different regional particularities, including for instance acidic and hypoxic regions, adding an additional layer of complexity and challenge to therapeutic strategies^{134,135}. The hypoxic niche in GBM is a key feature that provides malignant cell aggressiveness and promotes cancer progression, as well as treatment resistance^{134,135}. Hypoxia is associated with poor prognosis in patients because it activates various signaling pathways involved in apoptosis, autophagy, and DNA damage, thereby contributing to therapeutic resistance¹³⁶.

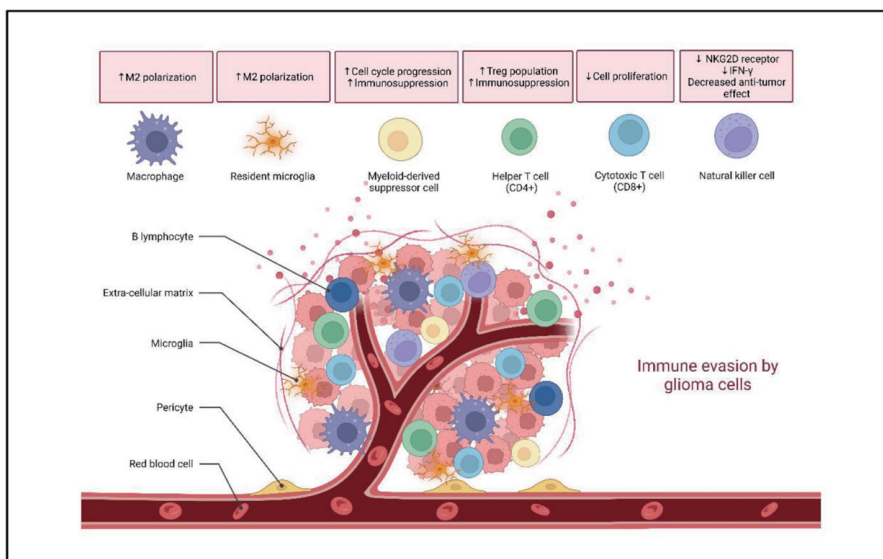


Figure 9 : Representation of GBM TME. GBM cells influence the immune landscape within the tumor microenvironment, leading to an immunosuppressive phenotype. They achieve this by secreting various factors that suppress the activation of T cells. Additionally, GBM cells promote the polarization of macrophages toward the anti-inflammatory M2-like phenotype and facilitate the recruitment of myeloid-derived suppressor cell (MDSCs) and T regulatory cells (Tregs) further enhancing the immunosuppressive environment. (Adapted from Mahajan et al. 2023)

2.6.6. The role of the subventricular zone

The subventricular zone (SVZ) is a 3-5 mm region of the adult brain which extends along the lateral walls of the lateral ventricles¹³⁷ (Fig.10). SVZ hosts a large population of neural stem cells capable of self-renewal and giving rise to neurons and glial cells¹³⁸. The structure of the SVZ as well as the mechanisms underlying adult neurogenesis have been and are yet under extensive characterization in murine models. In parallel, the study of post-mortem human brains also revealed the particular structure of the human SVZ, and the presence of stem-like neural cells that indicate the occurrence of neurogenic events¹³⁹.

In a subset of GBM patients, tumors develop in close proximity to the SVZ. Given the functional specificity of this area, several clinical studies have been carried out to determine whether the involvement of the SVZ had an impact on GBM patient survival. One study demonstrated that patients with SVZ-positive GBM had a higher risk of multifocal disease or distant progression¹⁴⁰. It was later revealed that the progression-free survival of patients with SVZ-positive tumor was lower compared to patients whose lesion was not in contact with the SVZ (Fig.11)¹⁴¹. Moreover, patients with GBM involving the SVZ had reduced overall survival¹⁴¹. Another study showed that contact with the SVZ but not with the *corpus callosum* or subgranular zone was associated with early recurrence and decreased survival¹⁴². Finally, it was shown that ionizing radiation directed to the SVZ was associated with an improvement in progression-free survival and overall survival in patients with GBM¹⁴³.

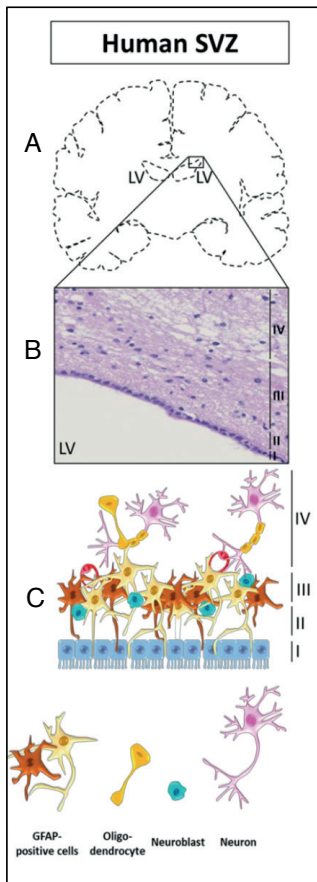


Figure 10 : Architecture of human subventricular zone (SVZ). **A**) Coronal section of human brain at the level of lateral ventricles. **B**) Enlarged images of human SVZ stained with hematoxylin and eosin. The human SVZ consisting of four layer (I to IV) from the lateral ventricle lumen to the parenchyma. **C**) Schematic representation of the cellular composition of human SVZ. The SVZ is composed of different layers: Layer I is a monolayer of ependymal cells responsible for the production and secretion of cerebrospinal fluid, layer II is known as hypocellular space as it is poorly populated with cellular processes, layer III is a cellular ribbon of GFAP-expressing cells and neuroblasts and layer IV, the outermost layer, is a transition zone of myelinated axons and oligodendrocytes (Adapted from Lombard et al. 2021)

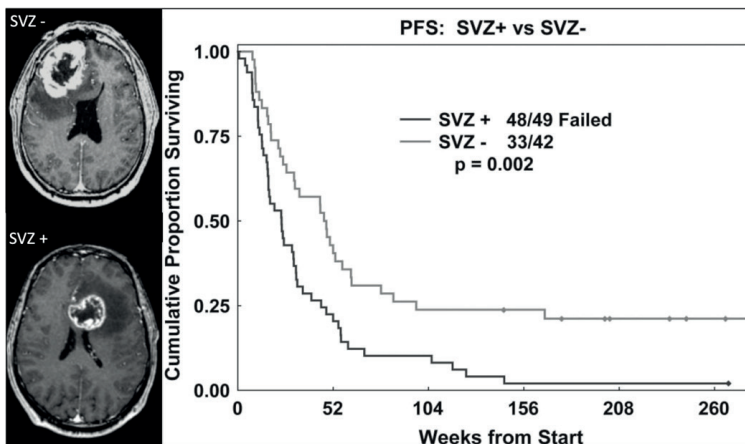


Figure 11 : Kaplan-Meier Curve of progression free-survival in patient presenting a tumor in contact with SVZ (SVZ+) or not (SVZ-) (Adapted from Jafri et al. 2013).

2.6.7. Background of the host lab

For several years, researchers in the laboratory have studied the cellular and molecular mechanisms underlying GBM recurrence. The main goal of was to understand the role of GBM stem-like cells (GSC) in disease development and mostly, in recurrence. Kroonen et al. demonstrated a particular interaction between GSC and the subventricular zone. They demonstrated that GBM cells injected into the right striatum of immunodeficient nude mice could migrate along the *corpus callosum* to reach and nest in the SVZ and from there, towards the olfactory bulbs (Fig. 12)¹⁴⁴. GBM cells isolated ex vivo from these two areas display huge tumorigenicity by forming a new tumor after second injection, suggesting that this tumoral cell population is enriched in GSCs¹⁴⁴. A fine characterization allowed them to demonstrate that these GBM cells express stem cell markers, such as Nestin and Sox2¹⁴⁴. Then, they noticed that GSCs expressed an important level of CXCR4 receptor at the surface¹⁴⁵. In parallel, they demonstrated that endothelial cells overlaying the SVZ secrete a high amount of CXCL12, the chemokine that binds to the CXCR4 receptor¹⁴⁵. These results allow them to suggest that CXCR4/CXCL12 signaling could play a significant role in the specific invasion of GSCs into the SVZ¹⁴⁵. To confirm this hypothesis, they treated GBM cells with an inhibitor of CXCR4 (AMD3100), which resulted in a disruption of GSC chemotactic attraction¹⁴⁵. These results were confirmed in an *in vivo* model where CXCR4-depleted GBM cells were grafted, and the invasion phenotype was abolished¹⁴⁵.

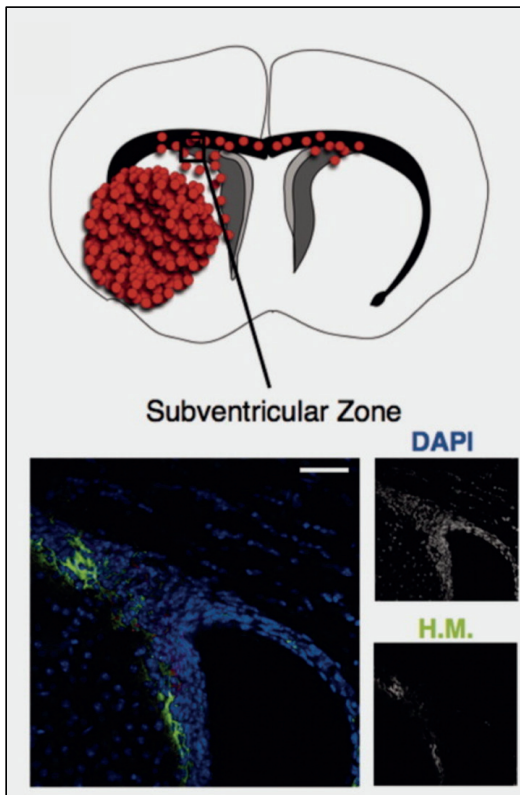


Figure 12: Immunodeficient mice injected with human U87 cells develop tumor mass in the right striatum at 3 weeks postinjection and invade the ipsilateral SVZ. Human mitochondrial (H.M.) marker was used to identify U87 cells. (Adapted from Kroonen et al. 2011)

The SVZ is considered as niche in which the local cellular and molecular environment support the maintenance and the proliferation of normal neural stem cells¹³⁸. The specific tropism of GSCs to this SVZ could thus be understood as if this would provide adequate local influences for their maintenance the survival. The SVZ could therefore constitute a reservoir for GSCs, putatively having a role in GBM recurrence. In this line, our host lab demonstrated that when these GBM cells reach SVZ, they became protected from ionizing radiation¹⁴⁶. *In vivo* xenograft experiments showed indeed that whole brain irradiation does not affect cells that have migrated into the SVZ to the same extend as cells present in the tumor mass¹⁴⁶. Moreover, disrupting the CXCL12/CXCR4 signaling axis sensitized these cells to IR¹⁴⁶. GSCs show enhanced resistance to double-stranded DNA damage. This could explain their ability to repair DNA damage to survive when in this favorable environment. They also observed that CXCL12 accelerates the repair of IR-induced double-stranded DNA damage in GSCs of the SVZ, increasing their survival¹⁴⁶.

They further investigated the phosphoproteome of CXCL12-treated GBM cells and identified the serine/threonine Aurora A (AurA) mitotic kinase as activated by CXCL12¹⁴⁷. AurA was overexpressed in GBM tissue compared to non-tumoral tissues¹⁴⁷. Further investigation demonstrated that in GBM cells, CXCL12 activates AurA through CXCR4 and ERK1/2 proteins¹⁴⁷. They identified various biological activities of AurA in GBM including cell survival, radio-resistance, self-renewal, proliferation, and migration¹⁴⁷. Finally, they showed that inhibition of AurA with alisertib decreases the number of GSCs invading the SVZ in mice model¹⁴⁷.

Additionally, they identified the nuclear MAP kinase phosphatase 1 (MKP1) which is another protein which phosphorylation is modulated by CXCL12¹⁴⁸. They found that MKP1 is increased in GBM and CXCL12 treatment GBM cells induced an increase in phosphorylation of MKP1¹⁴⁸. Our laboratory demonstrated that phosphorylated-MKP1 increases GBM cells radioresistance¹⁴⁸. In addition, MKP1 facilitates DNA repair through recruitment and stabilization of the DNA repair protein RAD51 at DNA double-stranded break sites¹⁴⁸.

3. Chemokines and chemokine receptors

CXCL12 and CXCR4 belong to a superfamily that is composed of many ligands and receptors. They constitute a complex interaction network where most chemokines bind to several chemokine receptors, and the majority of chemokine receptors have multiple chemokine type ligands (Fig. 13)¹⁴⁹.

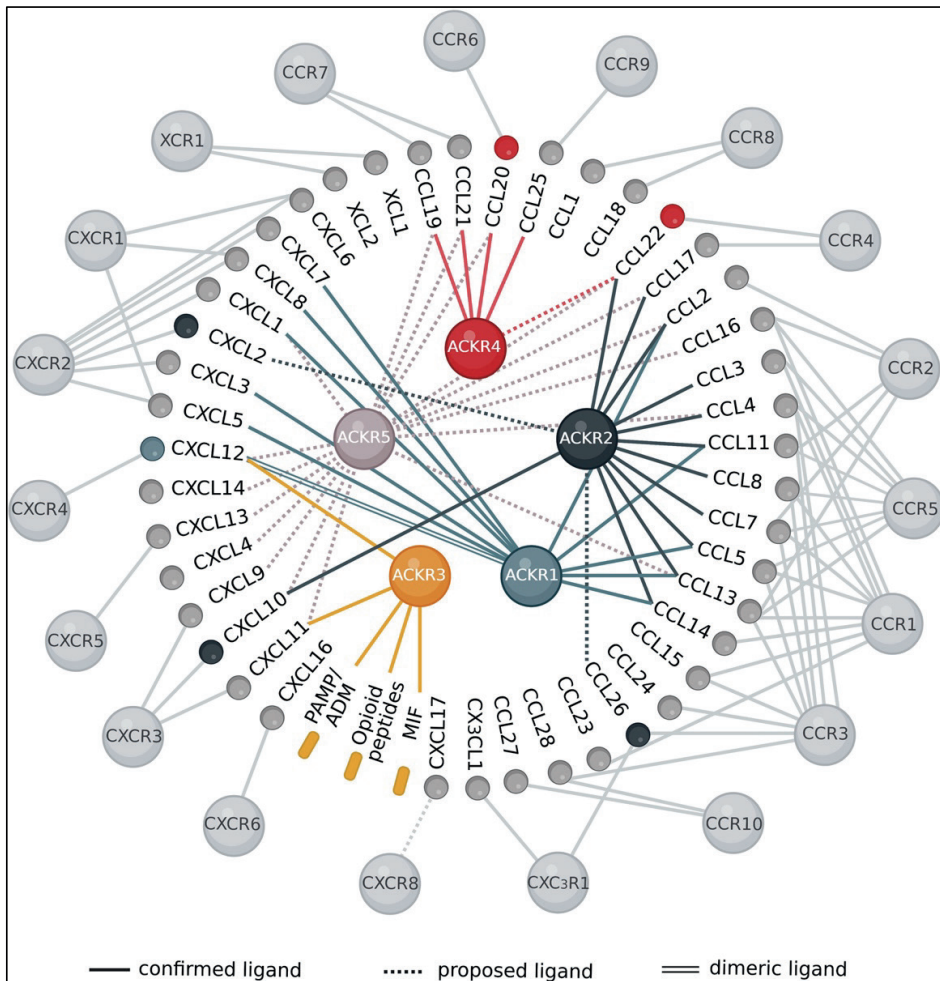


Figure 13 Interaction network of chemokines and chemokines receptors. Most chemokines can bind to multiple receptors, and most receptors have multiple ligands. Receptors and chemokines are represented as spheres, while non-chemokine ligands are represented as rectangles. The 19 classic chemokine receptors are shown in light gray (on the periphery of the schema), while the 5 atypical chemokine receptors are shown in color: ACKR1 (light blue), ACKR2 (black), ACKR3 (yellow), ACKR4 (red) and ACKR5 (light gray) and represented in the center of the schema. The colored chemokines and non-chemokine ligands represent interactions that have recently been identified and dotted lines indicate proposed ligands. (Adapted from Szpakowska et al. 2023)

3.1. Chemokines

Chemokines represent a subgroup of small chemotactic cytokine (8 to 12 kDa) that are secreted by numerous cell types in different tissues and are highly conserved¹⁴⁹. Chemokines act by interacting with G protein-coupled receptors (GPCRs) present on the cell surface, and participate in various biological processes such as development, immune response, and tissue repair. 43 chemokines have been described in the human genome and classified into four subfamilies (C, CC, CXC, and CX3C) based on the arrangement of cysteine residues in N-terminal position (Fig.17)¹⁴⁹. These cysteine residues are highly conserved and are crucial in maintaining the structural integrity, allowing a proper binding to their GPCRs¹⁴⁹. The C chemokine subfamily is the only one to contain a single cysteine residue in the N-terminal position. The CC, CXC and CX3C chemokines are made up of two cysteine residues which are adjacent (CC), separated by one amino acid (CXC) or by three amino acids (CX3C) (Fig.17)¹⁴⁹. In addition to their structural characteristics, chemokines can be classified based on their function as inflammatory or homeostatic chemokines¹⁵⁰. “Inflammatory chemokines” are highly regulated and mainly involved in immune cell recruitment during the inflammatory process, while “homeostatic chemokines” rather ensure the cellular trafficking under normal conditions. Some chemokines have mixed functions^{150–152}.

3.2. Chemokine receptors

Chemokine receptors are seven-transmembrane domain receptors that belong to the rhodopsin-like family of GPCRs, and are coupled to G α i proteins. The binding of the ligands induces a conformational change in the GPCR, leading to the activation of the G protein¹⁵³. The subunit α of the trimeric G protein complex exchanges guanosine diphosphate (GDP) into guanosine triphosphate (GTP). Subsequently, α -GTP dissociates from the $\beta\gamma$ subunit of the G protein complex, allowing both subunits, α and $\beta\gamma$, to interact with downstream effectors to propagate signals within the cell. The regulation of GPCR signaling is a complex and essential process for maintaining cellular homeostasis^{153–155}. A crucial part of this process is desensitization, in which

prolonged stimulation of GPCRs results in a decrease in their responsiveness. This phenomenon is facilitated by the phosphorylation of the GPCR by G protein-coupled kinases (GRKs), and their interaction with arrestins, which inhibit G protein activation^{156–158}. Simultaneously, the internalization of receptors into intracellular compartments constitutes another regulatory mechanism, reducing their bioavailability for ligands. In addition, GPCRs undergo recycling and degradation, contributing to the termination of signaling processes. There are four subfamilies of receptors based on the chemokine subfamilies to which they bind. To date, 19 classical chemokine receptors are shown to exhibit standard $G_{\alpha i}$ -dependent chemokine activity, while 5 atypical chemokine receptors (scavenging or recycling receptors) not dependent on a G protein for signalization^{153,159}.

3.2.1. CXCR4, the classical receptor for CXCL12

As mentioned, classical chemokine receptors translate signals via $G_{\alpha i}$ proteins and β -arrestins to induce cell migration, adhesion, and other biological responses¹⁶⁰. Currently, 19 classical receptors have been described, and are named according to the types of chemokines they bind (CCR, CXCR, CX3R and XCR) (Fig. 13)¹⁶⁰. However, the interaction network is complex, meaning that many chemokines bind to several receptors and in turn, receptors could interact with several ligands (Fig. 13). These receptors can exist as homodimers but can also form heterodimers with other receptors¹⁶⁰.

The chemokine receptor 4 (CXCR4) is a classical receptor that binds the chemokine CXCL12. It was first described for its important role in leukocyte trafficking and its ability to act as a co-receptor for the human immunodeficiency virus (HIV)¹⁶¹. Under physiological conditions, CXCR4 plays an important role in vascularization, angiogenesis, neurogenesis and the homing of immune cells in the bone marrow^{162–165}. Numerous studies have proved the crucial role of CXCR4/CXCL12 signaling in the progression of a wide range of cancers, including ovarian, breast, lung, and colon cancer, as well as GBM^{166–172}.

3.2.2. ACKR3, the atypical receptor for CXCL12

The family of atypical chemokine receptors (ACKRs) consists of five receptors: ACKR1, ACKR2, ACKR3, ACKR4 and ACKR5. As classical receptors, they can bind several chemokine or non-chemokine type ligands (Fig. 13)¹⁷³. Structurally, ACKRs are related to classical receptors, but they are functionally different. ACKRs are indeed unable to recruit G proteins to transduce signals leading to chemotactic and other cellular responses¹⁷³. This appears to be due to their lack of or alterations in the canonical DRYLAIV motif known to be required for most G proteins interaction, activation and signaling¹⁷³. These receptors are thus considered as silent/decoy or “scavenger” receptors, that use various strategies to regulate extracellular ligands responses by scavenging, internalization, and/or degradation. With this scavenger function, they appear more and more important regulators of immune and inflammatory responses, infectious diseases, and cancer¹⁷³.

In 1998, Heesen et al. discovered an orphan receptor (RDC1)¹⁷⁴, composed of seven transmembrane domains and was later considered as a chemokine receptor, renamed CXCR7¹⁷⁵(Fig. 14). Then this receptor was renamed atypical chemokine receptor 3 (ACKR3) due its incapacity to induce typical chemokine responses in cells by activating G protein dependent signaling¹⁷³. ACKR3 binds the chemokine CXCL12, ligand of the CXCR4 receptor, and CXCL11, one of the ligands of the CXCR3 receptor^{173,175,176}. ACKR3 presents a different activation mechanism, as some structural motifs required for CXCR3 and CXCR4 activation seem dispensable for ACKR3¹⁷⁷. ACKR3 can also bind the virus-encoded CC chemokine, vCCL2, and other non-chemokines ligands, including adrenomedullin (AM), macrophage migration inhibitory factor (MIF) and opioid peptides^{178–181}. The main function of ACKR3 receptor seems to rely in a scavenger activity for CXCL11, CXCL12 and AM, inducing internalization and degradation^{179,182}. Ray et al. showed that the deletion of ACKR3 C-terminus part prevents the internalization of the receptor and thereby impairs its role¹⁸³.

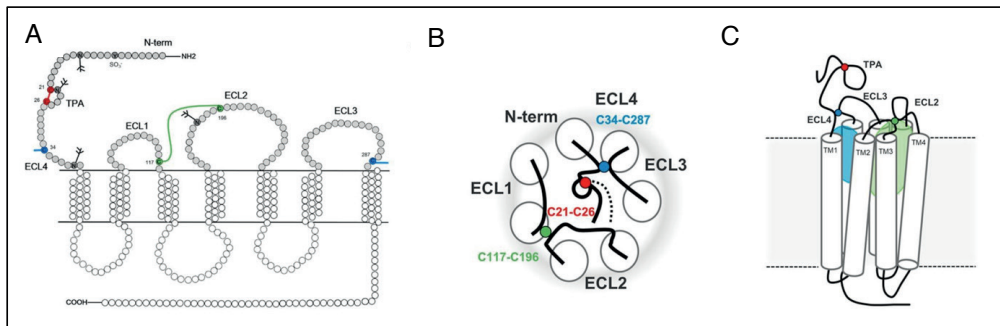


Figure 14 : A) Snake diagram of ACKR3 receptor highlighting post-translational modifications in the N-terminal and extracellular loops. Three disulfide bridges are identified: one within the N terminus (C21-C26, in red), another linking the N terminus to the top of the transmembrane domain 7 (C34-C287, in blue) and a third connecting transmembrane domain 3 to extracellular loop 2 (C117-C196, in green). Potential N-glycosylation sites (Ψ) and a sulfotyrosine modification (SO₃⁻) are marked in dark gray. B) Representation in top view of the extracellular disulfide bridges in ACKR3 receptor. The seven transmembrane segments are represented as white circles. C) ACKR3 architecture showing the position of different disulfide bridges on top of major (green) and minor ligand binding pockets. (Adapted from Szpakowska et al. 2018)

3.2.2.1. ACKR3 activation via CXCL12 and CXCL11

In 2005, ACKR3 was described as the second receptor of CXCL12¹⁷⁵. It has been demonstrated that ACKR3 interacts with CXCL12 (K_D of ~ 0.4 nM) with a 10-fold higher affinity than CXCR4^{175,184,185}. After ligand binding, ACKR3 is however unable to activate G α_i proteins pathways¹⁷⁶. CXCL12/ACKR3 interaction activates β -arrestin recruitment in a ligand-dependent manner, rather than G α_i -protein signaling and promotes CXCL12 internalization and degradation in endosome compartment (Fig.18)^{186,187}. It has been shown that ACKR3 act as scavenger to generate a gradient of CXCL12, modulating its bioavailability for the CXCR4 receptor^{188,189}. ACKR3 is also described as a major regulator of chemokine signaling by forming heterodimers with CXCR4 and modulating its activity (Fig.15)¹⁹⁰. After binding its ligand, ACKR3 is rapidly recycled back to the cell membrane, a process that is necessary for continued activation. This recycling is further improved in the presence of CXCL12¹⁸².

First discovered as a CXCR3 ligand, the CXCL11 chemokine (previously named ITAC) also binds ACKR3, though with a lower affinity than CXCL12 (K_D of ~ 4 nM)^{176,185,257}. CXCL11 binding to ACKR3 promotes different conformational changes in the receptor compared to CXCL12¹⁹¹. CXCL11 binding induces a faster ACKR3 internalization than CXCL12, and leads to a slower and delayed ACKR3 recycling, resulting in a prolong

intracellular presence of the receptor. This could be explained by a differential mechanism of endocytosis and transport¹⁹¹.

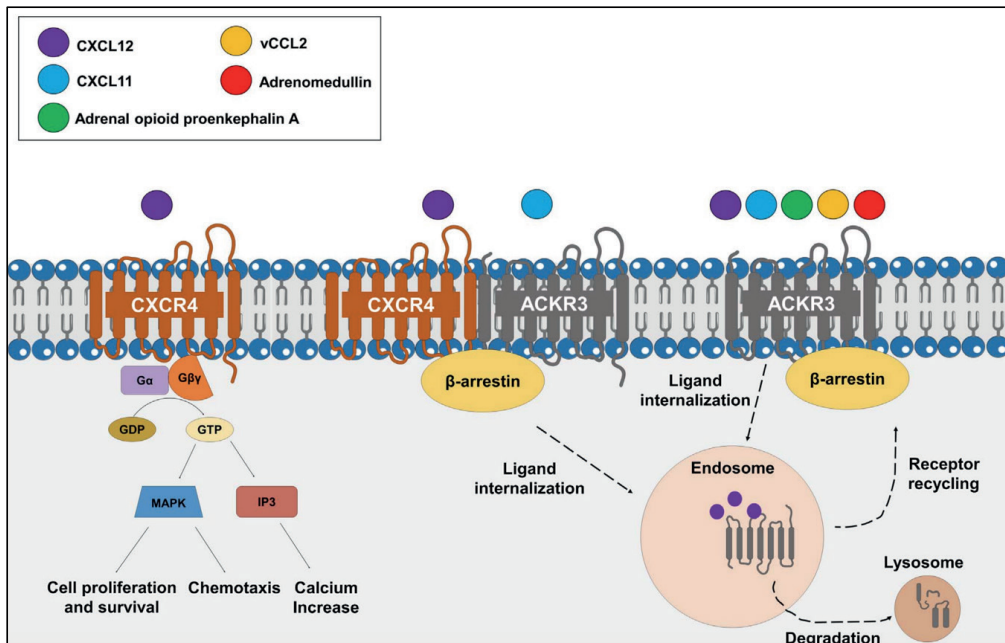


Figure 15: ACKR3 signaling. CXCL12 ligand binds to CXCR4 and activates classical signaling events including, cell proliferation, chemotaxis and calcium influx. ACKR3 can form a heterodimer with CXCR4, causing conformational rearrangements in G protein complexes and leading to a preference for β-arrestin over classical GPCR signaling in response to CXCL12 binding. This heterodimer effect is reduced by CXCL11. ACKR3 can also sequester the ligands CXCL12, CXCL11, adrenomedullin, adrenal opioid proenkephalin A, and vCCL2, leading to ligand internalization and degradation in lysosome via recruitment of β-arrestin. (Adapted from Quinn et al. 2018)

3.2.2.2. ACKR3 activation by non-chemokine ligands

ACKR3 was shown to bind adrenomedullin (AM) with a K_d of ~ 0.2 nM¹⁹². Like CXCL11 and CXCL12, AM does not induce canonical signaling after ACKR3 binding¹⁹³. Meyrath et al. confirmed that AM acts as a direct agonist of the ACKR3 receptor. Of note, ACKR3^{-/-} mice results in postnatal lethality due to a defect in cardiac development^{194,195} (see below). Wetzelschlag et al. have shown that overexpression of AM in mice model results in cardiac hypertrophy, which exhibit similar results observed in ACKR3^{-/-} mice¹⁹⁶. They have shown that the expression of ACKR3 on lymphatic vessels is important for scavenging and regulating AM concentration during cardiac development, since ACKR3 deletion promotes AM-mediated lymphatic vessels hyperplasia¹⁷⁹.

vCCL2 (also called VMIP-II) is a viral CC chemokine encoded by HHV-8 (Human Herpesvirus 8), known also as the Kaposi's sarcoma associated virus¹⁹⁷. vCCL2 interact with ACKR3 with an IC₅₀ of 53.6 nM and can also bind to a broad spectrum of chemokines receptors. vCCL2 is an agonist for ACKR3 and CCR3 receptors and an antagonist for CXCR4, CCR1 and XCR1 receptors^{198,178}. In response to vCCL2, ACKR3-expressing GBM cell lines are unable to trigger intracellular calcium mobilization or cAMP modulation, indicating that the chemokine does not activate G protein signaling pathways. However, like CXCL11, CXCL12 and AM, vCCL2 engenders β -arrestin recruitment upon ACKR3 binding, and change ACKR3 levels in a concentration-dependent manner¹⁷⁸.

Intermediate opioid peptides such as BAM22 and peptide E produced by the adrenal gland have been described as ligands for ACKR3¹⁹⁹. Ligand interaction can activate β -arrestin recruitment and induce anxiolytic effects by enhancing circadian oscillation of glucocorticoid levels in adrenal glands¹⁹⁹. More recently, Meyrath et al. have shown that ACKR3 can be activated by a large range of opioid peptides from different families, including enkephalin, dynorphin and nociception¹⁸¹. Once again, in response to endogenous opioid peptides, ACKR3 is unable to activate canonical G protein signaling but similarly to its role in chemokine gradient modulation, ACKR3 recruits β -arrestin and acts as a scavenger for regulating availability of opioid peptides for classical opioid receptors¹⁸¹.

3.2.2.3. The debate surrounding ACKR3: Scavenger or signaling receptor?

ACKR3 is described as an atypical receptor primarily acting as a scavenger by internalizing its ligands for degradation, preventing their interaction with classical receptors^{182,187,190}. However, its "signaling" properties remain debated, and whether ACKR3 directly or indirectly modulates key signaling pathways is still under investigation. Some studies suggest that ACKR3 can activate the MAP kinase pathway, specifically ERK1/2, independently of G proteins. In 2009, Levoe et al. demonstrated that when co-expressed with CXCR4, ACKR3 attenuates CXCR4-induced G protein signaling, either by regulating CXCR4 activity through

heterodimerization or by signaling independently via β -arrestin. This leads to reduced ERK pathway activation, as well as decreased immune cell migration and tumor progression¹⁹⁰. Décaillot et al. showed that when ACKR3 is co-expressed with CXCR4, CXCL12 modulates β -arrestin recruitment, which enhances ERK1/2 and MAPK pathways activation, promoting cell growth and migration, again independent of G proteins²⁰⁰.

Meyrath et al. support the hypothesis that ACKR3 functions as a scavenger receptor, binding ligands without inducing intracellular signaling. Indeed, their work has demonstrated that PAMP-12, an AM derivative, binds to ACKR3 without triggering G protein recruitment or ERK phosphorylation, confirming that ACKR3 regulates ligand availability without initiating signaling response²⁰¹. Similarly, Szpakowska et al. showed that the ligand vCCL2, by binding to ACKR3, causes β -arrestin recruitment and receptor internalization. However, this interaction does not trigger classical G protein-dependent signaling, reinforcing the role of ACKR3 as a non-signaling scavenger receptor²⁰². Finally, Meyrath et al. demonstrated that ACKR3 does not activate the MAPK pathway in response to opioid peptides, supporting the idea that this receptor regulates classical signaling without directly participating in intracellular signaling events²⁰³. Finally, the two hypotheses 'scavenger' versus 'signaling' are not necessarily mutually exclusive, as ACKR3 activity probably depends on the cellular context, presenting a significant challenge in determining its precise function.

3.3. The ACKR3 receptor – roles in physiopathology

3.3.1. ACKR3 function during embryonic development

ACKR3 plays important roles in cardiac and cerebral physiology. Most ACKR3-deficient mice die perinatally or *in utero* in late development stage, due to cardiovascular and cerebral defects^{194,195,204–206}. Considering these lethal defects, many studies have been focusing on ACKR3 functions in heart and brain development. For the heart modifications observed in ACKR3-deficient mice, two studies have highlighted a problem linked to cell proliferation. In 2008, Gerrith et al. observed cardiac hyperplasia among the 25% of ACKR3^{-/-} surviving mice¹⁹⁴. In 2011, Yu et al.

showed that ACKR3^{-/-} mice are characterized by an increased cell proliferation which prevented heart-valve development and, conducted to a lethal phenotype²⁰⁶.

Sanchez-Alcaniz et al. demonstrated that ACKR3 is expressed in the developing cortex, and is required for chemotaxis of interneurons in response to CXCL12. They proved that the ACKR3 deficiency led to an increase of CXCL12 levels, a failure in CXCL12 gradient and an accumulation of abnormal positioning interneurons in the cortex²⁰⁷. Recently, Trousse et al. showed that ACKR3 is required for the proper localization of Cajal-Retzius cells in the developing cortex. Cajal-Retzius cells play important function in laminar arrangement of cortical neurons after their radial migration. Indeed, they control the radial migration and position of pyramidal neuron by secreting Reelin protein²⁰⁴.

In addition, others ACKR3 roles have been described as in kidney development. Various studies have reported the role of CXCR4/CXCL12 axis in the proper development of renal vasculature and kidney morphogenesis^{206,208}. Subsequently, Haege et al. focused on ACKR3 in kidney development, and they founded ACKR3 depletion causes a decrease of CXCR4 immunoreactivity in nephrogenic zone and glomerular endothelium and leads to a malformation of the glomerular capillaries²⁰⁹.

ACKR3 receptor was predominantly expressed in the heart, kidney, lung, spleen and brain^{194,210-216}, where it is expressed in resident brain cells (glial cells and neurons), in the vascular system (smooth muscle and endothelial cells) and in the immune system (B, T cells)^{175,180,194,195,205,210,215-217}.

3.3.2. ACKR3 role in cancer

ACKR3 is expressed in a wide range of tumors, both by tumor cells and tumor-associated vascular cells. Generally, the activity of this receptor appears to promote tumor growth and has therefore been put forward as a potential therapeutic target^{218,219}.

3.3.2.1. *ACKR3 in breast cancer*

Many studies reported that ACKR3 plays a pivotal role in breast cancer progression and development of metastasis. Some reports demonstrated that ACKR3 expression was higher in human breast cancer samples compared to adjacent non tumoral samples and particularly found in tumor associated vasculature^{220,221}. ACKR3 participates to tumor growth and metastasis, as well as plays important role in vascular formation and angiogenesis^{220–223}. Furthermore, overexpression of ACKR3 in tumors was associated with worse prognosis in term of overall survival and a high chance to develop lymph node metastasis^{221,224}. In experimental models, genetic silencing or pharmacological inhibition of the receptor resulted in a reduction of tumor growth and metastasis^{221,225}. Another study showed that the ACKR3 knockdown reduced the expression of various stem cell markers (ALDH1, Oct4 and Nanog), and decreased the clonogenicity and proliferation capacities of breast cancer stem cells²²⁶.

Aiming at addressing ACKR3 mechanism of action, Salazar et al. indicated that ACKR3 receptor is expressed in estrogen receptor-positive breast cancer cells (MCF-7) and colocalizes with EGFR. They showed that the depletion of ACKR3 in MCF-7 cells reduced EGFR level and ERK1/2 phosphorylation, and decreased cell proliferation²²⁷. Hattermann et al. show that ACKR3 and CXCR4 are highly expressed together and interact closely in MCF-7 breast cancer cell line. After exposure to CXCL11 or CXCL12, the receptors were quickly internalized, either individually or near each other. Stimulation with antagonists for CXCR4 (AMD3100) or ACKR3 (CCX733) led to not only the individual internalization of the receptors but also, in some cases, their co-internalization. Additionally, both ligands reduced staurosporine-induced apoptosis and caspase-3/7 activation, although the selective inhibitors only partially blocked these biological effects²²⁸. Recently, Neves et al. analyzed the interaction between the CXCL12/CXCR4/ACKR3 axis and the signaling cascades induced by EGFR in different subtypes of breast cancer. They demonstrated that in MDA-MB-361 cells (luminal B subtype of breast cancer overexpressing Her2), there is a crosstalk between the ACKR3/CXCR4 receptors and EGFR, allowing to integrate signals from the TME and promote growth and tumor progression. This phenomenon was not

observed in MCF7 cells (luminal A subtype breast cancer) or MDA-MB-231 cells (triple negative breast cancer)²²⁹.

3.3.2.2. ACKR3 in lung cancer

Some studies suggest that ACKR3 may also play a role in different subtypes of lung cancer. Burns et al. showed that ACKR3 was highly expressed in lung carcinoma biopsies compared to healthy human lung samples¹⁷⁶. Additionally, Miao et al. confirmed these previous results and claimed that ACKR3 was found in tumor-associated vessels in lung carcinoma samples²²⁰. They highlighted that ACKR3 promotes lung tumor growth and enhances the formation of lung metastasis *in vivo*²²⁰. ACKR3 was shown upregulated in lung tumoral tissue whereas CXCR4 expression was similar in normal or tumoral tissue²³⁰. Moreover, it has been shown that overexpression of ACKR3 enhanced cell migration *in vitro* in lung cancer cell lines and promotes tumor growth and metastasis *in vivo*²³⁰. Pharmacological inhibition of ACKR3 by CCX754 displayed a reduction of the tumor growth¹⁷⁶. Furthermore, Iwakiri et al. demonstrated that ACKR3 is expressed in non-small cell lung cancer (NSCLC) and that recurrent metastatic samples express it to a greater extent than those without recurrence. In addition, patients with high expression of ACKR3 have a poor prognosis and a lower rate in disease-free survival²³¹. The study of Franco et al. underlines a high expression of ACKR3 in adenocarcinoma²³². Then it has been shown that the upregulation of ACKR3 is modulated by Transforming Growth Factor β -1 (TGF β -1). Depletion of ACKR3 leads to a reduction in migration, invasion, and epithelial mesenchymal transition (EMT) that are normally induced by TGF β -1. In patients, the combination of overexpression of TGF β -1 and ACKR3 is associated with an advanced stage of pulmonary adenocarcinoma and especially with a worse survival rate²³³.

3.3.2.3. ACKR3 and large B cell lymphoma

Diffuse large B-cell lymphoma (DLBCL) is the most common lymphoma and involvement of extra-nodal sites (bone marrow and CNS) is associated with an extremely bad prognosis. In an *in vivo* subcutaneous lymphoma model, ACKR3 was

shown to play a key role in DLBCL cells (VAL cells) lymph node, bone marrow and brain invasion²³⁴. A recent study consolidated previous findings by demonstrating that interfering with ACKR3 receptor significantly alters the migration of lymphoma cells towards CXCL12. To investigate the underlying mechanism, Antonello and his team developed ACKR3-knockout (VAL-KO) cells. Interestingly, deletion of ACKR3 does not affect CXCR4 expression. This study highlights that the migration of DLBCL cells towards CXCL12, mediated by CXCR4, requires the presence of ACKR3 *in vitro* and *in vivo*. Notably, cells which express ACKR3 on their surface can facilitate the migration of neighboring cells that do not express ACKR3. This mechanism is supported by the release of leukotriene B4 (LTB4) which acts synergistically with CXCL12 and CXCR4, thereby enhancing the overall migratory response of VAL cells²³⁵.

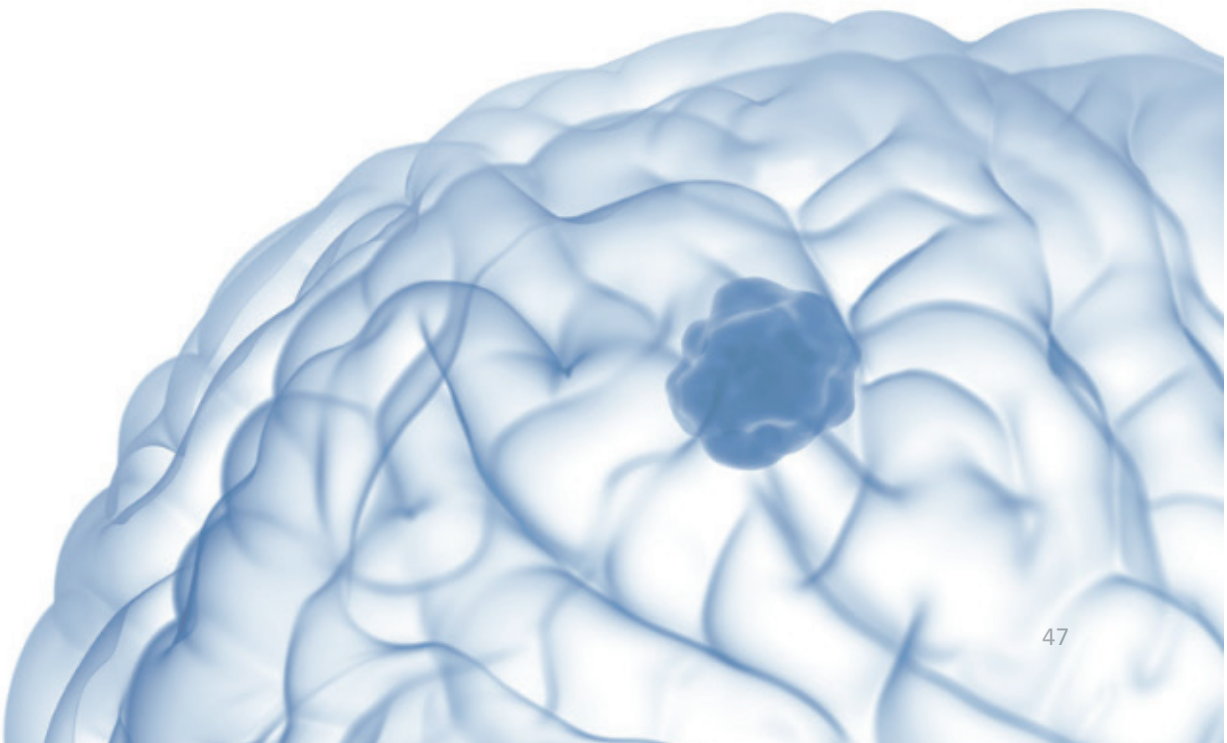
3.4. ACKR3 in glioblastoma – State of the art

Multivariate analyses helped to determine the prognostic significance of ACKR3 in GBM. This study showed that high expression of ACKR3 in GBM was strongly correlated with poor prognosis with poor overall survival²³⁶. Another study analyzed ACKR3 receptor expression in a cohort of matched primary and recurrent GBM samples. These results showed that ACKR3 and CXCL12 are expressed in high quantities, and that the receptor was downregulated in the matched recurrent samples²³⁷.

At the experimental level, Hattermann et al. revealed that there was a significant increase of ACKR3 transcript in high-grade glioma, compared to normal brain tissue. They demonstrated that in normal brain, ACKR3 is mainly expressed in endothelial cells. In GBM, a moderate expression was found in tumor vessels and more abundant expression was observed in glial cells (GFAP+), proliferative cells (Ki67+) and microglial/macrophage cells (Iba1+). ACKR3 is also expressed in different glioma cultures at both transcriptomic and protein levels. In addition, they showed that after treatment with camptothecin (an inhibitor of topoisomerase) or TMZ, ACKR3 inhibits glioma cell apoptosis while simultaneous treatment with a specific receptor antagonist (CCX733) restores the apoptotic process²³⁸. Another study showed that ACKR3 and CXCR4 are expressed in a comparable manner in malignant cells, higher than that in

tumor blood vessels. When analyzing the role of CXCR4 and ACKR3 in glioma cell proliferation, they demonstrated that an ACKR3 antagonist (CCX733) had a greater effect than CXCR4 antagonist (AMD3100) in reducing cell viability²³⁹. In three orthotopic models of GBM, the pharmacological inhibition of ACKR3 combined with irradiation led to tumor regression, blocked recurrence formation, and prolonged survival. The expression level of ACKR3 on tumor cells and associated vascular cells correlated with the neurosphere formation of human GBM cells after xenograft dissociation *ex vivo*. This correlation was abolished upon treatment with an ACKR3 inhibitor, suggesting that these events may be involved in vasculogenesis and/or proliferation of GBM tumor cells²⁴⁰. Salazar et al. demonstrated that targeting ACKR3 with monoclonal antibodies in combination with standard therapies could be effective in the treatment of GBM. They designed a single-chain chimeric antibody, X7Ab, to target the ACKR3 receptor in human and murine GBM cells. These results show that X7Ab alone or in combination with TMZ induces significant tumor reduction and prolongs overall survival. X7Ab kills GBM cells but also vascular endothelial cells that express ACKR3 via the activation of NK cell cytotoxic activity, and macrophage phagocytosis. In addition, X7Ab enhances the activation of M1-like macrophages *in vivo* to generate an anti-tumor immune response²⁴¹. A couple of additional studies have been conducted, to investigate ACKR3 function in GBM by using interfering RNA (siRNA) technology. Among other observations, the inactivation of ACKR3 has been associated to a decreased phosphorylation of the ERK1/2 signaling pathway in response to CXCL12, and a strongly reduced GBM cell proliferation, invasion and migration (mimicked by the ACKR3 antagonist, CCX771)²⁴². Another report highlighted that GBM cell lines expressed the ACKR3 receptor, and that hypoxia positively regulates this expression. Migration assays also showed that GBM cells expressing ACKR3 migrate towards CXCL12 under hypoxic conditions. In addition, they also show that when the receptor is inhibited, the phosphorylation of ERK1/2 and Akt decreases in response to CXCL12²⁴³.

PART 2: OBJECTIVES



PART 2: OBJECTIVES

Previous works from our laboratory have highlighted the critical importance of CXCL12/CXCR4 signaling axis in GBM. We demonstrated indeed that this signaling pathway plays a significant role in the invasion of GBM stem-like cells towards the SVZ of the brain and stimulates the DNA double-strands break repair induced by irradiation. These two observations suggest thus that the CXCL12/CXCR4 signaling pathway could play a significative role of the establishment of SVZ as a reservoir for GBM stem-like cells, easing the tumor relapse after the Stupp's therapeutic protocol. However, CXCL12 signaling is not limited to the sole CXCR4 receptor activation. Recently, atypical chemokine receptor 3 (ACKR3), previously known as RDC-1 and CXCR7, was identified as the second receptor for CXCL12.

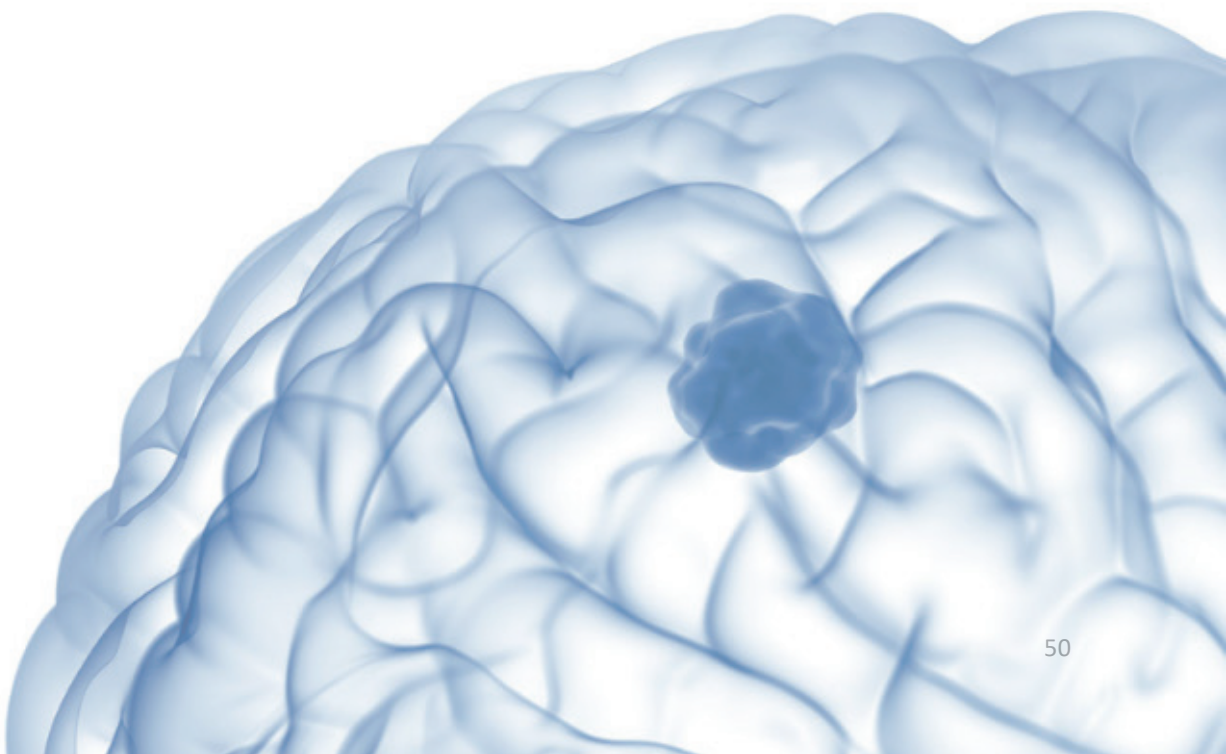
Given the high binding affinity of ACKR3 for CXCL12, and the growing evidence for its involvement in many oncological processes, we hypothesized that ACKR3 could play a complementary role to CXCR4 in GBM cell biology. Exploring the exact ACKR3 expression and function was therefore crucial for a more precise understanding of the mechanisms underlying GBM stem-like cell invasion and proliferation, which was the main objective of this thesis. To answer these questions, we conducted two distinct *in silico* analyzes which bring together transcriptomic data on the expression of several chemokine and chemokine receptors. Aside of assessing the relevance of CXCL12/CXCR4/ACKR3, these studies stratified the importance of the chemokine signaling pathways in GBM and summarize up-to-date, patient-oriented information about these axes in GBM. In parallel, experimental studies were carried out to study its expression within GBM stem-like cell cultures and tissues derived from GBM patients.

As previously mentioned, previous work in the laboratory has suggested the subventricular zone (SVZ) as an important niche harboring GBM stem-like cells and favorable for their resistance to radiotherapy. An important question remains whether these GBM cells in the SVZ effectively contribute to GBM recurrence. The second objective of this thesis was therefore to develop a strategy for labelling and tracking

OBJECTIVES

SVZ-nested GBM cells. We evaluated the effectiveness of an adeno-associated viral (AAV) vector injected intraventricularly into the mouse brain to specifically target cells that invade the SVZ. This project aims to provide an innovative tool to better understand cellular dynamics within the SVZ, in the context of GBM. This approach should make it possible not only to follow cell migration but also to understand the interactions between the SVZ and GBM cells.

**PART 3: *IN SILICO* ANALYSIS OF CHEMOKINES
AND CHEMOKINE RECEPTOR EXPRESSION IN
GLIOMA**



PART 3: *IN SILICO* ANALYSIS OF CHEMOKINES AND CHEMOKINE RECEPTOR EXPRESSION IN GLIOMA

I. Patient-Oriented Perspective on Chemokine Receptor Expression and Function in Glioma (Ischi et al. 2021)

1. Overview

The objective of this study was to refine our current understanding of the role of chemokine receptors in glioma, taking a step back from the cell line-based literature and focusing on a patient-centered perspective. We analyzed publicly available transcriptomic databases to identify a specific group of receptors that, based on their expression, appear to play a significant role in GBM patient samples. Considering the huge intra-tumor and inter-tumor diversity that characterizes gliomas, particularly GBM, we studied the expression of these receptors (1) regarding the severity of gliomas, (2) in specific histological niches in the tumors and (3) within different subtypes of cells that constitute the TME. It's important to note that bulk RNA sequencing (RNA-seq) and single-cell RNA sequencing (scRNA-seq) datasets are processed differently, which allows us to compare the broader tumor landscape with specific cellular contexts effectively. Additionally, we synthesize and re-discuss the most recent patient-oriented information from the literature based on these selected receptors. In conclusion, our study provides a clinically relevant and patient-centered overview summarizing the expression patterns and complex roles of chemokine receptors in gliomas. Additionally, this study highlights the importance of patient samples for the precise development and improvement of therapies that could target these receptors.

1.1. The Cancer Genome Atlas (TCGA) and Gliovis Platform

The Cancer Genome Atlas (TCGA) is a research project that has mapped the genetic, epigenetic, and proteomic alterations of tumors from different cancer types. The TCGA collects and shares complete genome sequencing data from thousands of cancer

patients and clinical data associated with these human samples. These massive data have been made publicly accessible to the scientific community to promote a deeper knowledge in cancer biology and to foster the development of new therapeutic approaches. The first TCGA study cohorts have helped to shed light on the tumor heterogeneity that poses such a major challenge in the treatment of GBM. In 2008, GBM was the first cancer studied by the TCGA, which provided significant progress by highlighting tumor complexity and genetic diversity. This study revealed the numerous genomic alterations and distinct molecular subtypes within GBM tumors, paving the way for more targeted and personalized treatment strategies⁹⁵. By using multidimensional analysis, this study reported analysis of DNA copy number, gene expression, DNA methylation aberrations and cataloged the most genome alterations encountered in a large cohort of human GBM (206 GBM samples)⁹⁵. Subsequently, all TCGA data were deposited in the DATA coordination center to allow public access. The results of this study highlighted mutations in the *TP53*, *PTEN* and *EGFR*, deletions of the *CDKN2A/B* genes as well as amplifications of *MDM2* and *CDK4*. Furthermore, this study discovered the existence of a disruption in three specific signaling axes: (i) the RTK/RAS/PI3K signaling pathway; (ii) the p53 signaling pathway and (iii) the RB signalization axis⁹⁵.

In 2016, Ceccarelli et al. extended the study to lower-grade gliomas (LGG) and comprehensively profiled 1122 diffuse gliomas newly selected by TCGA using molecular sequencing approaches. They identified new subgroups of diffuse gliomas with distinct molecular and clinical characteristics that allowed a classification of the different subtypes of gliomas. First, this study highlighted the *IDH1/2* mutation status as the main factor that allowed the separation of the sample cohort into *IDH1/2* mutant and *IDH1/2* wild-type groups, respectively enriched in LGG and GBM samples. The *IDH1/2* mutant tumors could be further segregated based on 1p/19q co-deletion. Then, this study identified the glioma-CPG island methylator phenotype (G-CIMP) phenotype as associated with *IDHmut* gliomas. Finally, DNA methylation signatures allow gliomas classification into 6 different subtypes (LGM1-6) with prognostic value²⁴⁴.

Gliovis portal is a powerful web platform that integrates genomic datasets from multiple sources, such as TCGA, Chinese Genome Atlas (CGGA) and others, currently containing 6500 tumor samples corresponding to adult and pediatric brain tumors. This intuitive tool helps researchers and clinicians to generate different types of data (Fig. 16)²⁴⁵.

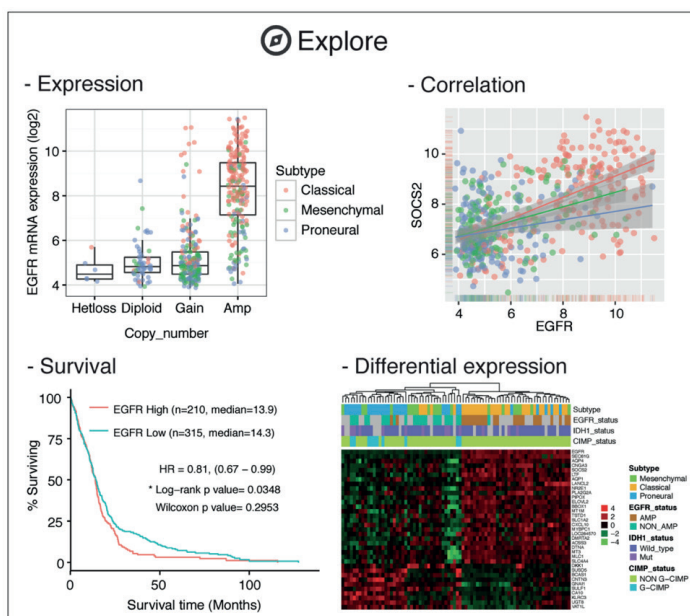


Figure 16 : example of data visualization by using Gliovis portal. Scatter dot plot of EGFR gene mutation expression in GBM subtypes; Correlation plot between EGFR and SOCS2 genes; Kaplan-Meier curve analyzing survival in EGFR high and EGFR low patient and heat map of EGFR differential expression. (Adapted from Browman et al. 2017).

1.2. Ivy Glioblastoma Atlas Project (IvyGAP project)

Years before the era of spatial transcriptomics, the study of Puchalski et al. (2018) significantly enriched our understanding of GBM spatial heterogeneity. This initiative used advanced technologies such as laser microdissection, RNA sequencing and *in situ* hybridization to obtain detailed transcriptional mapping of patient GBM samples, covering five different regions of the tumor to illustrate intra- and inter-tumoral heterogeneity. The laser microdissection allowed to precisely collect cells from different tumor regions, then RNA sequencing was used to determine gene expression

profiles from microdissected areas, whereas *in situ* hybridization allowed to visualization of gene expression in their anatomical context. The results highlighted the existence of distinct genetic profiles within the same tumor, which could potentially influence the response to treatments. Ultimately, this study generated a publicly available transcriptional atlas, The Ivy Glioblastoma Atlas Project (IvyGAP), providing a valuable resource for scientists wishing to further explore the molecular characteristics within five distinct GBM regions: Leading edge (LE), Infiltrating Tumor (IT), Cellular Tumor (CT), Microvascular Proliferation (MVP) and Pseudopalisading cells Around Necrosis (PAN). Each zone presents a specific different transcriptional profile (Fig. 17)²⁴⁶.

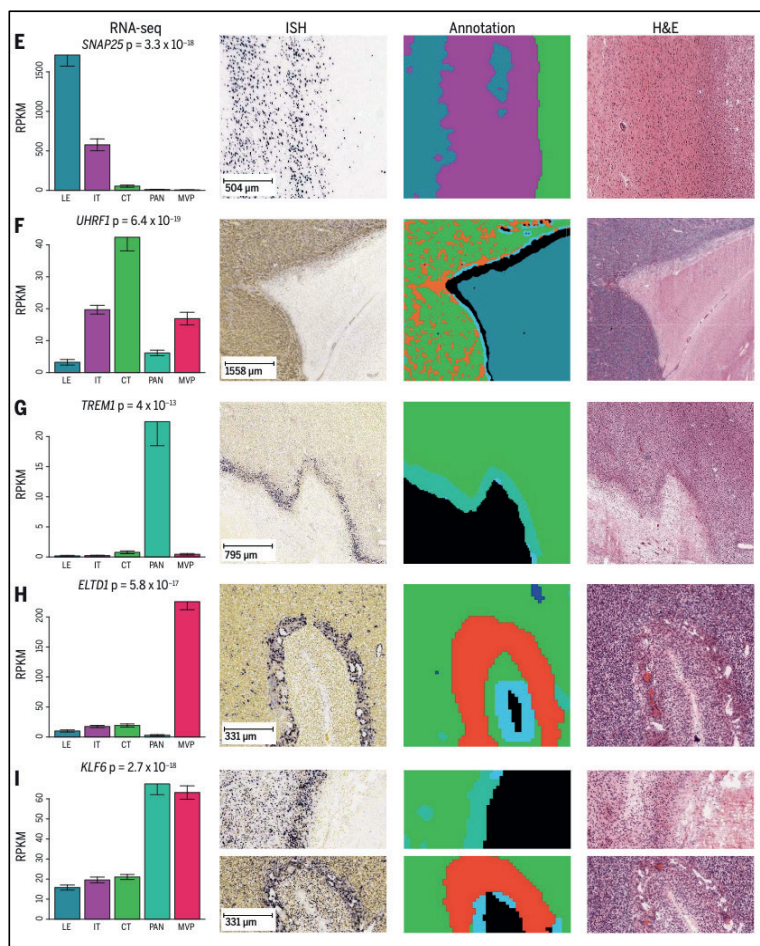


Figure 17 : Expression of SNAP25, UHRF1, TREM1, ELTD1 and KLF6 genes in five anatomical regions of human GBM samples. Data are represented by RNA sequencing (RNA-seq), in situ hybridization (ISH), annotation and by hematoxylin & eosin (H&E) staining. (Adapted from Puchalski et al. 2018).

1.3. Single-cell RNAseq data from Darmanis et al. (2017 Cell Reports)

The study of Darmanis et al. provided significant insights into cellular heterogeneity and immune infiltration in GBM. This study performed deep single-cell RNA sequencing on 4 GBM patients to better characterize tumor cells and define cellular diversity within GBM. To do this, they collected two distinct areas of the tumor from each GBM sample (the tumor core and the peritumoral brain) of which they isolated individual cells, to obtain specific molecular signature of infiltrating cells (vs. tumor core) and to analyze the effect of TME on immune/CNS cells (Fig. 18). Overall, they analyzed the sequencing of 3589 cells, including tumor cells and different cell types of the central nervous system (vascular cells, immune cells, neuronal and glial cells) (Fig. 19). Thanks to this approach, tumor cells that had migrated from the tumor to the surrounding tissue could be isolated and then, the effects of the TME could be compared on each of different cell types. These results provided a detailed analysis of different cell types present in GBM and their respective gene expression profiles²⁴⁷. These results were accessible on the GBMseq webtool.

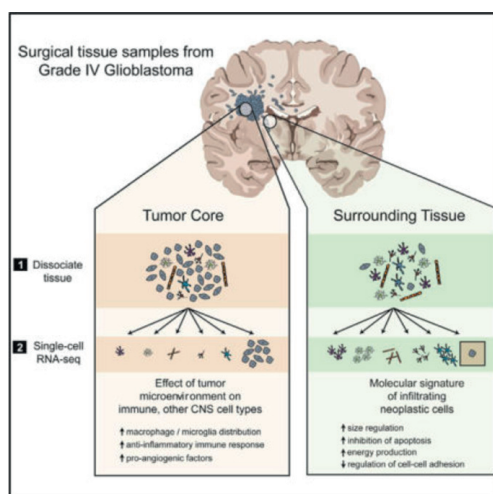


Figure 19: Schematic representation of study workflow (Adapted from Darmanis et al. 2017)

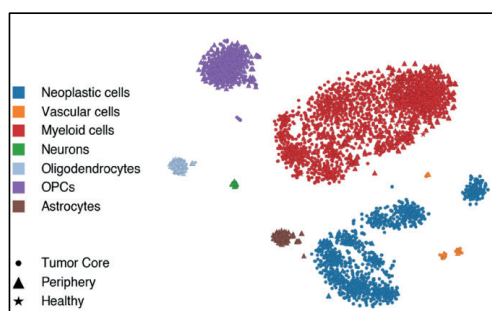


Figure 18: Classification of single cell from 4 GBM adult samples: tSNE plot of all single cells (Adapted from Darmanis et al. 2017)

1.4. Single-cell RNAseq data from Neftel et al. (2019 Cell)

Neftel et al. present another single-cell RNA sequencing study to investigate cellular diversity within 28 adult GBM samples. Cells were sorted using a viability marker and based on CD45 expression. Subsequently, tumor and non-tumor cells were classified by combining three different approaches: (i) they inferred chromosomal copy number alterations (CNA) based on the average expression of 100 genes, (ii) they analyzed gene expression corresponding to specific cell markers in cells devoid of CAN and then identified macrophages, T cells and oligodendrocytes (Fig. 20).

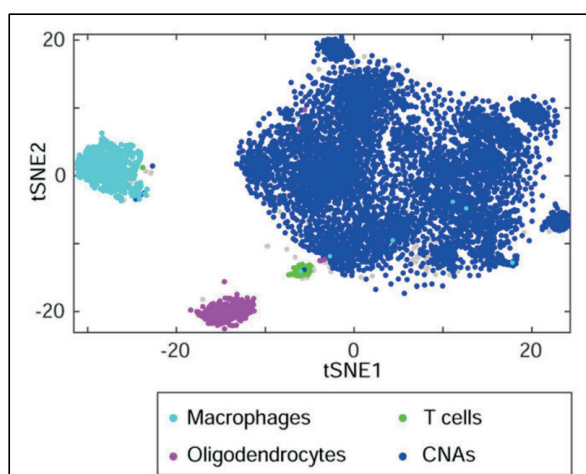


Figure 20 : Classification of single cell from 28 GBM adult samples: tSNE plot of all single cells. CNAs (Copy Number Alterations) is considered as a hallmark of cancer cells (Adapted from Neftel et al. 2019)

Focusing on malignant cells, this study highlighted four transcriptional states of GBM, based on their prominent gene expression profile: 1) Neural-progenitor cell-like (NPC-like); 2) Mesenchymal-like (MES-like); 3) astrocyte-like (AC-like), and 4) oligodendrocyte-progenitor cell-like (OPC-like). These cell states correlated with transcriptomic subgroups from the TCGA, and they demonstrated how malignant cells can transit from one state to another upon various environmental cues. This study provided valuable information on cell subtypes and on the level of interactions between tumor cells and non-malignant cells in the microenvironment⁹⁸.

2. Presentation and contributions to the manuscript

In this chapter, I will present and discuss in detail the main findings of our article entitled “***Patient-Oriented Perspective on Chemokine Receptor Expression and Function in Glioma (Ischi et al. 2021)***”. This paper highlights the expression and putative role of chemokine receptors in gliomas, with particular emphasis on patient-oriented data and findings. This study was designed and conducted with our collaborators from the Luxembourg Institute of Health (Andy Chevigné, Martyna Szpakowska, Giulia D’Uonno and May Wantz). Our main role was to conduct the analysis of chemokine receptor expression by interrogating the publicly accessible transcriptomic databases that were described above. In this work, we first attempted to study the expression of chemokine receptors in the different glioma subgroups in correlation with their severity/grade using the TCGA LGG-GBM dataset (513 patients with low grade glioma and 154 patients diagnosed with GBM). This allowed us to highlight 10 chemokine receptors based on their average mRNA expression within at least one subgroup of glioma. Then, the IvyGAP dataset allowed us to examine the expression of these 10 previously selected chemokine receptors within five different anatomical areas, and to correlate their expression with potential relevant biological activities. Finally, single-cell RNAseq datasets were used to determine the expression profile of chemokine receptors within different cell types present in GBM. We interpreted the results by highlighting the most prominent receptors playing a potential role in GBM, with the perspective to contribute to the understanding of GBM biology and to offer prospects for innovative therapies.

Review

Patient-Oriented Perspective on Chemokine Receptor Expression and Function in Glioma

Damla Isci ^{1,†}, Giulia D'Uonno ^{2,3,†}, May Wantz ², Bernard Rogister ^{1,4}, Arnaud Lombard ^{1,5}, Andy Chevigné ², Martyna Szpakowska ^{2,6} and Virginie Neirinckx ^{1,*}

- ¹ Laboratory of Nervous System Diseases and Therapy, GIGA Neuroscience, GIGA Institute, University of Liège, 4000 Liege, Belgium; Damla.Isci@uliege.be (D.I.); Bernard.Rogister@uliege.be (B.R.); alombard@chuliege.be (A.L.)
- ² Immuno-Pharmacology and Interactomics, Department of Infection and Immunity, Luxembourg Institute of Health, 1445 Strassen, Luxembourg; Giulia.Duonno@lih.lu (G.D.); May.Wantz@lih.lu (M.W.); Andy.Chevigne@lih.lu (A.C.); Martyna.Szpakowska@lih.lu (M.S.)
- ³ Faculty of Science, Technology and Medicine, University of Luxembourg, 4365 Esch-sur-Alzette, Luxembourg
- ⁴ Neurology Department, University Hospital, University of Liège, 4000 Liege, Belgium
- ⁵ Neurosurgery Department, University Hospital, University of Liège, 4000 Liege, Belgium
- ⁶ Tumor Immunotherapy and Microenvironment, Department of Oncology, Luxembourg Institute of Health, 1445 Strassen, Luxembourg
- * Correspondence: Virginie.Neirinckx@uliege.be
- † These authors contributed equally to this work.

Simple Summary: Chemokines and their receptors have been pointed out as key actors in a variety of human cancers, playing pivotal roles in multiples processes and pathways. The present study aims at deciphering the functions of several chemokine receptors in gliomas, starting from publicly available patient-derived transcriptomic data with support from the current literature in the field, and sheds light on the clinical relevance of chemokine receptors in targeted therapeutic approaches for glioma patients.



Citation: Isci, D.; D'Uonno, G.; Wantz, M.; Rogister, B.; Lombard, A.; Chevigné, A.; Szpakowska, M.; Neirinckx, V. Patient-Oriented Perspective on Chemokine Receptor Expression and Function in Glioma. *Cancers* **2022**, *14*, 130. <https://doi.org/10.3390/cancers14010130>

Academic Editor: Bernhard Moser

Received: 23 November 2021

Accepted: 24 December 2021

Published: 28 December 2021

Publisher's Note: MDPI stays neutral with regard to jurisdictional claims in published maps and institutional affiliations.



Copyright: © 2021 by the authors. Licensee MDPI, Basel, Switzerland. This article is an open access article distributed under the terms and conditions of the Creative Commons Attribution (CC BY) license (<https://creativecommons.org/licenses/by/4.0/>).

Abstract: Gliomas are severe brain malignancies, with glioblastoma (GBM) being the most aggressive one. Despite continuous efforts for improvement of existing therapies, overall survival remains poor. Over the last years, the implication of chemokines and their receptors in GBM development and progression has become more evident. Recently, large amounts of clinical data have been made available, prompting us to investigate chemokine receptors in GBM from a still-unexplored patient-oriented perspective. This study aims to highlight and discuss the involvement of chemokine receptors—CCR1, CCR5, CCR6, CCR10, CX3CR1, CXCR2, CXCR4, ACKR1, ACKR2, and ACKR3—most abundantly expressed in glioma patients based on the analysis of publicly available clinical datasets. Given the strong intratumoral heterogeneity characterizing gliomas and especially GBM, receptor expression was investigated by glioma molecular groups, by brain region distribution, emphasizing tissue-specific receptor functions, and by cell type enrichment. Our study constitutes a clinically relevant and patient-oriented guide that recapitulates the expression profile and the complex roles of chemokine receptors within the highly diversified glioma landscape. Additionally, it strengthens the importance of patient-derived material for development and precise amelioration of chemokine receptor-targeting therapies.

Keywords: glioma; chemokine receptor; patient-derived transcriptomic data; malignant processes; tumor microenvironment

1. Introduction

Gliomas are glial tumors of the central nervous system (CNS), which are categorized into different subtypes and clinical grades based on their histological features as well as molecular markers (according to the World Health Organization (WHO)) [1]. Adult-type

diffuse gliomas represent the majority of primary brain tumors detected in adults, glioblastoma (GBM) being the most malignant subtype [1]. It accounts for 48.3% of malignant tumors of the adult central nervous system [2] and systematically results in fatal outcome for patients. For over 15 years, standard-of-care treatment has combined maximal safe surgical resection, radiotherapy and concurrent temozolomide-based chemotherapy [3]. Despite extensive preclinical and clinical research continuously aiming to improve therapeutic efficacy, GBM recurrence is commonplace and patient survival from the time of diagnosis remains low [4]. Several mechanisms underlie tumor relapse: (1) the infiltrative nature of GBM that invades and disseminates through the whole brain tissue [5]; (2) the multilevel heterogeneity of GBM tumors, which exhibit inter-patient and intra-tumoral disparities [6], include diverse cell types and cellular states [7]; and (3) the ability of GBM cells to interact with and adapt to their microenvironment [8], to interconnect with neighboring tumor cells [9] or to harness healthy brain cells [10]. These devious mechanisms together support GBM to escape and resist treatment.

Chemokines are a subfamily of chemotactic cytokines secreted by a wide range of cell types in various tissues and are important regulators of developmental processes, immune responses and tissue repair [11]. Chemokines exert their effect by activating G protein-coupled receptors, which triggers downstream signaling pathways leading to cell migration, modulation of gene expression and cell phenotypes [12,13]. They are classified into four subfamilies—CC, CXC, CX3C and XC—based on the arrangement of the cysteine motif in their N-terminal part, while their receptors are classified according to the type of chemokines they bind (CCR, CXCR, CX3CR and XCR). Recently, four chemokine receptors have been grouped in a subfamily of “atypical chemokine receptors” (ACKRs) owing to their inability to activate the classical ligand-induced G protein signaling cascades. They do however have an important regulatory role and can act as scavengers by reducing chemokine availability in the extracellular environment [14,15]. Chemokines and chemokine receptors have been proposed as key actors in cancer cell growth, migration, invasion, neovascularization, as well as in the fine-tuned interplay between tumor cells and tumor-associated immune cells [16,17]. The growing interest in chemokine receptor function in GBM is of complex nature. Not only are chemokines and chemokine receptors involved in GBM cell malignant phenotype, they also play an important part in the immune cell recruitment to the tumor. These molecules are therefore being increasingly considered as potential targets in immunotherapy approaches for GBM [18].

The last decade has witnessed an unprecedented effort in collecting samples and clinical data from patients suffering from solid cancers, including brain tumors. International consortia and multicenter projects (e.g., The Cancer Genome Atlas (TCGA) [19], Glioma Longitudinal AnalySiS (GLASS) consortium [20], Gliogene [21], etc.) have gathered considerable patient cohorts that provided the neuro-oncology community with large multi-omics datasets, offering invaluable information for the classification and grading of tumors as well as for the understanding of molecular mechanisms underlying glioma biology. Whereas multiple therapeutic strategies have thus far failed to translate from the bench to the clinic because of limited research tools, the availability of patient data and biological material now facilitates clinically relevant research and fosters the development of personalized therapies [22,23].

Here, we aim to refine the current knowledge about the role of chemokine receptors in glioma from a patient-oriented perspective. We analyzed publicly available datasets and highlighted a subset of receptors that appear to be significant in GBM patients, for which we gather and discuss recent insight from the literature.

The purpose of this study is to provide researchers in the field with a clinically-relevant, up-to-date practical resource that could orient the next steps toward chemokine receptor-based treatment for glioma patients. We voluntarily highlight the literature that describes data generated from patient material and mention preclinical data on cellular and animal models when considered pertinent. We do not detail the mechanistic and functional aspects of each described receptor, which were exhaustively reviewed recently [24].

2. Methods

We aimed to highlight putative variations in the expression of chemokine receptors in different types of gliomas, as well as in different tumor subregions and cellular subsets. To do so, we browsed four different glioma patient datasets using available online tools and exploited the data related to the information of interest (Table 1). We focused on gene expression data, generated by RNA sequencing of patient-derived residual tumor tissue, obtained after surgical resection. We analyzed the expression of 22 genes encoding for chemokine receptors, namely CC receptors 1 to 10 (CCR1-10), CX3C receptor 1 (CX3CR1), CXCR receptors 1 to 6 (CXCR1-6), XC receptor 1 (XCR1) and the atypical chemokine receptors ACKR1 (or DARC), ACKR2 (or D6), ACKR3 (or CXCR7/RDC1) and ACKR4 (or CCRL1). The alternative gene names were used when required by the online platform. Original publications, online tools, RNA sequencing method as well as number of samples and patients included in the datasets are listed in Table 1. No recalculation nor modification of the existing data was performed. Figures included in this manuscript are either original heat maps displaying the unchanged data downloaded from the databases or were directly generated on the online platforms (for scRNAseq data).

Table 1. General information about the datasets used in the review.

	1	2	3	4
Publication, project	[25] The Cancer Genome Atlas (TCGA) Project	[26] Ivy Glioblastoma Atlas Project	[27]	[7]
Selected information	Gene expression in three glioma subgroups (correlated with severity)	Gene expression in five anatomical locations within GBM tumors	Gene expression in 4 different glioma-related cell subtypes	Gene expression in 7 different glioma-related cell subtypes
Online tool	http://gliovis.bioinfo.cnio.es [28] (accessed on 23 November 2021).	https://glioblastoma.alleninstitute.org (accessed on 23 November 2021).	http://gbmseq.org/ (accessed on 23 November 2021).	https://singlecell.broadinstitute.org/single_cell/study/SCP393/ (accessed on 23 November 2021).
Method	Bulk RNAseq (HiSeq)	Bulk RNAseq (HiSeq) after laser microdissection	Single cell RNAseq (NextSeq)	Single-cell RNAseq (SMART-Seq2)
Datasets, number of samples and patients	Brain lower grade glioma, LGG (513 patients) Glioblastoma, GBM (154 patients)	Glioblastoma (122 samples/ 10 patients)	Glioblastoma (3589 cells/ 4 patients)	Adult and pediatric glioblastoma (IDHwt) (7930 cells/28 patients)
Data expressed as	Log2 RSEM	Log2 RSEM	Log2 CPM	Log TPM

Legend: CPM: counts per million; IDHwt: IDH wild-type; RNAseq: RNA sequencing; RSEM: RNA-Seq by expectation maximization; TPM: transcripts per million.

3. Chemokine Receptor Expression in Gliomas

We first aimed to highlight which chemokine receptors are most abundantly expressed in gliomas. We unraveled the expression of 22 chemokine receptors in tumor tissue collected from newly diagnosed diffuse glioma patients using the TCGA LGG-GBM dataset (including 513 low-grade gliomas (LGG) and 154 GBM diagnosed patients with available RNAseq data). In an attempt to relate gene expression to glioma clinical subgroups associated with respective disease severity, we classified patients based on isocitrate dehydrogenase (IDH) mutation and 1p/19q co-deletion status, as these features were previously suggested to correlate with histological types and clinical grades. We therefore consider “IDH mutant 1p19q code1” gliomas as oligodendrogliomas, “IDH mutant 1p19q non code1” gliomas as enriched in low grade astrocytomas, “IDH wt” gliomas as enriched in high grade astrocytomas and glioblastomas [29,30] (Figure 1). Note that such enrichment does not imply the exclusivity of a group for a given histological assessment.

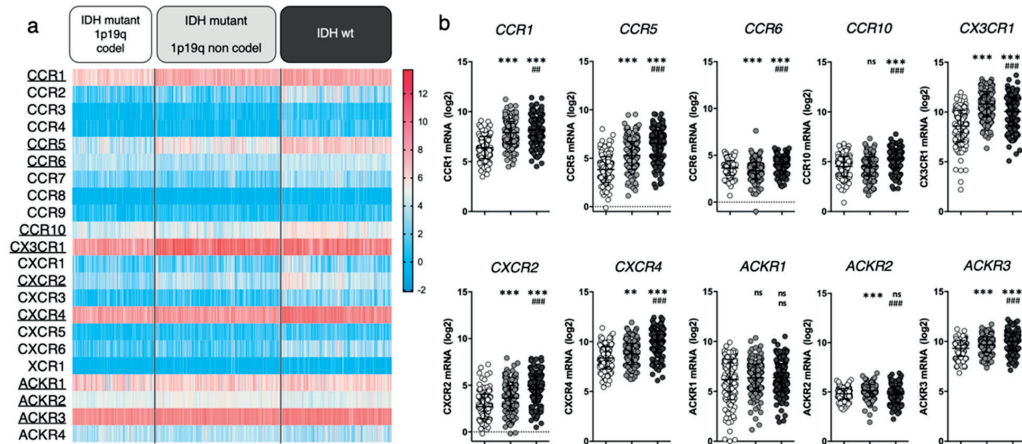


Figure 1. Chemokine receptor expression in glioma patients (TCGA LGG-GBM dataset [25], GlioVis platform²⁵). (a) Heatmap displaying log₂ RSEM value for the 22 receptors of interest. Each cell represents one patient. The receptors that will be highlighted in this review are underlined. (b) For every receptor, log₂ RSEM values were grouped into 3 categories (based on glioma genomic features). Each dot represents one patient. Data are downloaded from <http://gliovis.bioinfo.cnio.es> (accessed on 23 November 2021), data are represented as Mean \pm SD, and analyzed via one-way ANOVA (vs. “IDHmut 1p19q codelet”: ** $p < 0.01$; *** $p < 0.001$ and vs. “IDHmut 1p19q non codelet”: ### $p < 0.01$; ### $p < 0.001$).

We here highlighted CCR1, CCR5, CCR6, CCR10, CX3CR1, CXCR2, CXCR4, ACKR1, ACKR2 and ACKR3 based on their average mRNA expression within at least one patient subgroup (threshold arbitrarily placed at average RSEM ≥ 4). For most of the selected receptors, mRNA expression increases with glioma grade. Note that we do not rule out that unselected receptors may yet be of interest. We will therefore focus this manuscript on these ten chemokine receptors and unravel relevant literature data to further discuss their respective contribution to glioma biology.

In the last two decades [31], extensive evidence has proven CXCR4 as significantly related to glioma malignancy [32–34]. Its crucial contribution to the disease is supported by the phase I/II clinical testing of CXCR4 inhibitors for GBM treatment (e.g., plerixafor) [35,36], as further discussed in Section 4.1. The clinical relevance of the other selected chemokine receptors is supported by more or less abundant (pre)clinical data from the literature, which mostly analyzed mRNA/protein expression in glioma tissue sample cohorts (vs control tissue samples) and related these to tumor grade and patient survival. Among the receptors that appear highly expressed in all gliomas, CX3CR1 is a macrophage associated receptor, whose expression has been shown similar in patient tissue from both low and high grade gliomas [37,38], substantiating the TCGA data in Figure 1. Of note, a specific CX3CR1 defective polymorphism (V249I) correlates with increased patient survival in patients with GBM [39] and LGG [40], stressing its important role in tumor maintenance. ACKR3, formerly known as CXCR7/RDC1, has also been investigated in glioma patient tissue where its expression pattern appears quite inconstant: several studies highlight an increased mRNA expression in GBM tissue samples compared to non-malignant brain samples [41,42], while other studies do not [43]. Moreover, TCGA data show CCR1 expression in glioma samples. Although this has not been exhaustively documented in patient tissue thus far, insights in CCR1 activity in glioma are currently emerging (see Section 4). In comparison to the above-cited receptors, CCR5, CCR6, CCR10 and CXCR2 all display moderate expression in glioma patients from TCGA database. Their expression in tumor tissue has been assessed in diverse studies and was found upregulated in glioma (compared to non-tumor samples), correlating with the tumor grade as well as with shorter

disease-free and overall patient survival [44–47]. Higher expression of CCR5 and CXCR2 has also been associated with recurrent tumors [48,49]. The roles of ACKR1 and ACKR2 in tumor growth have also been evaluated in other cancer types [50,51] where their expression has been correlated with a reduced tumor growth and survival benefit (reviewed in [15,52]). However, the role of these atypical receptors in gliomagenesis remains to be elucidated.

4. Chemokine Receptors in Glioma Malignant Processes

GBM is an extremely heterogeneous tumor, endowed with high invasive capacity, harboring hypoxic areas, necrotic and proangiogenic environments. Such heterogeneity complicates GBM treatment and constitutes an immense challenge for neuro-oncologists. The Ivy Glioblastoma Atlas Project (IvyGAP) has addressed this intra- and inter-tumoral heterogeneity by correlating anatomic-histological features with gene expression data in a panel of GBM patients [26]. In this study, five separate areas were analyzed after laser microdissection: (1) leading edge (LE), outermost boundary of the tumor; (2) infiltrating tumor compartment (IT), intermediate zone; (3) cellular tumor (CT), core part of the tumor with high ratio of tumor cells vs. healthy cells; (4) pseudopalisading cells around necrosis (PAN), densely aligned tumor cells surrounding necrotic areas; (5) microvascular proliferation (MVP) marked by two or more blood vessels. This freely accessible anatomic-transcriptional atlas provides a valuable ground to interrogate gene function in GBM growth processes. Here, we utilize this IvyGAP resource to look at the expression of the selected chemokine receptors in these five regions of interest and further decipher their activity in these specific regions (Figure 2).

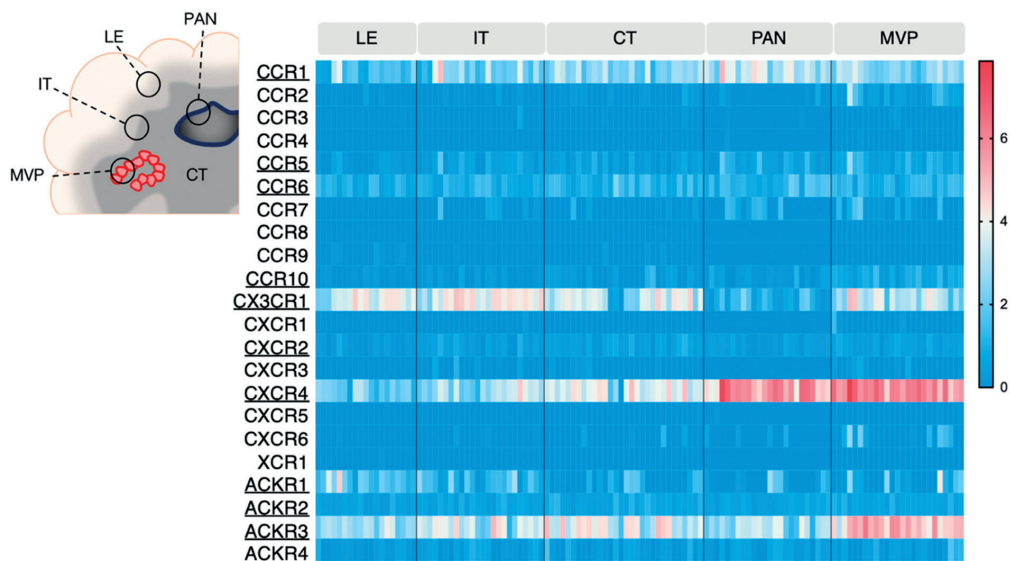


Figure 2. Chemokine receptor expression in various areas of GBM tumors (IvyGAP project). The heatmap displays log₂ RSEM value for each receptor, in the various tumor subregions. Each cell represents one sample. Legend: LE: leading edge; IT: infiltrative tumor; CT: cellular tumor; PAN: pseudopalisading cells around necrosis; MVP: microvascular proliferation. Data is downloaded from <https://glioblastoma.alleninstitute.org> (accessed on 23 November 2021).

CXCR4 once again stands out as highly expressed in the pseudopalisading cells around necrosis (PAN) and microvascular proliferation (MVP) regions, respectively described as related to hypoxia and angiogenesis/immune regulation [26]. ACKR3 also appears associated with MVP regions. Additionally, these two receptors are detected in the central tumor (CT), infiltrative tumor (IT) and leading edge (LE) regions, where their contribution

could be of variable nature (see Sections 4.1–4.3). CX3CR1 and CCR1 are also expressed and distributed in all tested regions. CCR5, CCR6, CCR10, CXCR2, ACKR1 and ACKR2 display moderate expression in GBM samples, regardless of the area, which is in line with the TCGA data from Figure 1.

Using a similar approach, another study described chemokine receptor profiling in different GBM subregions [53], which were isolated after 5-aminolevulinic acid (5-ALA) fluorescence-guided surgery of six newly diagnosed GBM patients [54]. GBM cells were isolated from the tumor core (strong fluorescence, ALA+), infiltrating area (pale fluorescence, ALA-PALE) and healthy tissue (no fluorescence, ALA-). CXCR4 and ACKR3 were found upregulated in tumor core GBM cells (without distinction of necrotic and/or angiogenic features) compared to infiltrating area and healthy tissue, which is supportive of the IvyGAP data. Conversely, CCR1 and CCR10 were found upregulated in GBM infiltrating area compared to the tumor core, which suggests a role for these receptors at the margin of the tumor, probably linked to cell invasion or communication with the tumor microenvironment (TME).

The different tumor subregions that were studied in this dataset were defined based on specific anatomopathological features, associated with important GBM-related mechanisms. In the following paragraphs, we will discuss the putative role of chemokine receptors in one or several key tumor processes that could be related to their expression in the aforementioned tumor areas.

4.1. Angiogenesis

Angiogenesis is an important feature of high-grade gliomas, supporting tumor cell survival and invasion [55]. In line with the IvyGAP analysis of chemokine receptor expression in MVP and PAN regions, studies have demonstrated that CXCR4 is largely expressed in endothelial cells of the normal brain, as well as in GBM blood vessels and hypoxic areas of necrosis [42]. CXCR4 is enriched in highly vascularized GBM tissue [56] and its role in hypoxia-induced angiogenesis has been widely documented [31,57]. CXCR4 inhibition using plerixafor was therefore proposed in combination with bevacizumab (anti-vascular endothelial growth factor monoclonal antibody) for diminishing resistance to this anti-angiogenic therapy and has thus far proven safe in patients with high-grade gliomas [36]. ACKR3 is also found in endothelial cells as well as in tumor cells and microglia in GBM patient tissue specimens [42,58]. Moreover, a role for ACKR3 in tumor neovascularization has been suggested using in vitro models of tube formation with glioma endothelial cells [59], breast cancer cells [60] or human umbilical vein endothelial cells [61]. In glioma cells, ACKR3 expression appears upregulated in hypoxic conditions [62]. Given the discernible expression of ACKR3 in MVP areas of GBM tumors, its contribution to the angiogenic mechanisms in glioma patients and its interplay with CXCR4 definitely warrant further investigation. Although less prominently expressed in the MVP region based on the IvyGAP data, CXCR2 has also been associated with neovascularization. It colocalizes with blood vessels in GBM patient tissue and functionally helps GBM cells to transdifferentiate and acquire an endothelial-like phenotype, inducing vascular mimicry [47]. Finally, a co-culture model of glioma cells with normal astrocytes suggests that astrocyte-mediated production of CCL20 facilitates CCR6-expressing GBM cell adaptation to hypoxic TME via upregulation of hypoxia-inducible factor 1-alpha (HIF1- α). In particular, xenografts lacking CCR6 showed an impaired vascularization and reduced adaptability to hypoxic stress, supporting a role for this axis in GBM [63].

4.2. GBM Cell Migration and Invasion

Although not extremely prominent, several of the selected receptors are expressed at the invasive front of the tumor, which may suggest their involvement in GBM cell incursion through the brain parenchyma. CXCR4 expression has been associated with the extent of tumor cell dissemination within the patient brain (based on tumor imaging features) [34]. Preclinical models of gliomas highlighted its role in mediating cell migration

and invasion [64,65], especially in the migration of specific “stem-like” cell subsets (see Section 4.3). In contrast, the activity of ACKR3 in glioma cell motility remains elusive and its function in the invasion of other cancer cell types is still a matter of debate. Indeed, in head and neck squamous cell carcinoma patients, ACKR3 expression has been associated with increased lymph node metastasis rate [66] and the relationship between CXCR4 and ACKR3 has also been linked to increased breast cancer metastasis in experimental models [67]. Contrasting results rather propose that CXCR4 and ACKR3 have distinct roles. CXCR4 seems to enhance cell invasiveness, while ACKR3 appears to be mainly associated with decreased invasive properties as well as inhibition of metastasis. ACKR3 is also suggested to promote tumor growth by stimulating angiogenesis [68].

Experimental data indicate that CCR5 and CXCR2 are involved in glioma cell invasion through tridimensional environments, when induced by co-cultured human mesenchymal stem cells [48,69] or endothelial cells [70] that were shown to secrete key chemokines. Hence, these receptors may play a role in GBM cell invasion through brain tissue.

4.3. GBM “Stem” Cell Properties and Resistance to Treatment

GBM progenitor/initiating/stem cell phenotype characterizes the self-renewing and plastic cell population within the tumor that sustains tumor growth and promotes resistance to treatment. Hence, significant efforts have been undertaken to specifically target these glioma stem cells (GSCs) (reviewed in [71]). GSCs have been associated with specific “vascular niches” within tumors [72], but also have been shown to be enriched in the cellular tumor (based on the IvyGAP data) [73]. CXCR4 was detected in cells expressing stem cell-associated markers (e.g., SOX2, KLF4, OCT4, NANOG) in both primary and recurrent GBM patient tissue sections [74]. Additionally, CXCR4 expression was found in patient-derived GSC primary cultures in vitro, where the receptor was implicated in cell survival, self-renewal and invasion upon xenografting [75–77]. Specifically, we previously showed that after orthotopic implantation, GSCs migrated toward the subventricular zone in an oriented, CXCR4-mediated fashion [78], which was associated with GSC protection from radiation therapy [79]. In contrast, only a minor subset of stem-like cells were found positive for ACKR3 in GBM patient tissue [74] and less information is available from in vitro patient-derived models. A study using selective ACKR3 modulators emphasized the involvement of ACKR3 in GSC growth in vitro together with CXCR4, although this report revealed that GSC tumor formation in vivo was independent of CXCR4 or ACKR3 activity [80]. Aside from sustaining tumor initiation, GSCs were shown to determine GBM cell response to therapy and were particularly suggested as crucial for the resistance to temozolomide (TMZ) [81]. A recent study has demonstrated that CXCR2 expression increased in patient-derived GSCs (expressing CD133, another stem cell-associated marker) upon treatment with TMZ in vitro. Activation of CXCR2-related pathways was indeed associated with alterations in the epigenomic landscape of cells, which impact GBM cell plasticity and resistance to TMZ [82]. Furthermore, CCR5 has been linked to TMZ resistance. Pericytes secrete CCL5 which activates CCR5 and downstream pathways in GBM cells. This leads to the activation of DNA damage response and thus reduces the efficiency of TMZ in killing GBM cells [83].

5. Chemokine Receptors in Diverse GBM Cell Subtypes

As mentioned above, the intratumoral heterogeneity of gliomas is largely accountable for therapeutic failure. Over the last years, the emergence of single-cell profiling technologies has deepened our understanding of glioma biology and the tumor heterogeneity that outreaches the anatomical level. Single-cell RNA sequencing is an advanced tool to decrypt the individual role of the different cell types forming the tumor, it allows to investigate the glioma heterogeneity at single-cell resolution. Several recent studies have shed light on the diverse malignant and non-malignant cell types that together compose gliomas and dictate their development, maintenance and response to therapy [6,7,27,84,85]. In high-grade gliomas, over a third of the tumor mass is constituted of non-malignant cells.

The TME includes neuronal and glial cells, macrophage/microglial cells, representing the major immune cells component, endothelial cells and a low number of T cells [86].

Within the tumor, malignant/neoplastic cells were distinguished from non-malignant TME cell types using inferred copy-number alterations, and specific cell clusters were further categorized into TME subtypes based on their gene expression profile (for more detailed information, please refer to the original publications [7,27]). In the process of deciphering chemokine receptor function in gliomas, we explored two publicly available single-cell RNAseq datasets obtained from glioma patient tissue [7,27]. We looked into the expression of CCR1, CCR5, CCR6, CCR10, CX3CR1, CXCR2, CXCR4, ACKR1, ACKR2 and ACKR3 in the various cell type-related signatures that were reported (Figure 3).

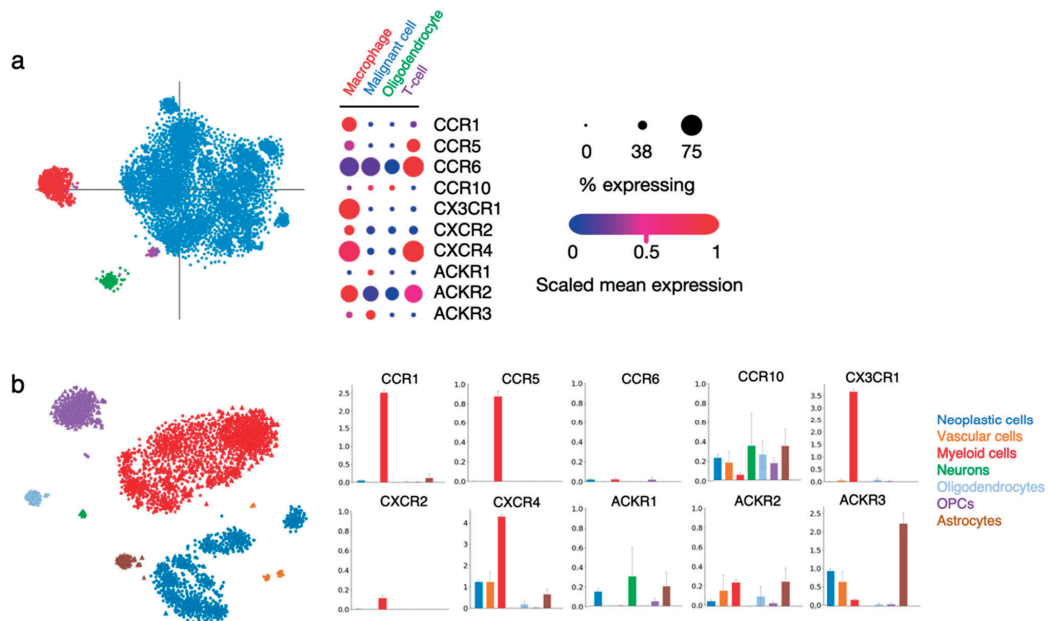


Figure 3. Chemokine receptor expression in various cell types within patient glioma samples. (a) Single cell RNAseq data from Neftel et al. (2019, Cell) [7] show the expression of the ten selected receptors in cells regrouped in four specific annotations (macrophage, malignant cell, oligodendrocyte and T-cell). The “% expressing” value indicates the proportion of cells in the signature that are positive for a given transcript, and the “scaled mean expression” is relative to each gene’s expression level (logTPM) across all cells within the signature (https://singlecell.broadinstitute.org/single_cell/study/SCP393/ (accessed on 23 November 2021)). (b) Single-cell RNAseq data from Darmanis et al. (2017, Cell Reports) [27] show the expression of the ten receptors of interest in cells regrouped in seven specific annotations (neoplastic cells, vascular cells, myeloid cells, neurons, oligodendrocytes, oligodendrocyte precursor cells (OPCs) and astrocytes). Bar plots indicate log2CPM values (<http://www.gbmseq.org/> (accessed on 23 November 2021)).

In both datasets, CCR1 and CX3CR1 expression strongly correlated with the “macrophage” and “myeloid cell” signatures, while the two receptors were virtually absent from other cell types, unsurprisingly pointing to their key role in immune cell recruitment and function in gliomas. A high expression of CCR5 and moderate expression of CXCR2 is found in the same groups. CCR5 expression is also detected in the minor population of “T-cells”, as well as CCR6. CXCR4 is abundantly present in cells assigned to the “macrophage” and “myeloid cell” signatures, as well as in “vascular cells” and “neoplastic cells”, which is in line with the various roles of this receptor in diverse tumor-related processes. ACKR3 is detected in “neoplastic cells” and “vascular cells”, again supporting the data obtained from

GBM patient tissue specimens [42,58]. Of note, this receptor is also abundantly expressed in “astrocytes” present in the tumor tissue. CCR10, ACKR1 and ACKR2 could be detected in different cell types at low level. The current knowledge on the function of these receptors in the respective cell entities will be further discussed in the following sections.

5.1. Tumor-Associated Macrophages (TAMs)

We previously mentioned that glioma TME largely contributes to the tumor bulk and influences tumor cell maintenance and growth. Tumor-associated macrophages (TAMs) derive from bone marrow circulating monocytes or from resident microglial cells and affect glioma progression in diverse manners depending on their activation status, interaction with TME components, phenotype or location within the tumor (reviewed in [87]). Thus far, TAMs are generally considered as supportive of GBM growth. CX3CR1-mediated macrophage infiltration into gliomas has been confirmed in patient tissue [88]. In GBM and LGG patients carrying the defective CX3CR1 V249I polymorphism [39,40], such infiltration is reduced which is associated with better prognosis.

Recently, a study investigated the single-cell transcriptome of multi-sector biopsies from 13 glioma patients (with various WHO grades) [89]. These data were used to reconstruct a ligand–receptor interaction map describing the most relevant chemoattractant relationships existing between tumor cells and TAMs in glioma TME. Nine chemokine receptors were detected in the 13 tumors, including CCR5, CCR6, CX3CR1, CXCR2 and CXCR4. This study reported that glioma cells overexpress CX3CL1, which is responsible for the recruitment of CX3CR1-expressing microglia and macrophages. CCR5 and CXCR4 were found on TAMs as well.

5.2. Tumor-Infiltrating Lymphocytes (TILs) and Other Immune Cell Types

Generally, gliomas are recognized as “cold” tumors endowed with poor immune response, where glioma cells expressing diverse immune checkpoint molecules (e.g., PD-L1) that hamper immune cell activation. Moreover, tumor infiltrating lymphocytes (TILs) poorly penetrate tumors, among which regulatory lymphocytes (T_{reg}) secrete immunosuppressive cytokines (IL10 and TGF- β) and cytotoxic T cells exhibit a specific exhaustion profile (expression of PD-1 and CTLA4). In addition to the extensive glioma heterogeneity, such immune suppressive environment makes glioma refractory to targeted immunotherapy [90]. Literature data suggest that the level of TILs varies between different glioma genomic subtypes, with high grade (IDHwt) gliomas showing the highest TIL amount and the worse prognosis [91,92]. This encourages to (1) consider genomic profiles for predicting response to immunotherapy and (2) better understand and modulate TIL function and access to the tumor. To that purpose, regulating chemokine receptor function is of interest. The aforementioned report on GBM single-cell transcriptome confirmed that TILs express CCR6 (corroborating the data from Figure 3), as well as CCR5 and CXCR4, which all could contribute to lymphocyte recruitment toward the tumor [89].

Other immune-related cell types such as neutrophils, dendritic cells, myeloid progenitors and hematopoietic stem cells could also be found in gliomas [86,93] and their roles in glioma development and response to therapy are still under investigation. The recent literature provides pieces of information regarding the activity of chemokine receptors in these subsets. Early studies of TME in mouse models allowed to identify immature and immune-suppressive myeloid cells within solid tumors, which were called myeloid-derived suppressor cells (MDSCs) (likely encompassing diverse cell entities). Although efforts are currently carried out to standardize nomenclature and characterization of these cells, the MDSC term is still often used. MDSCs isolated from glioma patient tissue could be classified in monocytic (M-MDSCs) and granulocytic subsets (G-MDSCs). G-MDSCs presented increased CXCR2 expression but showed minor accumulation in the tumors compared to M-MDSCs [94]. Accordingly, CXCR2 was associated with neutrophils in the aforementioned single cell mapping of glioma TME components [89]. Of note, the degree of neutrophil infiltration has been positively correlated with glioma severity [95,96].

Efforts still have to be carried out to decipher the functional aspects of the complex glioma-associated immune orchestra to eventually shed new light on effective treatment options, which could rely on the modulation of chemokine-mediated immune cell recruitment to the tumors.

5.3. Vascular Cells

Endothelial cells from brain capillaries, as well as contiguous pericytes and astrocytic feet, are key components of the blood-brain barrier (BBB), which constitutes a selective filter that tightly regulates brain penetration of a variety of molecules and compounds. The integrity of this BBB is compromised in brain tumors [97], and endothelial cells exhibit various molecular alterations that reflect on their dysfunction, anatomical location, and variable permeability [98]. The expression of chemokine receptors in endothelial cells from glioma tissue has been detailed in Section 4.1 together with their role in angiogenesis. The implication of CXCR4 and ACKR3 in this process has particularly been documented. However, CXCR4 and ACKR3 expression is not specific to glioma-associated endothelial cells, and both receptors are also detected in endothelial cells from the developing brain [99] or from the adult brain [100]. A recent study developed an ACKR3 knock-in mouse model and highlighted ACKR3 expression in the cerebral vasculature, distributed across various brain structures [101], thus stressing a role of this atypical chemokine receptor in brain physiology that deserves deeper investigation.

Pericytes also play a pivotal role in the BBB maintenance. In GBM, pericytes exhibit specific genetic alterations. They mostly derive from GBM stem cells, which are recruited to blood vessels via CXCL12/CXCR4-mediated axis and evolve toward pericytes that contribute to vascular niche remodeling [102] and modulate GBM cell activity. Pericytes secrete CCL5, which binds the CCR5 receptor expressed by GBM cells. This interaction triggers the activation of the DNA damage response, thereby overcoming TMZ-induced cell death. Inhibiting CCL5/CCR5 signaling abrogates the protective effects of pericytes against GBM and improves the efficacy of TMZ [83].

5.4. Non-Malignant Glial Cells and Neurons

As shown in Figure 3, ACKR3 as well as CXCR4 appear to be expressed also in non-malignant brain cells, notably in astrocytes. A study previously reported the presence of ACKR3 in adult rat astrocytes and further showed that its expression increases upon non-cancerous, neuroinflammatory conditions. ACKR3 is also detected in human astrocytes from the brain cortex and hippocampus and in oligodendrocytes and oligodendrocyte precursor cells (OPCs) [103]. In addition, preclinical models have shown the physiological role of ACKR3 in adult neuron physiology [104] and during development [105,106]. Overall, aside from the expression of ACKR3 and CXCR4 in glioma cells as well as in multiple cell subtypes from the TME, it appears that cell components of the neighboring healthy brain tissue require ACKR3 and CXCR4 for their maintenance and function, which could complexify their targeting in GBM therapy. Similarly, CCR10 and ACKR2 were also found to be expressed in astrocytes, albeit at lower level than ACKR3, while a small population of oligodendrocytes and OPCs express CCR6, CCR10 and ACKR2.

6. Conclusions

Gliomas are tumors of the central nervous system that remain associated with dismal prognosis in spite of innovative diagnostic strategies and modern therapies. Chemokines and their receptors play crucial roles in glioma development and progression and therefore constitute attractive candidates for targeted treatment. However, although their implication and targeting in *in vitro* and *in vivo* rodent models are well documented, especially for CXCR4 and ACKR3, their clinical relevance requires confirmation with patient data and biological material. Further analysis in terms of brain region distribution and by cell type enrichment is also necessary to better understand the complex roles of chemokine receptors within the highly diversified glioma landscape.

We found an overall good coverage and concordance of the different datasets used for the present analysis and congruence with targeted reports from the literature describing patient-derived material (Table 2). In this study, we focused on CCR1, CCR5, CCR6, CCR10, CX3CR1, CXCR2, CXCR4, ACKR1, ACKR2 and ACKR3, whose expression is detected in patient glioma tissue and rather well correlated with disease severity. With the aim of shedding light on chemokine receptor function in glioma physiopathology, this analysis integrated data from (1) publicly available bulk and single-cell transcriptomic datasets providing various types of information together with (2) evidence from the literature.

Table 2. Summary of chemokine receptor function in GBM tumorigenic processes and in GBM cell subtypes. Legend: TAMs: tumor-associated macrophages; TILs: tumor-infiltrating lymphocytes; **IV**: evidence from in vitro experiments (GSCs and others); **P**: evidence from patient tissue; **?**: still debated.

Role in	CCR1	CCR5	CCR6	CCR10	CX3CR1	CXCR2	CXCR4	ACKR1	ACKR2	ACKR3
Processes	Angiogenesis		IV			P	P			P
	Invasion		IV			IV	P			?
	Stem cell properties					IV	P			?
	Resistance		IV			IV	P			
Cell types	Tumor cells						P			P
	Vascular cells						P			P
	TAMs/Microglia		P			P	P			
	TILs		P	P			P			
	Neutrophils					P				
	Normal glial cells							P		P

CXCR4 emerged as the most prominent receptor expressed on many different cell types within the tumor and associated with various tumorigenic processes such as angiogenesis, cancer cell invasion and resistance to treatment. This review also highlights ACKR3 as a multifaceted player in almost every of these glioma-related cellular processes and subtypes and prompts researchers in the field to further apprehend the subtleties of the CXCR4/ACKR3/CXCL12 triad in glioma. The importance of the CXCL12/CXCR4//ACKR3 axis in GBM is emphasized by multiple efforts toward the clinical translation of related inhibitors largely validated at the preclinical level [32,36,107–109]. A phase I/II clinical trial (NCT04121455) is currently investigating the impact of the CXCL12 inhibitor olaptese pegol or NOX-A12 as part of combination therapy with radiation therapy and bevacizumab. Another phase I/II trial (NCT01977677), aiming at studying the safety and efficacy of the CXCR4 inhibitor plerixafor, after chemo/radiotherapy with the chemotherapeutic agent temozolomide (TMZ), suggests CXCR4-targeting as beneficial for patient survival and local control of tumor recurrence [35]. Finally, a clinical study (NCT03746080) has been recently initiated to better characterize the use of plerixafor in combination with whole-brain radiation therapy and TMZ.

Other receptors such as CCR5, CCR6, CXCR2 and CX3CR1 were mostly identified for their expression and function in immune cells from the tumor microenvironment. Despite the lack of supporting data from the literature, CCR1, CCR10, ACKR1 and ACKR2 also appear as significantly expressed in glioma tissue and deserve thus deeper investigation.

Although our study focuses on human classical and atypical chemokine receptors, Herpesviridae-encoded G protein-coupled receptors (GPCRs), homologous to human chemokine receptors, were also proposed to be important players in GBM. For instance, HCMV encodes for four viral GPCRs (US27, US28, UL33 and UL78) among which the oncomodulatory activities of US28 and UL33 have been recently described in GBM models [110–112].

Overall, this review highlights the intricacies of chemokine receptor activity in glioma, from central roles in glioma cells to key functions in TME partners and tumor-associated

vasculature. It also highlights the complex and sometimes opposing roles certain receptors may have in GBM and related TME, making their targeting challenging and the benefits thereof uncertain. Therefore, the present study constitutes a valuable tool to gain awareness on receptor expression and function in GBM, which is fundamental for the development of efficient therapeutic approaches that would have the chemokines-chemokine receptors axis as main target.

Author Contributions: Conceptualization: D.I., G.D., A.C. and V.N.; Investigation: D.I., G.D., M.W. and V.N.; Writing—original draft preparation, D.I., G.D., M.W. and V.N.; Writing—review and editing, B.R., A.L., A.C., M.S. and V.N.; Supervision, B.R., A.L., A.C., M.S. and V.N.; Funding acquisition, B.R., A.C., M.S. and V.N. All authors have read and agreed to the published version of the manuscript.

Funding: This work was supported by the University of Liège, and the Fonds Léon Frédéricq Association, Luxembourg Institute of Health (LIH), Luxembourg National Research Fund (INTER/FNRS grants 20/15084569, and PRIDE 11012546 “NextImmune” and 14254520 “I2TRON”), F.R.S.-FNRS-Télévie (grants 7.4593.19, 7.4529.19 and 7.8504.20). MS and AC are part of the Marie Skłodowska-Curie Innovative Training Networks ONCORNET2.0 “ONCOgenetic Receptor Network of Excellence and Training” (MSCA-ITN-2020-ETN).

Conflicts of Interest: The authors declare no conflict of interest.

References

- Louis, D.N.; Perry, A.; Wesseling, P.; Brat, D.J.; A Cree, I.; Figarella-Branger, D.; Hawkins, C.; Ng, H.K.; Pfister, S.M.; Reifenberger, G.; et al. The 2021 WHO Classification of Tumors of the Central Nervous System: A summary. *Neuro-Oncology* **2021**, *23*, 1231–1251. [[CrossRef](#)]
- Ostrom, Q.T.; Cioffi, G.; Gittleman, H.; Patil, N.; Waite, K.; Kruchko, C.; Barnholtz-Sloan, J.S. CBTRUS Statistical Report: Primary Brain and Other Central Nervous System Tumors Diagnosed in the United States in 2012–2016. *Neuro-Oncology* **2019**, *21*, v1–v100. [[CrossRef](#)] [[PubMed](#)]
- Stupp, R.; Mason, W.P.; van den Bent, M.J.; Weller, M.; Fisher, B.; Taphoorn, M.J.B.; Belanger, K.; Brandes, A.A.; Marosi, C.; Bogdahn, U.; et al. Radiotherapy plus Concomitant and Adjuvant Temozolomide for Glioblastoma. *N. Engl. J. Med.* **2005**, *352*, 987–996. [[CrossRef](#)] [[PubMed](#)]
- Rapp, M.; Baernreuther, J.; Turowski, B.; Steiger, H.-J.; Sabel, M.; Kamp, M. Recurrence Pattern Analysis of Primary Glioblastoma. *World Neurosurg.* **2017**, *103*, 733–740. [[CrossRef](#)]
- de Gooijer, M.C.; Navarro, M.G.; Bernardis, R.; Wurdinger, T.; van Tellingen, O. An Experimenter’s Guide to Glioblastoma Invasion Pathways. *Trends Mol. Med.* **2018**, *24*, 763–780. [[CrossRef](#)]
- Patel, A.P.; Tirosh, I.; Trombetta, J.J.; Shalek, A.K.; Gillespie, S.M.; Wakimoto, H.; Cahill, D.P.; Nahed, B.V.; Curry, W.T.; Martuza, R.L.; et al. Single-cell RNA-seq highlights intratumoral heterogeneity in primary glioblastoma. *Science* **2014**, *344*, 1396–1401. [[CrossRef](#)]
- Neftel, C.; Laffy, J.; Filbin, M.G.; Hara, T.; Shore, M.E.; Rahme, G.J.; Richman, A.R.; Silverbush, D.; Shaw, M.L.; Hebert, C.M.; et al. An Integrative Model of Cellular States, Plasticity, and Genetics for Glioblastoma. *Cell* **2019**, *178*, 835–849.e21. [[CrossRef](#)]
- Dirkse, A.; Golebiewska, A.; Buder, T.; Nazarov, P.V.; Muller, A.; Poovathingal, S.; Brons, N.H.C.; Leite, S.; Sauvageot, N.; Sarkisjan, D.; et al. Stem cell-associated heterogeneity in Glioblastoma results from intrinsic tumor plasticity shaped by the microenvironment. *Nat. Commun.* **2019**, *10*, 1787. [[CrossRef](#)]
- Osswald, M.; Jung, E.; Sahm, F.; Solecki, G.; Venkataramani, V.; Blaes, J.; Weil, S.; Horstmann, H.; Wiestler, B.; Syed, M.; et al. Brain tumour cells interconnect to a functional and resistant network. *Nature* **2015**, *528*, 93–98. [[CrossRef](#)] [[PubMed](#)]
- Venkatesh, H.S.; Morishita, W.; Geraghty, A.C.; Silverbush, D.; Gillespie, S.M.; Arzt, M.; Tam, L.T.; Espenel, C.; Ponnuswami, A.; Ni, L.; et al. Electrical and synaptic integration of glioma into neural circuits. *Nature* **2019**, *573*, 539–545. [[CrossRef](#)]
- Zlotnik, A.; Yoshie, O. The Chemokine Superfamily Revisited. *Immunity* **2012**, *36*, 705–716. [[CrossRef](#)]
- Griffith, J.W.; Sokol, C.L.; Luster, A.D. Chemokines and Chemokine Receptors: Positioning Cells for Host Defense and Immunity. *Annu. Rev. Immunol.* **2014**, *32*, 659–702. [[CrossRef](#)]
- Bachelierie, F.; Ben-Baruch, A.; Burkhardt, A.M.; Combadiere, C.; Farber, J.M.; Graham, G.; Horuk, R.; Sparre-Ulrich, A.H.; Locati, M.; Luster, A.D.; et al. International Union of Basic and Clinical Pharmacology. LXXXIX. Update on the Extended Family of Chemokine Receptors and Introducing a New Nomenclature for Atypical Chemokine Receptors. *Pharmacol. Rev.* **2013**, *66*, 1–79. [[CrossRef](#)] [[PubMed](#)]
- Nibbs, N.; Graham, G. Immune regulation by atypical chemokine receptors. *Nat. Rev. Immunol.* **2013**, *13*, 815–829. [[CrossRef](#)] [[PubMed](#)]
- Sjöberg, E.; Meyrath, M.; Chevigné, A.; Östman, A.; Augsten, M.; Szpakowska, M. The diverse and complex roles of atypical chemokine receptors in cancer: From molecular biology to clinical relevance and therapy. *Adv. Cancer Res.* **2020**, *145*, 99–138. [[PubMed](#)]

16. Murdoch, C.; Finn, A. Chemokine receptors and their role in inflammation and infectious diseases. *Blood* **2000**, *95*, 3032–3043. [[CrossRef](#)] [[PubMed](#)]
17. Nagarsheth, N.; Wicha, M.S.; Zou, W. Chemokines in the cancer microenvironment and their relevance in cancer immunotherapy. *Nat. Rev. Immunol.* **2017**, *17*, 559–572. [[CrossRef](#)]
18. Takacs, G.P.; Flores-Toro, J.A.; Harrison, J.K. Modulation of the chemokine/chemokine receptor axis as a novel approach for glioma therapy. *Pharmacol. Ther.* **2020**, *222*, 107790. [[CrossRef](#)]
19. The Cancer Genome Atlas Research Network. Comprehensive genomic characterization defines human glioblastoma genes and core pathways. *Nature* **2008**, *455*, 1061–1068. [[CrossRef](#)]
20. The GLASS Consortium; Aldape, K.; Verhaak, R.G.W. Glioma through the looking GLASS: Molecular evolution of diffuse gliomas and the Glioma Longitudinal Analysis Consortium. *Neuro-Oncology* **2018**, *20*, 873–884. [[CrossRef](#)]
21. Malmer, B.; Adatto, P.; Armstrong, G.; Barnholtz-Sloan, J.; Bernstein, J.L.; Claus, E.; Davis, F.; Houlston, R.; Il'Yasova, D.; Jenkins, R.; et al. GLIOGENE—An International Consortium to Understand Familial Glioma. *Cancer Epidemiol. Biomark. Prev.* **2007**, *16*, 1730–1734. [[CrossRef](#)]
22. Klein, E.; Hau, A.-C.; Oudin, A.; Golebiewska, A.; Niclou, S.P. Glioblastoma Organoids: Pre-Clinical Applications and Challenges in the Context of Immunotherapy. *Front. Oncol.* **2020**, *10*, 2755. [[CrossRef](#)]
23. Golebiewska, A.; Hau, A.-C.; Stieber, D.; Yabo, Y.A.; Baus, V.; Barthelemy, V.; Klein, E.; Bougnaud, S.; Keunen, O.; et al. Patient-derived organoids and orthotopic xenografts of primary and recurrent gliomas represent relevant patient avatars for precision oncology. *Acta Neuropathol.* **2020**, *140*, 919–949. [[CrossRef](#)]
24. Urbantat, R.M.; Vajkoczy, P.; Brandenburg, S. Advances in Chemokine Signaling Pathways as Therapeutic Targets in Glioblastoma. *Cancers* **2021**, *13*, 2983. [[CrossRef](#)] [[PubMed](#)]
25. Ceccarelli, M.; Barthel, F.; Malta, T.; Sabedot, T.S.; Salama, S.; Murray, B.A.; Morozova, O.; Newton, Y.; Radenbaugh, A.; Pagnotta, S.M.; et al. Molecular Profiling Reveals Biologically Discrete Subsets and Pathways of Progression in Diffuse Glioma. *Cell* **2016**, *164*, 550–563. [[CrossRef](#)]
26. Puchalski, R.B.; Shah, N.; Miller, J.; Dalley, R.; Nomura, S.R.; Yoon, J.-G.; Smith, K.A.; Lankerovich, M.; Bertagnolli, D.; Bickley, K.; et al. An anatomic transcriptional atlas of human glioblastoma. *Science* **2018**, *360*, 660–663. [[CrossRef](#)] [[PubMed](#)]
27. Darmanis, S.; Sloan, S.A.; Croote, D.; Mignardi, M.; Chemikova, S.; Samghababi, P.; Zhang, Y.; Neff, N.; Kowarsky, M.; Caneda, C.; et al. Single-Cell RNA-Seq Analysis of Infiltrating Neoplastic Cells at the Migrating Front of Human Glioblastoma. *Cell Rep.* **2017**, *21*, 1399–1410. [[CrossRef](#)]
28. Bowman, R.L.; Wang, Q.; Carro, A.; Verhaak, R.G.W.; Squatrito, M. GlioVis data portal for visualization and analysis of brain tumor expression datasets. *Neuro-Oncology* **2017**, *19*, 139–141. [[CrossRef](#)] [[PubMed](#)]
29. Eckel-Passow, J.E.; Lachance, D.H.; Molinaro, A.M.; Walsh, K.M.; Decker, P.A.; Sicotte, H.; Pekmezci, M.; Rice, T.W.; Kosel, M.L.; Smirnov, I.V.; et al. Glioma Groups Based on 1p/19q, IDH, and TERT Promoter Mutations in Tumors. *N. Engl. J. Med.* **2015**, *372*, 2499–2508. [[CrossRef](#)] [[PubMed](#)]
30. The Cancer Genome Atlas Research Network. Comprehensive, Integrative Genomic Analysis of Diffuse Lower-Grade Gliomas. *N. Engl. J. Med.* **2015**, *372*, 2481–2498. [[CrossRef](#)]
31. Rempel, S.A.; Dudas, S.; Ge, S.; Gutiérrez, J.A. Identification and localization of the cytokine SDF1 and its receptor, CXCR4 chemokine receptor 4, to regions of necrosis and angiogenesis in human glioblastoma. *Clin. Cancer Res.* **2000**, *6*, 102–111. [[PubMed](#)]
32. Rubin, J.B.; Kung, A.L.; Klein, R.S.; Chan, J.A.; Sun, Y.; Schmidt, K.; Kieran, M.W.; Luster, A.D.; Segal, R.A. A small-molecule antagonist of CXCR4 inhibits intracranial growth of primary brain tumors. *Proc. Natl. Acad. Sci. USA* **2003**, *100*, 13513–13518. [[CrossRef](#)]
33. Woerner, B.M. Widespread CXCR4 Activation in Astrocytomas Revealed by Phospho-CXCR4-Specific Antibodies. *Cancer Res.* **2005**, *65*, 11392–11399. [[CrossRef](#)]
34. Stevenson, C.B.; Ehteshami, M.; McMillan, K.M.; Valadez, J.G.; Edgeworth, M.L.; Price, R.R.; Abel, T.W.; Mapara, K.Y.; Thompson, R.C. CXCR4 Expression is Elevated in Glioblastoma Multiforme and Correlates with an Increase in Intensity and Extent of Peritumoral T2-weighted Magnetic Resonance Imaging Signal Abnormalities. *Neurosurgery* **2008**, *63*, 560–570. [[CrossRef](#)] [[PubMed](#)]
35. Thomas, R.P.; Nagpal, S.; Iv, M.; Soltys, S.G.; Bertrand, S.; Pelpola, J.S.; Ball, R.; Yang, J.; Sundaram, V.; Lavezo, J.; et al. Macrophage Exclusion after Radiation Therapy (MERT): A First in Human Phase I/II Trial using a CXCR4 Inhibitor in Glioblastoma. *Clin. Cancer Res.* **2019**, *25*, 6948–6957. [[CrossRef](#)]
36. Lee, E.Q.; Duda, D.G.; Muzikansky, A.; Gerstner, E.R.; Kuhn, J.G.; Reardon, D.A.; Nayak, L.; Norden, A.D.; Doherty, L.; LaFrankie, D.; et al. Phase I and Biomarker Study of Plerixafor and Bevacizumab in Recurrent High-Grade Glioma. *Clin. Cancer Res.* **2018**, *24*, 4643–4649. [[CrossRef](#)] [[PubMed](#)]
37. Erreni, M.; Solinas, G.; Brescia, P.; Osti, D.; Zunino, F.; Colombo, P.; Destro, A.; Roncalli, M.; Mantovani, A.; Draghi, R.; et al. Human glioblastoma tumours and neural cancer stem cells express the chemokine CXCL1 and its receptor CX3CR1. *Eur. J. Cancer* **2010**, *46*, 3383–3392. [[CrossRef](#)]
38. Locatelli, M.; Boiocchi, L.; Ferrero, S.; Boneschi, F.M.; Zavanone, M.; Pesce, S.; Allavena, P.; Gaini, S.M.; Bello, L.; Mantovani, A. Human glioma tumors express high levels of the chemokine receptor CX3CR1. *Eur. Cytokine Netw.* **2010**, *21*, 27–33. [[CrossRef](#)]
39. Rodero, M.; Marie, Y.; Coudert, M.; Blondet, E.; Mokhtari, K.; Rousseau, A.; Raoul, W.; Carpentier, C.; Sennlaub, F.; Deterre, P.; et al. Polymorphism in the Microglial Cell-Mobilizing CX3CR1 Gene Is Associated With Survival in Patients With Glioblastoma. *J. Clin. Oncol.* **2008**, *26*, 5957–5964. [[CrossRef](#)] [[PubMed](#)]

40. Lee, S.; Latha, K.; Manyam, G.; Yang, Y.; Rao, A.; Rao, G. Role of CX3CR1 signaling in malignant transformation of gliomas. *Neuro-Oncology* **2020**, *22*, 1463–1473. [[CrossRef](#)]
41. Madden, S.L.; Cook, B.P.; Nacht, M.; Weber, W.D.; Callahan, M.R.; Jiang, Y.; Dufault, M.R.; Zhang, X.; Zhang, W.; Walter-Yohrling, J.; et al. Vascular Gene Expression in Nonneoplastic and Malignant Brain. *Am. J. Pathol.* **2004**, *165*, 601–608. [[CrossRef](#)]
42. Hattermann, K.; Held-Feindt, J.; Lucius, R.; Mürköster, S.S.; Penfold, M.E.; Schall, T.J.; Mentlein, R. The Chemokine Receptor CXCR7 Is Highly Expressed in Human Glioma Cells and Mediates Antiapoptotic Effects. *Cancer Res.* **2010**, *70*, 3299–3308. [[CrossRef](#)] [[PubMed](#)]
43. Calatozzolo, C.; Canazza, A.; Pollo, B.; Di Pierro, E.; Ciusani, E.; Maderna, E.; Salce, E.; Sponza, V.; Frigerio, S.; Di Meco, F.; et al. Expression of the new CXCL12 receptor, CXCR7, in gliomas. *Cancer Biol. Ther.* **2011**, *11*, 242–253. [[CrossRef](#)] [[PubMed](#)]
44. Zhao, L.; Wang, Y.; Xue, Y.; Lv, W.; Zhang, Y.; He, S. Critical roles of chemokine receptor CCR5 in regulating glioblastoma proliferation and invasion. *Acta Biochim. Biophys. Sin.* **2015**, *47*, 890–898. [[CrossRef](#)] [[PubMed](#)]
45. Wang, L.; Qin, H.; Li, L.; Zhang, Y.; Tu, Y.; Feng, F.; Ji, P.; Zhang, J.; Li, G.; Zhao, Z.; et al. Overexpression of CCL20 and its receptor CCR6 predicts poor clinical prognosis in human gliomas. *Med. Oncol.* **2012**, *29*, 3491–3497. [[CrossRef](#)]
46. Chen, L.; Liu, X.; Zhang, H.-Y.; Du, W.; Qin, Z.; Yao, Y.; Mao, Y.; Zhou, L. Upregulation of chemokine receptor CCR10 is essential for glioma proliferation, invasion and patient survival. *Oncotarget* **2014**, *5*, 6576–6583. [[CrossRef](#)] [[PubMed](#)]
47. Angara, K.; Borin, T.F.; Rashid, M.H.; Lebedyeva, I.; Ara, R.; Lin, P.-C.; Iskander, A.; Bollag, R.J.; Achyut, B.R.; Arbab, A.S. CXCR2-Expressing Tumor Cells Drive Vascular Mimicry in Antiangiogenic Therapy-Resistant Glioblastoma. *Neoplasia* **2018**, *20*, 1070–1082. [[CrossRef](#)]
48. Novak, M.; Krajnc, M.K.; Hrastar, B.; Breznik, B.; Majc, B.; Mlinar, M.; Rotter, A.; Porčnik, A.; Mlakar, J.; Stare, K.; et al. CCR5-Mediated Signaling is Involved in Invasion of Glioblastoma Cells in Its Microenvironment. *Int. J. Mol. Sci.* **2020**, *21*, 4199. [[CrossRef](#)]
49. Liu, M.; Yang, L.; Liu, Z.; Wu, R.; Gu, Z.; Yao, Q. Correlation of C-X-C chemokine receptor 2 upregulation with poor prognosis and recurrence in human glioma. *Oncotargets Ther.* **2015**, *8*, 3203–3209. [[CrossRef](#)]
50. Sjöberg, E.; Meyrath, M.; Milde, L.; Herrera, M.; Lövrot, J.; Hägerstrand, D.; Frings, O.; Bartish, M.; Rolny, C.; Sonnhhammer, E.; et al. A Novel ACKR2-Dependent Role of Fibroblast-Derived CXCL14 in Epithelial-to-Mesenchymal Transition and Metastasis of Breast Cancer. *Clin. Cancer Res.* **2019**, *25*, 3702–3717. [[CrossRef](#)]
51. Wang, J.; Ou, Z.-L.; Hou, Y.-F.; Luo, J.-M.; Shen, Z.-Z.; Ding, J.; Shao, Z.-M. Enhanced expression of Duffy antigen receptor for chemokines by breast cancer cells attenuates growth and metastasis potential. *Oncogene* **2006**, *25*, 7201–7211. [[CrossRef](#)]
52. Morein, D.; Erlichman, N.; Ben-Baruch, A. Beyond Cell Motility: The Expanding Roles of Chemokines and Their Receptors in Malignancy. *Front. Immunol.* **2020**, *11*, 952. [[CrossRef](#)] [[PubMed](#)]
53. Manini, I.; Caponnetto, F.; Dalla, E.; Ius, T.; Pepa, G.; Pegolo, E.; Bartolini, A.; Rocca, G.; Menna, G.; Loreto, C.; et al. Heterogeneity Matters: Different Regions of Glioblastoma Are Characterized by Distinctive Tumor-Supporting Pathways. *Cancers* **2020**, *12*, 2960. [[CrossRef](#)]
54. Stummer, W.; Pichlmeier, U.; Meinel, T.; Wiestler, O.D.; Zanella, F.; Reulen, H.-J. Fluorescence-guided surgery with 5-aminolevulinic acid for resection of malignant glioma: A randomised controlled multicentre phase III trial. *Lancet Oncol.* **2006**, *7*, 392–401. [[CrossRef](#)]
55. Das, S.; Marsden, P.A. Angiogenesis in Glioblastoma. *N. Engl. J. Med.* **2013**, *369*, 1561–1563. [[CrossRef](#)] [[PubMed](#)]
56. Bian, X.-W.; Yang, S.-X.; Chen, J.-H.; Ping, Y.-F.; Zhou, X.-D.; Wang, Q.-L.; Jiang, X.-F.; Gong, W.; Xiao, H.-L.; Du, L.L.; et al. Preferential expression of chemokine receptor cxcr4 by highly malignant human gliomas and its association with poor patient survival. *Neurosurgery* **2007**, *61*, 570–579. [[CrossRef](#)]
57. Zagzag, D.; Lukyanov, Y.; Lan, L.; Ali, M.A.; Esencay, M.; Mendez, O.; Yee, H.; Voura, E.B.; Newcomb, E.W. Hypoxia-inducible factor 1 and VEGF upregulate CXCR4 in glioblastoma: Implications for angiogenesis and glioma cell invasion. *Lab. Investig.* **2006**, *86*, 1221–1232. [[CrossRef](#)]
58. Walters, M.J.; Ebsworth, K.; Berahovich, R.D.; Penfold, M.E.T.; Liu, S.-C.; Al Omran, R.; Kioi, M.; Chernikova, S.; Tseng, D.; Mulkearns-Hubert, E.; et al. Inhibition of CXCR7 extends survival following irradiation of brain tumours in mice and rats. *Br. J. Cancer* **2014**, *110*, 1179–1188. [[CrossRef](#)] [[PubMed](#)]
59. Yu, H.; Xue, Y.; Wang, P.; Liu, X.; Ma, J.; Zheng, J.; Li, Z.; Cai, H.; Liu, Y. Knockdown of long non-coding RNA XIST increases blood-tumor barrier permeability and inhibits glioma angiogenesis by targeting miR-137. *Oncogenesis* **2017**, *6*, e303. [[CrossRef](#)] [[PubMed](#)]
60. Qian, T.; Liu, Y.; Dong, Y.; Zhang, L.; Dong, Y.; Sun, Y.; Sun, D. CXCR7 regulates breast tumor metastasis and angiogenesis in vivo and in vitro. *Mol. Med. Rep.* **2018**, *17*, 3633–3639. [[CrossRef](#)]
61. Zhang, M.; Qiu, L.; Zhang, Y.; Xu, D.; Zheng, J.C.; Jiang, L. CXCL12 enhances angiogenesis through CXCR7 activation in human umbilical vein endothelial cells. *Sci. Rep.* **2017**, *7*, 8289. [[CrossRef](#)] [[PubMed](#)]
62. Esencay, M.; Sarfraz, Y.; Zagzag, D. CXCR7 is induced by hypoxia and mediates glioma cell migration towards SDF-1 α . *BMC Cancer* **2013**, *13*, 347. [[CrossRef](#)] [[PubMed](#)]
63. Jin, P.; Shin, S.H.; Chun, Y.S.; Shin, H.W.; Shin, Y.J.; Lee, Y.; Kim, D.; Nam, D.H.; Park, J.W. Astrocyte-derived CCL20 reinforces HIF-1-mediated hypoxic responses in glioblastoma by stimulating the CCR6-NF- κ B signaling pathway. *Oncogene* **2018**, *37*, 3070–3087. [[CrossRef](#)]

64. Ehtesham, M.; Winston, J.A.; Kabos, P.; Thompson, R.C. CXCR4 expression mediates glioma cell invasiveness. *Oncogene* **2006**, *25*, 2801–2806. [[CrossRef](#)] [[PubMed](#)]
65. Yadav, V.N.; Zamlar, D.; Baker, G.J.; Kadiyala, P.; Epstein, A.; Decarvalho, A.C.; Mikkelsen, T.; Castro, M.G.; Lowenstein, P.R. CXCR4 increases in-vivo glioma perivascular invasion, and reduces radiation induced apoptosis: A genetic knockdown study. *Oncotarget* **2016**, *7*, 83701–83719. [[CrossRef](#)]
66. Kim, N.; Ryu, H.; Kim, S.; Joo, M.; Jeon, H.J.; Lee, M.-W.; Song, I.-C.; Kim, M.-N.; Kim, J.-M.; Lee, H.J. CXCR7 promotes migration and invasion in head and neck squamous cell carcinoma by upregulating TGF- β 1/Smad2/3 signaling. *Sci. Rep.* **2019**, *9*, 18100. [[CrossRef](#)]
67. Luker, K.E.; Lewin, S.A.; Mihalko, L.A.; Schmidt, B.T.; Winkler, J.S.; Coggins, N.L.; Thomas, D.G.; Luker, G.D. Scavenging of CXCL12 by CXCR7 promotes tumor growth and metastasis of CXCR4-positive breast cancer cells. *Oncogene* **2012**, *31*, 4750–4758. [[CrossRef](#)]
68. Hernandez, L.; Magalhaes, M.A.O.; Coniglio, S.J.; Condeelis, J.S.; Segall, J.E. Opposing roles of CXCR4 and CXCR7 in breast cancer metastasis. *Breast Cancer Res.* **2011**, *13*, R128. [[CrossRef](#)]
69. Bajetto, A.; Pattarozzi, A.; Corsaro, A.; Barbieri, F.; Daga, A.; Bosio, A.; Gatti, M.; Pisaturo, V.; Siritto, R.; Florio, T. Different Effects of Human Umbilical Cord Mesenchymal Stem Cells on Glioblastoma Stem Cells by Direct Cell Interaction or via Released Soluble Factors. *Front. Cell. Neurosci.* **2017**, *11*, 312. [[CrossRef](#)]
70. McCoy, M.G.; Nyanyo, D.; Hung, C.K.; Goerger, J.P.; Zipfel, W.R.; Williams, R.M.; Nishimura, N.; Fischbach, C. Endothelial cells promote 3D invasion of GBM by IL-8-dependent induction of cancer stem cell properties. *Sci. Rep.* **2019**, *9*, 9069. [[CrossRef](#)]
71. Gimple, R.C.; Bhargava, S.; Dixit, D.; Rich, J.N. Glioblastoma stem cells: Lessons from the tumor hierarchy in a lethal cancer. *Genes Dev.* **2019**, *33*, 591–609. [[CrossRef](#)]
72. Gilbertson, R.J.; Rich, J.N. Making a tumour's bed: Glioblastoma stem cells and the vascular niche. *Nat. Rev. Cancer* **2007**, *7*, 733–736. [[CrossRef](#)] [[PubMed](#)]
73. Yu, D.; Khan, O.F.; Suvà, M.L.; Dong, B.; Panek, W.K.; Xiao, T.; Wu, M.; Han, Y.; Ahmed, A.U.; Balyasnikova, I.V.; et al. Multiplexed RNAi therapy against brain tumor-initiating cells via lipopolymeric nanoparticle infusion delays glioblastoma progression. *Proc. Natl. Acad. Sci. USA* **2017**, *114*, E6147–E6156. [[CrossRef](#)]
74. Flüh, C.; Hattermann, K.; Mehdorn, H.M.; Synowitz, M.; Held-Feindt, J.; Flüh, C. Differential expression of CXCR4 and CXCR7 with various stem cell markers in paired human primary and recurrent glioblastomas. *Int. J. Oncol.* **2016**, *48*, 1408–1416. [[CrossRef](#)] [[PubMed](#)]
75. Ehtesham, M.; Mapara, K.Y.; Stevenson, C.B.; Thompson, R.C. CXCR4 mediates the proliferation of glioblastoma progenitor cells. *Cancer Lett.* **2009**, *274*, 305–312. [[CrossRef](#)] [[PubMed](#)]
76. Gatti, M.; Pattarozzi, A.; Bajetto, A.; Würth, R.; Daga, A.; Fiaschi, P.; Zona, G.; Florio, T.; Barbieri, F. Inhibition of CXCL12/CXCR4 autocrine/paracrine loop reduces viability of human glioblastoma stem-like cells affecting self-renewal activity. *Toxicology* **2013**, *314*, 209–220. [[CrossRef](#)] [[PubMed](#)]
77. Schulte, A.; Günther, H.S.; Phillips, H.S.; Kemming, D.; Martens, T.; Kharbanda, S.; Soriano, R.H.; Modrusan, Z.; Zapf, S.; Westphal, M.; et al. A distinct subset of glioma cell lines with stem cell-like properties reflects the transcriptional phenotype of glioblastomas and overexpresses CXCR4 as therapeutic target. *Glia* **2011**, *59*, 590–602. [[CrossRef](#)]
78. Goffart, N.; Kroonen, J.; Di Valentin, E.; Dedobbeleer, M.; Denne, A.; Martinive, P.; Rogister, B. Adult mouse subventricular zones stimulate glioblastoma stem cells specific invasion through CXCL12/CXCR4 signaling. *Neuro-Oncology* **2015**, *17*, 81–94. [[CrossRef](#)]
79. Goffart, N.; Lombard, A.; Lallemand, F.; Kroonen, J.; Nassen, J.; Di Valentin, E.; Berendsen, S.; Dedobbeleer, M.; Willems, E.; Robe, P.A.; et al. CXCL12 mediates glioblastoma resistance to radiotherapy in the subventricular zone. *Neuro-Oncology* **2016**, *19*, 66–77. [[CrossRef](#)]
80. Liu, C.; Pham, K.; Luo, D.; Reynolds, B.A.; Hothi, P.; Foltz, G.; Harrison, J.K. Expression and Functional Heterogeneity of Chemokine Receptors CXCR4 and CXCR7 in Primary Patient-Derived Glioblastoma Cells. *PLoS ONE* **2013**, *8*, e59750. [[CrossRef](#)]
81. Eramo, L.; Ricci-Vitiani, A.; Zeuner, R.; Pallini, F.; Lotti, G.; Sette, E.; Pilozzi, L.M.; Larocca, C.; Peschle, R.D.M. Chemotherapy resistance of glioblastoma stem cells. *Cell Death Differ.* **2006**, *13*, 1238–1241. [[CrossRef](#)]
82. Hasan, T.; Caragher, S.P.; Shireman, J.M.; Park, C.H.; Atashi, F.; Baisiwala, S.; Lee, G.; Guo, D.; Wang, J.Y.; Dey, M.; et al. Interleukin-8/CXCR2 signaling regulates therapy-induced plasticity and enhances tumorigenicity in glioblastoma. *Cell Death Dis.* **2019**, *10*, 292. [[CrossRef](#)]
83. Zhang, X.-N.; Yang, K.-D.; Chen, C.; He, Z.-C.; Wang, Q.-H.; Feng, H.; Lv, S.-Q.; Wang, Y.; Mao, M.; Liu, Q.; et al. Pericytes augment glioblastoma cell resistance to temozolomide through CCL5-CCR5 paracrine signaling. *Cell Res.* **2021**, *31*, 1072–1087. [[CrossRef](#)]
84. Müller, S.; Kohanbash, G.; Liu, S.J.; Alvarado, B.; Carrera, D.; Bhaduri, A.; Watchmaker, P.B.; Yagnik, G.; Di Lullo, E.; Malatesta, M.; et al. Single-cell profiling of human gliomas reveals macrophage ontogeny as a basis for regional differences in macrophage activation in the tumor microenvironment. *Genome Biol.* **2017**, *18*, 234. [[CrossRef](#)]
85. Couturier, C.P.; Ayyadhury, S.; Le, P.U.; Nadaf, J.; Monlong, J.; Riva, G.; Allache, R.; Baig, S.; Yan, X.; Bourgey, M.; et al. Single-cell RNA-seq reveals that glioblastoma recapitulates a normal neurodevelopmental hierarchy. *Nat. Commun.* **2020**, *11*, 3406. [[CrossRef](#)]
86. Quail, D.F.; Joyce, J.A. The Microenvironmental Landscape of Brain Tumors. *Cancer Cell* **2017**, *31*, 326–341. [[CrossRef](#)] [[PubMed](#)]
87. Buonfiglioli, A.; Hambarzumyan, D. Macrophages and microglia: The cerberus of glioblastoma. *Acta Neuropathol. Commun.* **2021**, *9*, 54. [[CrossRef](#)] [[PubMed](#)]

88. Held-Feindt, J.; Hattermann, K.; Mürköster, S.S.; Wedderkopp, H.; Knerlich-Lukoschus, F.; Ungefroren, H.; Mehdorn, H.M.; Mentlein, R. CX3CR1 promotes recruitment of human glioma-infiltrating microglia/macrophages (GIMs). *Exp. Cell Res.* **2010**, *316*, 1553–1566. [[CrossRef](#)] [[PubMed](#)]
89. Yu, K.; Hu, Y.; Wu, F.; Guo, Q.; Qian, Z.; Hu, W.; Chen, J.; Wang, K.; Fan, X.; Wu, X.; et al. Surveying brain tumor heterogeneity by single-cell RNA-sequencing of multi-sector biopsies. *Natl. Sci. Rev.* **2020**, *7*, 1306–1318. [[CrossRef](#)]
90. Antunes, A.R.P.; Scheyltjens, I.; Duerinck, J.; Neyns, B.; Movahedi, K.; Van Ginderachter, J.A. Understanding the glioblastoma immune microenvironment as basis for the development of new immunotherapeutic strategies. *eLife* **2020**, *9*, e52176. [[CrossRef](#)]
91. Berghoff, A.S.; Kiesel, B.; Widhalm, G.; Wilhelm, D.; Rajky, O.; Kurscheid, S.; Kresl, P.; Wöhrer, A.; Marosi, C.; Hegi, M.E.; et al. Correlation of immune phenotype with IDH mutation in diffuse glioma. *Neuro-Oncology* **2017**, *19*, 1460–1468. [[CrossRef](#)]
92. Dejaegher, J.; Solie, L.; Hunin, Z.; Sciot, R.; Capper, D.; Siewert, C.; Van Cauter, S.; Wilms, G.; van Loon, J.; Ectors, N.; et al. DNA methylation based glioblastoma subclassification is related to tumoral T-cell infiltration and patient survival. *Neuro. Oncol.* **2021**, *23*, 240–250. [[CrossRef](#)]
93. Lu, I.-N.; Dobersalske, C.; Rauschenbach, L.; Teuber-Hanselmann, S.; Steinbach, A.; Ullrich, V.; Prasad, S.; Blau, T.; Kebir, S.; Sivek, J.T.; et al. Tumor-associated hematopoietic stem and progenitor cells positively linked to glioblastoma progression. *Nat. Commun.* **2021**, *12*, 3895. [[CrossRef](#)] [[PubMed](#)]
94. Alban, T.J.; Bayik, D.; Otvos, B.; Rabljenovic, A.; Leng, L.; Jia-Shiun, L.; Roversi, G.; Lauko, A.; Momin, A.A.; Mohammadi, A.M.; et al. Glioblastoma Myeloid-Derived Suppressor Cell Subsets Express Differential Macrophage Migration Inhibitory Factor Receptor Profiles That Can Be Targeted to Reduce Immune Suppression. *Front. Immunol.* **2020**, *11*, 1191. [[CrossRef](#)]
95. Han, S.; Liu, Y.; Li, Q.; Li, Z.; Hou, H.; Wu, A. Pre-treatment neutrophil-to-lymphocyte ratio is associated with neutrophil and T-cell infiltration and predicts clinical outcome in patients with glioblastoma. *BMC Cancer* **2015**, *15*, 617. [[CrossRef](#)] [[PubMed](#)]
96. Liang, J.; Piao, Y.; Holmes, L.; Fuller, G.; Henry, V.; Tiao, N.; De Groot, J.F. Neutrophils Promote the Malignant Glioma Phenotype through S100A4. *Clin. Cancer Res.* **2013**, *20*, 187–198. [[CrossRef](#)]
97. Xie, Y.; He, L.; Lugano, R.; Zhang, Y.; Cao, H.; He, Q.; Chao, M.; Liu, B.; Cao, Q.; Wang, J.; et al. Key molecular alterations in endothelial cells in human glioblastoma uncovered through single-cell RNA sequencing. *JCI Insight* **2021**, *6*, e150861. [[CrossRef](#)] [[PubMed](#)]
98. D’Arvanitis, C.; Ferraro, G.B.; Jain, R.K. The blood-brain barrier and blood-tumour barrier in brain tumours and metastases. *Nat. Rev. Cancer* **2021**, *20*, 26–41. [[CrossRef](#)] [[PubMed](#)]
99. Virgintino, D.; Errede, M.; Rizzi, M.; Girolamo, F.; Strippoli, M.; Wälchli, T.; Robertson, D.; Frei, K.; Roncali, L. The CXCL12/CXCR4/CXCR7 ligand-receptor system regulates neuro-glio-vascular interactions and vessel growth during human brain development. *J. Inherit. Metab. Dis.* **2013**, *36*, 455–466. [[CrossRef](#)]
100. Liu, K.K.Y.; Dorovini-Zis, K. Regulation of CXCL12 and CXCR4 expression by human brain endothelial cells and their role in CD4+ and CD8+ T cell adhesion and transendothelial migration. *J. Neuroimmunol.* **2009**, *215*, 49–64. [[CrossRef](#)]
101. Ehrlich, A.T.; Semache, M.; Couvineau, P.; Wojcik, S.; Kobayashi, H.; Thelen, M.; Gross, F.; Hogue, M.; Le Guill, C.; Darcq, E.; et al. Akr3-Venus knock-in mouse lights up brain vasculature. *Mol. Brain* **2021**, *14*, 151. [[CrossRef](#)]
102. Cheng, L.; Huang, Z.; Zhou, W.; Wu, Q.; Donnola, S.; Liu, J.K.; Fang, X.; Sloan, A.E.; Mao, Y.; Lathia, J.D.; et al. Glioblastoma Stem Cells Generate Vascular Pericytes to Support Vessel Function and Tumor Growth. *Cell* **2013**, *153*, 139–152. [[CrossRef](#)] [[PubMed](#)]
103. Kremer, D.; Cui, Q.-L.; Göttle, P.; Kuhlmann, T.; Hartung, H.-P.; Antel, J.; Küry, P. CXCR7 Is Involved in Human Oligodendroglial Precursor Cell Maturation. *PLoS ONE* **2016**, *11*, e0146503. [[CrossRef](#)] [[PubMed](#)]
104. Meyrath, M.; Szpakowska, M.; Zeiner, J.; Massotte, L.; Merz, M.P.; Benkel, T.; Simon, K.; Ohnmacht, J.; Turner, J.D.; Krüger, R.; et al. The atypical chemokine receptor ACKR3/CXCR7 is a broad-spectrum scavenger for opioid peptides. *Nat. Commun.* **2020**, *11*, 3033. [[CrossRef](#)] [[PubMed](#)]
105. Abe, P.; Mueller, W.; Schütz, D.; Mackay, F.; Thelen, M.; Zhang, P.; Stumm, R. CXCR7 prevents excessive CXCL12-mediated downregulation of CXCR4 in migrating cortical interneurons. *Development* **2014**, *141*, 1857–1863. [[CrossRef](#)]
106. Sánchez-Alcañiz, J.A.; Haegel, S.; Mueller, W.; Pla, R.; Mackay, F.; Schulz, S.; López-Bendito, G.; Stumm, R.; Marín, O. Cxcr7 Controls Neuronal Migration by Regulating Chemokine Responsiveness. *Neuron* **2011**, *69*, 77–90. [[CrossRef](#)] [[PubMed](#)]
107. Liu, S.-C.; Alomran, R.; Chernikova, S.B.; Lartey, F.; Stafford, J.; Jang, T.; Merchant, M.; Zboralski, D.; Zöllner, S.; Kruschinski, A.; et al. Blockade of SDF-1 after irradiation inhibits tumor recurrences of autochthonous brain tumors in rats. *Neuro-Oncology* **2013**, *16*, 21–28. [[CrossRef](#)]
108. Salazar, N.; Carlson, J.C.; Huang, K.; Zheng, Y.; Oderup, C.; Gross, J.; Jang, A.D.; Burke, T.M.; Lewén, S.; Scholz, A.; et al. A Chimeric Antibody against ACKR3/CXCR7 in Combination with TMZ Activates Immune Responses and Extends Survival in Mouse GBM Models. *Mol. Ther.* **2018**, *26*, 1354–1365. [[CrossRef](#)]
109. Szpakowska, M.; Decker, A.M.; Meyrath, M.; Palmer, C.B.; Blough, B.E.; Namjoshi, O.A.; Chevigné, A. The natural analgesic conolidine targets the newly identified opioid scavenger ACKR3/CXCR7. *Signal Transduct. Target. Ther.* **2021**, *6*, 209.
110. Van Senten, J.R.; Bebelman, M.P.; Fan, T.S.; Heukers, R.; Bergkamp, N.D.; Van Gasselt, P.; Langemeijer, E.V.; Slinger, E.; Lagerweij, T.; Rahbar, A.; et al. The human cytomegalovirus-encoded G protein-coupled receptor UL33 exhibits oncomodulatory properties. *J. Biol. Chem.* **2019**, *294*, 16297–16308. [[CrossRef](#)]

111. Heukers, R.; Fan, T.S.; De Wit, R.H.; van Senten, J.R.; De Groof, T.; Bebelman, M.; Lagerweij, T.; Vieira, J.; De Munnik, S.M.; Vries, L.S.-D.; et al. The constitutive activity of the virally encoded chemokine receptor US28 accelerates glioblastoma growth. *Oncogene* **2018**, *37*, 4110–4121. [[CrossRef](#)] [[PubMed](#)]
112. de Wit, R.H.; Mujić-Delić, A.; van Senten, J.R.; Fraile-Ramos, A.; Siderius, M.; Smit, M.J. Human cytomegalovirus encoded chemokine receptor US28 activates the HIF-1 α /PKM2 axis in glioblastoma cells. *Oncotarget* **2016**, *7*, 67966–67985. [[CrossRef](#)] [[PubMed](#)]

3. Discussion

It is widely recognized that chemokine receptors play a key role in the development and progression of cancers. In this context, it seemed crucial to study the implication of these receptors within the GBM, by analyzing their expression in different anatomical regions of the tumor but also in cells from the TME to better characterized expression pattern and to hypothesize about their possible roles. The importance of this study lies on its emphasis on data from patients. Although many publications address the roles of chemokine receptors in GBM, they often rely on cell lines or preclinical models where there is a notable lack of patient-centered data. This work provides thus an essential perspective on chemokine receptor in gliomas, shedding light on their potential role as therapeutic targets.

- **CXCR4**

CXCR4 appeared as the receptor mainly found and implicated in patient glioma samples with greater expression in GBM. CXCR4 is found in malignant cells but is mostly expressed in different cell types associated with the TME, and appeared involved in processes such as angiogenesis, cell invasion and resistance to treatment. The results from our study are consistent with experimental data from the literature, confirming the expression of the CXCR4 receptor in GBM cells, where it plays a significant role. This correlation reinforces the relevance of our approach.

- **Current views on CXCR4 as a diagnostic tool**

Jacobs et al. confirmed high and heterogeneous expression of CXCR4 receptor in GBM tissues. Their study also demonstrated that the use of [68Ga] Ga-Pentixafor for positron emission tomography (PET) imaging can be used to visualize CXCR4 expression, providing a valuable diagnostic tool²⁴⁸. They also suggest that the therapeutic potential of [177Lu] Lu-Pentixather, a radioligand specifically targeting CXCR4 could be tested in CXCR4-positive GBM patients²⁴⁸.

- **CXCR4 inhibition in the context of standard-of-care and anti-angiogenic therapies**

Clinical trials are currently underway to validate the therapeutic benefit of CXCR4 inhibition as add-on to existing GBM therapies. For example, the use of olaptosed pegol (NOX-A12), which neutralizes the CXCL12 ligand, shows encouraging results. The study focused on evaluating the safety and effectiveness of olaptosed pegol in combination with radiotherapy in newly diagnosed with GBM patients, including those with unmethylated *MGMT* promoter status (NCT04121455). Recently, Giordano et al. conducted a phase I/II trial combining radiotherapy with NOX-A12 to evaluate the safety of this treatment in 10 patients with newly diagnosed GBM without *MGMT* methylation. The primary endpoint was safety, while secondary endpoints included maximum tolerable dose, recommended phase II dose, plasma NOX-A12 levels, recurrence topography, quality of life, median progression-free survival (PFS), and overall survival (OS). The results showed that the treatment was safe, with no dose-limiting toxicity and no treatment-related deaths. All doses tested were tolerated, with a recommended dose of 600 mg/week for future studies. Nine of ten patients showed radiographic responses and four of them achieved partial remission. PFS was 174 days and OS was 389 days. In addition, a post-hoc analysis on tumor tissues revealed that a higher frequency of CXCL12⁺ endothelial cells and glioma cells was associated with a longer PFS with NOX-A12. These results suggest an improved clinical efficacy of NOX-A12 in the subgroup of patients with high CXCL12 positivity in CD31⁺ endothelial cells and GFAP⁺ glioma cells²⁴⁹.

Additionally, a phase I/II trial is exploring the use of plerixafor after radiotherapy and temozolomide, to study the side effects and the proper dose of plerixafor to use in the treatment of GBM patients. This study demonstrated that plerixafor could stop the growth of tumor cells by blocking blood flow to the tumor. This study shows that the use of plerixafor after standard treatment could be an effective therapy strategy against high-grade gliomas²⁵⁰.

Another clinical trial study the effectiveness of whole brain radiotherapy, this time by using plerixafor in combination with standard chemoradiotherapy with temozolomide in patients with GBM. This approach aims to capitalize on the multiple mechanisms of these treatments to target tumor growth and prevent recurrence (NCT03746080). And finally, a phase I/II investigation focused on the use of plerixafor to inhibit the CXCR4 receptor, a crucial element in the process of tumor revascularization after irradiation. The results of these studies demonstrated the tolerability of plerixafor in patients, as well as its potential to improve local control of tumor recurrence. These discoveries pave the way for new therapeutic strategies to treat GBM, by exploiting the specific biological mechanisms of the disease²⁵¹.

In addition, a phase I study was conducted to determine the safety of plerixafor (CXCR4 inhibitor) in combination with an anti-VEGF, bevacizumab in patients with recurrent GBM. The results showed that no dose-limiting toxicities were observed at the maximum dose of plerixafor, and bevacizumab and that the treatment was well tolerated. Dual inhibition of VEGF and CXCR4 led to an increase in inflammatory biomarkers such as plasma SDF1- α , increases in circulating CD3+ lymphocytes and CD14+ monocytes, and a decrease in IL8. In addition, the treatment decreased proangiogenic markers such as Ang-2, bFGF, and sMET ²⁵².

- **CXCR4 in the context of immunotherapy**

Mercurio et al. showed that inhibition of CXCR4 receptor using an antagonist, R-peptide, modifies GBM TME by modulating the activity of microglia, thus promoting their polarization towards the M1 phenotype. These changes in turn affect GBM cell proliferation, tumor growth and migration ²⁵³.

Wei et al. demonstrates that inhibition of CXCL12/CXCR4 signaling makes tumor cells more vulnerable to immunotherapeutic treatments and reduces tumor resistance by improving the immune response.

Wu et al. treated GBM-bearing mice with a combination therapy of anti-PD-1 and anti-CXCR4 and assessed the survival of the models as well as the cell population within the TME. Combination therapy conferred a survival benefit compared to control or monotherapy groups. The combination therapy showed modulation of the GBM microenvironment with an increase in CD4+ and CD8+ cells and helped increase levels of pro-inflammatory cytokines while reducing myeloid suppressor cells. In conclusion, they show that targeting myeloid cells with anti-CXCR4, allows anti-PD-1 to promote an antitumor response, thus improving survival²⁵⁴.

In the same context, Alghamri et al. have developed nanoparticles that target the CXCL12/CXCR4 signaling pathway via systemic injection. This team showed that the treatment blocked signaling and led to an inhibition of the GBM cells proliferation, a reduction of MDSC CXCR4+ cells infiltration, a BBB restoration and increase sensitivity to radiotherapy leading to anti-tumor immunity²⁵⁵.

- **Chemokine receptors not highlighted in the study**

We limited our analysis to 10 receptors that were found highly expressed in gliomas. However, a broader assessment of chemokine receptors could provide a more comprehensive view of GBM biology and potential therapeutic targets. Some receptors, such as CXCR3, CCR2, CCR3, CCR4 and CXCR6, although only weakly expressed in the GBM, could nonetheless play a role.

For instance, a study showed that the CXCR3 receptor is expressed in patient-derived GBM cells and involved in tumor growth²⁵⁶. Another study confirmed these results and highlights that high expression of CXCR3 was associated with an unfavorable prognosis and an invasive phenotype in patients with GBM. This study indicated there is a link between the CXCR3 receptor expression and GBM aggressiveness²⁵⁷. Furthermore, Boyé et al. highlighted the important role between the CXCR3 receptor and the LDL-associated protein receptor (LRP1) in brain tumor invasion. They demonstrate the roles of CXCR3 and LRP1 in tumor cell invasion and infiltration, by showing a downregulation of LRP1 in invasive areas which induces the accumulation

of CXCR3 at the cell membrane, thereby leading to sustained activation of CXCR3 and increased tumor cell invasion²⁵⁸. Finally, a team explored the use of a genetically engineered oncolytic adenovirus to express CXCL11 with CAR-T cells in the treatment of GBM. This study demonstrated that CXCL11 presence led to a TME modulation, promoting CAR-T cells infiltration, thus strengthening their ability to target and kill tumor cells. This study showed that the use of the chemokine CXCL11 could improve the effectiveness of CAR-T cells in the treatment of GBM²⁵⁹. Another paper highlights the importance of CCL2/CCR2 and CXCL10/CXCR3 signaling in GBM. This study reports that celecoxib-mediated modulation of CCL2/CCR2 and CXCL10/CXCR3 generated anti-tumor effects, leading to a reduction in the growth and progression of GBM in preclinical models^{260,261}. Zuo et al. demonstrated that glioma-associated fibroblasts (GAFs) play a crucial role in resistance to TMZ treatment. This study demonstrated that GAF secreted CCL2, which acts as a ligand for the CCR2 receptor expressed at the surface of GBM cells. The CCL2/CCR2 signaling axis in turn activated ERK1/2 expression which led to resistance to TMZ. These results were confirmed in GBM organoids where inhibition of CCR2 or MEK1/2 restored the sensitivity of organoids to TMZ²⁶¹. A recent study shows that combined inhibition of CCR2 and CCR5 receptors promotes better effectiveness of anti-PD1 therapy via modulation of the immunosuppressive TME of GBM. The results showed that inhibition of CCR2 and CCR5 receptors in combination with anti-PD-1 treatment reduced tumor growth in mouse models of GBM²⁶². Chia et al. examined the role of CXCL16/CXCR6 signaling in the interaction between T cells and GBM myeloid cells. Their study revealed that immunosuppressive myeloid cells express CXCL16, which leads to downregulation of T cell activity by decreasing their infiltration capacities and anti-tumor functions. On the other hand, they observe that the expression of the CXCR6 receptor facilitates the activation and infiltration of T cells towards the tumor site. The CXCL16-CXCR6 axis exhibits dual behavior, favoring the early stages of the T cell immune response and facilitating their infiltration into tumors. However, once inside the tumor, this axis contributes to immunosuppression²⁶³.

- **Strengths and limitations of the study**

The main strength of this study lies in its focus on large cohorts of patient-derived samples. Previous studies have often explored these receptors using GBM cell lines, or overexpression models, which, although easier to manipulate, are less representative of the biological complexity of human GBM tumors. Additionally, the rare studies involving patient samples have often been limited to small cohorts. In our work, we used a very large cohort allowing a more global and refined analysis of chemokine receptors, thus meeting an urgent need for patient-centered data. The goal of this study was to provide researchers and clinicians with a practical, clinically relevant resource and summary that can guide next steps toward treatments based on these receptors.

This study was carried out using web tools, publicly available databases which allow to easily reproduce results. This approach could inspire similar studies on large cohorts of patients with other types of cancer. The methodology employed could encourage other researchers to study the roles of chemokine receptors in similar ways in various cancer types, and to extrapolate these methods to expand our understanding of the molecular mechanisms involved in tumor progression in general.

This study has some limitations that are important to recognize. First, our analysis is purely based on transcriptomic data, without proteomic or functional validation. Therefore, it is imperative to conduct further experimental studies to corroborate and extend findings of our *in silico* analysis. *In vitro* and *in vivo* functional validations are indeed necessary to confirm the biological role of the identified chemokine receptors. Therefore, gene expression does not systematically translate into corresponding protein expression, which may limit the accuracy of conclusions drawn from transcriptomic data alone.

Additionally, most of the included transcriptomic analyses were performed at a single time point (generally reflecting the time of debulking surgery) and do not account for dynamic changes over time, or GBM cells plasticity. As GBM is a progressive and relapsing disease, it would be relevant to study the evolution of chemokine receptor

expression during disease progression, to better understand its development. In that regard, we could for instance exploit the data from the GLASS consortium²⁶⁴.

Moreover, additional patient-related information such as histology, survival, CIMP_status, or GBM transcriptomic subtypes was available, but not used in this study. We stratified gliomas solely based on their IDH status and 1p/19q codeletion. Likewise, information on treatments received by patients, which may impact receptor expression, was not used.

Before starting the study, we did not assess receptor expression in normal non-tumoral tissues, which could have provided a valuable basis for comparison.

Finally, this study focused on chemokine receptors without considering their ligands, the chemokines themselves. Chemokines play a crucial role by interacting with their receptors to induce intracellular signals. Future study aimed at characterizing chemokines and their interactions in GBM would be necessary to further our understanding of the biology of this disease as well as cell-to-cell communications in GBM TME.

II. Patient-based multilevel transcriptome exploration highlights relevant chemokines and chemokine receptor axes in glioblastoma" (D'Uonno, Isci et al. 2024)

1. Overview

The previous *in silico* transcriptomic study examined in detail the expression profile of chemokine receptors in GBM, without considering the expression and functions of their ligands, chemokines. To address this gap, we conducted a complementary study that unravel chemokine expression in gliomas. We were querying publicly available transcriptomic databases to study chemokine expression and function, and to infer putative chemokine-chemokine receptors interactions that take place within tumors. We aimed to provide a comprehensive patient-focused guide, highlighting the importance of interactions between chemokines and their receptors in glioma-related processes. Like in the first study, we used the TCGA database (via the Gliovis platform) to select chemokines of interest based on disease severity and study their expression and role within high-grade human gliomas. Next, we used again the IvyGAP database to determine the precise localization of their expression within different GBM sub-regions. Finally, to better understand the chemokine-receptor network at a single-cell resolution, we explored GBmap, a curated resource integrating multiple scRNAseq datasets from different published studies and exploited CellChat® to highlight putative interactions among cell types.

1.1. GBmap

GBmap is a curated resource that integrates several scRNAseq datasets from different published studies. To better understand the molecular basis of transcriptomic variation between different GBM samples, Ruiz-Moreno's team integrated data from 26 different databases, totaling 260 patients and more than a million cells. This broad integration of data from a large cohort of patients allowed the identification of underrepresented cell subtypes, thereby increasing the depth of the analysis (Fig. 24).

The team successfully mapped the composition of the GBM tumor microenvironment in details, creating the GBmap. This map revealed several tumor cell subtypes, converging into two distinct cellular phenotypes: stem/progenitor and differentiated cells. Additionally, subpopulations of immune cells (such as dendritic cells (DC), blood derived macrophages/monocytes (BDM), microglia (MG), CD4+ TILs, CD8+ TILs, natural killer (NK) and to a lesser extent B/plasma and mast cells have been gathered in the database, as well as glial cells and endothelial cells. The authors also integrated the four Neftel's malignant cell state signatures: AC-like, NPC-like, OPC-like and MES-like, among other transcriptomic profiles and programs. Each cellular subprogram is distinguished by characteristics such as hypoxia or high expression of major histocompatibility complex class II, particularly present in MES-like cells. On the other hand, OPC/NPC and AC-like cells are more associated with a proliferative character. This very large dataset allowed a robust characterization of particular GBM cell subpopulations. For instance, within TAMs, the BDM subgroup showed upregulation of genes such as interferon, pro-inflammatory cytokines, and tumor-promoting chemokines, whereas another BDM subgroup of characterized by MES-like cell gene expression and associated with a hypoxia phenotype. T cells are also present in distinct categories, highly expressing genes associated with cytotoxicity and cell proliferation. Furthermore, several subgroups of vascular cells have been identified, including arteriole-like endothelial cells, capillary-like endothelial cells as well as pericytes and mural cells.

Using the GBmap, the researchers constructed a cellular communication network based on the expression of ligand-receptor pairs in each cell type. For example, they highlighted the crucial role of neutrophils as potential new players shaping the tumor TME and cellular communication networks. The study also revealed functional interactions between neutrophils and cancer cells via the oncostatin M (OSM) pathway. Neoplastic MES-like cells interact with TAMs via the PROS pathway, while NECTIN3 expression by MES-like cells allows them to interact with T cells, suggesting a role in their exhaustion. They also have highlighted the prominent role of MES-like cells in the secretion of growth factors signaling neovascularization, such as VEGF, angiopoietin-like protein (ANGPTL) and calcitonin receptor (CALCR). They hypothesized that these

pro-angiogenic factors might play a positive feedback role in response to hypoxic metabolic signals in the TME. Finally, TAM-BDMs were identified as expressing wntless-related integration site family member 5A (WNT5A) and interacting with the Melanoma Cell Adhesion Molecule (MCAM) receptor on endothelial cells, thereby promoting the formation of new blood vessels. Furthermore, neutrophils were identified as the main source of Nicotinamide phosphoribosyltransferase (NAMPT), an enzyme involved in the VISFATIN pathway, contributing to angiogenesis in the GBM.

Finally, the study allowed to reconstruct tumor architecture using spatial transcriptomics. They explored the organization and architecture as well as cell-cell interactions and were able to precisely map the localization of GBM TME components. Their analysis revealed that AC-like, NPC-like, and OPC-like cells were widely distributed within the tumor, while MES-like cells formed distinct areas with an absence of other cellular phenotypes. AC-like and OPC-like cells were mainly localized around blood vessels, followed by an outline of MES-like cells. In addition, they identified the existence of five distinct compartments: compartment 5 was mainly populated by non-neoplastic glial and neuronal cells, usually adjacent to healthy tissues; compartments 2 and 3 were enriched in immune cells, facilitating communication with tumor cells; compartment 4 showed a predominance of AC and OPC cells, while compartment 1 was mainly occupied by MES-like cells. This detailed analysis underlines the complexity of tumor architecture in GBM and suggests that the spatial distribution of different cell types could play a crucial role in cellular interactions and immune responses within the tumor (Fig. 21)²⁶⁵.

In conclusion, the GBmap constitutes a robust and dynamic platform that integrates single-cell transcriptomic data from more than a million cells. This represents a significant advance for the scientific community, making it possible not only to map new data but also to build or explore new concepts.

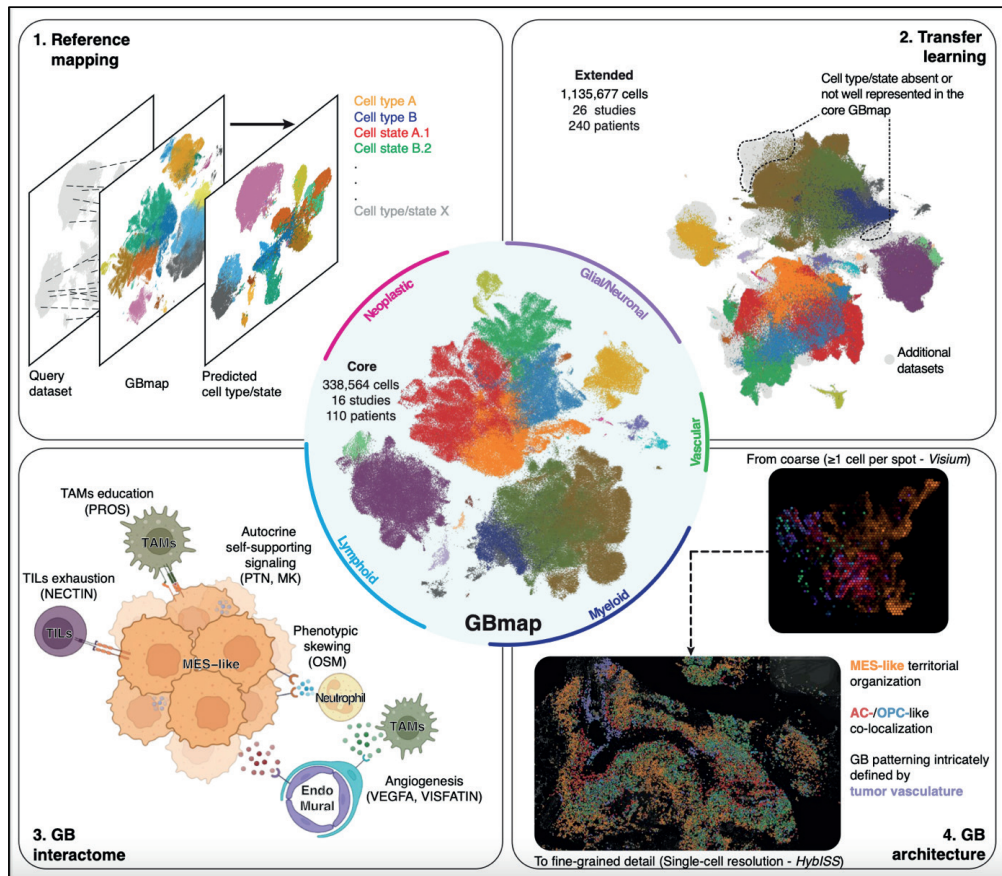


Figure 21: Illustrating schema of the main stages and results of the study using the GBmap database. 1) Reference mapping: prediction of various cell types by using a dataset, revealing cellular diversity within the GBM TME. 2) Transfer learning allows cellular mapping to be extended to include cell types or states underrepresented in the GBmap by integrating additional data from 240 patients from 26 studies. 3): GB Interactome: the cellular interaction network found within the GBM makes it possible to highlight important signaling mechanisms within GBM 4): GB architecture: reveals the detailed spatial organization of MES-like, AC/OPC-like and the structuring of the GBM defined by vascularization. (Adapted from Ruiz-Moreno et al. 2022).

1.2. CellChat package

To infer cell-cell communication within GBM TME, Ruiz Moreno's team used the GBmap as input to the CellChat Package in R. CellChat Package allows the scientific community to reconstruct and visualize signaling pathways and ligand-receptor interactions between TME GBM cells, based on single-cell sequencing data. This allows intercellular communication networks to be represented by weighted directed graphs, composed of significant communications where the interaction strength is defined as the communication probability²⁶⁶.

2. Presentation and contribution to the manuscript

This paper is published in *Computers in Biology and Medicine* in 2024 by D'Uonnolo & Isci et al. and analyze the expression of human chemokines in GBM with a particular focus patient-derived sample. This study was designed and conducted with our collaborators from the Luxembourg Institute of Health (Andy Chevigné, Martyna Szpakowska, Giulia D'Uonnolo, May Wantz, Bakhtiyor Nosirov, Petr V Nazarov and Anna Golebiewska). Our main role was to conduct bioinformatics analyzes of chemokines expression by interrogating the TCGA and IvyGAP databases. Similarly to what we did in the first 'receptors only' study, we studied the expression of chemokines in the glioma subgroups regarding tumor severity grade by using the TCGA LGG-GBM dataset (513 patients with low grade glioma and 154 GBM patients). This allowed us to bring out 18 chemokines based on their average mRNA expression within at least one subgroup of glioma. Then, Ivy GAP dataset allowed us to examine the expression of these selected chemokines within five different anatomical areas and to study more in depth their activity in these specific regions. Finally, GBmap was integrated to CellChat package in R to visualize network of intercellular communication within GBM TME.



Patient-based multilevel transcriptome exploration highlights relevant chemokines and chemokine receptor axes in glioblastoma

Giulia D'Uonnolo^{a,b,1}, Damla Isci^{c,1}, Bakhtiyor Nosirov^{d,e}, Amandine Kuppens^c, May Wantz^a, Petr V. Nazarov^e, Anna Golebiewska^d, Bernard Rogister^{c,f}, Andy Chevigné^{a,1}, Virginie Neirinckx^{c,*}, Martyna Szpakowska^{a,1}

^a Immuno-Pharmacology and Interactomics, Department of Infection and Immunity, Luxembourg Institute of Health, Luxembourg

^b Faculty of Science, Technology and Medicine, University of Luxembourg, Esch-sur-Alzette, Luxembourg

^c Laboratory of Nervous System Diseases and Therapy, GIGA Neuroscience, GIGA Institute, University of Liège, Belgium

^d NORLUX Neuro-Oncology Laboratory, Department of Cancer Research, Luxembourg Institute of Health, Luxembourg

^e Multiomics Data Science Research Group, Department of Cancer Research, Luxembourg Institute of Health, Luxembourg

^f University Hospital, Neurology Department, University of Liège, Belgium

ARTICLE INFO

Keywords:

Chemokines
Glioblastoma
Chemokine-receptor interactions
scRNAseq
CellChat

ABSTRACT

Chemokines and their receptors form a complex interaction network, crucial for precise leukocyte positioning and trafficking. In cancer, they promote malignant cell proliferation and survival but are also critical for immune cell infiltration in the tumor microenvironment. Glioblastoma (GBM) is the most common and lethal brain tumor, characterized by an immunosuppressive TME, with restricted immune cell infiltration. A better understanding of chemokine-receptor interactions is therefore essential for improving tumor immunogenicity. In this study, we assessed the expression of all human chemokines in adult-type diffuse gliomas, with particular focus on GBM, based on patient-derived samples. Publicly available bulk RNA sequencing datasets allowed us to identify the chemokines most abundantly expressed in GBM, with regard to disease severity and across different tumor subregions. To gain insight into the chemokines–receptor network at the single cell resolution, we explored GBmap, a curated resource integrating multiple scRNAseq datasets from different published studies. Our study constitutes the first patient-based handbook highlighting the relevant chemokine–receptor crosstalks, which are of significant interest in the perspective of a therapeutic modulation of the TME in GBM.

1. Introduction

Gliomas are glial primary tumours of the central nervous system (CNS), which are classified according to the World Health Organization (WHO) into different grades and subtypes depending on their histological features and molecular profile [1]. The importance of integrating molecular profiling with the histological characteristics, which have been the longstanding criteria for diagnosis of specific glioma types, has been introduced in the 2016 CNS WHO classification and confirmed in the 2021 edition [1,2]. Critical molecular features include mutations in the isocitrate dehydrogenase 1 or 2 (IDH1/2 mut) and codeletion of the short arm of chromosome 1 and the long arm of chromosome 19 (1p/19q code), which distinguish diffuse gliomas into low-grade WHO grade 2–3 oligodendrogliomas (IDHmut, 1p/19q code) and low-to

high-grade astrocytomas (IDHmut, 1p/19q intact). IDH wild-type tumours correspond to glioblastoma (GBM, IDHwt) [1,3,4], which is the most aggressive subtype that accounts for approximately 54.7% of adult gliomas [5] and is characterized by additional molecular features (e.g. chr7/chr10 copy number alterations, and/or TERT promoter mutations). With the standard-of-care therapy associating maximal safe resection and concomitant radio-chemotherapy with temozolomide (TMZ), the median survival after diagnosis is around 13 months [4,6,7]. The progression of the disease is characterized by systematic recurrences, mostly explained by the infiltrating nature of GBM cells that penetrate through the surrounding brain tissue, hampering complete tumour resection [8,9]. Plasticity and heterogeneity of GBM tumours additionally lead to intra-tumoural and inter-patient variability with regard to tumour progression and response to treatment [10–14].

* Corresponding author.

E-mail address: Virginie.Neirinckx@uliege.be (V. Neirinckx).

¹ These authors contributed equally to this work.

Finally, GBM tumours strongly rely on an immunosuppressive tumour microenvironment (TME) that supports their growth and resistance to therapy [13,15,16]. This TME is made up of different cell types, such as vascular cells and immunosuppressive cells which favour tumour maintenance. This close interaction between GBM cells and surrounding stroma influences disease progression and patient outcome [17]. Myeloid cell types within the GBM TME include microglia, infiltrating monocytes and macrophages, neutrophils, etc [18–22]. In contrast, GBM is characterized by a low number of tumour-infiltrating lymphocytes (TILs) [23]. TME composition and molecular features vary across tumours [24] but also over time, along tumour development [25].

In different solid tumours, including GBM, chemokines and chemokine receptors have been identified as critical players in shaping of the TME [26–28]. Chemokines are small soluble chemotactic cytokines that are able to bind and activate the related classical as well as atypical chemokine receptors [29,30]. So far, 43 human chemokines have been described and based on the positions of the first cysteine residues, they are classified into four classes (CCL, CXCL, CX3CL and XCL) [29–31]. They can be categorized on a functional basis [32], as (i) homeostatic, showing expression in steady-state conditions; (ii) inflammatory, whose expression is tightly regulated, and rapidly increases during inflammatory processes to specifically recruit immune cells; or (iii) mixed-function chemokines [32–34]. Chemokines and their receptors have been shown crucial for cancer cell proliferation, migration and invasion, in addition to mediating the crosstalk between cancer cells and tumour-associated immune cells [35–37]. Based on publicly available datasets, we have recently identified and described the chemokine receptors most highly expressed in glioma patient tissue and their putative role in malignant processes. This study confirmed the implication of CXCR4 and ACKR3 in GBM, and revealed a potential involvement of other receptors, although their exact role in brain tumours remains to be characterized [38]. This thorough receptor analysis did not, however, consider their ligands, chemokines, which all have their own unique expression profile and function [38]. Therefore, with the present study we aimed at providing a more exhaustive patient-based handbook, highlighting the impact of chemokine–receptor interactions in glioma processes. Using publicly available patient-related data, we explored the chemokines that are expressed in adult-type diffuse gliomas and elaborated on the important cellular crosstalks within the TME that rely on chemokines and their receptors.

2. Methods

2.1. Analysis of The Cancer Genome Atlas (TCGA), low grade glioma (LGG) – glioblastoma (GBM) dataset (2016)

Gene expression levels of the whole panel of human chemokines were inspected: the CC chemokine family (CCL1–5, CCL7, CCL8, CCL11, CCL13–28), the CXC chemokine family (CXCL1–14, CXCL16 and CXCL17), the two XCL chemokines (XCL1 and XCL2) and CX3CL1 by bulk RNA sequencing (HiSeq). Data were extracted from patient-derived tumour samples from adult-type diffuse gliomas by investigating the LGG-GBM TCGA [39] dataset with the use of the GlioVis platform (<http://gliovis.bioinfo.cnio.es/>). Patients from this dataset were grouped according to their IDH and 1p/19q codeletion status and clinical grade: (A) IDHmut, 1p/19q co-deleted tumours (WHO grade 2/3, n = 169), (B) IDHmut, 1p/19q intact astrocytomas of variable grade (WHO grade 2/3/4, n = 256), (C) IDHwt tumours (n = 229), that include GBMs (WHO grade 4) but also a subset of tumours that are assessed as WHO grade 2 or 3 in the initial dataset (n = 94), mostly based on histological aspects of astrocytomas/oligoastrocytomas. 67 % of these samples (57/85) show chr7/chr10 copy number alterations and/or TERT promoter mutations, which rather speaks for GBM IDHwt, WHO grade 4 according to the 2021 WHO CNS classification. However, substantial differences in chemokine expression could be noticed with respect to the initially described tumour grade, which we therefore displayed in two

subgroups.

2.2. Analysis of the Genotype-tissue expression (GTEx) normal tissue dataset (and comparison with the TCGA GBM dataset)

In order to further explore chemokine expression in gliomas, with particular focus on GBM, we used Gene Expression Profiling Analysis (GEPIA2) [40] was used to compare bulk RNAseq data from GBM TCGA dataset (163 GBM tissue samples) to normal human brain from GTEx (207 tissue samples). The RNAseq dataset GEPIA2 is based on the UCSC Xena project (<http://xena.ucsc.edu>). Bar graphs were generated by querying the whole panel of human chemokines (Supplementary Table 1) as multiple gene comparison. Tumour data and matched normal data were downloaded from <http://gepia2.cancer-pku.cn/#analysis>.

2.3. Analysis of the Ivy Glioblastoma Atlas Project (Ivy GAP) dataset (2018)

Chemokine expression was assessed in different GBM tumour subregions with the use of Ivy Glioblastoma Atlas Project (Ivy GAP) [41]. This dataset associates anatomic structural features and transcriptomes from bulk RNAseq GBM samples (122 samples from 10 GBM patients). In this study, five structures identified by hematoxylin-eosin staining and isolated by laser microdissection were screened. These include the three major anatomic regions of a tumour: (1) the leading edge (LE), namely the outermost margin of the tumour, (2) the infiltrating tumour area (IT), and (3) the cellular tumour core (CT). In addition, structural features can be observed within the tumour core like (4) microvascular proliferation (MVP), marked by the presence of at least two neighboring blood vessels and (5) pseudopalisading cells around necrosis (PAN), densely aligned tumour cells surrounding necrotic areas. We explored the expression levels of the different chemokines (CCL1–5, CCL7–8, CCL11, CCL17, CCL19–28, CXCL1–14, CXCL16–17, XCL1–2, CX3CL1) focusing on the five tumour subregions that were identified by reference histology as filtering criteria (LE, IT, CT, MVP and PAN). Data were downloaded from <https://glioblastoma.alleninstitute.org>.

2.4. Analysis of the GBmap resource

To decipher and determine chemokine expression in different cell subtypes associated with GBM, we explored the GBmap [42], a curated resource integrating multiple scRNAseq datasets from different published studies. The entire GBmap dataset was downloaded from the data link provided in the corresponding publication on BioRxiv. Here, we used the ‘core GBmap’ reference dataset (referred to as GBmap onwards) that contains over 330'000 cells from 110 patients [42]. As the GBmap data had already been integrated and pre-processed by the authors, it was not subjected to any additional preprocessing before we generated corresponding dot plots and intercellular ligand-receptor interaction plots. Cellular distribution of the human chemokines (and their receptors) in GBM was investigated using our gene list (Supplementary Table 1) as the values for the “features” parameter of the DotPlot function in the Seurat package for R to visualize gene expression changes in the form of a dot plot. Of note, the chemokines CCL1, CCL3, CCL11, CCL14, CCL15 and CCL16 and CCL21 were not detected in the GBmap dataset and were therefore excluded from the analysis. The chemokines CCL24, CCL25, CCL27, CXCL4 and CXCL17 were represented in the dataset at barely detectable levels, not differentially expressed across the different annotations in the GBmap.

GBmap was used as an input for CellChat [43] package in R to infer intercellular communication network and signalling pathways of selected chemokines (CCL2, CCL4, CCL5, CCL20, CXCL10, CXCL12, CXCL16, CXCL3) and related receptors (CCR1, CCR5, CCR6, CXCR3, CXCR4, CXCR6, ACKR3, CX3CR1). CellChat integrates gene expression data with literature-supported and manually-curated databases of

ligand–receptor interactions in human. The exploration, analysis and visualization of inferred networks were performed using default parameters of relevant CellChat functions. Different visualization packages of R were used to improve the quality of plots and plot annotations (Seurat, ggplot 2, cowplot and patchwork) [44–46].

The whole panel of human chemokines was investigated across the four datasets, however some genes were not included in Ivy GAP and/or GBmap. For each dataset, gene expression was displayed for the genes for which data were available (Supplementary Table 1). For chemokines showing multiple isoforms, the expression of the major isoform was reported. Original publications, online platforms, RNA sequencing methods, number of samples and patients included in the datasets are listed in Table 1. Original data were not subjected to any modification or recalculation, existing data were filtered to generate original heatmaps or dot plots.

3. Results

3.1. Global profiling of chemokine expression in gliomas

We have previously evaluated chemokine receptor expression in various types of gliomas, to decipher the complex chemokine-chemokine receptor network. To deepen this characterization, we here focused on the ligands of these receptors, the chemokines. We therefore investigated the relevance of the 43 human chemokines in glioma tissue by applying an approach similar to our previous analysis [38]. With the use of online platforms, we explored four publicly available datasets providing gene expression data for the target chemokines in glioma patient-derived material [12,39,41,47]. Bulk gene expression data from patient-derived tumour samples from the TCGA LGG-GBM dataset were extracted and their analysis allowed us to monitor the chemokines most abundantly expressed in different adult-type diffuse gliomas.

In GBM tumours, we observed a high expression of several chemokines, namely CCL2, CCL3, CCL4, CCL5, CCL8, CCL20, CXCL1, CXCL2, CXCL3, CXCL5, CXCL8, CXCL9, CXCL10, CXCL11, CXCL12, CXCL14, CXCL16 and CX3CL1 (threshold arbitrarily placed at average “log₂ (normalized count reads + 0.5)” expression value ≥ 3.5 , in the IDHwt, grade 4 tumours) (Fig. 1A–B). We selected these 18 chemokines for further description and investigation. For most of these chemokines, gene expression increases with disease severity (CCL2, CCL5, CCL8, CCL20, CXCL1, CXCL3, CXCL8, CXCL9, CXCL10, CXCL11 and at lower level CXCL14), suggesting their involvement in malignant processes. Note that histology-based grade within the IDHwt tumour group appeared associated with the level of chemokine expression. None of the chemokines were found downregulated in the IDHwt, grade 4 gliomas compared to other glioma subgroups. Other chemokines showed

elevated expression regardless of glioma grade (CCL3, CCL4, CXCL2, CXCL5, CXCL12, CXCL16 and CX3CL1). Importantly, the expression level in the normal brain should also be considered to truly spot the transcripts upregulated in the pathological condition. For example, CXCL14 and CX3CL1 showed an increased expression also in the normal brain (Supplementary Fig. 1A). Conversely, the chemokines CXCL12 and CXCL16, which were among the most prevalent in all glioma subgroups, showed moderate expression in normal human brain samples (Supplementary Fig. 1A).

Our analysis also revealed the IFN- γ -inducible chemokine CXCL16 as highly expressed in different gliomas, including GBM patients. Consistently, CXCL16 was previously reported to be expressed in gliomas, where it was suggested to play a critical role in microglia polarization towards a tumour-supportive phenotype, as well as contributing to glioma cell proliferation, migration and invasion [35,48] CX3CL1, also known as fractalkine, showed elevated expression across all glioma types (Fig. 1). This chemokine is proposed to be involved in CNS homeostasis by reducing brain inflammation. Although elevated in non-tumour brain tissue, its expression in human gliomas increases with tumour progression and correlates with disease severity [48].

CCL2 was also spotted among the most abundantly expressed chemokines in the different tumour entities in particular in GBM. These findings are in agreement with previous results showing CCL2 protein expression in tumour samples from different glioblastoma and astrocytoma patients [49]. Serum concentrations of CCL2 were higher in GBM patients when compared to healthy individuals, which was also the case for CCL5 [50].

CXCL12 appears highly expressed in all glioma subtypes, including GBM. Its biological relevance, together with the related classical and atypical receptors CXCR4 and ACKR3, is largely supported by numerous preclinical and clinical studies [12,35,51–59]. NOX-A12 (olaptesed pegol) an RNA-aptamer neutralizer of CXCL12, has recently been tested in a phase I/II clinical trial (GLORIA trial, NCT04121455) in combination with radiotherapy and immunotherapy in GBM patients.

Interestingly, these aforementioned chemokines CXCL12, CXCL16, CX3CL1 and partially CCL2 were already suggested as important for tumour maintenance [60].

CXCL8, also known as IL-8, was one of the first chemokine to be detected in human brain tumours [61]. Its increased expression was confirmed in our analysis, particularly in GBM (Fig. 1). Several studies highlighted its presence in patient-derived glioma tissues and glioblastoma stem cells (GSCs) [62,63].

Despite their accumulation in GBM, CXCL10 and CXCL14 (Fig. 1) have not been intensively investigated in patient-derived material. A recent study describes CXCL14 production by tumour cells in different types of astrocytomas [64].

Table 1

General information about the datasets used in this study.

	1	2	3	4
Publication, project	[39] The Cancer Genome Atlas (TCGA Project)	[41] Ivy Glioblastoma Atlas Project (Ivy GAP)	[42] Harmonized single-cell landscape, intercellular crosstalk and tumour architecture of Glioblastoma	Genotype-Tissue Expression (GTEx Project)
Selected information	Gene expression in glioma subgroups (correlated with severity)	Gene expression in five anatomical locations within GBM tumours	Gene expression in different GBM-related cell subtypes	Gene expression in GBM and human brain
Online tool	https://www.cbioportal.org , http://gliovis.bioinfo.cnio.es	https://glioblastoma.alleninstitute.org	NA → R software	http://gepia2.cancer-pku.cn/#index
Method	Bulk RNAseq (HiSeq)	Bulk RNAseq (HiSeq) after laser microdissection	scRNAseq	Bulk RNAseq
Datasets and number of samples and patients	Brain lower grade glioma, LGG (513 patients) Glioblastoma, GBM 154 patients)	Glioblastoma (122 samples/10 patients)	Glioblastoma (338'564 cells/110 patients)	Human brain (207 tissue samples)
Data expressed as	Log ₂ RSEM	Log ₂ RSEM	Normalized expression matrix (log-scale)	Log ₂ (TPM+1)

Legend: GBM: glioblastoma; GTEx: Genotype-Tissue Expression; LGG: low-grade glioma; RNAseq: RNA sequencing; scRNAseq: single-cell RNA sequencing; RSEM: RNAseq by expectation maximization; TPM: transcripts per million.

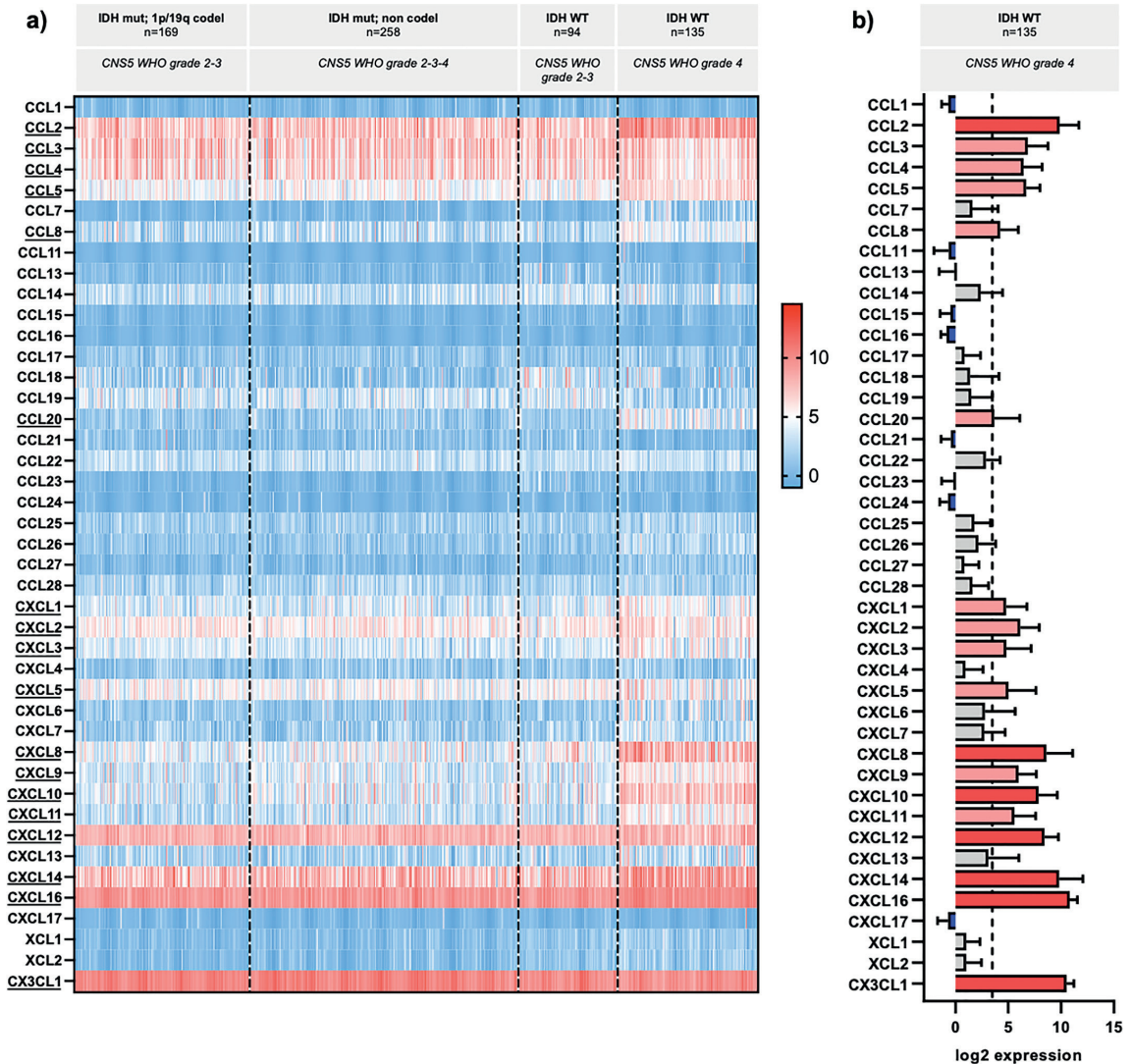


Fig. 1. Chemokine expression in glioma patients (TCGA LGG-GBM datasets) [39]. (A) The heatmap displays log₂ normalized counts (RSEM) for the 43 human chemokines. Each cell represents one patient. (B) Expression levels of chemokine genes in the IDH WT, grade 4 tumours (referred to as GBM). Chemokines with expression above arbitrary threshold of 3.5 (log₂ RSEM normalized counts) are displayed in red and selected for further description.

The chemokines CCL3, CCL4, CCL5, CCL8, CCL20, CXCL1, CXCL2, CXCL3, CXCL5, CXCL9 and CXCL11 showed only moderate expression in GBM (Fig. 1). Those able to activate the chemokine receptors CCR1 and CCR5, (CCL3, CCL4, CCL5 and CCL8) have been the body of investigation of different studies, with CCL8 being highly produced by glioma-associated macrophages and stimulating invasive abilities of tumour cells [65–67]. Among the CXC-chemokines able to activate CXCR2, a receptor responsible for neutrophils recruitment to inflammatory sites, CXCL1, CXCL2 and CXCL8 were shown elevated in GBM and their upregulation correlates with poor prognosis [68,69]. Also CCL20, together with its cognate receptor CCR6 was detected in brain tumor samples, in contrast to non-neoplastic brain samples [70]. CXCR3 ligands CXCL9, CXCL10 and CXCL11 have not been extensively characterized in gliomas. Only a few divisive studies propose them as

antitumour molecules, while others suggested a pro-tumoural role [71–74].

3.2. Unravelling chemokine expression in GBM subregions

In light of the notable increase of different chemokines in GBM, we further investigated this glioma subtype. The intra- and intertumoural heterogeneity of GBM constitutes one of the major challenges in neuro-oncology [13]. Various regions and niches have been described within these tumours, such as invasive, hypoxic, necrotic and vascularized areas. The Ivy Glioblastoma Atlas Project (IvyGAP) correlates the anatomic-histological features of GBM with genomic and gene expression patterns from a panel of GBM patients [41]. This freely accessible atlas allowed us to investigate the expression of 37/43 chemokines in

the five different tumour areas, suggestive of their activity in these regions (Fig. 2).

The assessment of RNAseq profiles revealed that certain previously highlighted chemokines displayed similar expression profiles across different tumour areas. The expression of CCL2 and CCL5 was well detectable in almost all areas. CXCL14 also showed noticeable expression in all regions, which is likely due to its basal expression in the brain tissue. On the other hand, we noted region-specific differences in the expression of several chemokines. The chemokines CCL3, CCL4, CXCL10 and CXCL16 were also detected in GBM but showed a rather heterogeneous distribution within the tumour mass. Chemokine enrichment in certain tumour regions may reveal their role in specific cell types or in regulating tumour-associated processes, e.g. angiogenesis or cell invasion. It could also indicate how a given chemokine is involved in GBM cell adaptation to its local environment. In the next paragraphs, we develop a few aspects of the existing knowledge about chemokine function with regard to their expression in the areas of interest, mainly MVP and PAN.

3.2.1. Chemokines mostly associated with microvascular proliferation (MVP) regions

The analysis showed the expression of CCL2 and CCL5 in the MVP regions, and to a lower extent also of CCL3 and CCL4 if compared to other areas (Fig. 2). Consistently, *in vitro* results have shown that CCL2, CCL3 and CCL5 were produced by brain endothelial cells upon inflammatory conditions [75], as well as CXCL8 and CXCL10 [76]. These chemokines have been also detected in endothelial cells from the brain of patients with multiple sclerosis [76]. Interestingly, CCL3 and CCL4 have been found in glioblastoma patient tissue as predominantly expressed in a specific subset of endothelial cells, associated with an inflammatory phenotype, as identified by single cell sequencing [77]. The inflammatory status of a tumour therefore appears as an important driver of chemokine expression in tumour-associated endothelial cells. CCL3 has also been described to promote the expression of the vascular endothelial growth factor-A (VEGF-A), an important inducer of angiogenesis involved in the progression of different cancers [78].

More evidently, CXCL12 was particularly abundant in the MVP

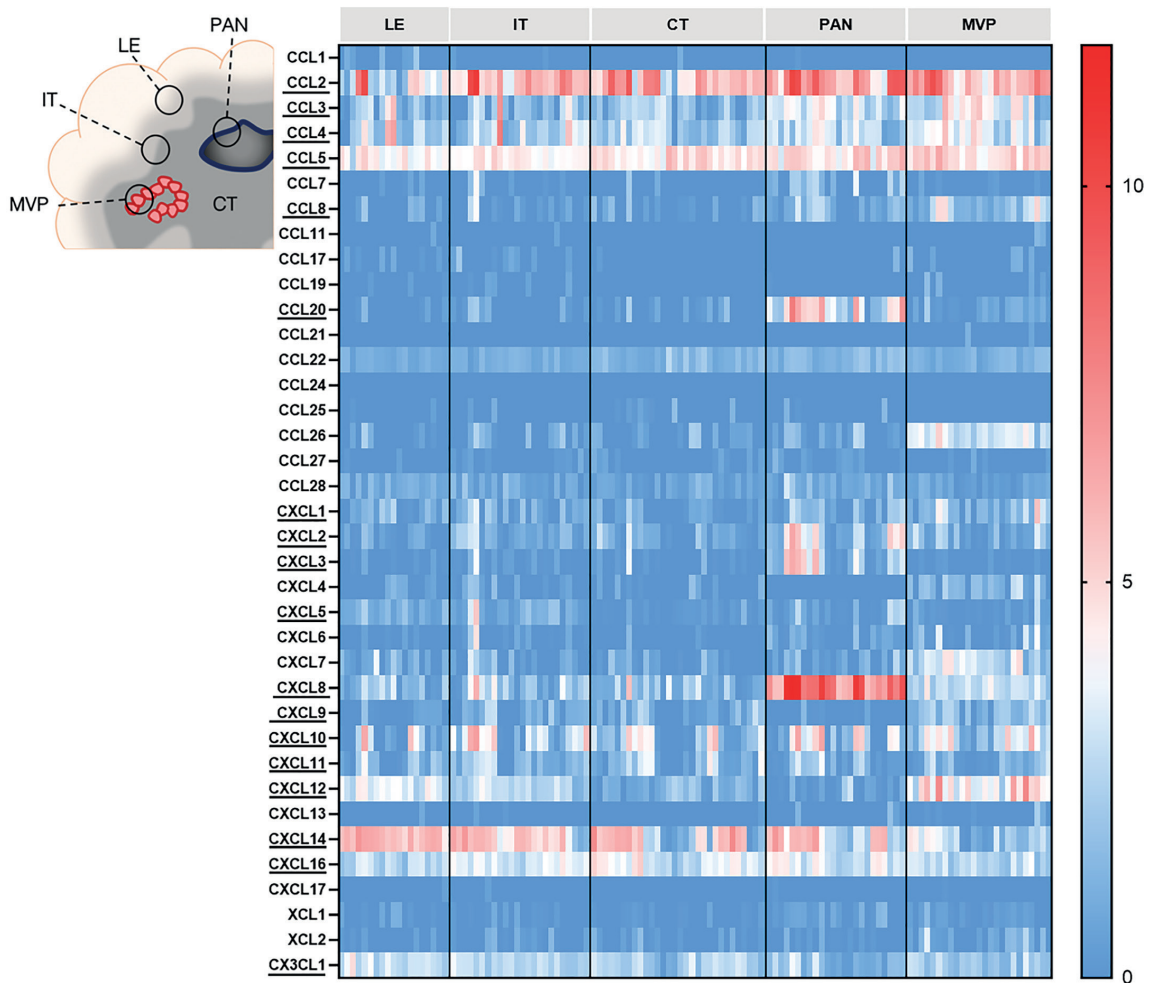


Fig. 2. Expression of chemokines in various areas of GBM tumours was analysed (IvyGAP project). The heatmap displays \log_2 RSEM normalized counts for each chemokine in the different tumour subregions. Each cell represents one sample. Legend: LE (leading edge); IT (infiltrative tumour); CT (cellular tumour); PAN (pseudopalisading cells around necrosis); MVP (microvascular proliferation). No data was available for CCL13, CCL14, CCL15, CCL16, CCL18, CCL23 in this dataset.

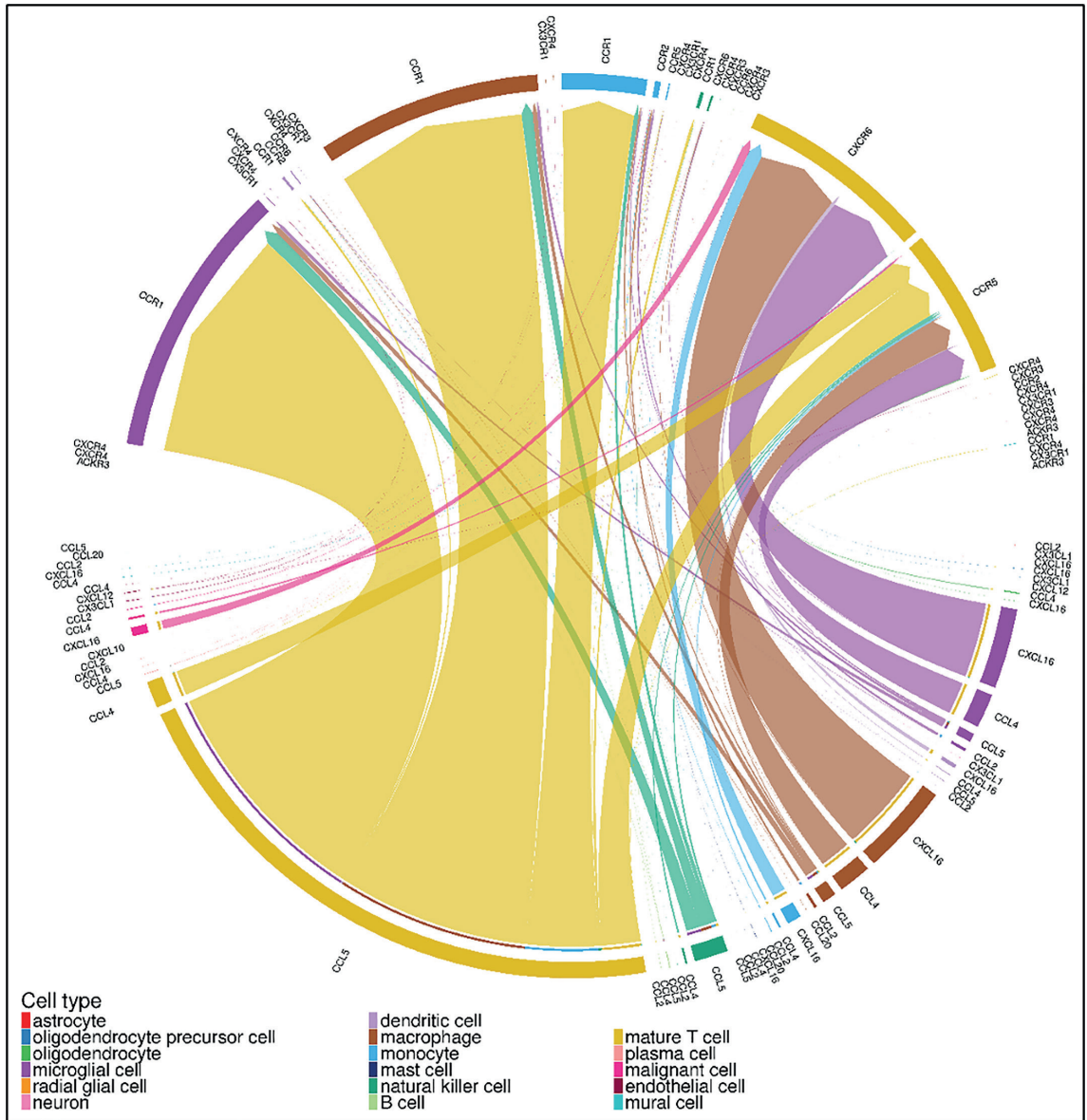


Fig. 5. The chord diagram of the inferred cell-cell interactions. All the significant interactions (p-value <0.05) shown were inferred through the CellChat calculations using the Gbmap data as input. The direction of communication is represented by arrows and the strength of communication is indicated by the width of the connecting lines.

yet been described. Although these interactions appeared less strong, annotated NK cells also express CCL5, also potentially modulating microglia, macrophages and monocytes via CCR1 (green arrows).

Other ligand-receptor pairs were highlighted, albeit with a “reduced” likelihood, as potentially involved in a wide diversity of cell-cell interactions. For instance, a putative action of CXCL12 produced by endothelial cells and oligodendrocyte precursor cells (OPCs) on various CXCR4-expressing cell types within the TME could be revealed (Supplementary Fig. 2B). Moreover, the involvement of

CX3CL1/CX3CR1 signalling in the communication between astrocytes and neurons, with diverse other tumour-associated cell types was suggested (Supplementary Fig. 2B).

In a similar fashion, a recent study emphasized the significance of the chemokine-receptor network in GBM. The receptor expression profile of GBM-infiltrating T cells, and the chemokine expression profile of non-lymphocyte GBM-associated cells was characterised using scRNAseq. It revealed that tumour infiltrating T cells were enriched in certain chemokine receptors (e.g. CCR2, CCR5, CXCR3, CXCR4, and CXCR6)

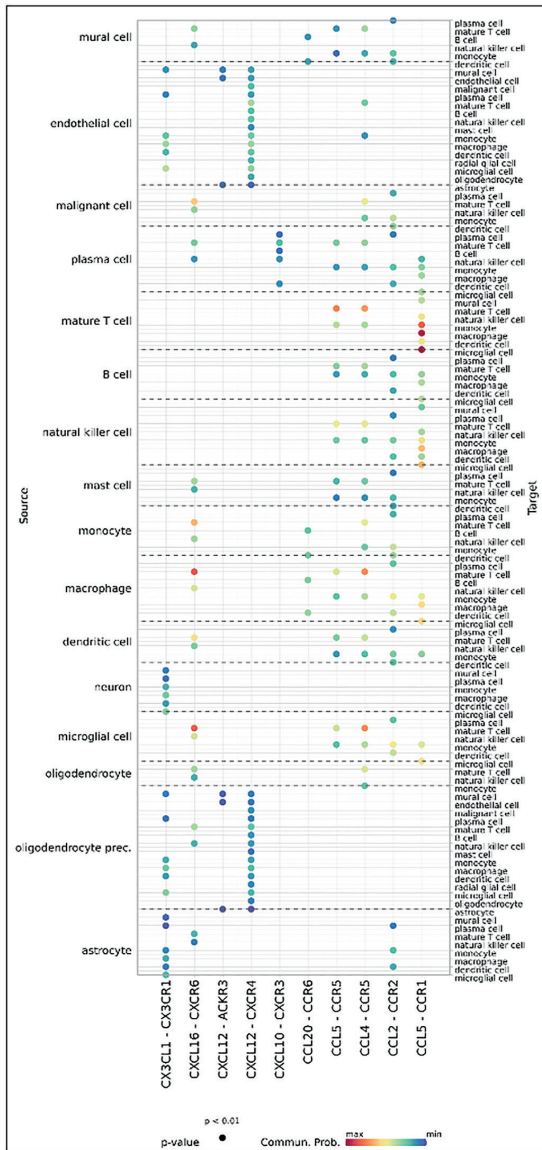


Fig. 6. The dot plot of inferred CellChat interactions from the Gbmap. The dot colour and size represent the calculated communication probability and p-values.

suggesting their role in directing T cell migration into GBM. As for the non-lymphocyte GBM-associated cells, various chemokines such as CCL2, CCL4, CCL5, CCL20, CXCL1, CXCL2, CXCL3, CXCL10, CXCL11, CXCL12, CXCL16, and CX3CL1 were detected, each with different enrichment scores. Notably, CCL4 and CXCL16 were predominantly expressed by GBM-associated macrophages and microglia [106].

4. Conclusions

Glioblastoma (GBM) tumour microenvironment (TME) is extremely important in driving tumour progression and response to therapy.

Unlike in other tumour types, most of the immunotherapeutic approaches failed in demonstrating global efficacy in GBM patients, owing to the immune-privileged brain tissue but also the acquired tumour cell resistance to therapy [107]. A better understanding of the mechanisms that dictate GBM TME organization and evolution is therefore needed for establishing effective treatments. In this study, we aimed to investigate the expression of chemokines and their receptors in an exhaustive, patient sample-based approach with unique single-cell resolution and representation.

The first part of the study was based on bulk RNAseq analyses of snap-frozen glioma tissue from different patient cohorts. It revealed that many chemokines were expressed in these tissues, some of them correlated with glioma severity. The Ivy GAP dataset offered a greater resolution by exploiting microdissected tissue regions to highlight the chemokine expression in discrete functional subregions within the tumours (e.g. pseudopalisading cells around necrosis, microvascular proliferation, etc). Among them, the presence of CCL20 and CXCL8 appeared localised to perinecrotic areas. This illustrates how histological specificities may influence chemokine expression, which was also reflected in chemokine expression in tumours from different histological grades (CCL2, CCL5, CCL8, CCL20, CXCL8 and CXCL10).

Therefore, the more recent gene expression data based on dissociated, single cells and excluding peripheral blood cell contamination, provided an unprecedented knowledge on cellular functions within the tumours. We explored the Gbmap resource, which, to date, constitutes the largest available scRNAseq dataset harmonized from previous studies. The most abundant cell annotations in this dataset are the malignant cells, macrophages, microglial cells and T-cells (Supplementary figure, 2A), whereas other neural or immune cell annotations are less represented. This scRNAseq data analysis essentially showed that chemokine expression is mostly associated with cells from the TME, including T cells, macrophages, or microglia. Consistently, the CellChat chemokine-receptor crosstalk analysis also linked these immune cell types, highlighting putative interactions with NK cells and monocytes. Our results show CCL5/CCR1 and CXCL16/CXCR6 axes as key duets in these immune cell crosstalks, which warrant further investigation. In parallel, the widely described CXCL12/CXCR4/ACKR3 axis appeared to dictate cell interactions within the tumour in a less prominent, but a rather universal manner. CXCL12 indeed appeared to be expressed by endothelial cells and OPCs, and to act on a plethora of cell types expressing variable levels of CXCR4. This data also suggests that malignant GBM cells have reduced chemokine expression, and also lower expression of chemokine receptors compared to non-malignant, TME cells.

It is crucial to note that the respective depiction of each annotation in the Gbmap dataset does not reflect the genuine proportion of corresponding cell types within GBM tumours *in situ*. Malignant cells remain the major components, while macrophages are the most abundant immune cells in the TME, representing up to 30 % of the tumour content. In contrast, infiltrative lymphoid cells are much scarcer [108,109]. Although this study provides key information about the cell types to which chemokine/receptor expression appear the most relevant (i.e. immune cells from the TME), it remains to be addressed to what extent it is also reflected clinically by immunomodulatory functions. Considering that gene expression data are captured as a tumour snapshot, further investigation using functional and dynamic GBM models is also warranted to determine whether chemokine-receptor signalling and related immune cell interactions actually drive tumour progression, emerge as a consequence of host tissue antitumour responses, or both.

The relevance of chemokines and their receptors in gliomas has already been analysed, mainly incorporating data from cell lines and murine models [35,36]. The main strengths and novelties of our study lie within the primary focus on patient tissue data, and on the comprehensive analysis of transcriptomic datasets that together highlight key chemokine-driven interactions and functions. Yet, a putative clinical translation of this study requires proteomic analyses and functional

validation. Of note, clinical information such as survival, CIMP status, or transcriptomic subtypes (e.g. Verhaak), and treatment regimen, were not considered in our study. Interestingly, a recent report focusing on chemokines in gliomas integrating 36 studies involving patients, used the related survival/clinical data to assess the predictive values of chemokines. The authors showed that the high expression of several chemokines/receptors (e.g. CXCL12, CXCR4, CCL2, among others) was associated with higher risk of glioma [110]. Most of the data included in our study relates to unique tissue samples, collected at debulking surgery and do not account for dynamic changes over time. It would therefore be relevant to also study the evolution of chemokine and chemokine receptor expression in longitudinal samples (e.g. from the GLASS consortium), to better understand their role in disease progression and recurrence.

Altogether, this analysis provides a comprehensive, in-depth assessment of chemokine and chemokine receptor expression in GBM cell types, using patient-based data, with important elaborations on how relevant cell types may work together in directing tumour outcome. The CCL5/CCR1, CXCL16/CXCR6, and CXCL12/CXCR4/ACKR3 pathways emerge from this analysis as relevant drivers of cell interactions between different cell types within tumours, including immune cells. Modulation of the immune system to improve tumour recognition and eradication has become a first-line priority in the cancer research field. Therefore, this study may not only serve as a guide for those interested in the relevance of chemokines in cancer but will also help to pave the way for novel immunomodulatory and antitumour approaches.

Availability of data and material

The datasets used/or analysed during the current study available from the corresponding author on reasonable request.

Funding

This work was supported by the University of Liège, the Luxembourg Institute of Health (LIH), the Cancer Foundation Luxembourg, Luxembourg National Research Fund (FNR) grants (INTER 20/15084569, C21/BM/15739125 “DIOMEDES”; C23/BM/18068832 “IMPACTT” PRIDE 16763386 “CANBIO2”, 16749720 “NextImmune2”, 14254520 “I2TRON”), F.R.S.-FNRS-Télévie (grants 7.4593.19, 7.4529.19 and 7.8504.20) and the European Cooperation in Science and Technology (COST) Action CA18133 European Research Network on Signal Transduction (ERNEST). GDU is a F.R.S.-FNRS-Télévie fellow (grant 7.4529.19). MS and AC are part of the Marie Skłodowska-Curie Innovative Training Networks ONCORNET2.0 “ONCOgenic Receptor Network of Excellence and Training” (MSCA-ITN-2020-ETN).

CRedit authorship contribution statement

Giulia D'Uonno: Writing – review & editing, Writing – original draft, Investigation, Conceptualization. **Damla Isci:** Writing – review & editing, Writing – original draft, Investigation, Conceptualization. **Bakhtiyor Nosirov:** Writing – review & editing, Writing – original draft, Investigation. **Amandine Kuppens:** Writing – review & editing. **May Wantz:** Writing – review & editing, Writing – original draft. **Petr V. Nazarov:** Supervision. **Anna Golebiewska:** Writing – review & editing, Supervision, Funding acquisition. **Bernard Rogister:** Writing – review & editing, Supervision, Funding acquisition. **Andy Chevigné:** Writing – review & editing, Supervision, Funding acquisition, Conceptualization. **Virginie Neirinckx:** Writing – review & editing, Writing – original draft, Supervision, Investigation, Funding acquisition, Conceptualization. **Martyna Szpakowska:** Writing – review & editing, Supervision, Funding acquisition, Conceptualization.

Declaration of competing interest

The authors declare that they have no known competing financial interests or personal relationships that could have appeared to influence the work reported in this paper.

Appendix A. Supplementary data

Supplementary data to this article can be found online at <https://doi.org/10.1016/j.compbimed.2024.109197>.

References

- [1] D.N. Louis, et al., The 2021 WHO classification of tumors of the central nervous system: a summary, *Neuro Oncol.* 23 (2021) 1231–1251.
- [2] D.N. Louis, et al., The 2016 world Health organization classification of tumors of the central nervous system: a summary, *Acta Neuropathol.* 131 (2016) 803–820.
- [3] Y. Zhang, et al., Prospective genomically guided identification of “early/evolving” and “undersampled” IDH-wildtype glioblastoma leads to improved clinical outcomes, *Neuro Oncol.* 24 (2022) 1749–1762.
- [4] X. Guo, et al., Histological and molecular glioblastoma, IDH-wildtype: a real-world landscape using the 2021 WHO classification of central nervous system tumors, *Front. Oncol.* 13 (2023) 1200815.
- [5] J.J. Miller, et al., Isocitrate dehydrogenase (IDH) mutant gliomas: a Society for Neuro-Oncology (SNO) consensus review on diagnosis, management, and future directions, *Neuro Oncol.* 25 (2023) 4–25.
- [6] R. Stupp, et al., Radiotherapy plus concomitant and adjuvant temozolomide for glioblastoma, *N. Engl. J. Med.* 352 (2005) 987–996.
- [7] H. Pinson, et al., Epidemiology and survival of adult-type diffuse glioma in Belgium during the molecular era, *Neuro Oncol.* (2023), <https://doi.org/10.1093/NEUONC/NOAD158>.
- [8] M. Rapp, et al., Recurrence pattern analysis of primary glioblastoma, *World Neurosurg* 103 (2017) 733–740.
- [9] P.Y. Wen, S. Kesari, Malignant gliomas in adults, *N. Engl. J. Med.* 359 (2008) 492–507.
- [10] A.P. Patel, et al., Single-cell RNA-seq highlights intratumoral heterogeneity in primary glioblastoma, *Science* 344 (2014) 1396.
- [11] A. Ou, W.K. Alfred Yung, N. Majd, Molecular mechanisms of treatment resistance in glioblastoma, *Int. J. Mol. Sci.* 22 (2021) 1–24.
- [12] C. Nefel, et al., An integrative model of cellular states, plasticity, and genetics for glioblastoma, *Cell* 178 (2019) 835–849.e21.
- [13] A. Dirkse, et al., Stem cell-associated heterogeneity in Glioblastoma results from intrinsic tumor plasticity shaped by the microenvironment, *Nat. Commun.* 10 (2019).
- [14] Y.A. Yabo, S.P. Niclou, A. Golebiewska, Cancer cell heterogeneity and plasticity: a paradigm shift in glioblastoma, *Neuro Oncol.* (2021), <https://doi.org/10.1093/NEUONC/NOAB269>.
- [15] F. Jacob, et al., A patient-derived glioblastoma organoid model and biobank recapitulates inter- and intra-tumoral heterogeneity, *Cell* 180 (2020) 188–204.e22.
- [16] M. Osswald, et al., Brain tumour cells interconnect to a functional and resistant network, *Nature* 528 (2015) 93–98.
- [17] R. Gargini, B. Segura-Collar, P. Sánchez-Gómez, Cellular plasticity and tumor microenvironment in gliomas: the struggle to hit a moving target, *Cancers* 12 (2020) 1–24.
- [18] D. Hambardzumyan, D.H. Gutmann, H. Kettenmann, The role of microglia and macrophages in glioma maintenance and progression, *Nat. Neurosci.* 19 (2016) 20.
- [19] M. Catalano, G. D'Alessandro, F. Trettel, C. Limatola, Role of infiltrating microglia/macrophages in glioma, *Adv. Exp. Med. Biol.* 1202 (2020) 281–298.
- [20] D.H. Gutmann, H. Kettenmann, Microglia/brain macrophages as central drivers of brain tumor pathobiology, *Neuron* 104 (2019) 442.
- [21] P.R. Gielen, et al., Elevated levels of polymorphonuclear myeloid-derived suppressor cells in patients with glioblastoma highly express S100A8/9 and arginase and suppress T cell function, *Neuro Oncol.* 18 (2016) 1253.
- [22] T.J. Alban, et al., Global immune fingerprinting in glioblastoma patient peripheral blood reveals immune-suppression signatures associated with prognosis, *JCI Insight* 3 (2018).
- [23] K. Maddison, et al., Low tumour-infiltrating lymphocyte density in primary and recurrent glioblastoma, *Oncotarget* 12 (2021) 2177–2187.
- [24] K. White, et al., Identification, validation and biological characterisation of novel glioblastoma tumour microenvironment subtypes: implications for precision immunotherapy, *Ann. Oncol.* 34 (2023) 300–314.
- [25] A.T. Yeo, et al., Single-cell RNA sequencing reveals evolution of immune landscape during glioblastoma progression, *Nat. Immunol.* 23 (6 2023) (2022) 971–984, 2022.
- [26] K. Kohli, V.G. Pillarisetty, T.S. Kim, Key chemokines direct migration of immune cells in solid tumors, *Cancer Gene Ther.* 29 (1 29) (2021) 10–21, 2021.
- [27] A.E. Vilgelm, A. Richmond, Chemokines modulate immune surveillance in tumorigenesis, metastasis, and response to immunotherapy, *Front. Immunol.* 10 (2019).

- [28] K. Franciszkiwicz, A. Boissonnas, M. Boutet, C. Combadière, F. Mami-Chouaib, Role of chemokines and chemokine receptors in shaping the effector phase of the antitumor immune response, *Cancer Res.* 72 (2012) 6325–6332.
- [29] A. Zlotnik, O. Yoshie, The chemokine superfamily revisited, *Immunity* 36 (2012) 705.
- [30] R. Bonecchi, G.J. Graham, Atypical chemokine receptors and their roles in the resolution of the inflammatory response, *Front. Immunol.* 7 (2016) 224.
- [31] F. Bachelierie, et al., New nomenclature for atypical chemokine receptors, *Nat. Immunol.* 15 (2014) 207–208.
- [32] A. Mantovani, R. Bonecchi, M. Locati, Tuning inflammation and immunity by chemokine sequestration: decoys and more, *Nat. Rev. Immunol.* 6 (12) (2006) 907–918, 2006.
- [33] K. Chen, et al., Chemokines in homeostasis and diseases, *Cell. Mol. Immunol.* 15 (2018) 324–334.
- [34] X. Blanchet, M. Langer, C. Weber, R. Koenen, P. von Hundelshausen, Touch of chemokines, *Front. Immunol.* 3 (2012).
- [35] M. Groblewska, A. Litman-Zawadzka, B. Mroczko, The role of selected chemokines and their receptors in the development of gliomas, *Int. J. Mol. Sci.* 21 (2020).
- [36] G.P. Takacs, J.A. Flores-Toro, J.K. Harrison, Modulation of the chemokine/chemokine receptor axis as a novel approach for glioma therapy, *Pharmacol. Ther.* 222 (2021).
- [37] Y. Zhou, P.H. Larsen, C. Hao, V.W. Yong, CXCR4 is a major chemokine receptor on glioma cells and mediates their survival, *J. Biol. Chem.* 277 (2002) 49481–49487.
- [38] D. Isci, et al., Patient-oriented perspective on chemokine receptor expression and function in glioma, *Cancers* 14 (2022) 130.
- [39] M. Ceccarelli, et al., Molecular profiling reveals biologically discrete subsets and pathways of progression in diffuse glioma, *Cell* 164 (2016) 550–563.
- [40] Z. Tang, B. Kang, C. Li, T. Chen, Z. Zhang, GEPIA2: an enhanced web server for large-scale expression profiling and interactive analysis, *Nucleic Acids Res.* 47 (2019) W556–W560.
- [41] R.B. Puchalski, et al., An anatomic transcriptional atlas of human glioblastoma, *Science* 360 (2018) 660–663.
- [42] C. Ruiz-Moreno, et al., Harmonized Single-Cell Landscape, *Intercellular Crosstalk and Tumor Architecture of Glioblastoma*, 2022, <https://doi.org/10.1101/2022.08.27.505439>.
- [43] GitHub - sqjin/CellChat: R toolkit for inference, visualization and analysis of cell-cell communication from single-cell data, <https://github.com/sqjin/CellChat>.
- [44] H. Wickham, *ggplot2* elegant graphics for data analysis, Use R! series (2016) 211.
- [45] Arranging plots in a grid • cowplot, https://wilkelab.org/cowplot/articles/plot_grid.html.
- [46] Authors and Citation • patchwork, <https://patchwork-data-imaginist.com/authors.html#citation>.
- [47] S. Darmanis, et al., Single-cell RNA-seq analysis of infiltrating neoplastic cells at the migrating front of human glioblastoma, *Cell Rep.* 21 (2017) 1399.
- [48] M. Erreni, et al., Human glioblastoma tumours and neural cancer stem cells express the chemokine CX3CL1 and its receptor CX3CR1, *Eur. J. Cancer* 46 (2010) 3383–3392.
- [49] I. Desbaillets, et al., Human astrocytomas and glioblastomas express monocyte chemoattractant protein-1 (MCP-1) in vivo and in vitro, *Int. J. Cancer* 58 (1994) 240–247.
- [50] B.K. Khandani, et al., The intricate expression of CC chemokines in glial tumors: evidence for involvement of CCL2 and CCL5 but not CCL11, *Acta Med. Iran.* 53 (2015) 770–777.
- [51] E. Kokovay, et al., Adult SVZ lineage cells home to and leave the vascular niche via differential responses to SDF1/CXCR4 signaling, *Cell Stem Cell* 7 (2010) 163–173.
- [52] N. Goffart, et al., Adult mouse subventricular zones stimulate glioblastoma stem cells specific invasion through CXCL12/CXCR4 signaling, *Neuro Oncol.* 17 (2015) 81.
- [53] M. Gatti, et al., Inhibition of CXCL12/CXCR4 autocrine/paracrine loop reduces viability of human glioblastoma stem-like cells affecting self-renewal activity, *Toxicology* 314 (2013) 209–220.
- [54] E.Q. Lee, et al., Phase I and biomarker study of plerixafor and bevacizumab in recurrent high-grade glioma, *Clin. Cancer Res.* 24 (2018) 4643–4649.
- [55] R.P. Thomas, et al., Macrophage exclusion after radiation therapy (MERT): a first in human phase I/II trial using a CXCR4 inhibitor in glioblastoma, *Clin. Cancer Res.* 25 (2019) 6948–6957.
- [56] H. K. et al., The chemokine receptor CXCR7 is highly expressed in human glioma cells and mediates antiapoptotic effects, *Cancer Res.* 70 (2010) 3299–3308.
- [57] M. Neves, et al., The role of ACKR3 in breast, lung, and brain cancer, *Mol. Pharmacol.* 96 (2019) 819–825.
- [58] N. Salazar, et al., A chimeric antibody against ACKR3/CXCR7 in combination with TMZ activates immune responses and extends survival in mouse GBM models, *Mol. Ther.* 26 (2018) 1354.
- [59] S.M. Jacobs, et al., CXCR4 expression in glioblastoma tissue and the potential for PET imaging and treatment with [68Ga]Ga-Pentixafor/[177Lu]Lu-Pentixafor, *Eur. J. Nucl. Med. Mol. Imag.* 49 (2022) 481–491.
- [60] V. Adamski, et al., Entry and exit of chemotherapeutically-promoted cellular dormancy in glioblastoma cells is differentially affected by the chemokines CXCL12, CXCL16, and CX3CL1, *Oncogene* 39 (22) (2020) 4421–4435, 2020.
- [61] T. Nitta, M. Allegretta, K. Okumura, K. Sato, L. Steinman, Neoplastic and reactive human astrocytes express interleukin-8 gene, *Neurosurg. Rev.* 15 (1992) 203–207.
- [62] I. Sharma, A. Singh, F. Siraj, S. Saxena, IL-8/CXCR1/2 signalling promotes tumor cell proliferation, invasion and vascular mimicry in glioblastoma, *J. Biomed. Sci.* 25 (2018).
- [63] D.W. Infanger, et al., Glioblastoma stem cells are regulated by interleukin-8 signaling in a tumoral perivascular niche, *Cancer Res.* 73 (2013) 7079–7089.
- [64] A. Kumar, et al., CXCL14 promotes a robust brain tumor-associated immune response in glioma, *Clin. Cancer Res.* 28 (2022) 2898–2910.
- [65] M.K. Kranjc, M. Novak, R.G. Pestell, T.T. Lah, Cytokine CCL5 and receptor CCR5 Axis in glioblastoma multiforme, *Radiol. Oncol.* 53 (2019) 397.
- [66] Y. Wang, et al., Hypoxia and macrophages promote glioblastoma invasion by the CCL4-CCR5 axis, *Oncol. Rep.* 36 (2016) 3522–3528.
- [67] X. Zhang, et al., CCL8 secreted by tumor-associated macrophages promotes invasion and stemness of glioblastoma cells via ERK1/2 signaling, *Lab. Invest.* 100 (2020) 619–629.
- [68] J. Hu, et al., Regulation of tumor immune suppression and cancer cell survival by CXCL1/2 elevation in glioblastoma multiforme, *Sci. Adv.* 7 (2021).
- [69] W. Alafate, et al., Elevation of CXCL1 indicates poor prognosis and radioresistance by inducing mesenchymal transition in glioblastoma, *CNS Neurosci. Ther.* 26 (2020) 475–485.
- [70] L. Wang, et al., Overexpression of CXCL20 and its receptor CCR6 predicts poor clinical prognosis in human gliomas, *Med. Oncol.* 29 (2012) 3491–3497.
- [71] K. Shono, et al., Downregulation of the CCL2/CCR2 and CXCL10/CXCR3 axes contributes to antitumor effects in a mouse model of malignant glioma, *Sci. Rep.* 10 (2020).
- [72] G. Wang, et al., CXCL11-armed oncolytic adenoviruses enhance CAR-T cell therapeutic efficacy and reprogram tumor microenvironment in glioblastoma, *Mol. Ther.* (2022), <https://doi.org/10.1016/j.ymthe.2022.08.021>.
- [73] Z. Wang, et al., The CXCL family contributes to immunosuppressive microenvironment in gliomas and assists in gliomas chemotherapy, *Front. Immunol.* 12 (2021).
- [74] T.Y.H. Chan, J.S.Y. Wong, K.M.-Y. Kiang, C.W.Y. Sun, G.K.-K. Leung, The duality of CXCR3 in glioblastoma: unveiling autocrine and paracrine mechanisms for novel therapeutic approaches, *Cell Death Dis.* 14 (12) (2023) 1–13, 2023.
- [75] R. Chui, K. Dorovini-Zis, Regulation of CCL2 and CCL3 expression in human brain endothelial cells by cytokines and lipopolysaccharide, *J. Neuroinflammation* 7 (2010) 1–12.
- [76] E.A. Subileau, et al., Expression of chemokines and their receptors by human brain endothelium: implications for multiple sclerosis, *J. Neuropathol. Exp. Neurol.* 68 (2009) 227–240.
- [77] Y. Xie, et al., Key molecular alterations in endothelial cells in human glioblastoma uncovered through single-cell RNA sequencing, *JCI Insight* 6 (2021).
- [78] Y.Y. Liao, et al., CCL3 promotes angiogenesis by dysregulation of miR-374b/VEGF-A axis in human osteosarcoma cells, *Oncotarget* 7 (2016) 4310.
- [79] A. Bajetto, et al., Expression of CX chemokine receptors 1-5 and their ligands in human glioma tissues: role of CXCR4 and SDF1 in glioma cell proliferation and migration, *Neurochem. Int.* 49 (2006) 423–432.
- [80] D. Zagzag, et al., Hypoxia- and vascular endothelial growth factor-induced stromal cell-derived factor-1 α /CXCR4 expression in glioblastomas: one plausible explanation of scherer's structures, *Am. J. Pathol.* 173 (2008) 545.
- [81] Identification, Localization of the Cytokine SDF1 and Its Receptor, CXCR4 Chemokine Receptor 4, to Regions of Necrosis and Angiogenesis in Human Glioblastoma |, *Clin. Cancer Res.* 6 (2000) 102–111.
- [82] S. Rao, et al., CXCL12 mediates trophic interactions between endothelial and tumor cells in glioblastoma, *PLoS One* 7 (2012).
- [83] A. Salmaggi, et al., CXCL12 in malignant glial tumors: a possible role in angiogenesis and cross-talk between endothelial and tumoral cells, *J. Neuro Oncol.* 67 (2004) 305–317.
- [84] D. Dai, et al., miR-24 regulates angiogenesis in gliomas, *Mol. Med. Rep.* 18 (2018) 358–368.
- [85] X. Guo, H. Jiao, L. Cao, F. Meng, Biological implications and clinical potential of invasion and migration related miRNAs in glioma, *Front. Integr. Neurosci.* 16 (2022).
- [86] T. Oishi, S. Koizumi, K. Kurozumi, Molecular mechanisms and clinical challenges of glioma invasion, *Brain Sci.* 12 (2022).
- [87] J.S. So, H. Kim, K.S. Han, Mechanisms of invasion in glioblastoma: extracellular matrix, Ca²⁺ signaling, and glutamate, *Front. Cell. Neurosci.* 15 (2021).
- [88] M. Li, R.M. Ransohoff, Multiple roles of chemokine CXCL12 in the central nervous system: a migration from immunology to neurobiology, *Prog Neurobiol* 84 (2008) 116–131.
- [89] D.S. Mithal, G. Banisadr, R.J. Miller, CXCL12 signaling in the development of the nervous system, *J. Neuroimmune Pharmacol.* 7 (2012) 820.
- [90] A. Dar, O. Kollet, T. Lapidot, Mutual, reciprocal SDF-1/CXCR4 interactions between hematopoietic and bone marrow stromal cells regulate human stem cell migration and development in NOD/SCID chimeric mice, *Exp. Hematol.* 34 (2006) 967–975.
- [91] J.H. Park, H.K. Lee, Current understanding of hypoxia in glioblastoma multiforme and its response to immunotherapy, *Cancers* 14 (2022).
- [92] M. Domènech, A. Hernández, A. Plaja, E. Martínez-balibrea, C. Balaña, Hypoxia: the cornerstone of glioblastoma, *Int. J. Mol. Sci.* 22 (2021).
- [93] S.H. Ahn, et al., Necrotic cells influence migration and invasion of glioblastoma via NF- κ B/AP-1-mediated IL-8 regulation, *Sci. Rep.* 6 (1) (2016) 1–12, 2016.
- [94] D.J. Brat, A.C. Bellail, E.G. Van Meir, The role of interleukin-8 and its receptors in gliomagenesis and tumoral angiogenesis, *Neuro Oncol.* 7 (2005) 122–133.
- [95] R.M. Urbantat, et al., The CXCL2/IL8/CXCR2 pathway is relevant for brain tumor malignancy and endothelial cell function, *Int. J. Mol. Sci.* 22 (2021) 1–19.

- [96] S. Conroy, F.A.E. Kruyt, M. Wagemakers, K.P.L. Bhat, W.F.A. den Dunnen, IL-8 associates with a pro-angiogenic and mesenchymal subtype in glioblastoma, *Oncotarget* 9 (2018) 15721.
- [97] Y. Jung, et al., MCP-1 and MIP-3 α secreted from necrotic cell-treated glioblastoma cells promote migration/infiltration of microglia, *Cell. Physiol. Biochem.* 48 (2018) 1332–1346.
- [98] P. Jin, et al., Astrocyte-derived CCL20 reinforces HIF-1-mediated hypoxic responses in glioblastoma by stimulating the CCR6-NF- κ B signaling pathway, *Oncogene* 37 (23 37) (2018) 3070–3087, 2018.
- [99] A.L. Chang, et al., CCL2 produced by the glioma microenvironment is essential for the recruitment of regulatory T cells and myeloid-derived suppressor cells, *Cancer Res.* 76 (2016) 5671–5682.
- [100] J.P. Böttcher, et al., NK cells stimulate recruitment of cDC 1 into the tumor microenvironment promoting cancer immune control, *Cell* 172 (2018) 1022–1037.e14.
- [101] M.T. Chow, A.D. Luster, Chemokines in cancer, *Cancer Immunol. Res.* 2 (2014) 1125–1131.
- [102] A.J. Ozga, M.T. Chow, A.D. Luster, Chemokines and the immune response to cancer, *Immunity* 54 (2021) 859–874.
- [103] N. Nagarsheth, M.S. Wicha, W. Zou, Chemokines in the cancer microenvironment and their relevance in cancer immunotherapy, *Nat. Rev. Immunol.* 17 (9 17) (2017) 559–572, 2017.
- [104] K. Yu, et al., Surveying brain tumor heterogeneity by single-cell RNA-sequencing of multi-sector biopsies, *Natl. Sci. Rev.* 7 (2020) 1306–1318.
- [105] F. Lepore, et al., CXCL16/CXCR6 axis drives microglia/macrophages phenotype in physiological conditions and plays a crucial role in glioma, *Front. Immunol.* 9 (2018) 2750.
- [106] P.M. Kollis, et al., Characterising distinct migratory profiles of infiltrating T-cell subsets in human glioblastoma, *Front. Immunol.* 13 (2022).
- [107] V.A. Arrieta, et al., Immune checkpoint blockade in glioblastoma: from tumor heterogeneity to personalized treatment, *J. Clin. Invest.* 133 (2023).
- [108] E. Karimi, et al., Single-cell spatial immune landscapes of primary and metastatic brain tumours, *Nature* 614 (7948 614) (2023) 555–563, 2023.
- [109] V. Wischnewski, et al., Phenotypic diversity of T cells in human primary and metastatic brain tumors revealed by multiomic interrogation, *Nature Cancer* 4 (6 4) (2023) 908–924, 2023.
- [110] S. Yang, et al., Relationship between chemokine/chemokine receptor and glioma prognosis and outcomes: systematic review and meta-analysis, *Int. Immunopharm.* 133 (2024) 112047.

3. Discussion

The results of this analysis put forward the CXCL16/CXCR6 and CCL5/CCR1 signaling pathways as key players in cellular interactions in GBM.

- **CXCL16/CXCR6 signaling in the GBM TME**

A couple of preclinical studies also reveal the importance of CXCL16/CXCR6 in the interactions occurring among cell types within GBM TME.

Hattermann et al. demonstrated that in healthy brain, CXCL16 is produced mainly by endothelial cells while its receptor, CXCR6, is absent. On the other hand, in the context of GBM, CXCL16 is upregulated and produced mainly by a population of proliferating tumor cells, but also infiltrating microglia/macrophages. They also demonstrated that the expression of the CXCR6 receptor is restricted to stem-like cells ²⁶⁷.

Another study reveals the dual role of this axis in the interactions between myeloid cells and T cells, within GBM tissues. They discovered that CXCR6 expression was limited to T cells, particularly CD8+, which can be activated and exhausted. In parallel, they show that CXCL16 is expressed at the membrane of immunosuppressive myeloid cell but secreted as a chemokine by microglial cells. They concluded that the CXCL16/CXCR6 axis plays an initial role in T cell infiltration in the tumors, but later seem to drive immunosuppression by promoting T cell interaction with immunosuppressive myeloid cells²⁶³.

Lepore et al. reported that CXCL16 released by tumor cells leads to promote GBM-associated microglia/macrophage modulation toward an anti-inflammatory/pro-tumoral phenotype. They demonstrated that CXCL16/CXCR6 signaling promotes the growth, migration and invasion of murine and human GBM cells²⁶⁸.

- **CCL5/CCR1 signaling in the GBM TME**

Regarding CCL5/CCR1 signaling, very few information is available in the literature. The lack of data may be attributed to the low immune infiltration observed in GBM. It is important to note that despite the presence of a huge population of myeloid cells in GBM TME, T cells are in reduced proportion and very rare. Therefore, isolated studies studying limited number of tumor models may therefore not highlight all the signaling axes that are at play in T cell modulation.

It is however worth noting that a research team recently generated an oncolytic herpes simplex virus type 1 expressing a secreted single-chain variable fragment of the cetuximab, linked to CCL5 (OV-Cmab-CCL5). This virus specifically targets EGFR⁺ GBM cells and continuously produces CCL5 in GBM TME. Infection of GBM cells with this virus inhibited EGFR signaling, but also significantly improved migration and activation of NK, macrophage and T cells, altogether leading to a significant reduction in tumor size and to a prolonged survival of preclinical GBM models ²⁶⁹.

- **Strengths and limitations of the study**

In the present study, we thus included an in-depth investigation of chemokine expression and their potential role in GBM. Furthermore, this study integrates an additional dimension by evaluating the probabilities of cellular communication based on chemokines and chemokines receptors, which considerably enriches our hypothesis about the dynamics within the GBM TME. Another aspect reinforcing the robustness of this study is the analysis of the expression of chemokines and their receptors in healthy brains, thus allowing a more precise and relevant selection of important signaling pathways to be investigated.

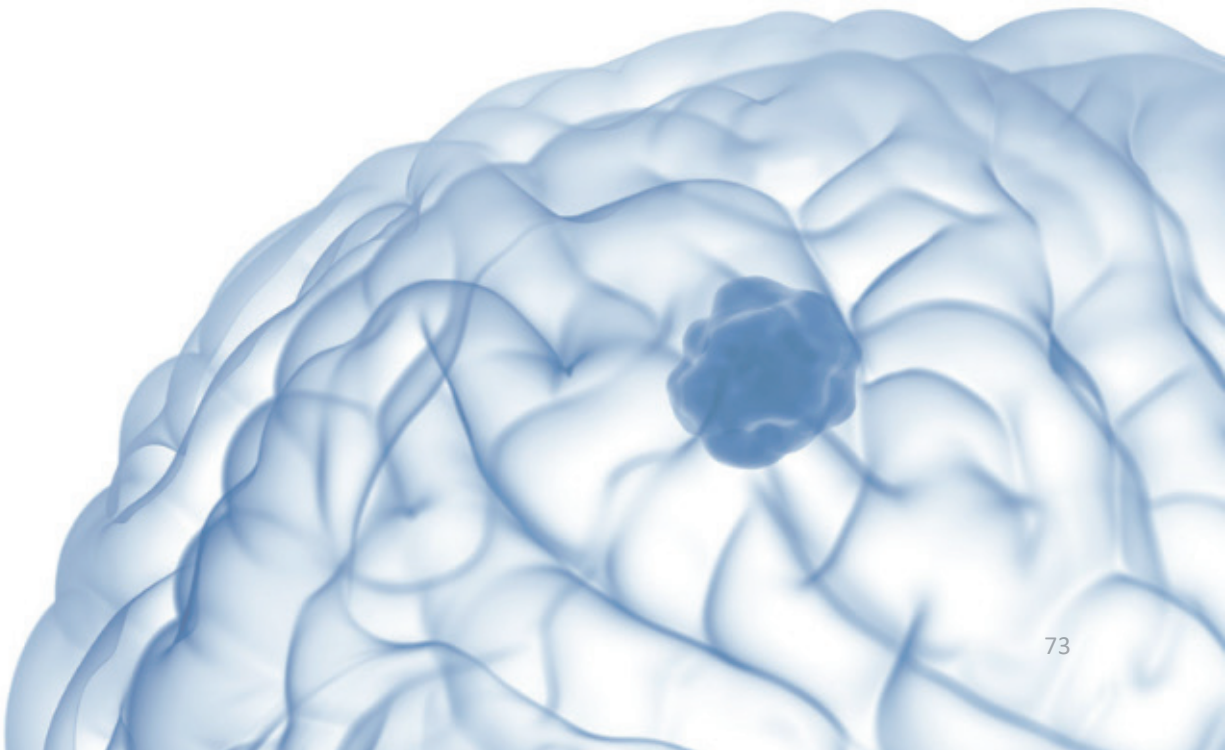
Once again, the major strength of this study lies in the use of transcriptomic data from a large cohort of patients, excluding any analysis based on cell lines, and focusing only on clinical data. In addition, the use of the GBmap database, one of the most exhaustive in terms of transcriptomic data from GBM patients, gives great robustness

to our results. Furthermore, application of the CellChat tool to predict cellular interactions based on chemokine and receptor expression further strengthens the findings of this study.

However, *in silico* analyzes still require additional validation through proteomic studies and experimental and functional analyses. These validations are crucial to confirm the hypotheses and predictions generated by our bioinformatics analyses, and to ensure the clinical and biological relevance of our findings. Also, the fact that we did not relate gene expression data with clinical information (e.g. gender, age, survival, genetics, etc.) is once again a point that could be improved. It would have been also interesting to classify patient cohorts based on the amount of immune infiltrate in tumors, before investigating cell-cell interactions. For example, separating populations with a low vs high immune infiltrate may have revealed hidden intercellular communications, providing additional and potentially revolutionary insights into the mechanisms underlying immune and tumor interaction.

In conclusion, although our study provides significant advances and addresses several weaknesses identified in the previous work (Ischi et al. 2024 Cancers), the challenges inherent to *in silico* analyzes highlight the need for future experimental validations to strengthen and confirm our results.

PART 4: ANALYSIS OF ACKR3 AND ITS ROLE IN GBM



PART 4: ANALYSIS OF ACKR3 AND ITS ROLE IN GBM

I. **Heterogeneous expression of the atypical chemokine receptor ACKR3 in glioblastoma patient-derived tissue samples and cell cultures. (Isci et al. 2024)**

1. Overview

Over the past decades, ACKR3 has attracted significant attention due to its presumed role in the progression of various types of cancers, where the CXCL12/CXCR4/ACKR3 axis has been suggested to take part in the development and progression of brain tumors. Based on existing literature and after having demonstrated the significance of the CXCR4/CXCL12 axis in GBM cell invasion, our team naturally envisaged to analyze the expression and role of ACKR3 receptor. Furthermore, the transcriptomic analysis of chemokine receptors in various cohorts of GBM patient tissue (see Part 3) revealed a high expression of *ACKR3* in glioma tissues, which several reports have previously associated with poorer disease prognosis. In this experimental study, we examined ACKR3 protein expression in patient-derived GBM tissues as well as in stem-like cell cultures (GSCs). Our main objective was to better understand the function and role of this protein in GBM biology, to possibly guide towards the development of new therapeutic strategies targeting ACKR3.

2. Presentation and contribution to the manuscript

This manuscript is published in Scientific Reports. The main objective was to explore ACKR3 expression in GBM patient tissue samples as well as in corresponding cell cultures. With this study, we attempted to clarify previously published reports on the expression and function of ACKR3 in GBM, that could appear contradictory based on what we observed in the laboratory. This study paves the way for a better understanding of the potential role of ACKR3 in the GBM TME which is important for the development of new innovative therapies. My role in this study covered the design

of the research, the execution of experiment to collect the results and analyze the data, and the writing and submission of the paper.

3. Validation of ACKR3 detection tools

The detection of ACKR3 receptor as a protein is difficult and a widely recognized challenge in the chemokine receptor research field. Indeed, the lack of reliability and specificity of classical commercial antibodies has complicated its detection and analysis²⁷⁰. Numerous studies that attempt to characterize this receptor (e.g. for characterizing pharmacological features) make use of reporter genes to locate ACKR3 in cells and tissues, most regularly in overexpression systems.

A genetically modified mouse was recently established to label ACKR3 in a physiological context. This Knock-in ACKR3-Venus mouse, expressing a functional endogenous ACKR3 receptor fused to the mVenus protein, allows the reliable detection of ACKR3 and helped to highlight that ACKR3 receptor is mainly found in the cerebral vasculature²⁷¹

Several notable advances have emerged through the development of various pharmacological tools and compounds for ACKR3 detection these last years²⁷². Three fluorescent probes specific to ACKR3 have been developed and have shown binding with affinities ranging from pKd 6.8 to 7.8, highlighting their usefulness in the specific detection of the receptor²⁷³. In parallel, nanobodies (NB1, NB2 and NB3) have been generated against ACKR3 by Mussang et al. and have shown varying abilities to inhibit CXCL12 binding. NB2 and NB3 induced complete inhibition of CXCL12 binding, while NB1 showed partial inhibition despite its high affinity²⁷⁴. The antibody X7ab, developed by Salazar et al. constitutes another significant advance, specifically designed to inhibit CXCL12 signaling via the fusion of a single chain variable fragment with a portion of FC of IgG1. This opens the way to potential therapeutic applications in pathological contexts where CXCL12 signaling is dysregulated²⁷⁵. Thelen's team generated a chimeric chemokine that selectively binds to ACKR3. This chimera consists of the N-terminus of CXCL11 and the main body of the C-terminus of CXCL12²⁷⁶. In addition, agonists such as VUF11207 have been used in experimental models of thrombosis or

hypertension specifically targeting ACKR3²⁷⁷⁻²⁷⁹. This agonist shows promising potential to reduce thrombo-inflammatory complications suggesting their future use in therapies against these pathologies.

Moreover, An ACKR3 antagonist has also been developed, ACT-1004-1239, and has been used in several studies^{280,281}. Use of this antagonist results in a decrease in immune infiltration into the CNS, which translates into a reduction in inflammatory lesions in a model of experimental autoimmune encephalomyelitis (EAE)²⁸¹. This decrease in immune infiltrate has also been shown in models of acute lung injury following use of the ACKR3 antagonist²⁸⁰. Finally, the LIH383 peptide, developed by Andy Chevigné's team, stands out as a particularly potent and selective agonist of ACKR3, surpassing the natural chemokines CXCL11 and CXCL12 in its effectiveness in inducing the recruitment of b-arrestin. This makes it a valuable tool not only for modulating the ACKR3 receptor but also for detecting cells expressing this receptor²⁰³.

In our hands, we decided to validate a few of these detection probes. A flow cytometry experiment was conducted to test three distinct probes for detecting ACKR3 at the surface of different cell types. U87 cells were used as a negative expression control, while U87 overexpressing ACKR3 (U87 ACKR3) and MCF-7 cells served as positive controls. Three detection tools were exploited:

- (i) the commercial monoclonal antibody 8F11-M16 coupled to the APC fluorochrome, which targets the ACKR3 protein at the cell surface;
- (ii) the Cy5-coupled LIH383 probe, a highly selective and potent ACKR3 agonist, allowing reliable detection of ACKR3-expressing cells in human and rodent models²⁰³;
- (iii) hCM11-12 coupled to AZ647, a chemokine-type chimera that selectively binds to ACKR3. This chimera is composed of the N terminus of CXCL11 and the main body and C terminus of CXCL12 and selectively interacts with ACKR3 with high affinity²⁷⁶.

The results showed that all detection tools are reliable for ACKR3 detection (Fig. 25). The antibody 8F11-M16, the probe LIH383-cy5 (used at 5nM) and the chimeric chemokine hCM11-12-AZ647 showed a strong signal in U87-ACKR3 and in MCF-7

cells, while no signal was observable in U87 cells. However, using the LIH383-Cy5 probe at 25 nM showed a visible background in U87 cells and it was not possible to make a direct comparison at this stage, as the three tools were used at different concentrations and are coupled to distinct fluorochromes, making any quantitative comparison difficult. Despite these limitations, all three tools proved to be reliable and specific (Fig. 22).

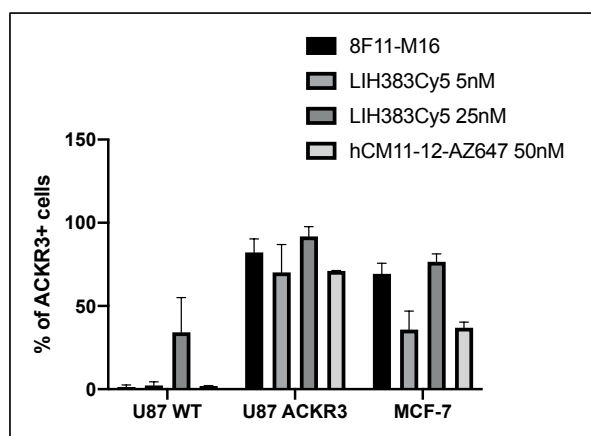


Figure 22: Percentage of ACKR3 positive cells by using 8F11-M16, LIH383Cy5 and hCM11-12-AZ647 detection tools via flow cytometry.

In the present study, we will use the 8F11-M16 antibody to detect ACKR3 and evaluate the expression in different patient-derived GSCs, since it appears to be specific.



OPEN Heterogeneous expression of the atypical chemokine receptor ACKR3 in glioblastoma patient-derived tissue samples and cell cultures

Damla Isci¹, Amandine Kuppens¹, Joshua Scalisi¹, Julie Cokaiko¹, Giulia D'Uonno^{2,3}, May Wantz², Martyna Szpakowska², Andy Chevigné², Bernard Rogister^{1,4} & Virginie Neirinckx¹✉

Glioblastoma (GBM) is the most aggressive glial tumor of the adult brain, associated with invariably fatal outcome, and a deeper understanding of the underlying malignant mechanisms is necessary to address the current therapeutic failure. We previously demonstrated the role of the CXCL12/CXCR4 axis in GBM cell migration and resistance to ionizing radiation. The atypical chemokine receptor ACKR3, responsible for CXCL12 scavenging, was previously suggested as additional important player in the context of GBM. Following validation of the detection tools, we observed that ACKR3 is expressed within GBM patient tumor tissue, distributed in diverse cell types. In contrast to CXCR4, ACKR3 expression in patient-derived stem-like cells (GSCs) remains however low, while ACKR3 gene expression by tumor cells appears to be modulated by the in-vivo environment. Using overexpression models, we also showed that in vitro ACKR3 had no significant direct effect on cell proliferation or invasion. Altogether, these results suggest that in vitro ACKR3 plays a minor role in malignant GBM cell biology and that its expression is possibly regulated by in-vivo influences. The subtle and multifaceted functions ACKR3 could exert in GBM should therefore only be tackled within a comprehensive tumor microenvironment considering tumoral but also non-tumoral cells.

Keywords Glioblastoma, Chemokines receptors, ACKR3, CXCR4

Gliomas are glial primary tumors of the central nervous system (CNS) which are classified by the World Health Organization (WHO) based on their specific histological characteristics and molecular features¹. According to this classification, glioblastoma (GBM) is identified as the most common and aggressive grade 4 glioma and is distinguished by a set of genetic alterations^{1,2}. These include the absence of the isocitrate dehydrogenase (*IDH*) mutation, designating GBM as an IDH wild-type (IDH WT) tumor, the presence of mutations in the telomerase reverse transcriptase (*TERT*) promoter and copy number alterations in chromosome 7 and 10 (+7/-10), most often associated with epithelial growth factor receptor (*EGFR*) amplification^{1,2}. The standard-of-care therapy associating maximal safe surgery and concomitant radio-chemotherapy using temozolomide (TMZ) allows a median survival of about 16 months from diagnosis³. Moreover, the progression of the disease is characterized by a systematic recurrence that relies on (1) GBM cell infiltration through the brain tissue, hindering total resection of the tumor⁴, and (2) an extreme heterogeneity⁵ of GBM cells that transit through diverse functional states⁶⁻⁸, which overall lead to therapeutic resistance.

Chemokines constitute a subgroup of chemotactic cytokines secreted by various cell types in different tissues and playing an important role in inducing and guiding cell migration⁹. They are important regulators of various processes such as development, immune responses and tissue repair⁹. Chemokine receptors, which are

¹Laboratory of Nervous System Diseases and Therapy, GIGA Neuroscience, GIGA Institute, University of Liège, Liège, Belgium. ²Immuno-Pharmacology and Interactomics, Department of Infection and Immunity, Luxembourg Institute of Health, Strassen, Luxembourg. ³Faculty of Science, Technology and Medicine, University of Luxembourg, Esch-sur-Alzette, Luxembourg. ⁴Neurology Department, University Hospital, University of Liège, Liège, Belgium. ✉email: virginie.neirinckx@uliege.be

G protein-coupled receptors, have been widely studied for their role in cancer development and metastasis^{10,11}. Besides malignant cells, chemokines and their receptors are also expressed by a wide range of cell subtypes found within the tumor bed including tumor-associated macrophages, tumor infiltrating-lymphocytes, vascular cells, non-malignant glial cells and neurons, and play diverse roles in GBM growth, angiogenesis and resistance to treatment¹².

We have previously demonstrated the function of CXCR4, the receptor for the CXCL12 chemokine, in the migration of GBM cells towards the subventricular zone (SVZ) in orthotopic xenografts models, as well as in the CXCL12-mediated protection from radiation therapy^{13,14}. ACKR3 (formerly named CXCR7), a second receptor for CXCL12, expressed in diverse cell types, including leukocytes, neurons or endothelial cells was identified^{15,16}. ACKR3 was subsequently demonstrated to play a crucial role in regulating CXCL12-dependent processes including cardiovascular and neuronal development as well as in the migration and homing of hematopoietic stem/progenitor cells^{17–20}. Unlike CXCR4 which signals via G protein pathways to induce cell migration and proliferation, ACKR3 activity relies mainly on β -arrestin recruitment and its ability to signal through G protein-independent pathways is still controversial. ACKR3 is proposed to act as a scavenger or “sink” receptor for CXCL12, shaping its gradient and regulating its availability, thereby controlling the directional migration and homing of CXCR4-expressing cells^{21–25}. So far, the exact role and expression of ACKR3 in GBM and its crosstalk with CXCR4 through their shared ligand, CXCL12, remain to be elucidated.

ACKR3 can also heterodimerize with CXCR4 and modify its signaling properties²⁶. Several years ago, different studies reported high expression of ACKR3 in brain tumor cell lines and tissue samples, which correlated with bad prognosis and increased aggressiveness in preclinical models²³. ACKR3 was also shown to be expressed on cells delimiting the SVZ in the mouse brain^{27,28}, which suggests an important role ACKR3 could play in glioma²⁹. On that basis, we decided to investigate the precise function ACKR3 could exert in GBM cells, in a potential interplay with CXCL12 and CXCR4, using patient-derived models. Recently, based on large-scale patient-based transcriptomic data, we have shown that ACKR3 is one of the most abundant chemokine receptor-encoding genes in glioma tissue¹². However, how these results are correlated to detection of the corresponding protein *ex vivo* and in various patient-derived cell cultures remain elusive.

In this study, we assessed the expression of ACKR3 protein expression in patient-derived GBM tissue and GBM stem-like cells, in different *in vitro* and *ex vivo* settings, with the ultimate aim to better understand its function and impact on GBM and to guide novel ACKR3-targeting therapeutic strategies.

Results

Validation of monoclonal antibodies for the detection of ACKR3 at the cell membrane

Detecting ACKR3 at the protein level is a widely acknowledged challenge in the field. While genetic models (e.g. reporter genes) can be employed for this purpose^{12,21}, the crucial requirement remains the recognition under native conditions, especially in order to elucidate ACKR3 role and relevance in cancer. In this study, we first aimed to assess the efficacy of two ACKR3-specific monoclonal antibodies: the 8F11-M16 antibody and the 11G8 antibody, commonly employed in our experiments for ACKR3 detection using flow cytometry and immunofluorescence, respectively. Results indicate that both antibodies yield a strong signal in U87 stably expressing ACKR3 (Fig. 1A). No signal was observed in U87 and U87 CXCR4 cells, showing a good specificity of both antibodies for ACKR3 (Fig. 1A). Additionally, we provide experimental evidence that, among several antibodies that fail to specifically detect the receptor, the 11G8 antibody reliably identifies ACKR3 in immunostaining and immunoblotting experiments using overexpression GBM cell models, as well as in MCF-7 breast cancer cells, which were previously described to endogenously express ACKR3^{23,24}. (Fig. 1B–C). In contrast, diverse other commercially available antibodies provided signals that appeared similar in both U87 and U87 ACKR3. Based on these results, we consider that both 8F11-M16 and 11G8 antibodies are reliable tools for ACKR3 detection, using flow cytometry and immunostaining experiments.

ACKR3 exhibits diverse expression patterns in GBM tissue

Over the last years, different studies reported ACKR3 expression in numerous cancer cell lines and tissue²³. Based on data from The Cancer Genome Atlas (TCGA) and Genotype-Tissue Expression (GTEx) databases (via the GEPIA platform), ACKR3 expression appears higher in low-grade gliomas (LGGs) and GBM samples compared to normal brain (Fig. 2A), which speaks for a potential role of ACKR3 in malignant cells. In line with this, we performed immunofluorescence staining to detect ACKR3 at the protein level in patient-derived FFPE tissues. We observed that ACKR3 is expressed in both glioma tissue and non-tumoral brain tissue with high inter- and intra-tumoral heterogeneity. We identified three different expression patterns of ACKR3 expression (named here after type 1, 2 and 3). In most GBM samples, ACKR3 appeared present around cell nuclei (“type 1”). Similar pattern was found in non-GBM brain samples, such as the hippocampus (HIPPO) or the subventricular zone (SVZ). In “type 2”, ACKR3 positive regions displayed blood vessel-like shapes and were found in GBM tissue, as well as in the non-tumoral SVZ, in line with previous reports showing the expression of ACKR3 on tumor-associated vasculature³⁰. Finally, in several samples, ACKR3 was detectable in the whole tissue, without apparent specificity to any cell type or structure (“type 3”). No ACKR3 expression was found in non-tumoral cortical (CORTEX) tissue samples (Fig. 2B–C).

Different co-staining experiments have been performed to analyze the cell types that appeared positive for the receptor. ACKR3 was expressed in SOX2+ cells (“stem-like”) and in GFAP+ cells (astrocytes), with “type 1” features. ACKR3 did not colocalize with PDGFR β (pericytes) or Iba1 (microglia) markers. Importantly, EGFR+ cells in tumor tissue were rarely ACKR3+ (Fig. 3A–B). Blood vessel-like (“type 2”) CXCR4+ cells also appeared ACKR3+ (Fig. 3B). Altogether, these results show that ACKR3 expression within GBM tissue is rather heterogeneous, and it can be distributed among different cell types, which mostly correspond to SOX2, GFAP,

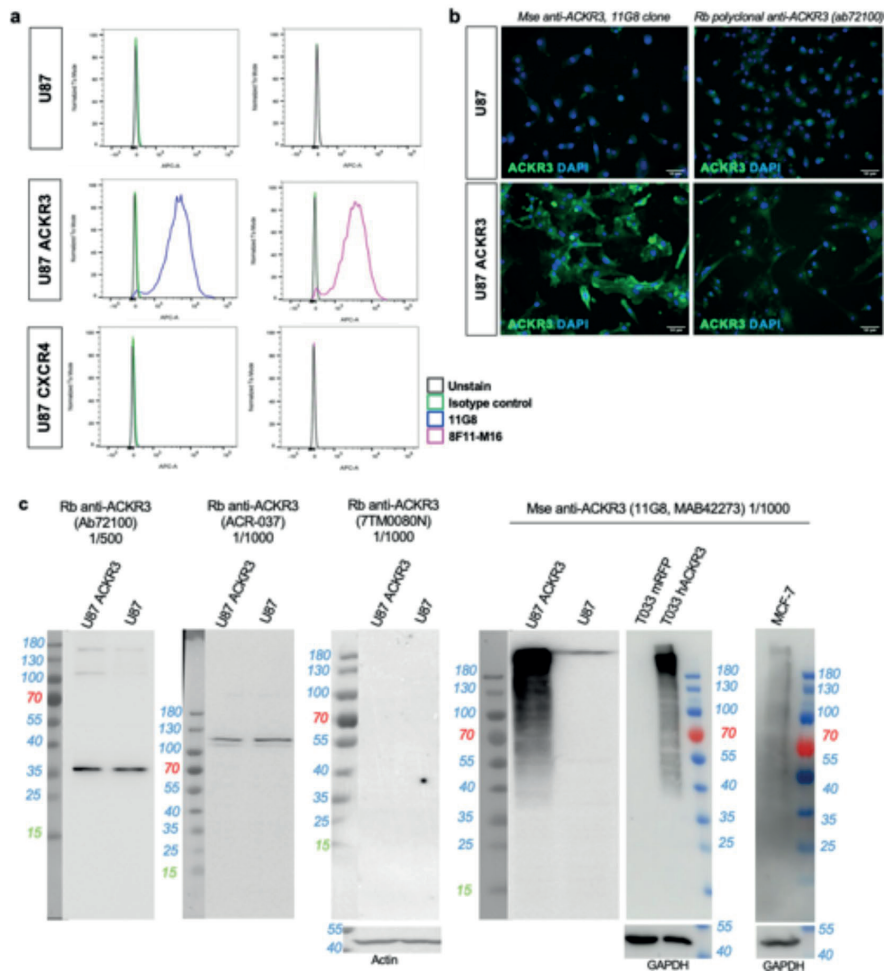


Fig. 1. ACKR3 tool validation using flow cytometry. **(A)** Cell surface ACKR3 expression in U87, U87 ACKR3 and U87 CXCR4 cell lines by using 8F11-M16 and 11G8 antibodies. **(B)** Immunofluorescent staining of ACKR3 (green) in U87 and U87 ACKR3 cells using 11G8 MAB42273 antibody against ACKR3. DAPI (blue) was used to counterstain nuclei. Scale bar = 50 μ m. **(C)** Western Blot (WB) analysis of ACKR3 in protein extracts from U87, U87 ACKR3, T033-mRFP, T033-hACKR3 and MCF-7 cells, using different commercially available antibodies (11G8/MAB42273, ab72100, ACR-037 and 7TM0080N). Original blots/gels are presented in Supplementary Figure S3.

and CXCR4-expressing cells. This is in line with single-cell RNAseq data showing that ACKR3 is expressed, although at a low level, in cells assigned to various categories (Fig. 3C).

Patient-derived GBM stem-like cell cultures express low levels of ACKR3 at the membrane

Fresh tumor tissue obtained after surgical resection was processed in order to obtain patient-derived GBM stem-like cells (GSCs) cultured as floating, 3D tumorspheres (Fig. 4A). The expression of ACKR3 was assessed at mRNA level by qRT-PCR as well as at the cell membrane by flow cytometry. ACKR3 mRNA was detected in patient-derived GSCs (Fig. 4B), although weakly expressed, e.g. compared to the SOX2 gene (Figure S1A). Using flow cytometry, we aimed at detecting ACKR3 at the cell surface of GSCs. The signal intensity for ACKR3 appeared rather close to the negative control values (Fig. 4C). The percentage of ACKR3-positive cells in each GSC culture was as follows: T08 = $1.22 \pm 0.76\%$; T013 = $3.91 \pm 1.78\%$; T018 = $2.90 \pm 0.66\%$; T033 = $0.78 \pm 0.18\%$ (vs. U87 ACKR3 = $81.40 \pm 2.31\%$) (Fig. 4D). We selected T018 and T033 GSCs to assess whether ACKR3 expression at the cell membrane could be upregulated upon stimulation with the ACKR3-binding chemokines

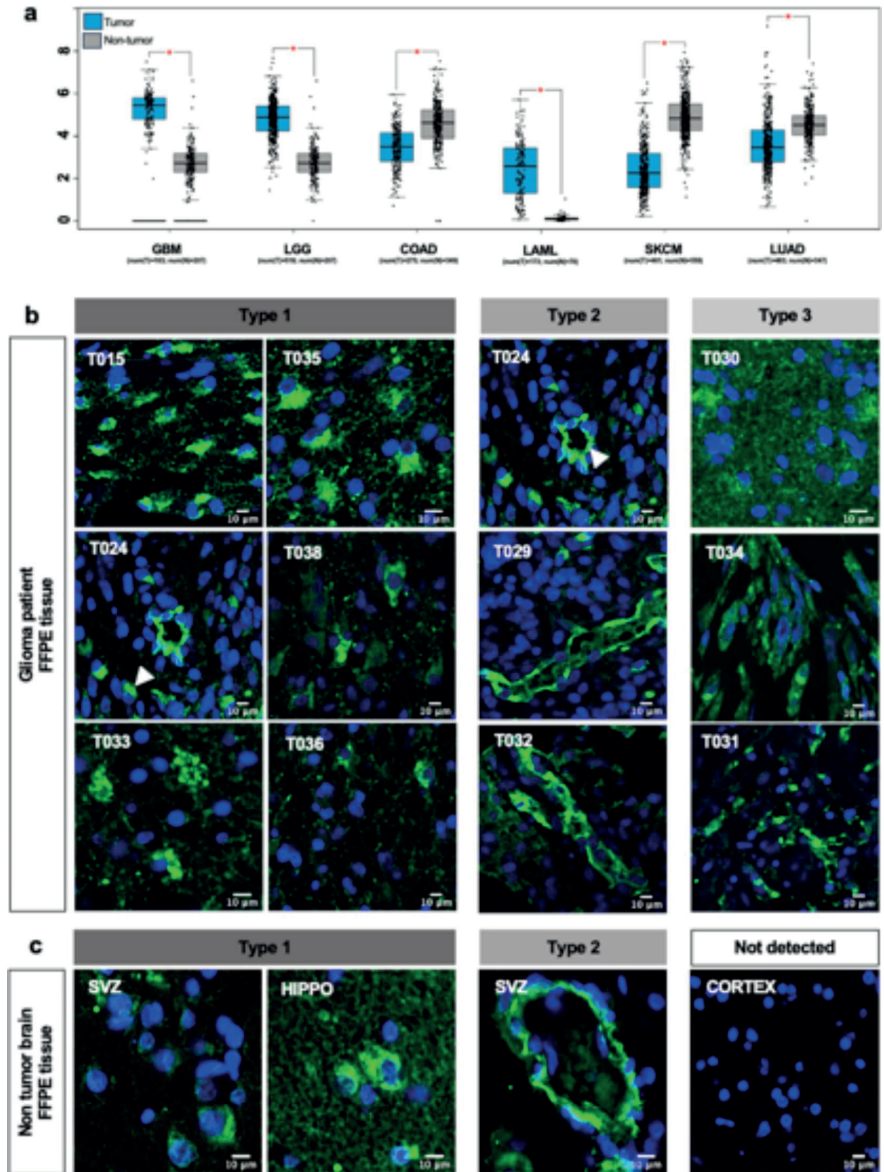


Fig. 2. ACKR3 is expressed in different patterns in human glioma tissue and non-tumor brain tissue. **(A)** In blue, ACKR3 expression in GBM, Low Grade Glioma (LGG), Colon Adenocarcinoma (COAD), Acute Myeloid Leukemia (LAML), Skin Cutaneous Melanoma (SKCM) and Lung adenocarcinoma (LUAD) (TCGA data) vs. in grey, non-tumoral samples (GTEx data, using GEPIA tool in TCGA database). **(B)** Immunofluorescent staining of ACKR3 (green) in glioma patient FFPE tissue. White arrow indicates ACKR3 expression patterns. **(C)** ACKR3 immunofluorescent staining (green) in various regions of non-tumoral FFPE brain tissue: subventricular zone (SVZ), hippocampus (HIPPO), and cortex. of non-tumoral FFPE brain tissue. DAPI (blue) was used to counterstain nuclei. Scale bar = 10 μ m.

CXCL12 and CXCL11. T018 and T033 cells were incubated for 24–48 h with different concentrations of chemokines and flow cytometry analysis was performed to detect ACKR3 as well as CXCR4, which also binds CXCL12 but not CXCL11. When T018 cells were stimulated for 24 h with 10 nM of CXCL12, we discovered a statistically significant decrease of the percentage of CXCR4-positive cells ($82.6 \pm 4.8\%$), compared to untreated

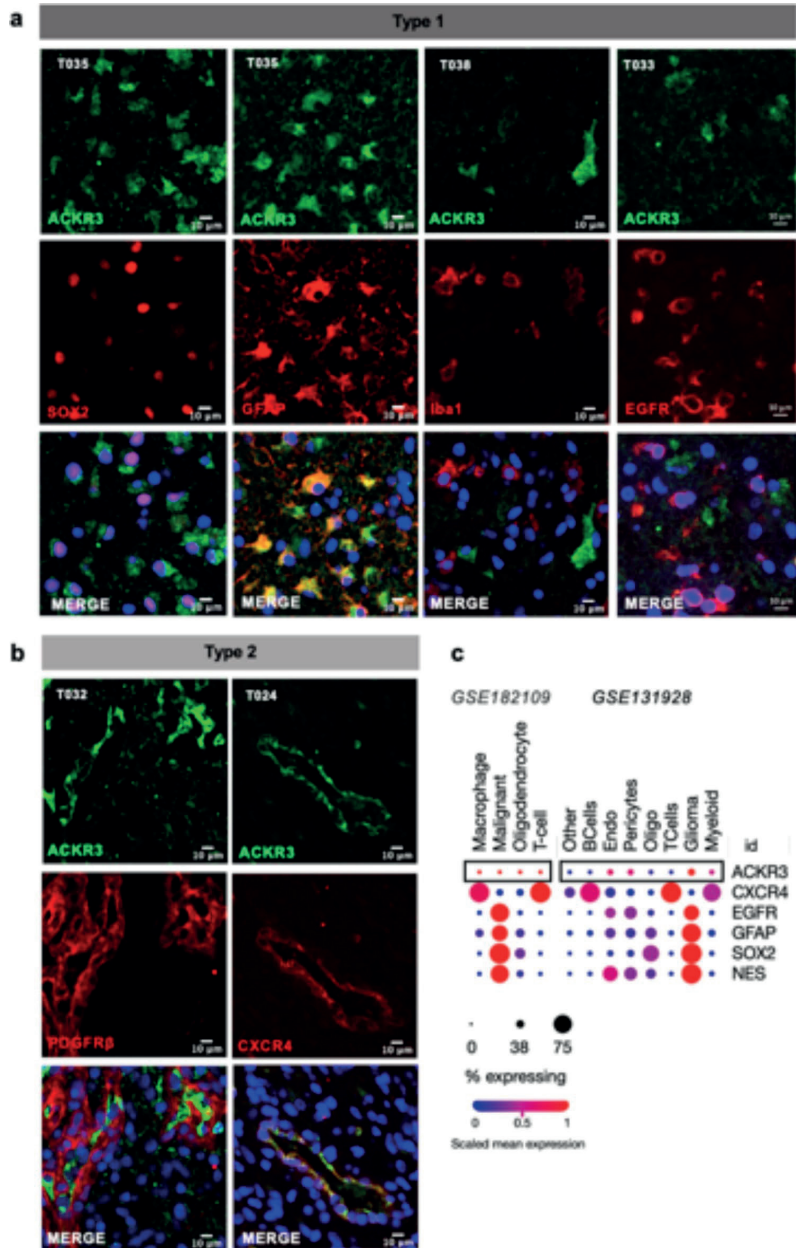


Fig. 3. Characterization of ACKR3-positive cells in glioblastoma tissue. (A–B) Immunofluorescent staining of ACKR3 (green) and cell type specific markers, including SOX2, GFAP, Iba1, EGFR, PDGFRb and CXCR4 (red). DAPI (blue) was used to counterstain nuclei. Scale bar = 10 μ m. (C) ACKR3 expression in various cell types within patient glioma samples. Single cell RNAseq data from Neftel 2019 dataset⁸ show ACKR3 expression in different cell types. The “% expressing” value indicates the proportion of cells in the signature that are positive for a given transcript, and the “scaled mean expression” is relative to each gene expression level (logTPM) across all cells within the signature (using Single Cell Portal online platform).

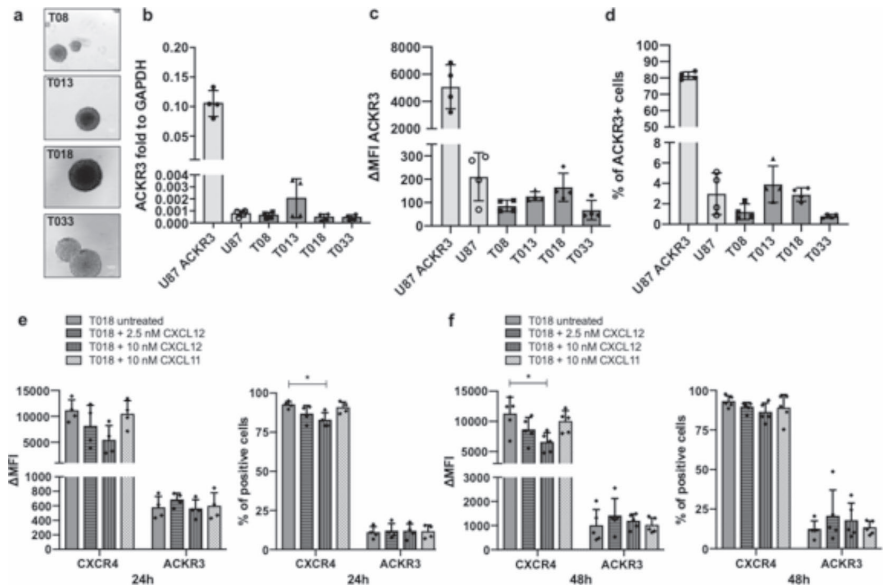


Fig. 4. ACKR3 surface expression in patient-derived GSCs is low and remains unchanged upon CXCL11 or CXCL12 stimulation. **(A)** Phase-contrast images of patient-derived GSCs (T08, T013, T018 and T033) cultured as 3D tumorospheres (scale bar = 100 μ m). **(B)** ACKR3 mRNA expression relative to GAPDH mRNA expression in patient-derived GSCs and U87 cells (*U87* overexpressing ACKR3 were used as positive control) ($n=4$). **(C)** Fluorescence intensity of ACKR3 membrane staining in patient-derived GSCs and U87 cells using flow cytometry (*U87* overexpressing ACKR3 were used as positive control) ($n=4$). **(D)** Percentage of ACKR3 positive cells in patient-derived GSCs using flow cytometry. **(E–F)** ACKR3 and CXCR4 fluorescence intensity (and % of positive T018 GSCs) after CXCL11 or CXCL12 stimulation for 24–48 h ($n=4$). Statistical significance was determined by one-way ANOVA (* $p < 0.05$).

cells ($92.4 \pm 2.2\%$), which suggested CXCL12-mediated CXCR4 downregulation ($N=4$; $p=0.03$) (Fig. 4E). No differences of CXCR4 expression were observed when T018 cells were stimulated with a lower concentration of CXCL12 (2.5 nM) or with CXCL11 (10 nM) (Fig. 4E). After 48 h of stimulation, we observed again a reduced expression of the CXCR4 receptor at the membrane (Fig. 4F). Importantly, no difference was observed for ACKR3 expression upon stimulation with CXCL12 or CXCL11, for 24–48 h (Fig. 4E–F). Whereas reduction in CXCR4-positive cells was suggested in T033 cells as well after 24 h of stimulation by CXCL12, no significant differences were recorded. Again, the expression of ACKR3 remained very low across all conditions (Figure S1B–C). We observed a strong signal for ACKR3 detection in U87 genetically modified for expressing stably ACKR3 (positive control), but also in MCF-7 breast cancer cells, considered as positive control for endogenous ACKR3 expression^{23,24}. Then, we tested a 5-minute incubation of CXCL12, which revealed a significant decrease in ACKR3 signal, revealing receptor internalization in the MCF-7 cells endogenously expressing ACKR3 ($N=4$ or 5; $p=0.014$), but the signal in GSCs remained close to zero due to scarce surface expression of ACKR3 (Figure S1D). In conclusion, these results indicate that ACKR3 is not detected at the membrane of patient-derived GSCs, irrespective of chemokine presence in the culture medium. To make sure ACKR3 is not localized exclusively inside the cells and therefore not detected by surface staining, we used immunofluorescence and high-magnification microscopy. This revealed a very mild ACKR3 staining, without specific colocalization with Rab5, ruling out a restricted localization of ACKR3 in endosomes in GSCs (Figure S1E).

ACKR3 overexpression does not directly influence GBM cell proliferation and invasion

To investigate the role ACKR3 could play in GBM cells that initially express low levels of this receptor, we took advantages of U87 cells and U87 ACKR3 cells and carried out various assays to determine whether the expression of ACKR3 in GBM cells influenced cell proliferation (Fig. 5A). Cell counting revealed no changes in proliferation between U87 ACKR3 and U87 parental cells. CFSE labeling experiments confirmed these results (Fig. 5B–C). We further modified patient-derived GSC T033 via lentiviral transduction to overexpress the ACKR3 receptor (Fig. 5D). Again, no difference in cell proliferation was observed in T033 hACKR3 cells compared to T033 mRFP in the presence or absence of CXCL12 (Fig. 5E–F). Next, we aimed at comparing T033 mRFP and T033 hACKR3 tumorigenicity in vivo. Cells were engrafted in the right striatum of immunodeficient nude mice. After 10 weeks, we observed that both cell types developed large, highly invasive tumors that spread all over the mouse brain. No obvious difference could be observed in T033 hACKR3 compared to mRFP, in terms of growth or invasiveness (Fig. 5G). We also checked in vitro whether ACKR3 expression modified the

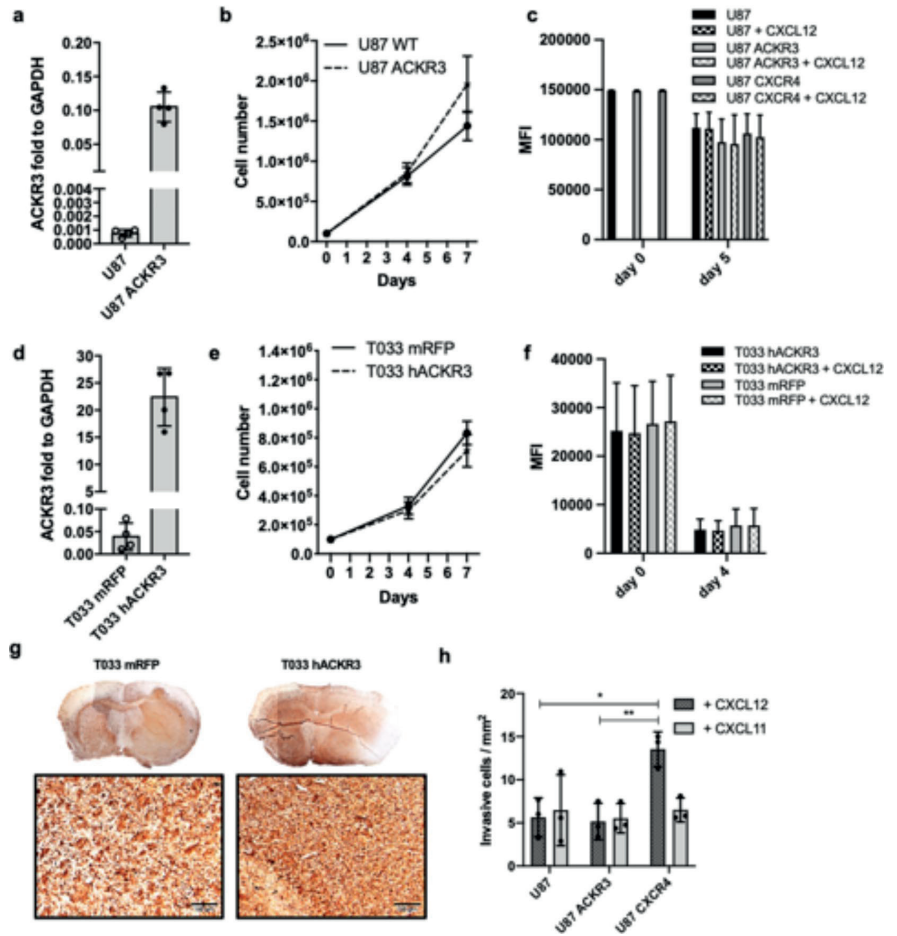


Fig. 5. ACKR3 expression in U87 and T033 cells does not modify cell proliferation or invasion (A) ACKR3 mRNA expression relative to GAPDH in U87 vs. U87 ACKR3 cells ($n=4$). (B) Proliferation assay on U87 vs. U87 ACKR3 cells. Cells were counted at day 0, 4 and 7. ($n=5$) (C) CFSE assay (Cell Trace proliferation assay) on U87, U87 ACKR3 and U87 CXCR4 cells after 5 days with or without CXCL12 (10 nM) ($n=3$) (D) ACKR3 mRNA expression relative to GAPDH in T033 mRFP vs. T033 hACKR3 cells. (E) Proliferation assay on T033 mRFP and T033 hACKR3 cells. Cells were counted at day 0, 4 and 7. (F) CellTrace Violet assay on T033 GSCs after 4 days with or without CXCL12 (10 nM). (G) T033 mRFP and T033 hACKR3 cells were engrafted in the right striatum of nude mice, sacrificed 10 weeks post engraftment, and detected using immunohistochemistry staining against human vimentin. (H) Transwell invasion assay on U87, U87 ACKR3 and U87 CXCR4 cells for 24 h with CXCL11 or CXCL12 ($n=3$) (* $p < 0.05$; ** $p < 0.01$).

invasive properties of U87 cells using Boyden chamber assays. The invasive capacities of U87 ACKR3 cells were not modified compared to U87 wild-type cells, even upon stimulation with CXCL12 or CXCL11. Conversely, the presence of CXCL12 increased the invasiveness of U87 CXCR4 cells, which was not observed upon CXCL11 stimulation ($p=0,010$) (Fig. 5H).

ACKR3 protein expression is not detected in orthotopic tumors, but gene expression is upregulated ex vivo

In vivo, T033 GSCs induce the formation of a highly infiltrative tumors within a few weeks (Figure S2A). At 7 weeks post-graft, immunohistochemistry against human vimentin shows that T033 cells had invaded the whole right hemisphere and reached the contralateral hemisphere via white matter tracts (Figure S2B). We verified that the tumor core was enriched in CXCR4-positive cells, but ACKR3 expression was not detected (Figure S2C). In a second experiment, in vivo engrafted T033 GSCs expressing the RFP and luciferase genes (T033-RFP-Luc) were harvested from different brain regions at 6 weeks post-implantation (before clinical endpoint), dissociated

and put back in culture. We were particularly interested in the impact of the subventricular zone on GBM cell behavior³¹. Interestingly, RFP-positive T033 cells were detected in the tissue harvested from the right SVZ (“SVZ in”) as well as in the right temporal cortex, away from the SVZ (“SVZ out”). We let RFP-positive T033 cells “SVZ in” and “SVZ out” form new tumorspheres in serum-free culture for seven days, then collected them to analyze their *ACKR3* gene expression. Of note, only few RFP-positive cells could be harvested from the contralateral SVZ and cortex which did not regrow. Surprisingly, quantitative RT-PCR analysis showed a significant increase of *ACKR3* expression of T033 GSCs ex vivo, especially from “SVZ in”, compared to T033 in vitro (Fig. 6A–B). Given that, endothelial cells present on the lateral wall of ventricle is described as a major source of CXCL12³², we stimulated T033 GSC with CXCL12 in vitro. However, no differences were observed in terms of *ACKR3* gene expression when GSCs were stimulated with CXCL12 (Fig. 6C). These results suggest that *ACKR3* gene expression is modulated by specific brain microenvironments which does not only rely on CXCL12.

Discussion

The chemokine receptor *ACKR3* has gained increased therapeutic interest in the last years, along with the in-depth elucidation of its atypical mechanism of action, implication in different physiopathological processes and the development of new pharmacological modulators^{33–41}. Together with its CXCL12/CXCR4 signaling partners, it has been suggested as an important player in cancer, including in brain tumors²³. Additionally, our recent transcriptomic analysis of large patient cohorts showed a high expression of *ACKR3* in glioma tissues¹², which several reports have previously associated with disease prognosis. *ACKR3* has therefore been endowed with significant therapeutic potential.

In the 2010’s, several studies described a high *ACKR3* expression in glioma patient tissue and in GBM cells in vitro, mostly using RT-PCR, immunostainings and immunoblots^{25,42–44}. Regrettably, not only did many of these studies focus on cell lines in vitro but they also made use of polyclonal antibodies against *ACKR3* (e.g. ab12780 and ab72100), that had previously been suggested as unspecific⁴⁵, and which we confirm here as not reliable for *ACKR3* detection. These studies are nowadays still cited^{46,47} to support the biological relevance of *ACKR3* in gliomas, setting the ground for clinical trials⁴⁸, and we wished to confront current knowledge with an updated evaluation of this receptor in GBM tissues and cells. After verifying that the 11G8 and 8F11-M16 monoclonal antibodies consistently allow *ACKR3* detection, as previously suggested⁴⁵, we analysed the expression of *ACKR3* in glioblastoma patient-derived tissue samples and cell cultures, using proper controls of *ACKR3* overexpression (U87 *ACKR3*) and endogenous expression (e.g. MCF-7 cells). We report in-situ stainings, paying particular attention to *ACKR3* expression pattern and to the type of cells that express it. *ACKR3* appears associated with blood vessels in tumor tissue (“Type 2”), and present in GFAP+/SOX2 + cells, however not present in EGFR + cells (“Type 1”). We must consider that GFAP+/SOX2 + cells may include intra-tumoral reactive astrocytes, which were previously described as *ACKR3* + in different models of brain pathologies⁴⁹. In line with our results, Walters et al. used the 11G8 antibody to show that *ACKR3* is expressed in tumor cells as well as endothelial cells, in GBM patient tissue⁵⁰. In a very similar manner, Birner et al.⁵¹ describe *ACKR3*-positive cells as “vascular *ACKR3* cells (vas*ACKR3* + cells detected in 58.1% of 320 cases) and much rarer “tumor cell *ACKR3*” (tc*ACKR3* cells in 11.6% of 320 cases). Interestingly, they described the number of vas*ACKR3* + cells as a bad prognosis marker in IDH mutant gliomas, the number of tc*ACKR3* + cells having no prognosis value⁵¹. The role of *ACKR3* + in endothelial cells within GBM tumors warrants further investigation. In that line, Salazar et al. developed a scFv-based chimeric antibody against *ACKR3* that triggers NK-mediated toxicity against both tumor and endothelial cells⁵². Elaborating an *ACKR3*-targeted therapeutic strategy in cancer indeed requires to identify the cell types of interest, and it is now of significant importance to orient future research endeavors considering *ACKR3* in non-malignant cells from the TME (e.g. vascular cells, glial cells, putatively immune cells).

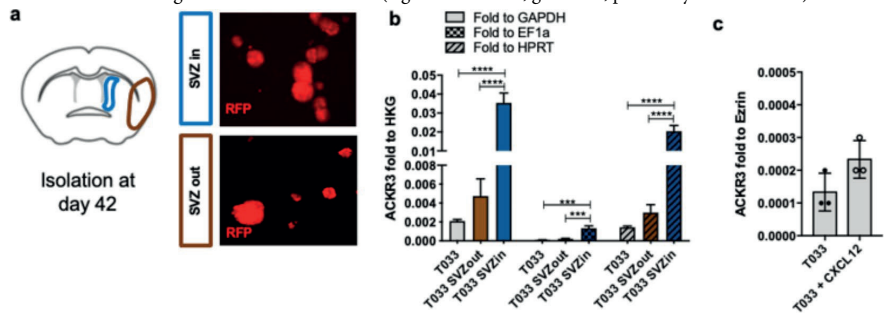


Fig. 6. (A) T033-RFP-LUC cells were engrafted in the right striatum of nude mice, sacrificed 42 days post-engraftment. Two different brain regions were isolated (“SVZ in” and “SVZ out”) and cells were cultured for 7 days before RT-qPCR analyses were performed. (B) Quantitative RT-qPCR analysis allowed to detect *ACKR3* mRNA expression normalized to HKG (GAPDH, EF1a, HPRT) in T033 (in vitro), T033 “SVZ in” (in vivo) and T033 “SVZ out” (in vivo). Statistical significance was determined by one-way ANOVA (*** $p < 0.001$, **** $p < 0.0001$). (C) *ACKR3* mRNA expression relative to *Ezrin* used as HKG in T033 GSCs vs. T033 GSCs stimulated with CXCL12 (10nM).

The putative clinical relevance of ACKR3 in glioma has also emerged from RNAseq data pointing to its high expression. However, bulk GBM tissue data stem from a large mixture of cell types, including peripheral blood, and do not allow to delineate the full picture of ACKR3 function within a tumor. More recently, single-cell RNAseq data helped to shed light on gene expression across different cell subgroups¹². Although such data indicate *ACKR3* as expressed in malignant cells, we firmly demonstrated here that in spite of expressionist presence at the transcript level, ACKR3 protein is undetected in patient-derived GBM cells in vitro, under various conditions. It strongly suggests that mRNA amount may not always be a reliable indicator of the protein abundance. In a different tumor model, Antonello et al. show that ACKR3 surface expression is detected only in a fraction of B-cell lymphoma cells, yet both ACKR3+ and ACKR3- cells have similar levels of mRNA⁵³. Such results can partially be explained by the preferred localization of ACKR3 in intracellular compartments, e.g. endosomes^{54,55}. It has also been shown that ACKR3 surface expression in the same lymphoma cells is increased upon in-vivo “conditioning” in subcutaneous grafts and further ex-vivo isolation, without any modification in *ACKR3* gene expression, again suggesting a particular trafficking of the receptor from intracellular compartments to the plasma membrane⁵⁶. Here however, we do not detect the receptor inside patient-derived GBM cells using immunofluorescence or western-blotting on whole cell lysates. It remains puzzling to observe that in vivo “conditioning” in orthotopic brain xenografts strikingly increases *ACKR3* expression in ex vivo isolated cells although the protein was not detected in tumor tissue.

All in all, whether ACKR3 plays a key role in GBM tumors is still a matter of debate. Here, we concluded that patient-derived GSCs, widely used as in vitro models of GBM tumors in mechanistic studies or drug testing, do not express detectable levels of ACKR3 protein. However, we do not rule out that ACKR3 expression may be tightly regulated upon variable conditions. Given the fine-tuned chemokine-dependent cell-cell interactions, we now consider imperative to study ACKR3 as well as other chemokine receptor function in an exhaustive, well vascularized, immunocompetent tumor microenvironment.

Materials and methods

Human tissues – All human GBM samples were obtained from residual tumor tissue after surgical resection, in collaboration with the Neurosurgery department of the Liège University Hospital (CHU), and the University Hospital Biobank (BHUL, Liège, Belgium), in accordance with relevant guidelines and legal regulations on human body material. None of the included patients opposed to the use of residual human body material, according to the legal regulations in Belgium. Fresh tissue was further (1) dissociated to establish patient-derived glioblastoma stem-like cell cultures (GSCs), (2) formalin-fixed and paraffin-embedded (FFPE) to be used for immunohistochemistry, (3) flash-frozen in liquid nitrogen for molecular biology analyses. Non-tumoral brain tissue was obtained from the BHUL, from brain donations or residual tissue following epileptic foci resections. None of the included patients opposed to the use of residual human body material, according to the legal regulations in Belgium.

Cell culture – In-house patient-derived GSC cultures (T08, T013, T018 and T033) were established from resected adult GBM tumors, and cultured as 3D tumorospheres in Dulbecco’s modified Eagle’s medium and Nutrient Mixture F-12 (DMEM/F12 with GlutaMAX, Gibco) supplemented with 2% of B27 without vitamin A (Gibco), 100 U/mL penicillin and 100 µg/mL streptomycin (ThermoFisher Scientific), 1 µg/mL of heparin (LEO pharma), 20 ng/mL of human EGF (Peprotech) and 20 ng/mL of bFGF (Peprotech). GSC cultures informations are listed in Table S1. T033 cells were stably transduced with a lentiviral vector LV-CMV-hACKR3 or LV-CMV-mRFP for the control vector. For in vivo monitoring, T033 were stably transduced with a lentiviral vector pLV-IRES-Luciferase-mRFP. Plasmid design and related experiments were carried out with the help of the GIGA Viral Vectors platform. The U87 human GBM cell line was obtained from ATCC. U87 cells were transfected with pIRES-puro-ACKR3-WT to overexpress the human ACKR3 or with pIRES-puro-CXCR4-WT to overexpress the human CXCR4, and further selected using puromycin (1 µg/mL and 0.5 µg/mL respectively). The MCF-7 human breast cancer cell line was obtained from ATCC. These cell lines were all cultivated as adherent cell monolayers in Dulbecco’s modified Eagle’s medium (DMEM) containing 10% fetal bovine serum (FBS, Invitrogen), 100 U/mL penicillin and 100 µg/mL streptomycin (ThermoFisher Scientific). Mycoplasma tests were performed on a regular basis.

Immunofluorescent stainings - FFPE human brain tissue sections were heated at 60 °C, dewaxed with 100% xylene (2×20 min), and rehydrated through a set of alcohol baths: 100% ethanol (2×5 min), 95% ethanol, 80% ethanol, 75% ethanol and water (1×2 min each). An antigen retrieval step was performed using Tris-EDTA buffer (10 mM Tris-base, 1 mM EDTA solution, 0.05% Tween 20, pH 9.0). Slices were heated in a pressure cooker for 3 min then were left to cool down at room temperature. Slices were permeabilized with PBS + 0.2% Triton-X100 for 10 min, incubated 30 s with TrueBlack Lipofuscin Autofluorescence Quencher (Biotium), blocked with PBS + 10% normal donkey serum, then incubated with antibodies overnight at 4 °C. ACKR3 (R&D systems, #MAB42273, clone 11G8) was co-stained with SOX2 (Cell Signaling Technology, #3579), PDGFRβ (R&D systems, #AF385), Iba1 (Abcam, #ab5076), GFAP (Abcam, #ab4674), EGFR (Cell Signaling Technology, #4267), Rab5 (Cell Signaling Technology, #3547) and CXCR4 (Abcam, #ab124824). After washing steps, slides were incubated for 1 h with conjugated secondary antibodies (Jackson ImmunoResearch Laboratories) and nuclei were counterstained with DAPI (Sigma). Cells coated on coverslips were fixed in 4% PFA for 10 min at room temperature, permeabilized with PBS + 0.1% Triton-X100, incubated with primary antibodies overnight at 4 °C, then with fluorescently labelled secondary antibodies (Jackson ImmunoResearch Laboratories) for 1 h at 4 °C. Image acquisition was performed with an epifluorescence microscope (Zeiss Apotome) and analyzed on ZENlite and ImageJ 2 (Fiji) softwares. Antibodies are listed in Table S2.

Flow cytometry - Cells were collected by centrifugation at 300 g for 5 minutes. The supernatant was removed, and cells were washed with PBS. Cells were dissociated with 1 mL Accutase (StemCell Technologies) and incubated at 37 °C for 5 minutes. Twice the volume of flow buffer (PBS with 1% BSA, 1 mM EDTA, 0.1% Azide)

were added to quench Accutase action. Cells were collected by centrifugation at 300 g for 5 minutes. Cell pellet was resuspended in 1 mL of flow buffer and were counted to prepare 3×10^5 cells in 100 μ L. APC-conjugated ACKR3 antibody (Biolegend, #331114, clone 8F11-M16) or mouse-anti ACKR3 (R&D systems, #42273, clone 11G8) were added and incubated for 1 h at 4 °C, in the dark. Cells were washed three times by adding 1 mL of flow buffer. A centrifugation step at 300 g for 4 min at 4 °C was performed. After the third wash, supernatant was removed, and cells were resuspended in flow buffer to a final volume of 300 μ L. Samples were recorded on a flow cytometer Canto II (BD Biosciences). Percentage of positive cells as well as Mean Fluorescence Intensity values (Δ MFI = MFI of stained cells – MFI of unstained cells) were analyzed using FlowJo 10 software.

CXCL11 and CXCL12 stimulation - Cells were collected by centrifugation at 300 g for 5 minutes. The supernatant was removed, and cells were washed with PBS. Cells were dissociated with 1 mL Accutase (StemCell Technologies) and incubated at 37 °C for 5 minutes. 3×10^5 cells were plated in a 6-well plate with 1 mL of medium and 2.5 nM or 10 nM human CXCL12 (Peprotech) or 10 nM of human CXCL11 (Peprotech) were added for 24 to 48 h. Flow cytometry analysis was performed using FlowJo 10 software as described above.

Quantitative RT-PCR – Total RNA was isolated using the RNA isolation Nucleospin kit (Macherey-Nagel). RNA was reverse transcribed by using ProtoScript II First Strand cDNA Synthesis Kit (New England Biolabs) with random primers mix. For qRT-PCR reaction samples, a mix of a total volume of 5 μ L was prepared. qRT-PCR Mix contained 2 μ L of the diluted cDNA (10 ng per reaction), 2.5 μ L of SYBRGreen (Eurogentec) and 0.25 μ L of each primer (reverse and forward). Quantitative RT-PCR was performed using LightCycler 480 Roche. Primer sequences are listed in Table S2.

Cell counting – 1×10^5 cells were seeded in 1 mL of medium and incubated at 37 °C for 4 and 7 days. Then, cells were dissociated with trypsin-EDTA (Gibco) and counted with trypan blue staining by using an automatic cell counter (Countess™ II Automated Cell Counter, Thermo Fisher Scientific).

Cell Trace/CFSE – GSCs were stained with CellTrace Violet Stain (Invitrogen, 5 μ M / 10^6 cells) and incubated for 15 min at 37 °C in the dark. Medium was added to quench the excess of dye and centrifuged at 300 g for 3 min. Supernatant was removed and cells were resuspended in culture medium and incubated for 30 min at 37 °C. Then, a cell suspension of 3×10^5 cells was prepared for each condition. The CXCL12 condition was treated with 10 nM human recombinant CXCL12. Cells were incubated for 4 days at 37 °C in the dark. Before flow cytometry analysis, cells were stained with 100 μ L of a 1/1000 Zombie NIR fixable viability dye (SONY) and incubated for 15 min at RT. Cells were analyzed with FACS Canto II (Becton Dickinson).

U87 and U87 ACKR3 cells were stained with CellTrace CFSE Cell Proliferation kit (Invitrogen, 0.25 μ M / 2.10^6 cells) for 15 min at 37 °C in the dark. The excess of free dye was quenched with medium during 5 minutes at 37 °C in the dark. The cells were washed with complete medium and incubated for additional 10 min at 37 °C to allow the reagent to undergo acetate hydrolysis. Then, part of the cells (2.5×10^5 cells per condition) were washed with PBS and stained with Zombie NIR fixable viability dye (Biolegend, dilution 1/3000) during 30 min at 4 °C. The cells were again washed with PBS and analyzed by FACS using a NovoCyte Quanteon Flow Cytometer (Agilent) (condition day 0). The remaining cells (7.5×10^5 cells per condition) were seeded in 6 cm culture dishes either in complete medium (untreated control) or in complete medium supplemented with 10 nM of CXCL12. The cells were incubated for 5 days at 37 °C in the dark. After 5 days, the cells were detached using Versene (Gibco), washed with PBS and stained with Zombie NIR fixable viability dye (Biolegend, dilution 1/3000) during 30 min at 4 °C. The cells were washed with PBS and analyzed by FACS using a NovoCyte Quanteon Flow Cytometer (Agilent). Flow cytometry analysis was performed using FlowJo 10 software as described above.

Invasion assay – For in vitro invasion assays, transwell chambers (Boyden chambers with 8 μ m pore diameter, Thincert, Greiner) were coated with a 1:1 mixture of 0.05 mg/mL collagen type I (Gibco) and 0.5 mg/mL protein of ECM gel (Sigma-Aldrich) in 1:1 PBS-DMEM for 2 h at 37 °C. U87, U87 ACKR3 and U87 CXCR4 cells were detached using Versene (Gibco), washed with PBS and seeded in the upper compartment of the previously coated inserts (3×10^4 cells) in DMEM supplemented with 100 U/mL penicillin and 100 μ g/mL streptomycin (Gibco). DMEM was added as chemoattractant in the lower compartment. After 24 h, cells were fixed with 4% formaldehyde (VWR) in the presence of 1 μ g/mL of Hoechst 33,342 (Thermo Fisher Scientific) for 15 min at room temperature. Non-invading cells were removed, and the invasion was assessed by counting the cells on the lower side of the membrane under fluorescence microscope (Axio Observer Z1, Zeiss). The cell number was determined using QuPath software.

Western blotting – Whole cell lysates were treated with RIPA (Thermo Fisher Scientific) buffer, and extracted proteins were then denatured for 5 min at 95 °C. 20 μ g of proteins were loaded on a 10% acrylamide/bis-acrylamide gel for SDS-PAGE, then transferred onto a PVDF membrane. The membrane was later incubated with blocking solution for 1 h at room temperature, and with primary antibody overnight at 4 °C. Horseradish peroxidase (HRP)-conjugated secondary antibodies (Jackson ImmunoResearch) were then incubated for 1 h at room temperature and signals were revealed with a chemiluminescent HRP substrate before being imaged using the ImageQuant LAS 4000. Antibodies are listed in Table S2.

In vivo orthotopic xenografts – Adult female immunodeficient mice (CrI: NU-Foxn1tm) were obtained from Charles River Laboratories and were used for xenograft experiments. Mice were anesthetized in a cage containing isoflurane. Mice were placed in a stereotaxic frame and kept under isoflurane anesthesia. After a precise bone drill, 1×10^5 T033 (GSCs) cells suspended in 2 μ L of PBS were slowly infused into the right striatum (from Bregma: -0.5 mm AP, +2 mm VL, +2.5 mm DV). Monitoring of tumor growth was performed with in vivo bioluminescence imaging (IVIS, Xenogen), mice health status was evaluated daily, and body weight was recorded every week. Mice were sacrificed when they showed first clinical signs of significant discomfort or suffering. All animal experiments were approved by the ethical committee of the University of Liège (#2290). All experiments were performed in accordance with ARRIVE guidelines.

Mouse brain tissue processing and immunohistochemistry – Mice were euthanized with intraperitoneal injection of 400 mg/kg of Euthasol vet in NaCl 0.9% and immediately perfused intracardially with ice-cold NaCl

0.9% solution containing heparin (LEO Pharma) and then with 4% paraformaldehyde (PFA) in PBS. Brains were removed and postfixed in 4% PFA for 24 h. Brains were cryoprotected in PBS + 30% sucrose for 24 h before being frozen at -80°C . Coronal brain slices of $14\ \mu\text{m}$ were generated with a cryostat and stored at -20°C . For the detection of T033 cells in mouse brain tissue, sections were stained with human Vimentin antibody (MAB3400, Millipore), with the Enzo PolyView IHC kit, according to the manufacturer's instructions.

Ex vivo isolation of cells after tumor growth— Mice were sacrificed by cervical dislocation and brain were collected. Brains were dissected into thick coronal sections at the level of the dorsal horn of the lateral ventricles. In both hemispheres, restricted tissue areas were removed, (1) in the close proximity of the lateral wall of the lateral ventricle (“SVZ in”) and (2) in the temporal cortex, distant from the lateral ventricle (“SVZ out”). Tissue pieces were mechanically and enzymatically dissociated in a solution of Hibernate-A (Fisher Scientific) containing $10\ \text{U/mL}$ DNase and $2.5\ \text{U/mL}$ papain and then incubated for 10 min at 37°C under gentle agitation. DMEM/F12 was then added to dilute the enzymes and the solution was passed through a $100\ \mu\text{m}$ strainer to remove debris. Cells were collected by centrifugation ($160\ \text{g}$ for 10 min) and resuspended in DMEM/F12 supplemented with 2% of B27 without vitamin A (Gibco), $100\ \text{U/mL}$ penicillin and $100\ \mu\text{g/mL}$ streptomycin (ThermoFisher Scientific), $1\ \mu\text{g/mL}$ of heparin (LEO pharma), $20\ \text{ng/mL}$ of human EGF (Peprotech) and $20\ \text{ng/mL}$ of bFGF (Peprotech). Cells were maintained in culture for 7 days, enriched in RFP-positive tumor cells, then collected before a qRT-PCR analysis.

Statistical analyses— The GraphPad Prism 8 software was used for generating graphs and for statistical analysis. The normal distribution of data was verified, and independent comparisons were further performed using unpaired t-tests, Kruskal-Wallis or parametric one-way ANOVA tests. Data were represented as mean \pm SD, with the n representing the number of independent experiments. A p -value ≤ 0.05 was considered as statistically significant.

Data availability

All data used and/or analyzed during the current study available from the corresponding author upon reasonable request.

Received: 30 April 2024; Accepted: 13 September 2024

Published online: 20 September 2024

References

- Louis, D. N. et al. The 2021 WHO classification of tumors of the Central Nervous System: A summary. *Neuro Oncol.* **23**, 1231–1251 (2021).
- Ostrom, Q. T. et al. CBTRUS Statistical Report: Primary brain and other Central Nervous System tumors diagnosed in the United States in 2016–2020. *Neuro Oncol.* **25**, IV1–IV99 (2023).
- Stupp, R. et al. Radiotherapy plus concomitant and adjuvant temozolomide for glioblastoma. *N. Engl. J. Med.* **352**, 987–996 (2005).
- Wen, P. Y. & Kesari, S. Malignant gliomas in adults. *N. Engl. J. Med.* **359**, 492–507 (2008).
- Patel, A. P. et al. Single-cell RNA-seq highlights intratumoral heterogeneity in primary glioblastoma. *Science* **344**, 1396 (2014).
- Nefel, C. et al. An integrative model of cellular states, plasticity, and genetics for glioblastoma. *Cell* **178**, 835–849e21 (2019).
- Dirkse, A. et al. Stem cell-associated heterogeneity in glioblastoma results from intrinsic tumor plasticity shaped by the microenvironment. *Nat. Commun.* **10** (2019).
- Yabo, Y. A., Niclou, S. P. & Golebiewska, A. Cancer cell heterogeneity and plasticity: A paradigm shift in glioblastoma. *Neuro Oncology*. <https://doi.org/10.1093/NEUONC/NOAB269> (2021).
- Zlotnik, A. & Yoshie, O. Chemokine Superfamily Revisit. *Immun.* **36**, 705 (2012).
- Zlotnik, A. Chemokines and cancer. *Int. J. Cancer* **119**, 2026–2029 (2006).
- Poeta, V. M., Massara, M., Capucetti, A. & Bonocchi, R. Chemokines and chemokine receptors: New targets for cancer immunotherapy. *Front. Immunol.* **10**, 379 (2019).
- Isci, D. et al. Patient-oriented perspective on chemokine receptor expression and function in glioma. *Cancers* **14**, 130 (2022).
- Goffart, N. et al. Adult mouse subventricular zones stimulate glioblastoma stem cells specific invasion through CXCL12/CXCR4 signaling. *Neuro Oncol.* **17**, 81–94 (2015).
- Kroonen, J. et al. Human glioblastoma-initiating cells invade specifically the subventricular zones and olfactory bulbs of mice after striatal injection. *Int. J. Cancer* **129**, 574–585 (2011).
- Balabanian, K. et al. The chemokine SDF-1/CXCL12 binds to and signals through the Orphan receptor RDC1 in T lymphocytes. *J. Biol. Chem.* **280**, 35760–35766 (2005).
- Yen, Y. C. et al. Structures of atypical chemokine receptor 3 reveal the basis for its promiscuity and signaling bias. *Sci. Adv.* **8**, 8063 (2022).
- Shimizu, S., Brown, M., Sengupta, R., Penfold, M. E. & Meucci, O. CXCR7 protein expression in human adult brain and differentiated neurons. *PLoS ONE* **6** (2011).
- Gerrits, H. et al. Early postnatal lethality and cardiovascular defects in CXCR7-deficient mice. *Genesis* **46**, 235–245 (2008).
- Sierro, F. et al. Disrupted cardiac development but normal hematopoiesis in mice deficient in the second CXCL12/SDF-1 receptor, CXCR7. *Proc. Natl. Acad. Sci.* **104**, 14759–14764 (2007).
- Wang, Y. et al. CXCR4 and CXCR7 have distinct functions in regulating Interneuron Migration. *Neuron* **69**, 61 (2011).
- Fumagalli, A. et al. The atypical chemokine receptor 3 interacts with Connexin 43 inhibiting astrocytic gap junctional intercellular communication. *Nat. Commun.* **11** (2020).
- Koenen, J., Bachelier, F., Balabanian, K., Schlecht-Louf, G. & Galleo, C. Atypical chemokine receptor 3 (ACKR3): A comprehensive overview of its expression and potential roles in the immune system. *Mol. Pharmacol.* **96**, 809–818 (2019).
- Neves, M. et al. The role of ACKR3 in breast, lung, and brain cancer. *Mol. Pharmacol.* **96**, 819–825 (2019).
- Hattermann, K. et al. Effects of the chemokine CXCL12 and combined internalization of its receptors CXCR4 and CXCR7 in human MCF-7 breast cancer cells. *Cell. Tissue Res.* **357**, 253–266 (2014).
- Hattermann, K. et al. The chemokine receptor CXCR7 is highly expressed in human glioma cells and mediates antiapoptotic effects. *Cancer Res.* **70**, 3299–3308 (2010).
- Levoye, A., Balabanian, K., Baleux, F., Bachelier, F. & Lagane, B. CXCR7 heterodimerizes with CXCR4 and regulates CXCL12-mediated G protein signaling. *Blood* **113**, 6085–6093 (2009).
- Berachovitch, R. D. et al. Endothelial expression of CXCR7 and the regulation of systemic CXCL12 levels. *Immunology* **141**, 111 (2014).

28. Naumann, U. et al. CXCR7 functions as a scavenger for CXCL12 and CXCL11. *PLoS ONE* **5**, e9175 (2010).
29. Gonçalves, T. L. & de Araújo, L. P. Pereira Ferrer, V. Tamoxifen as a modulator of CXCL12-CXCR4-CXCR7 chemokine axis: A breast cancer and glioblastoma view. *Cytokine* **170**, 156344 (2023).
30. Ehrlich, A. T. et al. ACR3-Venus knock-in mouse lights up brain vasculature. *Mol. Brain* **14** (2021).
31. Goffart, N. et al. CXCL12 mediates glioblastoma resistance to radiotherapy in the subventricular zone. *Neuro Oncol.* **19**, 66–77 (2017).
32. Goffart, N. et al. Adult mouse subventricular zones stimulate glioblastoma stem cells specific invasion through CXCL12/CXCR4 signaling. *Neuro Oncol.* <https://doi.org/10.1093/neuonc/nou144> (2015).
33. Cebo, M. et al. Platelet ACKR3/CXCR7 favors antiplatelet lipids over an atherothrombotic lipidome and regulates thromboinflammation. *Blood* **139**, 1722–1742 (2022).
34. Del Barrio, I. M., Wilkins, G. C., Meeson, A., Ali, S. & Kirby, J. A. Breast Cancer: An examination of the potential of ACKR3 to modify the response of CXCR4 to CXCL12. *Int. J. Mol. Sci.* **19** (2018).
35. Song, B. et al. Stromal cell-derived factor-1 exerts opposing roles through CXCR4 and CXCR7 in angiotensin II-induced adventitial remodeling. *Biochem. Biophys. Res. Commun.* **594**, 38–45 (2022).
36. Walters, M. J. et al. Inhibition of CXCR7 extends survival following irradiation of brain tumours in mice and rats. *Br. J. Cancer* **110**, 1179–1188 (2014).
37. Smit, M. J. et al. The CXCL12/CXCR4/ACKR3 Axis in the Tumor Microenvironment: Signaling, crosstalk, and therapeutic targeting. *Annu. Rev. Pharmacol. Toxicol.* **61**, 541–563 (2021).
38. Bayrak, A. et al. Discovery and Development of First-in-class ACKR3/CXCR7 superagonists for platelet degranulation modulation. *J. Med. Chem.* **65**, 13365–13384 (2022).
39. Szpakowska, M. et al. The natural analgesic conolidine targets the newly identified opioid scavenger ACKR3/CXCR7. *Signal. Transduct. Target. Ther.* **6** (2021).
40. Meyrath, M. et al. The atypical chemokine receptor ACKR3/CXCR7 is a broad-spectrum scavenger for opioid peptides. *Nat. Commun.* **11** (2020).
41. Sjöberg, E. et al. The diverse and complex roles of atypical chemokine receptors in cancer: From molecular biology to clinical relevance and therapy. *Adv. Cancer Res.* **145**, 99–138 (2020).
42. Bianco, A. M. et al. CXCR7 and CXCR4 expressions in Infiltrative Astrocytomas and their interactions with HIF1 α expression and IDH1 mutation. *Pathol. Oncol. Res.* **21**, 229–240 (2015).
43. Calatozzolo, C. et al. Expression of the new CXCL12 receptor, CXCR7, in gliomas. *Cancer Biol. Ther.* **11**, 242–253 (2011).
44. Esencay, M., Sarfraz, Y. & Zagzag, D. CXCR7 is induced by hypoxia and mediates glioma cell migration towards SDF-1 α . *BMC Cancer.* <https://doi.org/10.1186/1471-2407-13-347> (2013).
45. Berahovich, R. D., Penfold, M. E. T. & Schall, T. J. Nonspecific CXCR7 antibodies. *Immunol. Lett.* **133**, 112–114 (2010).
46. Neves, M. et al. Special section: From insight to modulation of CXCR4 and ACKR3 (CXCR7) function—minireview the role of ACKR3 in breast, lung, and brain cancer. <https://doi.org/10.1124/mol.118.115279>
47. Samus, M. & Rot, A. Atypical chemokine receptors in cancer. *Cytokine* **176**, 156504 (2024).
48. Giordano, F. A. et al. L-RNA aptamer-based CXCL12 inhibition combined with radiotherapy in newly-diagnosed glioblastoma: Dose escalation of the phase I/II GLORIA trial. *Nat. Commun.* **15**(1), 1–14 (2024).
49. Puchert, M. et al. Astrocytic expression of the CXCL12 receptor, CXCR7/ACKR3 is a hallmark of the diseased, but not developing CNS. *Mol. Cell. Neurosci.* **85**, 105–118 (2017).
50. Walters, M. J. et al. Inhibition of CXCR7 extends survival following irradiation of brain tumours in mice and rats. *Br. J. Cancer.* <https://doi.org/10.1038/bjc.2013.830> (2014).
51. Birner, P., Tchorbanov, A., Natchev, S., Tuettenberg, J. & Guentchev, M. The chemokine receptor CXCR7 influences prognosis in human glioma in an IDH1-dependent manner. *J. Clin. Pathol.* **68**, 830–834 (2015).
52. Salazar, N. et al. A chimeric antibody against ACKR3/CXCR7 in combination with TMZ activates Immune responses and extends survival in mouse GBM models. *Mol. Ther.* **26**, 1354–1365 (2018).
53. Antonello, P. et al. ACKR3 promotes CXCL12/CXCR4-mediated cell-to-cell-induced lymphoma migration through LTB4 production. *Front. Immunol.* **13**, 1067885 (2023).
54. Szpakowska, M. et al. Human herpesvirus 8-encoded chemokine vCCL2/vMIP-II is an agonist of the atypical chemokine receptor ACKR3/CXCR7. *Biochem. Pharmacol.* **114**, 14–21 (2016).
55. Neves, M., Marolda, V., Mayor, F. & Penela, P. Crosstalk between CXCR4/ACKR3 and EGFR signaling in breast Cancer cells. *Int. J. Mol. Sci.* **23** (2022).
56. Puddinu, V. et al. ACKR3 expression on diffuse large B cell lymphoma is required for tumor spreading and tissue infiltration. *Oncotarget* **8**, 85068–85084 (2017).

Acknowledgements

The authors would like to thank the patients and the Neurosurgery department of the Liège University Hospital Belgium. We also would like to thank the GIGA-ULiège Flow cytometry and Cell Imaging (S. Ormenese and colleagues), the NCP platform from LIH (Fanny Hedin, Giovanna Radicchio and Dominique Revets) and Viral Vector (E. Di Valentin and colleagues) platforms for their expert advice and technical support.

Author contributions

DI and VN designed the study. Entire experiments and data analysis were mainly performed by DI and partially by other authors. The manuscript was written by DI and revised by VN, BR, AC and MS. All authors read and approved the final manuscript.

Funding

This work was supported by the National Fund for Scientific Research (FNRS, Télévie) (grants 7.4593.19, 7.4529.19 and 7.8504.20) and the Leon Frédéricq Foundation (Liège, Belgium), the Luxembourg Institute of Health (LIH) through the NanoLux platform, Luxembourg National Research Fund (INTER/FNRS grant 20/15084569 and CORE C23/BM/18068832).

Declarations

Competing interests

The authors declare no competing interests.

Ethics statement

All animal experiments were approved by the ethical committee of the University of Liège (#2290) and were performed in accordance with relevant guidelines and regulations. All animal research reported in this paper was in accordance with the ARRIVE guidelines.

Additional information

Supplementary Information The online version contains supplementary material available at <https://doi.org/10.1038/s41598-024-73064-w>.

Correspondence and requests for materials should be addressed to V.N.

Reprints and permissions information is available at www.nature.com/reprints.

Publisher's note Springer Nature remains neutral with regard to jurisdictional claims in published maps and institutional affiliations.

Open Access This article is licensed under a Creative Commons Attribution-NonCommercial-NoDerivatives 4.0 International License, which permits any non-commercial use, sharing, distribution and reproduction in any medium or format, as long as you give appropriate credit to the original author(s) and the source, provide a link to the Creative Commons licence, and indicate if you modified the licensed material. You do not have permission under this licence to share adapted material derived from this article or parts of it. The images or other third party material in this article are included in the article's Creative Commons licence, unless indicated otherwise in a credit line to the material. If material is not included in the article's Creative Commons licence and your intended use is not permitted by statutory regulation or exceeds the permitted use, you will need to obtain permission directly from the copyright holder. To view a copy of this licence, visit <http://creativecommons.org/licenses/by-nc-nd/4.0/>.

© The Author(s) 2024

II. TME data on ACKR3

Aside to verifying ACKR3 expression in patient-derived tissues and cells, we attempted to verify its expression in TME cells. To do so, it was necessary to work in an immunocompetent mouse model (C57/black6) and switch from human GCSs to GBM mouse cell lines such as CT2A and GL261 cells. To assess the presence of ACKR3 at the cell surface of GBM TME cells, we conducted an *in vivo* experiment. We implanted 50.000 murine GBM cells (GL261 and CT2A) into the brains of immunocompetent C57/Black6 mice and waited for tumor formation. Seventeen days after transplantation, mice were sacrificed and perfused with saline solution and brains were collected. Mechanical dissociation followed by enzymatic dissociation using DNase and Collagenase D was performed 30 minutes at 60°C for brain dissociation. The dissociated tissue was then filtered through a 70µm filter to obtain a single-cell suspension. Then, cells were resuspended in 90% Percoll, and a Percoll gradient was performed in a 15ml tube to isolate cells (Fig. 23). The 15ml tube was centrifuged for 15 minutes at 450g with slow acceleration (acc: 3) and no deceleration (dec: 0) (Fig. 26). After centrifugation, the myelin layer was removed, and the CNS cell ring was recovered for cell labeling. The cells were first labeled with a viability dye (Zombie NIR), incubated for 20 minutes in the dark and then rinsed. Then, cells were labeled with an antibody cocktail, incubated for 30 minutes in the dark and then rinsed again (see the list of antibodies and gating strategy for details) (Fig. 24-25). Cells were analyzed by spectral flow cytometry using the SONY ID700 instrument and analyzed according to a gating strategy via the ID700 analysis software.

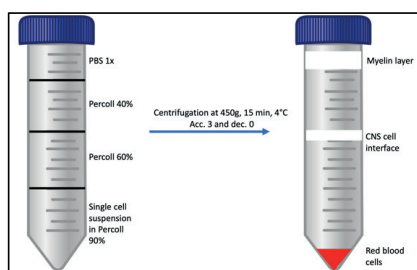


Figure 24: Schematic representation of Percoll gradient to isolate CNS cells.

Target	Fluorochrome
CD45	PE/Cy7
CD49b	PE/DAZZLE
Ly-6G	Spark NIR™ 594
CD19	APC/Fire™ 810
CD11b	Brilliant Violet 711™
I-A/I-E (MHCII)	Brilliant Violet 785™
CD4	Brilliant Violet 421™
CD8a	PerCP/Cyanine5.5
Ly-6C	Alexa Fluor® 700
CD3e	Brilliant Violet 605™
Viability	Zombie NIR™
F4/80	Pacific Blue™
CD163	PE
CD80	Brilliant Violet 650™
CD11c	BUV737
CD25	BUV395
CD125	PE-Cy5
ACKR3	APC

Figure 23 : Table of antibodies for immune cells labelling

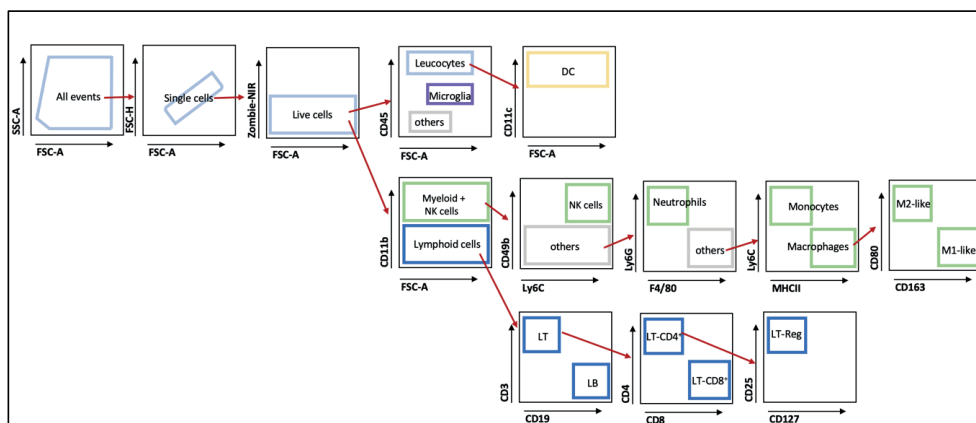


Figure 25: Gating strategy for spectral flow cytometry analysis

This experiment allowed us to determine the immune infiltrate in immunocompetent mouse models bearing GBM. The results showed a predominance of microglial cells in the CT2A and GL261 groups, with the presence of other populations of immune cells in lower quantities, such as T lymphocytes, macrophages and monocytes, dendritic and NK cells. (Fig. 26).

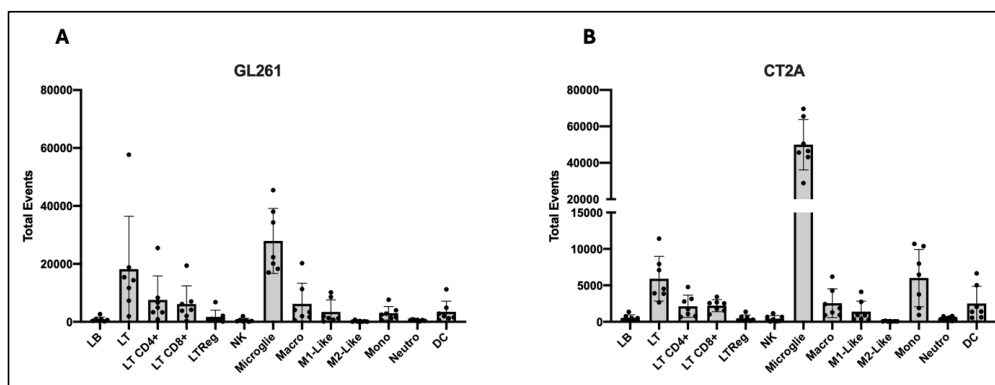


Figure 26 : Flow cytometry experiment showing total events of immune cells in GL261 and CT2A groups.

We next examined ACKR3 expression on the surface of these cells. The results showed that microglial cells, although the majority in the TME, were negative for the receptor, while other cells, such as monocytes, NK cells, T cells, neutrophils and dendritic cells, were positive for ACKR3 receptor (Fig. 27).

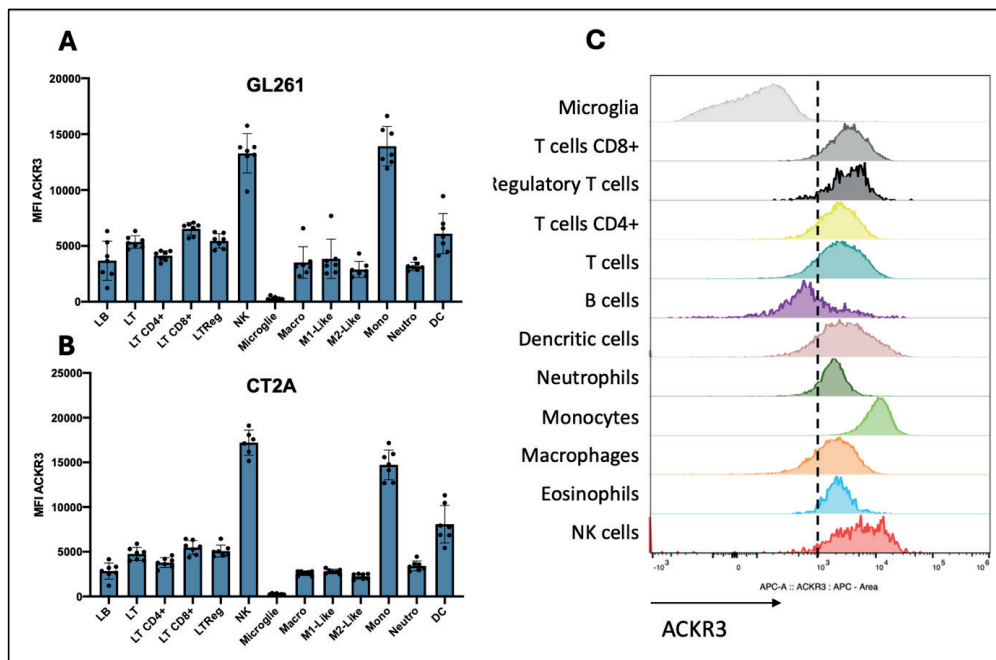


Figure 27: A-B) Mean fluorescence intensity (MFI) of ACKR3 in immune cells of GL261 and CT2A group. C) Histogram of ACKR3 MFI in immune cells.

4. Discussion

ACKR3 receptor is important in cancer signaling particularly with CXCL12 and CXCR4, but detecting it is challenging due to the lack of specific antibodies, complicating the accurate analysis of ACKR3 expression. In 2010, Berahovich et al. already published a report denouncing the non-specificity of the majority of ACKR3 antibodies and recommended the use of the 11G8 antibody, which it found specific and suitable for flow cytometry and immunostaining.

Numerous studies have defined a role for ACKR3 in GBM, using antibodies of questionable specificity. For instance, report of Liu et al. (2010), Salmaggi et al. (2009) and Hattermann et al. (2010) used antibodies later found to be non-specific^{282–284}. Obviously, this issue extends beyond GBM^{285,286} to other cancer like prostate cancer²⁸⁷.

However, recent studies using the 11G8 antibody have provide more reliable data. For example, Flüh et al. showed ACKR3 co-localizes with stem cell markers in GBM, while Liu et al. demonstrated that targeting ACKR3 reduces GBM cell proliferation and migration^{242 237}. Finally, Birner et al. showed that ACKR3 expression in endothelial cells with IDH1 mutation was associated with a better prognosis²⁸⁸.

Therefore, caution is advised when interpreting results and drawing conclusions with new antibodies. In this context, we made sure to use validated antibodies in our study. We employed ACKR3-positive MCF-7 and U87-ACKR3 cells as positive controls and U87 cells as negative controls. Although we faced challenges establishing an ACKR3 knockout model, our immunostaining with 11G8 antibody was reliable. For flow cytometry, we used the APC coupled 8F11-M16 antibody, tested also for its specificity against ACKR3.

We also tested three new specific ACKR3 detection tools: the 8F11-M16 antibody coupled to the APC fluorochrome for surface ACKR3 detection, the LIH383 probe coupled to Cy5 and the hCM11-12 chimera coupled to AZ647. Unfortunately, new non-

specific antibodies continue emerged, such as the ACR-037 and 7TM0080N underscoring the need for careful validation.

In this study, we observed the expression of the ACKR3 receptor in the resected tissues of patients with GBM. The receptor was detected in SOX2, GFAP, and CXCR4⁺ cells. However, at this point in our research, it was challenging to determine if the receptor was present in tumor cells or non-tumor cells, as these markers are found in both healthy and GBM cells. Then, our patient-derived cells in cultures exhibited a very weak, almost negligible signal for membrane ACKR3 expression. This expression did not change even when the cells were treated with the chemokines CXCL11, CXCL12. Therefore, we conclude that tumoral GBM cells in cultures do not express the ACKR3 receptor.

Additionally, ACKR3 overexpression in GBM cell lines and patient-derived cells did not alter their phenotype. Nonetheless, we noted an upregulation of the ACKR3 gene in patient-derived *ex vivo* cells that contacted the SVZ during an *in vivo* experiment. In the same context, Puddinu et al. compared the surface expression of ACKR3 on lymphoma B cells cultured *in vitro* and extracted from xenografts in NOD/SCID mice. Their results showed that *ex vivo* cells had increased ACKR3 expression compared to cells in culture, where expression was low. After 2-3 weeks of culture, *ex vivo* cells could no longer be distinguished from starting cells, indicating a strong influence of the *in vivo* environment on ACKR3 expression. Interestingly, the increase of ACKR3 expression by *ex vivo* cells was not accompanied by variations in gene transcripts²³⁴.

Although ACKR3 does not appear to play a role or is not found on the surface of GBM cells in our study, we propose that it might have a potential function in TME, given its surface expression on immune cells. This finding opens new avenues for future research into the potential role of ACKR3 in the TME of GBM.

Our *in vivo* experiments show that the ACKR3 receptor is expressed on the surface of TME cells and more particularly in monocytes, NK cells and T lymphocytes. Some studies have already analyzed the expression of the receptor in lymphocyte cells. Hartmann et al. observed low expression of ACKR3 at the surface of T cells, while

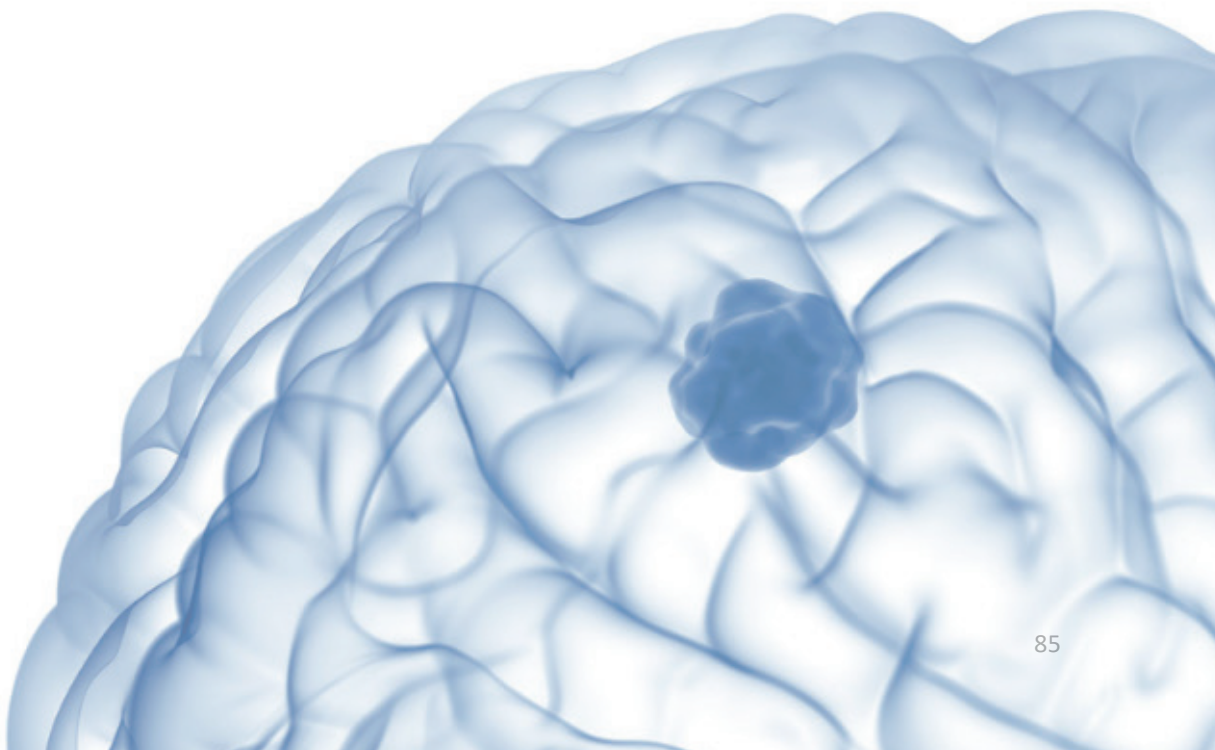
CXCR4 was highly expressed. In contrast, ACKR3 was mainly localized intracellularly in cytosolic compartments of T cells, whereas CXCR4 was exclusively present at the cell surface. This paper highlights the role of ACKR3 in modulating CXCR4-induced integrin activation in T lymphocytes and CD34⁺ progenitor cells in response to CXCL12. Despite its mainly intracellular localization and its weak presence at the membrane, ACKR3 plays a crucial role in integrin signaling and T cell motility, in cooperation with CXCR4²⁸⁹. It would therefore be interesting to study both receptors simultaneously in future experiments and maybe analyze also its intracellular localization.

It would be also intriguing to explore the pharmacological modulation of ACKR3 in preclinical GBM models to determine if using an agonist (VUF11207) or antagonist (ACT1004-1239) could influence immune cell recruitment and/or tumor growth.

A recent study revealed how ACKR3 activation can reshape immunity in the context of GBM. The team of Chang found a correlation between CXCL12 and PD-L1 expression at the surface of TAM through NF- κ B signaling, promoting T cell exhaustion. This mechanism allows tumor to evade the immune system. However, they showed that ACKR3 downregulates CXCL12 expression in GBM cells. They showed that ACKR3 knockdown increases CXCL12 expression, which in turn conduct to PD-L1 expression on TAM leading to CD8⁺T cell exhaustion and creation of immunosuppressive TME. To counteract this effect, they treated preclinical models with ACKR3 agonist, VUF11207. VUF11207 treatment restored T cell activity, previously inhibited by TAM. Additionally, mice treated with the combination of VUF11207 and anti-PD-L1 antibody showed a significant reduction of tumor mass and improved survival. These results suggest that ACKR3 activation could make GBM cells more sensitive to immune checkpoint blockade treatment, thus inducing a potent anti-tumor effect²⁹⁰. One has to note that in this paper, the researchers only assess ACKR3 expression via qPCR experiments, and with only one western-blot analysis on U87 cells, obtained with an antibody we are unsure of, provided as supplementary data.

Concurrently, it would be pertinent to study CXCR4 signaling to see if it is affected or upregulated in response to treatment with an ACKR3 modulators. Treatment with an ACKR3 antagonist might activate more CXCR4 signaling and maybe increase tumor growth. Such an approach could provide valuable insights into the interaction between these two signaling pathways and their roles in immune regulation and tumor progression. This dual investigation into the pharmacological modulation of ACKR3 and CXCR4 signaling could open new perspectives for developing combination therapies aimed at enhancing immune responses and reducing tumor growth in GBM.

PART 5: APPROACHES OF GBM TARGETING VIA VIRUSES



PART 5: APPROACHES OF GBM TARGETING VIA VIRUSES

I. Development of an intraventricular Adeno-Associated Virus-based labelling strategy for glioblastoma cells nested in the subventricular zone. (Lombard, Isci et al. 2024)

1. Overview

Increasing evidence suggest the subventricular zone (SVZ) of the adult brain as a crucial neurogenic area related to GBM initiation, growth and relapse. Many clinical studies associate the proximity of GBM with the SVZ with worst prognosis. In previous studies, we showed that GBM cells infiltrate the brain parenchyma through the white matter tracts and nest in this neurogenic zone. These cells express stem cell markers and become particularly inaccessible to surgery and resistant to conventional radio- and chemotherapy treatments. It becomes imperative to develop targeted methods to specifically reach these SVZ-nested cells. In this regard, our study presents an innovative approach that consists of an intracerebroventricular injection of a recombinant adeno-associated virus (rAAV), aiming to precisely target and track GBM cells established in the SVZ.

2. Adeno-associated viruses (AAVs)

Adeno-associated viruses (AAVs) belong to *Parvovirus* family and were discovered for the first time in 1965 as a contaminant of adenovirus isolates²⁹¹. AAVs are characterized by an unenveloped icosahedral capsid and contain a single-stranded DNA genome (approximately 4.7 kb) composed of poly A, promoter, a replication gene (*Rep*), a structural capsid gene (*Cap*) and an assembly activation protein (AAP) with inverted terminal repeats (ITR)²⁹² (Fig. 28).

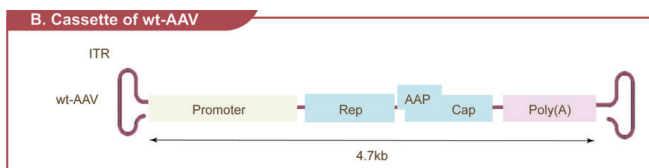


Figure 28: Genome structure of wild type AAV (Adapted from Kang et al. 2023)

1.1. Advantages of AAVs

AAVs have many characteristics that make them attractive and powerful tools for viral gene therapy:

- 1) Unlike many other viruses, AAVs are not associated with human disease, thus considered as non-pathogenic making them “safe” viral vector for genetic therapy^{293,294};
- 2) AAVs are unable to replicate on their own and require the presence of an “helper” virus for propagation. In the absence of this helper virus, AAVs remain stable and enter in latent stage within host genome, reducing the risk of insertional mutation²⁹⁵;
- 3) AAVs can infect a wide variety of cell types allowing them to target many types of tissues and organs. (e.g.: AAV-2 can transduce muscle, liver, brain, retina and lungs²⁹⁶ ;
- 4) AAVs have capacity to stay for a long period in nuclei without any toxicity²⁹⁵;
- 5) The small genome size facilitates their genetic manipulation²⁹⁶ .

1.2. Recombinant AAVS (rAAVs)

Triple co-transfection is the most used technique to produce rAAVs. This method involves co-transfection of HEK293 cells with three plasmids (Fig. 29)²⁹⁷:

- 1) A helper plasmid that delivers *E2A*, *E4*, *VA RNA* genes of the Adenovirus;
- 2) A plasmid that expresses the *Rep* and *Cap* genes;
- 3) And a plasmid that harbors the transgene of interest flanked by ITR.

However, other techniques have also been developed to improve efficiency and stability such as adenovirus-HEK293, recombinant herpes simplex virus-HEK293 and recombinant baculovirus-*Spodoptera frugiperda* (Sf9)²⁹⁸.

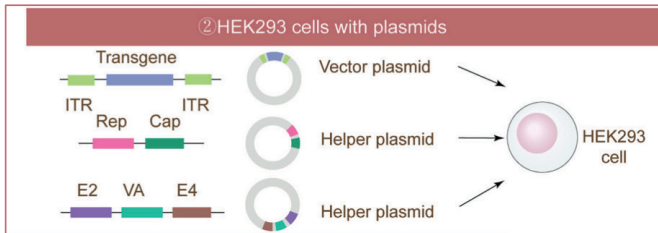


Figure 29 : Triple co-transfection of HEK293 cells for rAAVs production. (Adapted from Kang et al. 2023)

1.3. Ways to administrate rAAVs to the CNS

There are three different ways to administer recombinant AAV to the CNS: intraparenchymal, intra CSF, and intravenous administration (Fig. 30). Intraparenchymal delivery is the most popular route that uses a stereotaxic framed surgical system to deliver high concentrations of vectors directly to target regions of the brain, providing increased precision and successful use in various areas like the striatum and thalamus. Intra-CSF administration allows more widespread distribution into the brain or spinal cord via the intrathecal, intracerebroventricular, and intracisterna *magna* routes, but may provoke a more severe immune response. Intravenous administration, the least invasive, relies on the ability of AAV9 and AAVrh10 serotypes to cross the blood-brain barrier, but requires high doses and can result in hepatotoxicity and an immune response, although these effects are rare thanks to effective immunosuppression strategies^{299,300}.

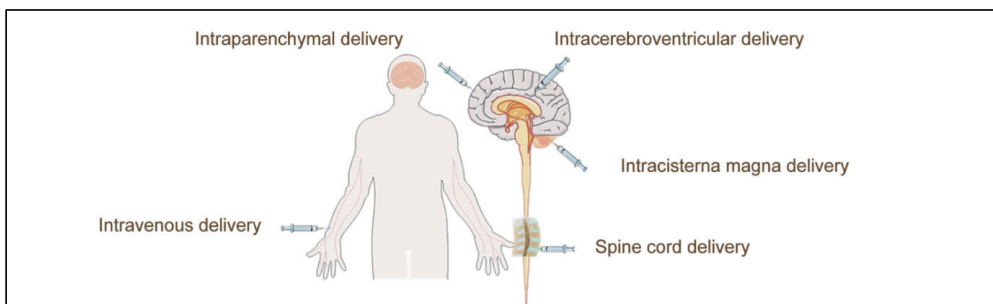


Figure 30: Different way to administrate rAAV. (Adapted from Kang et al. 2023)

1.4. rAAVs in clinical applications

AAVs have already shown promising results in several clinical studies for several CNS diseases, such as neurodegenerative diseases, and neuromuscular diseases. Currently, there are three FDA-approved, commercially available AAV drugs focus on neurological disorders:

- **Upstaza® for aromatic L-amino acid decarboxylase (AADC) deficiency**

AADC deficiency is due to a mutation in the *dopa decarboxylase (DDC)* gene that produces the AADC enzyme. This enzyme is important to produce dopamine for controlling movement. Patients with AADC deficiency don't have a properly working enzyme conducting to a low dopamine production in the brain. This therapy consists of an AAV which deliver *DDC* gene into nerve cells to produce the missing and enabling dopamine production³⁰¹.

- **Luxturna® for inherited retinal dystrophy (IDR)**

IDR is due to a mutation in *retinal pigment epithelium-specific protein 65-kD (RPE65)* gene which leads to a complete blindness in untreated patients. This therapy uses AAV to deliver a functioning copy of *RP65E* in retinal cells. These improvements were durable for 4 years after treatment^{302,303}.

- **Zolgensma® for spinal muscular atrophy (SMA)**

SMA is caused by a defect in *human survival motor neuron (SMN1)* gene. SMA is a genetic disease that causes muscle weakness and infant with SMA leads to disability and death before the age of 2 years. This therapy consists of AAV which is administrated as one time intravenously to deliver a functional copy of *SMN1* gene to motor neuron cells, improving survival and motor function. These improvements were durable for 5 years³⁰⁴.

3. Presentation and contribution to the manuscript

In this part we will present and discuss in detail the findings of our paper entitled “***Development of an intraventricular Adeno-Associated Virus-based labeling strategy for glioblastoma cells nested in the subventricular zone***”, published by Lombard & Isci et al. in 2024 in *Neuro-Oncology Advances*. This project formed the basis of Arnaud Lombard’s thesis, who designed and implemented the entire study. He primarily conducted the initial experiments with GB1 cells, collected the results, and analyzed all the data. Initially, my role in the study focused on performing *in vitro* experiments to select the AAV that best transduced GB1 cells. Finally, I conducted additional *in vitro* and *in vivo* experiments, including those with T033 and T049-LRLG, two *in-house* patient-derived GBM cell cultures. Finally, I analyzed all new results, co-wrote the manuscript with Arnaud Lombard and Virginie Neirinckx, and was responsible for the submission.

Neuro-Oncology Advances

Development of an intraventricular Adeno-Associated Virus-based labelling strategy for glioblastoma cells nested in the subventricular zone.

Arnaud Lombard[†], Damla Isci[†], Gilles Reuter, Emmanuel Di Valentin, Alexandre Hego, Didier Martin, Bernard Rogister, Virginie Neirinckx

Laboratory of Nervous System Diseases and Therapy, GIGA Neuroscience, University of Liège, Belgium; CHR Citadelle, Neurosurgery Department, Liège, Belgium; University Hospital, Neurosurgery Department, Liège, Belgium; GIGA Viral Vectors Platform, University of Liège, Belgium; GIGA Cell Imaging Platform, University of Liège, Belgium; University Hospital, Neurology Department, Liège, Belgium.

[†]These authors contributed equally to this work.

Corresponding author: Virginie Neirinckx ; GIGA Neurosciences - Tour 4 (B36) Quartier Hôpital Avenue Hippocrate 15 B-4000 Liège ; +32 4 366 36 70 ; virginie.neirinckx@uliege.be

Abstract

Background. Glioblastoma (GBM) is a dreadful brain tumor, with a particular relationship to the adult subventricular zone (SVZ) that has been described as relevant to disease initiation, progression, and recurrence.

Methods. We propose a novel strategy for the detection and tracking of xenografted GBM cells that locate in the SVZ, based on an intracerebroventricular (icv) recombinant adeno-associated virus (AAV)-mediated color conversion method. We used different patient-derived GBM stem-like cells (GSCs), which we transduced first with a retroviral vector (LRLG) that included a lox-dsRed-STOP-lox cassette, upstream of the eGFP gene, then with rAAVs expressing the Cre-recombinase. Red and green fluorescence is analyzed *in vitro* and *in vivo* using flow cytometry and fluorescence microscopy.

Results. After comparing the efficiency of diverse rAAV serotypes, we confirmed that the *in vitro* transduction of GSC-LRLG with rAAV-Cre induced a switch from red to green fluorescence. In parallel, we verified that rAAV transduction was confined to the walls of the lateral ventricles. We therefore applied this conversion approach in two patient-derived orthotopic GSC xenograft models and showed that the icv injection of an rAAV-DJ-Cre after GSC-LRLG tumor implantation triggered the conversion of red GSCs to green, in the periventricular region. Green GSCs were also found at distant places, including the migratory tract and the tumor core.

Conclusions. This study not only sheds light on the putative outcome of SVZ-nested GBM cells, but also shows that icv injection of rAAV vectors allows to transduce and potentially modulate gene expression in hard to reach GBM cells of the periventricular area.

Key points

- This study details a new AAV-based method to specifically detect and track glioblastoma cells that nest in the subventricular zone.
- GBM cells nesting in the SVZ shortly leave this region to migrate towards other brain areas, including the initial tumor core.

Importance of the study

Many studies support that the adult subventricular zone (SVZ) can be considered as a specific niche allowing glioblastoma (GBM) initiation, progression, and recurrence. In this context, we aimed to develop a new strategy to label and track the SVZ-nested GBM cells in a preclinical patient-derived orthotopic xenograft model. Such tools that allow to reliably detect hard-to-reach GBM cells in the SVZ will help to shed light on their contribution to disease progression and relapse, and open new perspectives on the genetic modulation of these SVZ-nested cells in a therapeutic context.

Glioblastoma (GBM) is the most frequent malignant brain tumor with dismal prognosis. After a maximal safe debulking surgery and subsequent radio-chemotherapy¹, tumors repeatedly relapse, typically in the margin of the resection cavity but also at more distant places². This secondary progression of the disease seems to originate from the persistence of tumor cells that escaped surgery, resisted treatment, and initiated new tumor formation. Those specific features have classically been associated with GBM stem-like cells (GSCs), long considered as significant actors in tumor maintenance and recurrence³.

The subventricular zone (SVZ) is a neurogenic area in the adult mammalian brain, running along the lateral walls of lateral ventricles (LV)⁴. Adult neural stem cells (NSCs) that locate in this region have been extensively characterized in mice, and were also detected in the SVZ of the adult human brain⁵. Increasing clinical evidence highlighted that the proximity of GBM tumors with the SVZ was associated with greater tumor invasiveness⁶ and poor prognosis⁷⁻⁹. Different studies demonstrated that the accumulation of mutations in SVZ NSCs result in glioma initiation in genetically engineered mouse models^{10,11}. In 2018, Lee et al. demonstrated that NSCs carrying low-level driver gene mutations (e.g. *TP53*, *PTEN*, *EGFR* and *TERT*) are detected in the SVZ of GBM patients, and match with the mutational burden of the tumors. They also used genetic models to show that NSCs with key driver mutations migrate out of the SVZ and develop GBM-like tumors at distant areas¹².

Using glioma patient-derived orthotopic xenograft (PDOX) models, we and others

previously revealed glioma cell chemoattraction and infiltration within the SVZ^{13,14}. These SVZ-nested GBM cells display stem-like features¹⁵, and show modified sensitivity to ionizing radiation (IR)¹⁶. Another study suggested that SVZ-nested GBM cells support tumor resistance to chemotherapy¹⁷. As a whole, these data point out the key contribution of the SVZ in GBM initiation and progression, and putatively in GBM recurrence.

In this context, we aimed to establish an experimental model to specifically detect and track SVZ-nested GBM cells in a PDOX setting. We designed a model that consists in the engraftment of patient-derived GBM stem-like cells (GSCs) that are initially red, and conditionally turn green upon invasion in the SVZ where they would be transduced by an adeno-associated viral (AAV) vector. AAVs are small, non-pathogenic single-stranded DNA (ssDNA) viruses and recombinant AAV (rAAV) vectors have been extensively tested as gene delivery carriers in experimental as well as clinical investigations. In our approach, GSCs were transduced with a retroviral vector including a floxed dsRed/STOP cassette, upstream of the eGFP gene. Upon intracerebroventricular (icv) injection of rAAV delivering the Cre recombinase in the periventricular areas, the floxed dsRed/STOP cassette is excised to allow the expression of eGFP. In this study, we first validated the rAAV-mediated color conversion *in vitro*, and further showed how SVZ-nested GSCs can be detected and tracked *in vivo*, using regular microscopy but also tridimensional lightsheet microscopy after brain tissue clarification. Altogether, these results validate the establishment of an rAAV-based tracking method of GSCs that relocate in the SVZ, and pave the way for further investigation of the SVZ role in GBM biology.

Materials and Methods

Cell culture

Patient-derived GBM stem-like cells (GSCs) (GB1^{18,19}, T033 and T049) were established from residual tumor tissue after surgical resection, in collaboration with the Neurosurgery department of the Liège University Hospital (CHU), and the University Hospital Biobank (BHUL, Liège, Belgium), in accordance with the legal regulations on residual human body material. Relevant data on T033 and T049 patients and GSC cultures are found in Table S1).

GSCs were cultured as neurospheres in serum-free medium, consisting of DMEM/F12 containing 1x B27 without vitamin A (Thermo Fisher), 1% Penicillin-Streptomycin and supplemented with recombinant human epidermal growth factor (EGF) 20 ng/mL, and recombinant human fibroblast growth factor 2 (FGF-2), 10 ng/mL (Preprotech). For two-dimensional cultures, GB1 cells were cultured in DMEM supplemented with 5% fetal bovine serum (FBS) (Lonza) for the time of the experiment. Mycoplasma tests were performed on a regular basis. In culture, cells were maintained in a 5% CO₂ humidified incubator, at 37°C.

Viral vector production

Production of the LRLG retroviral vector: HEK-293T cells were co-transfected together with gene transfer plasmid pMSCV-lox-dsRed/STOP-lox-eGFP-Puro-WPRE [LRLG, Addgene plasmid # 3270]²⁰, packaging plasmid [CellBiolabs # RV-111] and a VSV-G encoding plasmid. Retroviral supernatants were collected, concentrated, filtrated (0.22 μM) and used to transduce GB1, T033 and T049 cells.

Production of recombinant adeno-associated viral (rAAV) vectors: Briefly, pAAV-CMV-mRFP1, pAAV-EF1A-Cre-T2A-eYFP or pAAV-EF1a-Cre plasmids were co-transfected into 293AAV Cell Line (Cell Biolabs, AAV-100) together with a helper plasmid (Part No. 340202 VPK-401 kit) and REP-Cap plasmid (various serotypes: pAAV-1, pAAV-2, pAAV-5, pAAV-8, pAAV-9, pAAV-10²¹ and pAAV-DJ, an artificial capsid that was generated by DNA family

shuffling technology). After collection of the cell supernatant, rAAV vectors were titrated using ABM good kit (#GE931) at a concentration of 1E+12 genome copy/mL (GC/mL) (see Supplementary methods).

rAAV transduction of GSCs and flow cytometry analysis

For the screening of rAAV serotypes, 50.000 naïve GB1 cells were seeded in 6-well plates then cultured either in 2D or in 3D. After 6 hours, culture medium was supplemented with 2.5μL (2.5E+09gc) of rAAVs from different serotypes (1, 2, 5, 8, 9, 10, DJ), expressing RFP. After 72 hours, cells were collected in 500μL of PBS and RFP expression was analyzed using a Fortessa flow cytometer (BD Biosciences) and FlowJo software.

For the in vitro color conversion protocol, 50.000 GB1-LRLG, T033-LRLG and T049 cells were seeded in 6-well plates and supplemented with 2.5μL (2.5E+09gc) rAAV-DJ-Cre, rAAV-1-Cre or r-AAV-5-Cre. At day 3 or 7 of exposition, cells were collected in 500μL of PBS or maintained in culture for 7 additional days with fresh medium without rAAVs (to reach day 14). At each time point, cells were observed in live fluorescent imaging, DsRed and eGFP positivity was assessed by flow cytometry (Fortessa, BD Biosciences) and analyzed on FlowJo software.

Animal experiments

Intracranial transplantation of GSC-LRLG: Crl:NU-Foxn1^{nu} female mice were positioned in a stereotactic frame upon maintained isoflurane anesthesia. A hole was drilled on the skull bone (coordinates from bregma: 0.5 mm AP, +2 mm ML, 2.5 mm DV) and 50.000 GB1-LRLG or 100.000 T033-LRLG cells suspended in 2 μl PBS were injected into the right striatum, as previously described²².

Intraventricular rAAV injection: At 1 week or 4 weeks post-transplantation, a hole was drilled on the skull bone. Then, 1 μL (1E+09gc) of rAAV-DJ-Cre-eYFP (to evaluate virus spreading without tumor) or rAAV-DJ-Cre (to excise the floxed cassette in tumor cells) were injected into the left lateral ventricle (coordinates from bregma: 0.2 mm AP, +0.8

mm ML, 2 mm DV). The needle was left in place for 2 minutes to prevent backflow before withdrawal.

Brain tissue processing

Mice were anaesthetized with an injection of Nembutal® (Pentobarbital 60 mg/mL, Ceva Sante Animal) before an intracardiac perfusion with NaCl 0.9% (VWR International) followed by ice-cold PFA 4% in PBS. Brains were collected, postfixed in 4% PFA overnight at 4°C and then conserved in PBS at 4°C for a maximum of 7 days.

Brain tissue clearing: Clarification of the right and left half-brains was performed as described before²³. First, a 4°C-cocktail of hydrogel monomers (acrylamide with bisacrylamide), formaldehyde and thermally triggered initiators is infused into the tissue, for 24 hours. Then, the hydrogel polymerization is triggered at 37°C for 3 hours, followed by brain extraction and washing in borate-buffered 4% sodium-dodecyl-sulfate (SDS) solution at 37°C for 24h. After that, the brain is cleared using X-Clarity™ Tissue Clearing System II in an Electrophoretic Tissue Clearing Solution for 24 hours at room temperature, to remove the lipids without losing native tissue components. The resulting lipid-extracted and structurally stable tissue–hydrogel hybrid is then washed in PBS with 0,1% of Triton X-100, for 2 days at room temperature, and finally stored in PBS-azide at 4°C. Then, half-brains are immersed in a refractive index (RI) homogenization solution (Refractive Index Matching Solution; RI~1.460) to render it transparent to light.

Lightsheet microscopy: Half-brain images were acquired with a dual illumination lightsheet Z1 fluorescence microscope (Zeiss), equipped with a 5x/0.16 NA dry objective at a zoom of 0.36. Samples were illuminated with 515 nm at 15%, 561 nm at 20% and 638 nm at 15% lasers. 1240 x 1240 pixel images (scaling x,y = 2.538 μm) were acquired using 2 sCMOS (pco.edge) camera with 30 ms exposure time. For Z-stack imaging, between 500 and 650 slices were acquired with a 9 μm z-step size. Images were stitched and reconstructed using Arivis Vision 4D software. Images were analyzed using Imaris (version 9.0) software and referenced

using Allen Mouse Brain Atlas. To determine the distance between the LV and the transduced cells in the CP, we reconstructed the whole volume of the LV by contouring it on serial coronal sections (every 10 μm) and measured the distance to the surface of the reconstructed LV volume.

Immunostainings

Immunohistochemistry and fluorescence on brain sections: Brain tissue was processed as described above. 14 μm-thick coronal brain slices were generated with a cryostat and stored at -20°C. Xenografted T033-LRLG cells were detected with human Vimentin antibody, with the Enzo PolyView IHC kit, according to the manufacturer's instructions. Brain slices were permeabilized and blocked with PBS + 0,3% Triton-X100 + 10% donkey serum for 1 hour and then incubated with anti-eGFP antibody overnight at 4°C. After washing steps with PBS, slides were incubated for 1 hour with Cy5-conjugated secondary antibody, to ensure the specificity of the signal (Jackson ImmunoResearch Laboratories). Antibodies against Ki67 and SOX2 were used for costainings. Nuclei were counterstained with DAPI (Sigma). Image acquisition was performed with an epifluorescence microscope (Zeiss Apotome) and analyzed on ImageJ (Fiji) software (see Supplementary methods).

Immunofluorescence on cells: 20.000 GB1 cells were transduced with rAAVs expressing RFP (serotypes 1, 2, 5, 8, 9, 10 and DJ). After 72 hours, cells were fixed with paraformaldehyde (PFA) 4% and incubated with anti-RFP antibody diluted in PBS + 0.1% donkey serum and 0.1% Triton X-100, followed by a second incubation with Rhodamine red X-conjugated antibodies (Jackson ImmunoResearch Laboratories). Nuclei were counterstained with Hoescht (Thermo Fisher Scientific cat#62249), and images were acquired with a Zeiss AxioImager Z1 epifluorescence microscope (see Supplementary methods).

Statistics

Statistics were realized thanks to GraphPad Prism v8. Normality was assessed by a Shapiro-Wilk test and either Student-t test, one-

way ANOVA or 2way ANOVA were performed for group comparisons. Statistical significance was set at 0.05. Data are indicated as mean +/- standard deviation, with the number of independent experiments/animals indicated as N in the figure legends.

Study approval

Patient tissue was obtained in collaboration with the Neurosurgery department of the Liège University Hospital (CHU), and the University Hospital Biobank (BHUL, Liège, Belgium), in accordance with the legal regulations on human body material. This study was approved by the local human ethics committee.

CrI:NU-Foxn1^{nu} female mice were purchased at Charles River laboratories, housed in group of four individuals (ZT0: 7am, ZT12: 7pm). Mice health status was evaluated daily, and body weight was recorded every week. Tumor endpoint and animal sacrifice was considered at the first signs of significant discomfort or suffering. No mice had to be sacrificed at an early timepoint in this study. All animal experiments were approved by the ethical committee of the University of Liège (local protocol number 1737).

Results

In vitro assessment of rAAV transduction efficiency using diverse serotypes

First, we determined the efficiency of various AAV serotypes in transducing patient-derived GSCs in vitro. As a first screening, GB1 cells were infected with rAAVs from seven different serotypes (rAAV-1, rAAV-2, rAAV-5, rAAV-8, rAAV-9, rAAV-10 and rAAV-DJ) all expressing the red fluorescent protein (RFP), and then analyzed by flow cytometry (**Fig1, A**). In 2D-culture conditions, the percentage of RFP⁺ GB1 cells after three days was higher than 50% with rAAV-1 (97.78±1.77%), rAAV-5 (67.23±4.42%) and rAAV-DJ (60.09±1.29%). In contrast, the transduction efficiency was significantly reduced for rAAV-2, rAAV-8, rAAV-9, rAAV-10 ($p < 0.0001$) (**Fig1, B & FigS1 A,C**). When GB1 cells were cultured in 3D neurospheres, the percentage of RFP⁺ tumor cells was again

higher for rAAV-1 (64.69±5.1%), rAAV-5 (56.98±4.1%) and rAAV-DJ (60.11±8.3%), with again a significantly reduced transduction for rAAV-2, -8, -9, and -10 (p -values ranging from <0.05 to <0.001) (**Fig1, C & FigS1, B-C**). Those results were confirmed with an anti-RFP immunostaining performed on coated GB1 cells after three days of exposition to rAAV-1, rAAV-5 and rAAV-DJ (**Fig1, C**). Altogether, we concluded that rAAV-1, rAAV-5 and rAAV-DJ are the most efficient serotype for GSC transduction in vitro.

In vitro validation of rAAV-Cre-mediated color conversion of GSC-LRLG

Prior to applying the red-to-green conversion in an in vivo setting, we verified the ability of the rAAV serotypes 1, 5 and DJ to induce such conversion in patient-derived GSCs in culture. T033, T049 and GB1 GSCs were stably transduced with a retroviral vector including a floxed dsRed/STOP cassette, upstream of the eGFP gene (LRLG vector). T033-LRLG, T049-LRLG and GB1-LRLG were further exposed to rAAV-1-Cre, rAAV-5-Cre or rAAV-DJ-Cre (**Fig2, A**). Globally, all rAAV serotypes induced a progressive color conversion of T033-LRLG, from dsRed⁺ (red) to dsRed⁺/GFP⁺ (orange) and finally eGFP⁺ only (green) (**Fig2, B-E**). At 14 days, the rAAV-DJ-Cre induced 75.92±5.24% eGFP⁺ cells in T033-LRLG, which is significantly higher than rAAV-5-Cre (56.87±4.20%; $p=0.0193$), and slightly increased compared to rAAV-1-Cre (62.99±10.91%; $p=0.0309$). The % of eGFP⁺ cells was significantly higher at day 14 compared to day 7 in rAAV-DJ-Cre transduced T033-LRLG ($p=0.0314$) (**Fig2, F-G**). A similar time-dependent color conversion was observed upon transduction of T049-LRLG with the three rAAV serotypes (**Fig2, H-J**). The rAAV-DJ-Cre induced 81.78±5.42% eGFP⁺ cells at day 14, while lower number of eGFP⁺ were induced with rAAV-5-Cre (66.45±11.39%; $p=0.2419$), and with rAAV-1-Cre (69.49±6.36%; $p=0.1324$). Again, the % of eGFP⁺ cells was significantly higher at day 14 compared to day 7 in rAAV-DJ-Cre transduced T049-LRLG ($p=0.0027$) (**Fig2, K-L**). We also tested the rAAV-DJ-Cre in GB1-LRLG and observed a progressive increase of

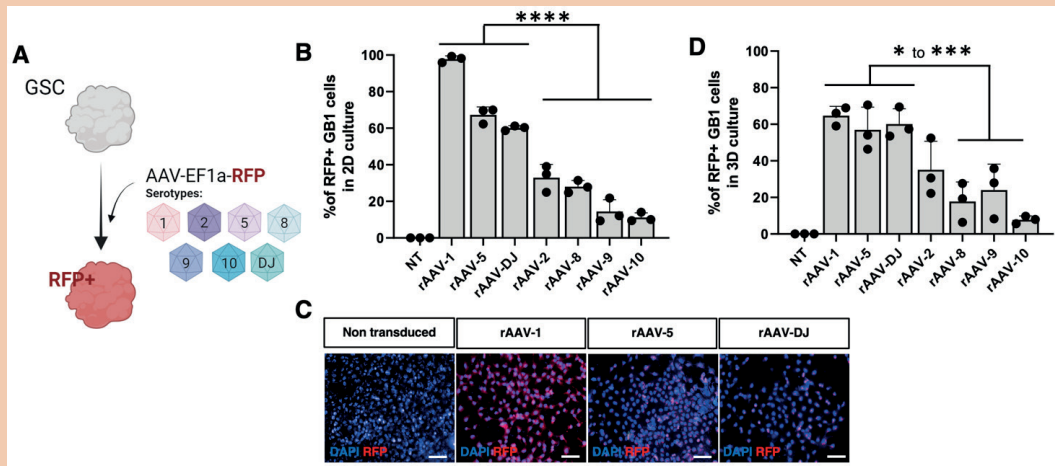


Figure 1: rAAV-1, rAAV-5 and rAAV-DJ efficiently transduce patient-derived GBM stem-like cell (GSC) cultures. (A) Flowchart representing the rAAV-RFP transduction of GSCs for the screening of most efficient serotypes (created with BioRender®). (B) % GB1 cells expressing RFP in 2D-culture after a three-day exposition to rAAVs (n=3 independent experiments) (one-way ANOVA, p-values for each comparison in FigS1, A). (C) Immunofluorescent staining of the RFP protein (red) after rAAV-DJ-RFP transduction of GB1 cells (Scale bar = 50 μ m). (D) % GB1 cells expressing RFP in 3D-culture after a three-day exposition to rAAVs (n=3 independent experiments) (one-way ANOVA, p-values for each comparison in FigS1, B).

eGFP⁺ cells, reaching 63.36 \pm 0.14% at day 14 (Fig S1, D-E). Based on these results, we concluded that the three rAAV serotypes adequately transduce GSC-LRLG and induce red-to-green conversion in vitro, with the rAAV-DJ emerging as the most efficient.

Dissemination of rAAV-Cre-eYFP after icv injection in the naïve brain

After injection in the brain, the dissemination of the AAV-DJ serotype is reported as more confined compared to other serotypes²¹. Here, we wanted to evaluate the spreading of rAAV-Cre vectors upon intracerebroventricular (icv) injection, to assess whether rAAV transduction would be restricted to the walls of the lateral ventricles. rAAV-1-Cre-eYFP, rAAV-5-Cre-eYFP and rAAV-DJ-Cre-eYFP were icv injected in naïve nude mice (n=3 mice per group), and brains were collected 1 week after injection. Imaging of the brain sections showed that eYFP signal is tightly limited to the borders of the lateral ventricles (Fig3, A), which would ensure that rAAV transduction of GBM cells in a xenograft model would be restricted to cells within the SVZ.

Furthermore, we could analyze mice that were icv injected with rAAV-DJ-Cre-eYFP, at 4 weeks post-injection, after brain tissue clearing and lightsheet microscopy, to precisely quantify rAAV spreading at longer term. We determined the volume of YFP-positive signal for different regions adjoining the lateral (LV) and the third (V3) ventricles (n=5 mice) (Fig3, B). Medially to the LV, we observed YFP-positive signal in the Lateral Septal nucleus (LSc) (Fig3, B-C, yellow arrow). Laterally to the LV, YFP-positive signal was detected in a few layers of cells in the SVZ and in the medial part of the caudoputamen (mCP), anteriorly (Fig3, B-C, orange arrow) and in its dorsolateral part (dlCP), posteriorly (Fig3, B-C, purple arrow). In the nearby of LV posterior wall, we also highlighted the transduction of few cells in the fimbria (Fi) (Fig3, B-C, red arrow) and in the Ammon's horn of the hippocampus (HPF), where the YFP⁺ area was the larger (Fig3, B-C green arrow). Some isolated cells in the corpus callosum (CC) (Fig3, B-C, grey arrow) were also detected. The YFP⁺ area was significantly higher in the HPF compared to the mCP (p=0.0409), to the Fi (p=0.0236) and to the CC (p=0.0268), which suggests that cells are more likely transduced in structures enriched in

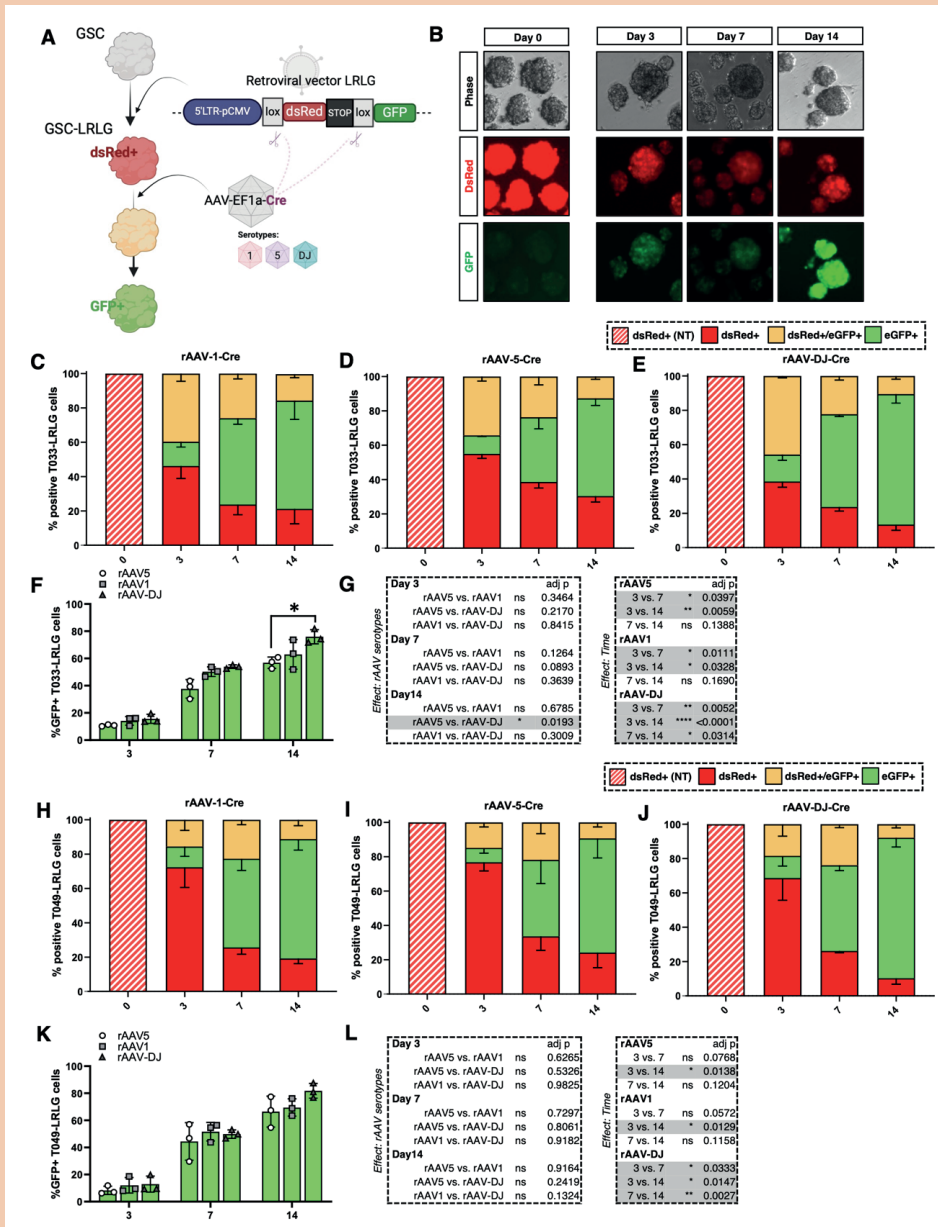


Figure 2: rAAV-1, rAAV-5 and rAAV-DJ efficiently convert GSC-LRLG cells in culture from dsRed⁺ to eGFP⁺. (A) Flowchart representing of dsRed gene excision and fluorescent eGFP gene expression in GSCs induced by rAAV-mediated Cre recombinase (created with BioRender®). (B) Representative images of the dsRed and eGFP signals in T033-LRLG cultures transduced with rAAV-DJ-Cre, over 14 days. (C-D-E) % T033-LRLG cells that are found dsRed⁺ (red), dsRed⁺/eGFP⁺ (orange) or eGFP⁺ only (green) at 3, 7 and 14 days post-transduction with rAAV-1-Cre (C), rAAV-5-Cre (D) and rAAV-DJ-Cre (E) (NT= non transduced, at day 0). (F) % eGFP⁺ T033-LRLG cells over time, with the three rAAV serotypes (n=3 independent experiments). (G) Results from the 2way ANOVA, providing the statistical effect of the serotype and the effect of time. (H-I-J) % T049-LRLG cells that are found dsRed⁺ (red), dsRed⁺/eGFP⁺ (orange) or eGFP⁺ only (green) at 3, 7 and 14 days post-transduction with rAAV-1-Cre (H), rAAV-5-Cre (I) and rAAV-DJ-Cre (J) (NT= non transduced, at day 0). (K) % eGFP⁺ T049-LRLG cells over time, with the three rAAV serotypes (n=3 independent experiments). (L) Results from the 2way ANOVA, providing the statistical effect of the serotype and the effect of time.

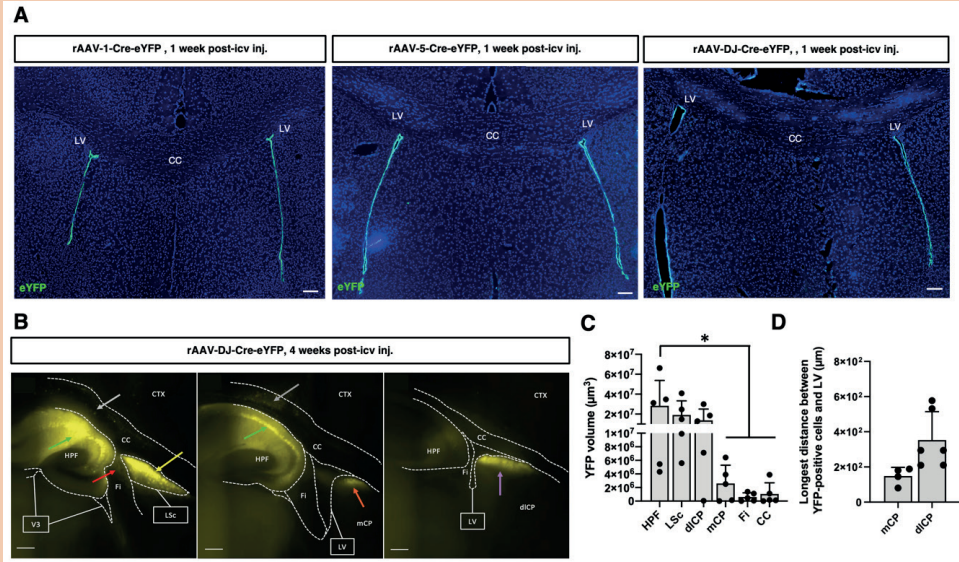


Figure 3. The rAAV-DJ-Cre-eYFP has LV-restricted spreading 1 week after icv injection and disseminates to adjacent neuron-rich structures after 4 weeks. **(A)** rAAV-1-eYFP, rAAV-5-eYFP and rAAV-DJ-eYFP remain confined to the lateral ventricle walls one week after icv injection. Images are representative of $n=3$ mice per serotype tested (scale bars = $100\ \mu\text{m}$). **(B)** Sagittal views at the VL medial wall ($400\ \mu\text{m}$ laterally to Bregma), through the VL (1mm laterally to Bregma) and at the VL lateral wall ($1500\ \mu\text{m}$ laterally to Bregma) to visualize YFP⁺ cells (scale bars = $400\ \mu\text{m}$). **(C)** Comparison of the volume (in μm^3) of YFP fluorescence in transduced areas in the LV neighboring ($n=5$ mice) (one-way ANOVA, p -values for each comparison in FigS2, A). **(D)** Longest distance (μm) between the further YFP⁺ cells in the mCP and dLCP and the lateral wall of the VL ($n=5$). Legend: *LSc* : lateral septal nucleus, *mCP* : medial caudoputamen, *dLCP* : dorsolateral caudoputamen, *Fi* : fimbria, *CC* : corpus callosum, *HPF* : hippocampus.

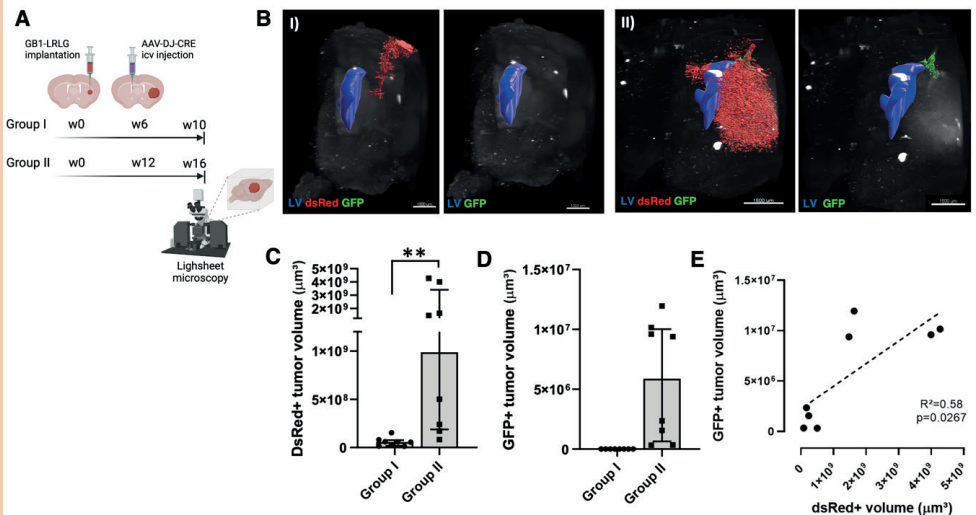


Figure 4. rAAV-DJ-Cre icv injection induces red-to-green conversion of GB1-LRLG that reached the subventricular zone (SVZ) in an orthotopic xenograft model. **(A)** Flowchart representing the experimental workflow. GB1-LRLG cells were implanted in nude mice and rAAV-DJ-Cre-YFP was icv injected at week 6 (group I) or week 12 (group II). Then mice were sacrificed at week 10 or week 16 respectively. **(B)** Analysis of right hemispheres with a lightsheet microscope, highlighting dsRed and eGFP-positive tumor areas. **(C)** Quantification of the dsRed-positive tumor area in mice from groups I and II (Mann-Whitney U-test, $n=8$ mice per group). **(D)** Quantification of the eGFP-positive tumor area in mice from groups I and II ($n=8$ mice per group). **(E)** Correspondence between dsRed⁺ and eGFP⁺ volumes in group II animals (linear regression).

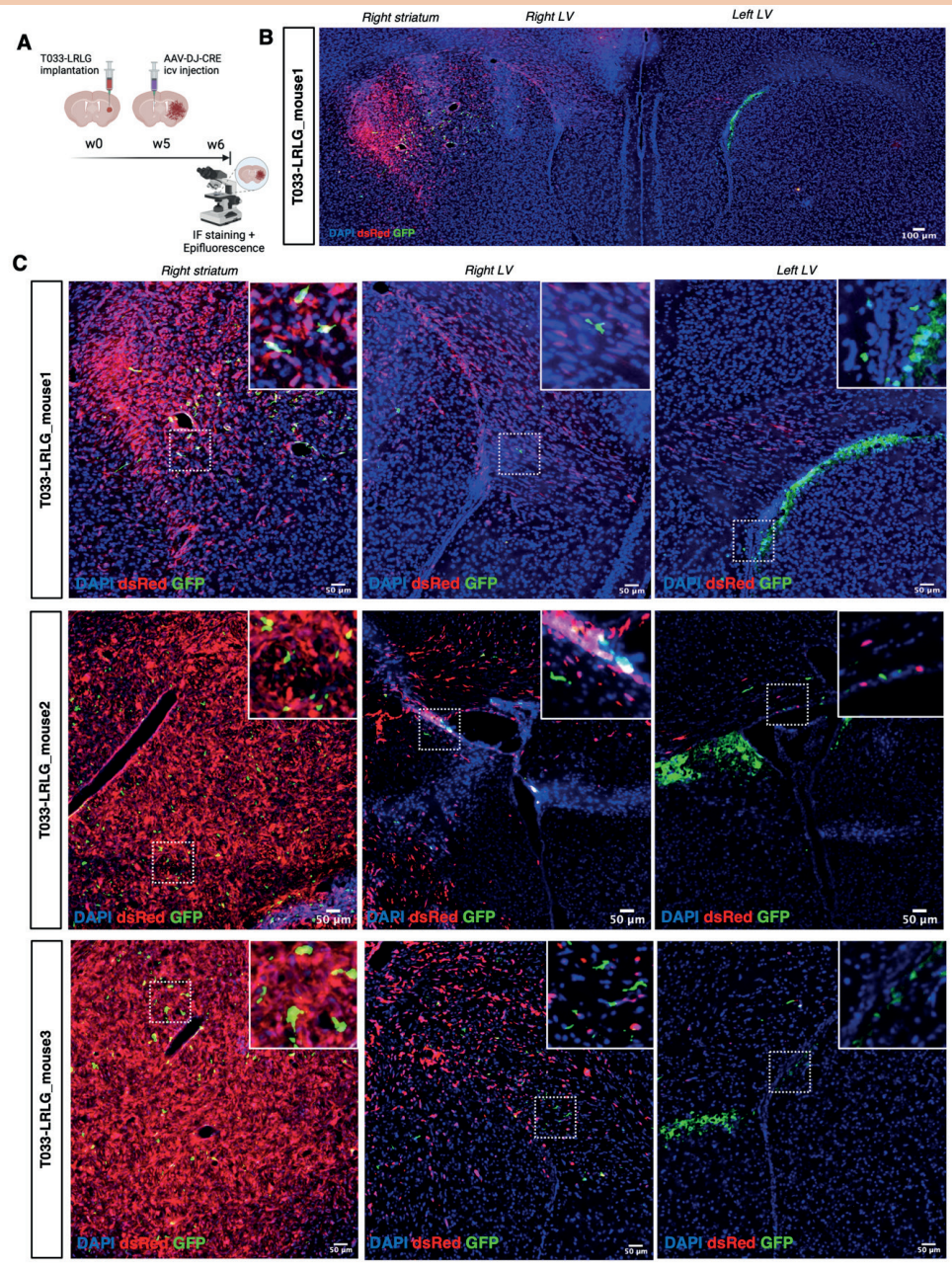


Figure 5. rAAV-DJ-Cre icv injection induces red-to-green conversion of T033-LRLG that reached the subventricular zone (SVZ) in an orthotopic xenograft model. **(A)** Flowchart representing the experimental workflow. T033-LRLG cells were implanted in nude mice and rAAV-DJ-Cre-YFP was icv injected intraventricularly at week 5, and mice were sacrificed at week 6. **(B-C)** Immunofluorescence stainings of eGFP+ (green) and dsRed+ (red) cells in different regions of the mouse brain (right striatum, right lateral ventricle, left lateral ventricle). Sections of three different animals are displayed (scale bar = 50 or 100 μm).

neuronal bodies (HPF, LSc, CP), rather than in white matter tracts (Fi, CC). Finally, we measured the longest distance between the LV and the transduced cells in the mCP (P25<median<P75: 128,75<162,5<182 μ m) and in the dlCP (210 μ m-294 μ m-531,67 μ m) (Fig3, D). This data shows that 4 weeks after injection, the rAAV-DJ-C-eYFP spreads towards other structures distant from the LV, although below five hundred micrometers.

In vivo validation of rAAV-Cre-mediated color conversion of GSC-LRLG that invaded the subventricular zone (SVZ)

Previous work from our group has shown that GB1-LRLG cells form a symptomatic tumor upon implantation in the striatum of nude mice within 12 to 16 weeks, associated to an invasion of the subventricular zone (SVZ)²². Hence, we icv injected the rAAV-DJ-Cre at week 6 after GB1-LRLG cell engraftment, before SVZ invasion (group I, n=8 mice), and at week 12, after SVZ invasion (group II, n=8 mice). We finished the experiment 4 weeks later, respectively at week 10 (group I) and at week 16 (group II) (**Fig4, A**). Brain tissue was cleared, and the right hemispheres were imaged with a lightsheet microscope, and analyzed with Imaris[®] software, for highlighting dsRed⁺ and eGFP⁺ tumor cells. As expected, the median volume of dsRed-positive tumors in the CP was reduced in group I μ m³ (P25<median<P75: 2.40<5.73<6.66 $\times 10^7 \mu$ m³) compared to group II (2.23<9.88<2.23 $\times 10^9 \mu$ m³) (p=0.0016) (Fig4, B-C). In group I, we did not observe any contact of the tumor with the SVZ and no eGFP⁺ signal was detected (**Fig4, B-D**). However, we observed eGFP⁺ signal in most animals from group II (volume of P25<median<P75: 1.25<5.88<9.74 $\times 10^6 \mu$ m³), especially those with the largest dsRed⁺ tumor volume (R²:0.58, p=0.0267) (**Fig4, D-E**).

We also tested the ability of the rAAV-DJ-Cre to promote red-to-green conversion in another GSC intrastriatal xenograft, within a different timeframe. At 6 weeks, T033-LRLG cells establish a large infiltrating tumor that invade both the right and left LV lateral walls via the corpus callosum (FigS2). The rAAV-DJ-Cre was icv injected in the left LV at week 5 post-

engraftment (**Fig5, A**). One week later, mice were sacrificed, and brains collected. Immunostainings showed dsRed⁺ T033-LRLG cells scattered in the right hemisphere, as well as in the right and left LV. Not only are eGFP⁺ cells detected near the left LV, but also in the proximity of the right LV and within the tumor core (**Fig5, B-C**). These eGFP⁺ cells are SOX2⁺ and Ki67⁺, which indicates a maintained potential for proliferation (**Fig6**). These results support the hypothesis that dsRed⁺ tumor cells develop and migrate out of the tumor mass to reach the LV walls, where they switch from dsRed⁺ to eGFP⁺. Interestingly, these eGFP⁺ cells appear to leave the LV and reinvade the initial tumor core. In absence of tumor cells in the LV surroundings (i.e. for tumors that did not grow sufficiently large), we did not see any eGFP⁺ cell at all (FigS3), which is in line with the restricted diffusion of the rAAV and further supports the specificity of the SVZ-located transduction. Altogether, these results demonstrate the relevance of an icv AAV-based color conversion approach to detect GBM cells that invade the LV wall/SVZ. These results also shed light on the putative role of SVZ-nested GBM cells in tumor evolution and recurrence.

Discussion

Many studies have evidenced the key contribution of the subventricular zone (SVZ) of the adult brain in glioblastoma (GBM) initiation, maintenance and recurrence. At the clinical level, the proximity of GBM tumors with the SVZ (SVZ⁺ GBM) has been associated with worse prognosis⁷⁻⁹, and different experimental findings have demonstrated the protective role of the SVZ environment against therapy^{16,17}. SVZ⁺ GBM is associated to particular methylation signatures²⁴, and recent single cell transcriptomic data suggest a differential cell type enrichment and related therapeutic vulnerabilities²⁵. Such data fosters deeper investigation of the molecular mechanisms that underlie the influence of SVZ environment on GBM cell fate and phenotype, and the development of experimental tools to do so. In this study, we harnessed different types of viral

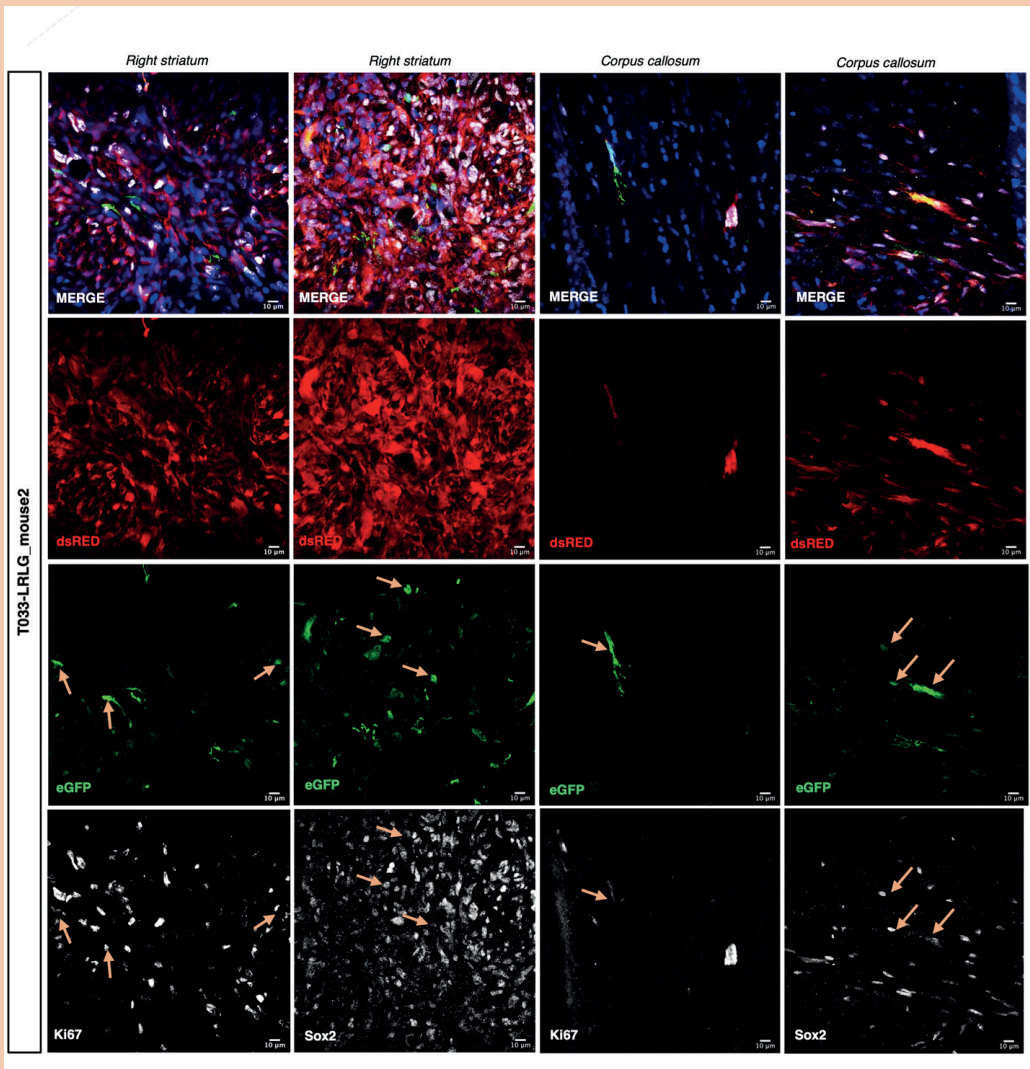


Figure 6. Characterization of eGFP+ T033-LRLG cells. Immunofluorescence costainings of SOX2 and Ki67 (white) with eGFP+ (green) and dsRED+ (red) cells in different regions of the mouse brain implanted with T033-LRLG and one week after rAAV-DJ-Cre icv injection. Sections of three different animals are displayed (scale bar = 100 µm).

vectors to label and track GBM cells invading the SVZ in an orthotopic xenograft model. Using a color-conversion approach, we observed that implanted dsRed⁺ patient-derived GBM stem-like cells (GSCs) do infiltrate the brain and reach the SVZ where they turn eGFP⁺, with the help of a recombinant adeno-associated viral (rAAV) delivering a Cre recombinase inside the lateral ventricle. To our knowledge, this study proposes an original approach to study SVZ-nested GBM cells, and also is the first to suggest that GBM cells nesting in the SVZ may actually leave this region to repopulate other brain areas. Of note, this experimental strategy is versatile, and the SVZ-restricted color-conversion approach could be further refined. Whereas a similar LRLG vector-based method has previously been used for monitoring transduction efficiency²⁶, or for lineage tracing²⁷, other studies further exploited this strategy, to monitor environmental influences on cancer cells, i.e. for fate-mapping post-hypoxic breast cancer cells and investigating their phenotype and role in the metastatic process, using a HIF1 α -dependent expression of Cre recombinase^{28,29}. Such conditional Cre expression may also be applied and highly relevant in the exploration of SVZ molecular influences on GBM cells. For example, it would be interesting to use a Cre recombinase that would be dependent on a particular component in the cerebrospinal fluid, or in the SVZ vasculature, to assess how these are influencing GBM cells nested in the periventricular area.

The many natural and engineered rAAV capsid serotypes that are reported or under ongoing development have distinct but overlapping tropisms and distribution^{30,31}. Whereas we here selected AAV-DJ as an efficient serotype for GSC transduction among a panel of AAV serotypes, other novel rAAV constructs may be envisaged for specific properties, e.g. restricted surface of action, or more specific GBM cell transduction. A recent high-throughput screening of 177 AAV capsid variants has shown that AAV1-P5 most effectively transduces NSCs in the naïve adult brain after icv injection, and these can be tracked up to their final destination in the olfactory bulb³². The

AAV-SCH9 also efficiently transduces adult NSCs³³. To what extent this NSC-oriented tropism would be recapitulated on SVZ-nested GSCs remains to be investigated.

The transgene of interest may also be replaced, e.g. for modulating gene expression in the target cells in a therapeutic purpose, for inducing cell death, reducing proliferation or stimulating immune recognition. For instance, AAV intraventricular injection has already been described in GBM models, e.g. for the delivery of interferon γ (IFN γ). A first report show that icv AAV2/rh8-IFN γ preferentially distributes in the corpus callosum and the hippocampus, similar to what we observed here with AAV-DJ (at lower viral titration), and reduces tumor growth in a U87 model³⁴. Later, they showed that icv AAV9-IFN γ reduced tumor growth and increases survival in an invasive patient-derived xenograft model, as well as in an immunocompetent model, and synergizes with temozolomide treatment³⁵. AAV9 armed with the sTRAIL proapoptotic protein has also shown promising therapeutic effect in GBM models, upon systemic injection³⁶. It would be of huge interest to induce therapeutic genes in SVZ-nested GBM cells to ascertain their contribution to tumor resistance to treatment and recurrence.

In addition to these molecular developments that could apply to this approach, we also point out the importance of considering clinically relevant, therapy-like models to be combined to our color-conversion protocol. For example, it would be interesting to observe whether eGFP⁺, SVZ-relocated GBM cells are able to repopulate an experimental resection cavity, for instance using microsurgery models³⁷.

Altogether, this work exposes the development of an rAAV-based approach for the specific and restricted labelling of GBM cells that get in close contact with the subventricular zone (SVZ), after tumor development in a xenograft mouse model. This experimental approach is highly relevant to the clinical context describing the poor prognosis associated with GBM proximity to the SVZ. This versatile model could be optimized for both investigational and therapeutic perspectives and will help to shed

light on the spatiotemporal aspects of GBM 3.33. progression and recurrence.

Funding

This work is supported by the Fond National de la Recherche Scientifique (FNRS), the TELEVIE, the University of Liège and the 4.44. Fondation Léon Frédéricq.

Authorship statement

AL, EDV, BR, VN: Study design. DM, BR, VN: 5.55. Project supervision. AL, GR, DM: Tissue collection. AL, DI, AH: Experimental work. AL, DI, AH: Data analysis. AL, DI: Initial draft writing. AL, DI, AH, EDV, GR, DM, BR, VN: 6.66. Review and final draft writing. All authors read and approved the final manuscript.

Conflict of Interest Statement

None declared

Acknowledgements

We thank the colleagues from the GIGA-Viral Vector platform, the Neurosurgery Department the University Hospital Biobank. Plasmids 8.88. pAAV8, pAAV9, pAAV10 were kind gifts from Miguel Sena-Esteves (UMass Chan Medical School). The plasmid pMSCV-loxp-dsRed-loxp-eGFP-Puro-WPRE was a gift from Hans Clevers (Addgene plasmid #32702; <http://n2t.net/addgene:32702> ; 9.99. RRID:Addgene_32702).

Data availability

The data are available from the corresponding author upon request.

References

1. Stupp R, Mason WP, van den Bent MJ, et al. Radiotherapy plus concomitant and adjuvant temozolomide for glioblastoma. *N Engl J Med.* 2005;352(10):987-996. doi:10.1056/NEJM0A043330
2. Rapp M, Baernreuther J, Turowski B, Steiger HJ, Sabel M, Kamp MA. Recurrence Pattern Analysis of Primary Glioblastoma. *World Neurosurg.* 2017;103:733-740. doi:10.1016/J.WNEU.2017.04.053
3. Ignatova TN, Kukekov VG, Laywell ED, Suslov ON, Vrionis FD, Steindler DA. Human cortical glial tumors contain neural stem-like cells expressing astroglial and neuronal markers in vitro. *Glia.* 2002;39(3):193-206. doi:10.1002/GLIA.10094
4. Alvarez-Buylla A, García-Verdugo JM. Neurogenesis in adult subventricular zone. *Journal of Neuroscience.* Published online 2002. doi:10.1523/jneurosci.22-03-00629.2002
5. Sanai N, Tramontin AD, Quinones-Hinojosa A, et al. Unique astrocyte ribbon in adult human brain contains neural stem cells but lacks chain migration. *Nature.* 2004;427(6976):740.
6. Lim DA, Cha S, Mayo MC, et al. Relationship of glioblastoma multiforme to neural stem cell regions predicts invasive and multifocal tumor phenotype. *Neuro Oncol.* Published online 2007. doi:10.1215/15228517-2007-023
- 7.77. Jafri NF, Clarke JL, Weinberg V, Barani IJ, Cha S. Relationship of glioblastoma multiforme to the subventricular zone is associated with survival. *Neuro Oncol.* 2013;15(1):91-96. doi:10.1093/NEUONC/NOS268
- 8.88. Mistry AM, Hale AT, Chambless LB, Weaver KD, Thompson RC, Ihrie RA. Influence of glioblastoma contact with the lateral ventricle on survival: a meta-analysis. *J Neurooncol.* 2017;131(1):125-133. doi:10.1007/S11060-016-2278-7
- 9.99. Adeberg S, Bostel T, König L, Welzel T, Debus J, Combs SE. A comparison of long-term survivors and short-term survivors with glioblastoma, subventricular zone involvement: A predictive factor for survival? *Radiation Oncology.* Published online 2014. doi:10.1186/1748-717X-9-95
- 10.10. Wang Y, Yang J, Zheng H, et al. Expression of mutant p53 proteins implicates a lineage relationship between neural stem cells and malignant astrocytic glioma in a murine model. *Cancer Cell.* 2009;15(6):514-526. doi:10.1016/j.ccr.2009.04.001
- 11.11. Alcantara Llaguno S, Sun D, Pedraza AM, et al. Cell-of-origin susceptibility to glioblastoma formation declines with neural lineage restriction. *Nature Neuroscience 2019 22:4.* 2019;22(4):545-555. doi:10.1038/s41593-018-0333-8

12. Lee JH, Lee JE, Kahng JY, et al. Human glioblastoma arises from subventricular zone cells with low-level driver mutations. *Nature*. Published online 2018:1.
13. Goffart N, Kroonen J, Di Valentin E, et al. Adult mouse subventricular zones stimulate glioblastoma stem cells specific invasion through CXCL12/CXCR4 signaling. *Neuro Oncol*. Published online 2015. doi:10.1093/neuonc/nou144
14. Qin EY, Cooper DD, Abbott KL, et al. Neural Precursor-Derived Pleiotrophin Mediates Subventricular Zone Invasion by Glioma. *Cell*. Published online 2017. doi:10.1016/j.cell.2017.07.016
15. Kroonen J, Nassen J, Boulanger YG, et al. Human glioblastoma-initiating cells invade specifically the subventricular zones and olfactory bulbs of mice after striatal injection. *Int J Cancer*. Published online 2011. doi:10.1002/ijc.25709
16. Goffart N, Lombard A, Lallemand F, et al. CXCL12 mediates glioblastoma resistance to radiotherapy in the subventricular zone. *Neuro Oncol*. Published online 2017. doi:10.1093/neuonc/now136
17. Piccirillo SGM, Spiteri I, Sottoriva A, et al. Contributions to drug resistance in glioblastoma derived from malignant cells in the subependymal zone. *Cancer Res*. 2015;75(1):194-202. doi:10.1158/0008-5472.CAN-13-3131/651340/AM/CONTRIBUTIONS-TO-DRUG-RESISTANCE-IN-GLIOBLASTOMA
18. Willems E, Dedobbeleer M, Digregorio M, et al. Aurora A plays a dual role in migration and survival of human glioblastoma cells according to the CXCL12 concentration. *Oncogene*. Published online 2019. doi:10.1038/s41388-018-0437-3
19. Dedobbeleer M, Willems E, Lambert J, et al. MKP1 phosphatase is recruited by CXCL12 in glioblastoma cells and plays a role in DNA strand breaks repair. *Carcinogenesis*. Published online 2020. doi:10.1093/carcin/bgz151
20. Koo BK, Stange DE, Sato T, et al. Controlled gene expression in primary Lgr5 organoid cultures. *Nat Methods*. 2012;9(1):81.
21. Haery L, Deverman BE, Matho KS, et al. Adeno-Associated Virus Technologies and Methods for Targeted Neuronal Manipulation. *Front Neuroanat*. 2019;13. doi:10.3389/FNANA.2019.00093
22. Goffart N, Lombard A, Lallemand F, et al. CXCL12 mediates glioblastoma resistance to radiotherapy in the subventricular zone. *Neuro Oncol*. 2017;19(1):66-77. doi:10.1093/neuonc/now136
23. Tomer R, Deisseroth K. Advanced CLARITY Methods for Rapid and High-Resolution Imaging of Intact Tissues. Published online 2014.
24. Adeberg S, Knoll M, Koelsche C, et al. DNA-methylome-assisted classification of patients with poor prognostic subventricular zone associated IDH-wildtype glioblastoma. *Acta Neuropathologica*. 2022;144(1):129-142. doi:10.1007/S00401-022-02443-2
25. Licón-Muñoz Y, Avalos V, Subramanian S, et al. Single-nucleus and spatial landscape of the sub-ventricular zone in human glioblastoma.
26. Schubert L, Le AT, Hinz TK, et al. A functional sgRNA-CRISPR screening method for generating murine RET and NTRK1 rearranged oncogenes. Published online 2023. doi:10.1242/bio.059994
27. Guo Y, Lei I, Tian S, et al. Chemical suppression of specific C-C chemokine signaling pathways enhances cardiac reprogramming. *Journal of Biological Chemistry*. 2019;294(23):9134-9146. doi:10.1074/JBC.RA118.006000/ATTACHMENT/EEC4CC7E-2357-425D-93E5-0568CBCEE9A5/MMC1.ZIP
28. Godet I, Shin YJ, Ju JA, Ye IC, Wang G, Gilkes DM. Fate-mapping post-hypoxic tumor cells reveals a ROS-resistant phenotype that promotes metastasis. *Nature Communications*. 2019;10(1):1-18. doi:10.1038/s41467-019-12412-1
29. Rocha HL, Godet I, Kurtoglu F, et al. A persistent invasive phenotype in post-hypoxic tumor cells is revealed by fate mapping and computational modeling. *iScience*. 2021;24(9):102935. doi:10.1016/J.ISCI.2021.102935
30. Haery L, Deverman BE, Matho KS, et al. Adeno-Associated Virus Technologies and Methods for Targeted Neuronal Manipulation.

- Front Neuroanat.* 2019;13:493120. doi:10.3389/FNANA.2019.00093/BIBTEX
31. Xu X, Chen W, Zhu W, et al. Adeno-associated virus (AAV)-based gene therapy for glioblastoma. *Cancer Cell Int.* 2021;21(1):1-10. doi:10.1186/S12935-021-01776-4/TABLES/2
 32. Kremer LPM, Cerrizuela S, Dehler S, et al. High throughput screening of novel AAV capsids identifies variants for transduction of adult NSCs within the subventricular zone. *Mol Ther Methods Clin Dev.* 2021;23:33-50. doi:10.1016/J.OMTM.2021.07.001
 33. Ojala DS, Sun S, Santiago-Ortiz JL, Shapiro MG, Romero PA, Schaffer D V. In Vivo Selection of a Computationally Designed SCHEMA AAV Library Yields a Novel Variant for Infection of Adult Neural Stem Cells in the SVZ. *Molecular Therapy.* 2018;26(1):304-319. doi:10.1016/J.YMTHE.2017.09.006/ATTACHMENT/C5A91BE4-4B73-4495-8A18-35FD1DC90D6B/MMC1.PDF
 34. Meijer DH, Maguire CA, Leroy SG, Sena-Esteves M. Controlling brain tumor growth by intraventricular administration of an AAV vector encoding IFN- β . *Cancer Gene Therapy 2009* 16:8. 2009;16(8):664-671. doi:10.1038/cgt.2009.8
 35. Guhasarkar D, Neiswender J, Su Q, Gao G, Sena-Esteves M. Intracranial AAV-IFN- β gene therapy eliminates invasive xenograft glioblastoma and improves survival in orthotopic syngeneic murine model. *Mol Oncol.* 2017;11(2):180-193. doi:10.1002/1878-0261.12020
 36. Crommentuijn MHW, Kantar R, Noske DP, et al. Systemically administered AAV9-sTRAIL combats invasive glioblastoma in a patient-derived orthotopic xenograft model. *Mol Ther Oncolytics.* 2016;3:16017. doi:10.1038/mto.2016.17
 37. Oudin A, Moreno-Sanchez PM, Baus V, Niclou SP, Golebiewska A. Magnetic resonance imaging-guided intracranial resection of glioblastoma tumors in patient-derived orthotopic xenografts leads to clinically relevant tumor recurrence. *BMC Cancer.* 2024;24(1):1-14. doi:10.1186/S12885-023-11774-6/FIGURES/5

4. Discussion

The use of the CRE-Lox system to specifically label and track tumor cells in an *in vivo* environment represents a significant methodological advance in the context of GBM. This strategy makes it possible not only to visualize the location of labeled cells, but also to study their phenotype in response to specific biological signals acting locally *in vivo*. This innovative approach makes it possible to explore the dynamics of tumor cells in detail. Using this method, we could, for example, isolate eGFP+ and dsRED+ cells *ex vivo* to characterize and compare them in depth. This approach has already been successfully implemented in our laboratory in a previous project. More precisely, we could study the genomic instability of these cells after irradiation and TMZ treatment, by analyzing the expression of DNA double-strand break markers, such as γ H2AX and 53BP1. Moreover, *in vivo* studies could be conducted to compare not only the viability, proliferation rate of eGFP+ and dsRED+ cells (with or without irradiation + TMZ), but also analyze their migration and invasion capacity.

- **GBM cells invade the SVZ and rapidly leave this area**

Moreover, this study makes a significant contribution by demonstrating the ability of GBM cells to migrate bidirectionally between the tumor mass and the SVZ, a previously unexplored dynamic. This observation could be helpful to decipher mechanisms underlying GBM recurrence. Our previous reports showed that tumor cells can invade the brain parenchyma using white fibers to nest in the SVZ. However, we had not yet demonstrated that these cells could leave this area, and invade other regions, including the initial tumor mass. We hypothesize a possible phenotypic modulation of SVZ-nested GBM cells, which would adopt an increased aggressiveness. This observation challenges our understanding of cellular plasticity in GBM and highlights the ability of tumor cells to modify their migration trajectory in response to specific environmental stimuli. Therefore, again it would be interesting to extract and analyze/compare these eGFP+ and dsRED+ cells to better understand the molecular events and the impact of the GBM TME on these cells. Further characterization could reveal therapeutic targets and clarify the molecular basis of their migration.

Moreover, the clinical correlation between the proximity of GBM cells to the SVZ and an unfavorable prognosis highlights the clinical importance of our study. Furthermore, observations on the resistance of cells nested in the SVZ to radiotherapy underline the importance of the development of new SVZ-targeted treatments.

- **Methods for rAAVs delivery into the brain, in the context of GBM**

The intracerebroventricular injection allows effective drug delivery into the brain through the cerebrospinal fluid (CSF), overcoming the limitations of local injections that cannot target and eliminate infiltrating GBM cells. Unlike systemic injections, which can cause toxicities to other organs, this method offers better specificity and minimization of adverse effects by allowing more direct and controlled delivery of therapeutic agents into the brain. Since the safety of intracerebral injection has already been studied in others context and shown to be effective in recent clinical trials, this tool could also serve as a therapeutic strategy.

Currently, advanced medical devices (e.g. Ommaya® reservoir) are designed specifically for intracerebral delivery on a chronic basis, rather than an acute one³⁰⁵. Indeed, this device allows chronic access to the intrathecal space via an intraventricular catheter, providing an effective and safe method to deliver treatments directly into the brain. Recently, a clinical trial demonstrated the feasibility and safety of this device for injecting CAR-T cells targeting EGFRvIII for patients with recurrent GBM, marking a significant advance in the treatment of this complex disease³⁰⁶. This fits perfectly with the goals and future perspectives of this project. By using this intrathecal delivery approach demonstrated in these recent clinical trials, our research could potentially improve the precision and efficiency of targeting these difficult-to-reach GBM cells via the use of rAAVs.

- **Genes of interest for possible therapeutic rAAVs in the future**

The genes of interest that could be expressed by rAAVs may include inhibitors of cell proliferation, cell migration, angiogenesis or even stimulators of the immune response, to offer new treatment avenues.

Among possible options, miRNAs targeting GBM-specific oncogenes and pro-apoptotic factors like TRAIL (TNF-Related Apoptosis-Inducing Ligand) could be expressed via AAV to induce GBM cell death. It has been shown that miR-7 can inhibit tumor growth by targeting signaling pathways involved in survival and proliferation. It also enhances the sensitivity of cancer cells to apoptosis, making it particularly effective against GBM that are resistant to TRAIL. In this context, Bhere et al. engineered an AAV encoding miR-7 and investigated the efficacy of a combined treatment involving stem cell releasing soluble form of TRAIL and AAV-miR-7 in GBM. Their results showed that the combined treatment induces a downregulation of EGFR and the phosphorylated form of Akt and activates NF- κ B pathway. This leads to an upregulation of the death receptor 5 (DR5) to sensitize GBM cells to TRAIL. In addition, they demonstrated that a single administration of AAV-miR-7 significantly reduces tumor volume and increases DR5 expression, thereby increasing cell death via TRAIL and significantly improving mouse survival³⁰⁷. This construct could be interesting since we have demonstrated that SVZ-nested cells were more resistant to irradiation. SVZ-nested GBM cells may also be resistant to apoptotic death via TRAIL. This method could be considered after resection surgery to eliminate the remaining cells.

In the same perspective, several studies have generated AAVs encoding molecules inducing cell death. Mizuno et al. designed an AAV that encodes a suicide gene, the herpes simplex virus thymidine kinase gene (HSV-tk) to evaluate its effect in GBM. The results showed complete regression and prolonged survival after multiple injections of this AAV-tk followed by intraperitoneal administration of ganciclovir³⁰⁸. Zhong et al. used an AAV delivering the Apoptin peptide and showed a decrease in tumor growth and prolonged survival in treated mice. They show that injection of AAV-

apoptin into the left hemisphere effectively prevented ipsilateral tumor growth but was not sufficient to prevent distal tumor growth in the contralateral hemisphere³⁰⁹.

Furthermore, immunomodulatory cytokines, such as interferon-beta (IFN- β), IL12 and IL15, can be generated as part of an AAV vector to stimulate and enhance an antitumor immune response. Meijer et al. demonstrated that peritumoral parenchymal transduction with AAV-hIFN- β was effective in eradicating tumor cells. However, the high infiltrative and migratory nature of GBM cells can leave a significant number of tumor cells outside the treatment area. Therefore, they decided to treat mice with this AAV but this time by icv injection and they showed that the treatment not only prevents tumor growth but also improves mice survival³¹⁰. Guhasarkar et al. Evaluates the therapeutic efficacy of systemic injection of AAV-hIFN- β in an invasive orthotopic model of GBM. The results showed that the treatment leads to a complete regression of tumors in a dose-dependent manner³¹¹. These results are totally related to our method and summarizes our technique. Again, we could consider using such a type of AAV and injecting it icv, in order to kill eGFP+ cells that are difficult to access.

Moreover, anti-angiogenic factors like anti-VEGF could be expressed via AAV to reduce angiogenesis. Hicks et al. engineered an AAV vector encoding for bevacizumab, an anti-human VEGF monoclonal antibody. Local administration to the area of GBM xenograft reduced tumor growth *in vivo* and increased survival. Moreover, they confirmed these results with early passage GBM patient derived cells³¹².

In order to limit tumor invasion, the team of Yanamandra et al. studied the effect of an AAV that expresses tissue factor pathway inhibitor-2 (TFPI-2), a protein that plays a role in the degradation of the extracellular matrix. The results showed that *in vitro* use of AAV-TFPI-2 leads to a reduction in capillary formation and *in vivo* the treatment inhibited the formation of microvessels and significantly reduced tumor growth³¹³.

The integration into our AAV molecules with the specific capacity to inhibit tumor growth, induce cell death or suppress migration represents a promising strategy for our future research. By exploiting these advanced methods, we could precisely target

tumor cells that are particularly difficult to access and potentially responsible for recurrence. The application of this approach in addition to standard treatment procedures would not only improve the efficacy of treatment by eliminating the last remaining residual cells but also minimize recurrences.

In conclusion, this study opens new perspectives for the labeling, monitoring and treatment of GBM cells nested in the SVZ, thus offering a promising tool for the development of targeted therapies.

II. Nanobody-based retargeting of an oncolytic herpesvirus for eliminating CXCR4+ GBM cells: A proof of principle (Sanchez Gil et al. 2022)

1. Presentation and contribution to the manuscript

In this chapter, we will briefly present the main findings of our article entitled “**Nanobody®-based retargeting of an oncolytic herpesvirus for eliminating CXCR4+ GBM cells: A proof of principle (Sanchez Gil et al. 2022)**”. This paper led by the laboratory of Catherine Sadzot (GIGA-highlights the *in vitro* and *in vivo* efficiency of CXCR4-based, Nanobody®-retargeted and armed oncolytic herpesvirus (oHSV) in GBM. Our main role was to generate an oncolytic virus against CXCR4+ GBM cells. The objective was to generate an oncolytic virus specifically targeting GBM cells expressing CXCR4, to induce their death by cell lysis and apoptosis via the secretion of the soluble form of TRAIL protein. We focused on CXCR4 as it is expressed by GBM cells and involved in the SVZ-oriented invasion. In this work, we first attempted to study the effectiveness of retargeting to CXCR4 GBM cells and the arming with TRAIL. Subsequently, we evaluated the therapeutic efficacy of this retargeted oHSV using an orthotopic GBM xenograft model. This proof-of-concept study suggests that Nanobodies® specific for various GBM cell markers could be used to retarget and “personalize” oHSVs, providing a potential complement to current standard therapeutic approaches.

Nanobody-based retargeting of an oncolytic herpesvirus for eliminating CXCR4⁺ GBM cells: A proof of principle

Judit Sanchez Gil,¹ Maxime Dubois,¹ Virginie Neirinckx,² Arnaud Lombard,^{2,3} Natacha Coppieters,² Paolo D'Arrigo,¹ Damla Isci,² Therese Aldenhoff,² Benoit Brouwers,² Cédric Lassence,¹ Bernard Rogier,^{2,4} Marielle Lebrun,¹ and Catherine Sadzot-Delvaux¹

¹Laboratory of Virology and Immunology, GIGA Infection, Inflammation and Immunity (GIGA I3), University of Liège, 4000 Liège, Belgium; ²Laboratory of Nervous System Disorders and Therapy, GIGA-Neurosciences, University of Liège, 4000 Liège, Belgium; ³Department of Neurosurgery, CHU of Liège, 4000 Liège, Belgium; ⁴Department of Neurology, CHU of Liège, 4000 Liège, Belgium

Glioblastoma (GBM) is the most aggressive primary brain tumor in adults, which remains difficult to cure. The very high recurrence rate has been partly attributed to the presence of GBM stem-like cells (GSCs) within the tumors, which have been associated with elevated chemokine receptor 4 (CXCR4) expression. CXCR4 is frequently overexpressed in cancer tissues, including GBM, and usually correlates with a poor prognosis. We have created a CXCR4-retargeted oncolytic herpesvirus (oHSV) by insertion of an anti-human CXCR4 nanobody in glycoprotein D of an attenuated HSV-1 (ΔICP34.5, ΔICP6, and ΔICP47), thereby describing a proof of principle for the use of nanobodies to target oHSVs toward specific cellular entities. Moreover, this virus has been armed with a transgene expressing a soluble form of TRAIL to trigger apoptosis. *In vitro*, this oHSV infects U87MG CXCR4⁺ and patient-derived GSCs in a CXCR4-dependent manner and, when armed, triggers apoptosis. In a U87MG CXCR4⁺ orthotopic xenograft mouse model, this oHSV slows down tumor growth and significantly improves mice survival. Customizing oHSVs with diverse nanobodies for targeting multiple proteins appears as an interesting approach for tackling the heterogeneity of GBM, especially GSCs. Altogether, our study must be considered as a proof of principle and a first step toward personalized GBM virotherapies to complement current treatments.

INTRODUCTION

The chemokine receptor 4 (CXCR4), first described for its role in leukocyte trafficking or HIV infection,¹ is a largely studied G-protein-coupled receptor that activates various signaling pathways upon binding of its unique ligand CXCL12, also known as stromal-cell-derived factor 1. CXCR4 overexpression has been reported in a wide range of tumors, including glioblastoma multiforme (GBM),^{2–5} and increasing evidence has suggested its central role in cancer progression.⁶ Multiple preclinical or clinical studies have demonstrated that the disruption of CXCR4 downstream signaling via several approaches (CXCR4 short hairpin RNA [shRNA], CXCL12 mimetic

peptide, anti-CXCR4 antibodies, or nanobodies) diminishes tumor growth and synergizes with chemo- or radiotherapy.^{7–13}

GBM is the most frequent primary malignant brain tumor, classified by the World Health Organization as a grade 4 glioma.¹⁴ Despite standard therapies that associate surgical resection with radio- or chemotherapy, the prognosis remains dramatically poor, with a median survival of 16 months from diagnosis.¹⁵ GBM is indeed highly diffuse and tumor cells infiltrate healthy brain tissue, making the total resection of the tumor rather difficult or even impossible. GBM recurrences frequently develop within the margin of the resection cavity or at distant sites.¹⁶ In addition, GBM is characterized by a high degree of heterogeneity at the genetic, epigenetic, and transcriptomic levels. Many studies reported the presence of self-renewing, multipotent subsets of GBM cells endowed with high tumorigenic capacity, considered as GBM stem-like cells (GSCs).^{17–19} GSCs have been associated with the expression of specific markers, form tumorspheres *in vitro* upon limiting dilution, and are able to initiate a tumor when serially transplanted in mice brain. GSCs have long been considered as key actors in GBM relapse, and the mechanisms underlying GSC development, maintenance, and phenotypic plasticity yet remain intensively investigated.²⁰ We previously have shown that, upon GBM xenotransplantation, CXCR4⁺ GSCs escape the tumor core and reach the subventricular zones (SVZs) based on a CXCR4/CXCL12-dependent signaling.^{21,22} GSCs hosted in the SVZ display an improved DNA double-strand break repair and hence are resistant to radiotherapy.^{22,23} These observations have been confirmed in GBM patients, in which GSCs can be found both in the tumor core, where the hypoxic environment constitutes an appropriate niche, and in the SVZ, reinforcing the role of these CXCR4⁺ cells in GBM recurrence.^{24,25} Importantly, a

Received 5 May 2022; accepted 1 June 2022;
<https://doi.org/10.1016/j.omto.2022.06.002>

Correspondence: Catherine Sadzot-Delvaux, Laboratory of Virology and Immunology, GIGA Infection, Inflammation and Immunity (GIGA I3), University of Liège, 11 Avenue de l'Hôpital, 4000 Liège, Belgium.
E-mail: csadzot@uliege.be



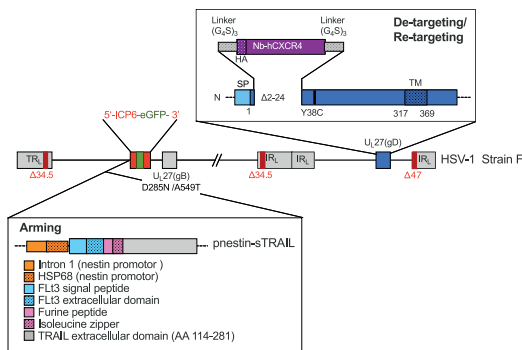


Figure 1. Schematic representation of oHSV/Nb-gD and oHSV/Nb-gD:sTRAIL genomes

high expression of CXCR4 positively correlates with tumor size, tumor progression, recurrence, and ultimately with patient survival.^{3,5} Targeting GSCs and particularly CXCR4⁺ cells therefore provides an opportunity to reach tumor cells that escape current treatments.²⁶

Over the last decade, virotherapy has emerged as a promising approach for cancer treatment.²⁷ Oncolytic viruses (OVs) are currently at different stages of preclinical investigations, and numerous clinical trials are ongoing. In the context of GBM, virotherapy and oncolytic herpesviruses (oHSVs) in particular are currently being evaluated as an alternative or complementary therapeutic approach for patients resistant to traditional therapies.²⁸ oHSV efficacy depends on the capacity of the virus to specifically infect cancer cells. However, it is estimated that about 20% of the GBM cells are not efficiently infected by oHSV, partly due to a low expression of CD111 (nectin-1, one of the HSV-1 natural receptors).^{29,30} A virus able to target cancer cells and GSCs in particular through its interaction with a membrane protein specifically expressed by these cells would thus allow to reach cells that have escaped standard therapeutic approaches. One strategy for oHSV retargeting is to replace the domain responsible for glycoprotein D (gD) interaction with its natural cellular receptors by a ligand able to interact with a protein of interest expressed by the target cells. Single-chain immunoglobulin (scFv) or ligands, such as cytokines or peptides, have been successfully introduced in gD to target cancer cells.^{31–36} Nanobodies are a single heavy variable domain of camelid antibodies and constitute an interesting alternative to retarget an oHSV. They can be selected from a synthetic or immune library with a huge diversity and can recognize cryptic antigens with a high affinity. These nanobodies therefore open the possibility to develop a panel of tailored oHSVs for personalized therapy.

In this context, we have developed, as a proof of principle, an oncolytic HSV-1 specifically targeting CXCR4, thanks to the insertion in gD of an anti-human CXCR4 nanobody previously described for its capacity to efficiently recognize CXCR4 (WO2016156570A1). This virus (oHSV/Nb-gD) has been further armed with a transgene express-

ing the soluble form of TRAIL (oHSV/Nb-gD:sTRAIL), whose efficacy to trigger the extrinsic apoptosis pathway has been previously documented.^{37–40} We demonstrated that the engineered virus infects U87MG CXCR4⁺ and patient-derived GSCs in a CXCR4-dependent manner and can replicate efficiently in these cells and lead to sTRAIL expression, thereby triggering apoptosis. When used in an *in vivo* orthotopic xenograft GBM model, oHSV/Nb-gD armed or not with sTRAIL had a clear impact on tumor progression and significantly improved mice survival. These results confirm nanobodies as appropriate tools for retargeting oHSVs toward specific cell subsets and constitute a proof of principle of an oHSV design strategy that could be considered for personalized treatment.

RESULTS

Construction of a nanobody-retargeted and armed oncolytic herpesvirus

To specifically target GBM cells expressing CXCR4, we engineered an oHSV that was first detargeted from its natural receptors HVEM and nectin-1, prior to being retargeted to CXCR4 (Figure 1). These modifications were introduced within fQuick-1 (kind gift from Prof. E.A. Chiocca), a bacterial artificial chromosome (BAC) containing the HSV-1 genome (strain F; Δ ICP34.5/ Δ ICP6/EGFP⁺). This backbone was further deleted from US12 coding for ICP47, this deletion being important to partly overcome the attenuation resulting from γ 34.5 deletion.⁴¹ The detargeting and retargeting was achieved by replacing the residues 2–24 of gD within the HVEM-binding domain by an anti-human CXCR4 nanobody.⁴² In addition, the residue 38 of gD was mutated (Y38C) to impair gD interaction with nectin-1, another natural receptor.⁴³ Moreover, two mutations (D285N and A549T) shown to improve the fusion capacity of glycoprotein B (gB) were introduced in UL27.⁴⁴ Finally, the virus was armed with a transgene expressing sTRAIL⁴⁵ under the control of a nestin promoter. After transfection of these constructs into Vero cells previously transduced with the human CXCR4, oHSVs were produced in the supernatant and further purified and titrated. In this publication, they are referred to as oHSV/gD (non-retargeted; non-armed), oHSV/Nb-gD (CXCR4 retargeted; non-armed), and oHSV/Nb-gD:sTRAIL (CXCR4 retargeted; sTRAIL armed).

Efficacy of the CXCR4 retargeting

To verify the detargeting efficacy, J1.1–2 hamster cells resistant to HSV due to the lack of HVEM or nectin-1 expression at the cell surface,⁴⁶ as well as their modified version J/A and J/C expressing, respectively, human HVEM⁴⁷ or nectin-1⁴⁸ (kind gift from Prof. G. Campadelli Fiume), were infected with oHSV/gD or oHSV/Nb-gD (MOI: 0.01, 0.1, and 1). Contrary to oHSV/gD, which led to numerous infectious foci in J/A and J/C, no foci were detected upon oHSV/Nb-gD infection, demonstrating that oHSV/Nb-gD was properly detargeted (Figure 2A). To evaluate the capacity of oHSV/Nb-gD to specifically infect CXCR4⁺ cells, glioblastoma U87MG cells that express CXCR4 at a very low level (Figures S1A and S1B) were transduced with a lentivirus expressing the human CXCR4. The ectopic expression of CXCR4 was confirmed by flow cytometry (Figures S1A and S1B). U87MG and U87MG CXCR4⁺ were

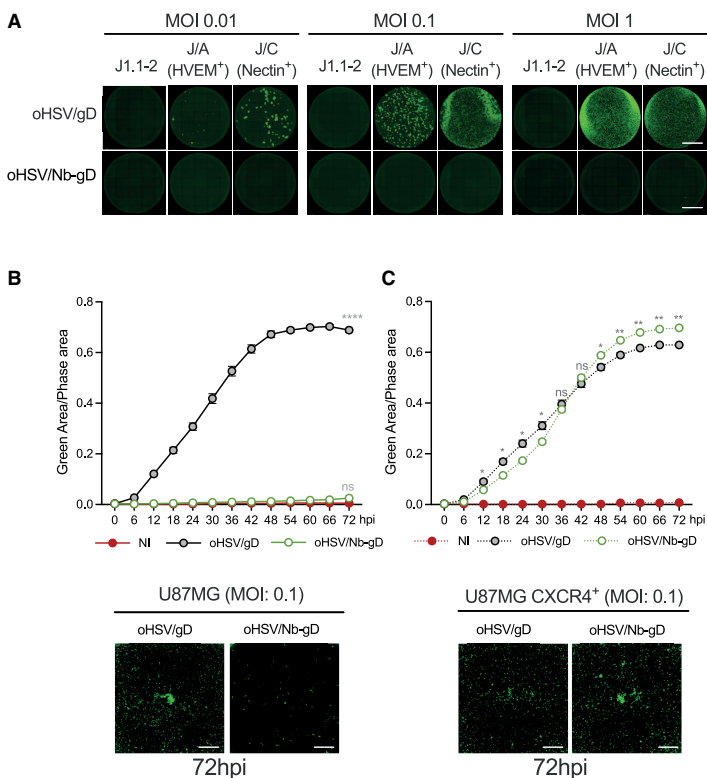


Figure 2. Efficacy of the oHSV detargeting and retargeting

(A) Detargeting was evaluated by infection of J1.1-2, J/A (J1.1 HVEM⁺), and J/C (J1.1 nectin-1⁺) cells infected for 72 h at different MOIs with the recombinant oHSVs expressing either wild-type (WT) gD (oHSV/gD) or gD modified by the insertion of an anti-hCXCR4 nanobody (oHSV/Nb-gD). Both viruses express EGFP under the control of pICP6, allowing the visualization of infected cells by epifluorescence microscopy. Scale bars represent 5 mm. (B and C) Retargeting was evaluated on U87MG (B) and U87MG CXCR4⁺ (C) cells. Cells were plated in 96-well plates, infected with oHSV/gD or oHSV/Nb-gD (MOI 0.1) and incubated in Incucyte S3 for real-time analyses during 72 h. EGFP expression and cell confluency were quantified every 6 h. Circles represent the ratio between the green and the phase area expressed as the mean \pm SEM of four wells. Statistical significance was determined by ordinary two-way ANOVA with Bonferroni multiple comparisons of means with a single pooled variance (ns, non-significant; * $p < 0.05$, ** $p < 0.01$, **** $p < 0.0001$). Images were taken every 6 h, and representative images taken at 72 hpi are shown. Scale bars represent 2 mm. Additional representative whole-well images taken at 24, 48, and 72 h are shown in Figure S2. See also growth curve of oHSV/gD and oHSV/Nb-gD in U87MG CXCR4⁺ cells in Figure S3

then infected with oHSV/gD or oHSV/Nb-gD (MOI: 0.1), and the level of infection was evaluated by real-time GFP imaging and quantification with Incucyte S3 (Figures 2B, 2C, and S2). As expected, oHSV/gD efficiently replicated in both cell lines independently of CXCR4 expression. On the contrary, oHSV/Nb-gD infection remained very low in U87MG cells, with only very few cells infected, as reflected by a very weak EGFP expression and no statistical difference with the non-infected cells. This clearly contrasted with numerous foci and overtime increasing EGFP signal in oHSV/Nb-gD-infected U87MG CXCR4⁺ cells, confirming that oHSV/Nb-gD infection relies on the expression of CXCR4. Importantly, the efficacy of infection of oHSV/gD and oHSV/Nb-gD in U87MG CXCR4⁺ cells was similar. This was further confirmed by a growth curve of both oHSVs in U87MG-CXCR4⁺ cells. No statistical difference was observed (Figure S3).

CXCR4-dependent infection of patient-derived GSCs by oHSV/Nb-gD

The efficacy of oHSV/gD and oHSV/Nb-gD was further evaluated on four different GSC cultures (T08, T013, T018, and T033) directly established from residual GBM tissue obtained from surgical resection (Department of Neurosurgery, CHU Liège, Belgium) and main-

tained as tumorspheres. In opposition to U87MG cells, GSCs express high levels of SOX2, POU3F2, and SALL2 (Figure S4). The percentage of CXCR4⁺ cells among the four different GSC cultures analyzed by flow cytometry was highly variable (Figures 3A and 3B). While less than 3% of T08 cells were positive for CXCR4, around 75% of T033 expressed this chemokine receptor, T013 and T018 being intermediate. As expected, the endogenous expression of CXCR4 was much lower than the ectopic expression by U87MG CXCR4⁺ cells (Figures 3A and 3B). To evaluate the efficacy of the retargeted oHSV and to compare it with the non-retargeted virus efficacy, primary GSCs were cultured as tumorspheres and infected with oHSV/gD or oHSV/Nb-gD (10^6 plaque-forming units [PFUs]/mL). Forty-eight hours post-infection, cells were dissociated and the percentage of EGFP-positive cells was analyzed by flow cytometry.

Interestingly, the percentage of oHSV/Nb-gD-infected cells clearly reflected the level of CXCR4 expression (Figure 3C). T033 that expresses CXCR4 at a high level was the most infected (34.8% of EGFP cells on an average; 48 h post-infection [hpi]), while less than 2% of T08 cells that do not express CXCR4 or express it at a very low level were positive for EGFP. As expected, in most primary cells, oHSV/gD led to a higher percentage of infected cells compared with oHSV/Nb-gD (Figures 3C and S5). However, an Incucyte S5 overtime analysis of T033 cells infected with a high titer (10^7 /mL) indicated that both the dynamics and the EGFP fluorescence were similar for both viruses (Figure S6). Finally, it is worth mentioning that, although

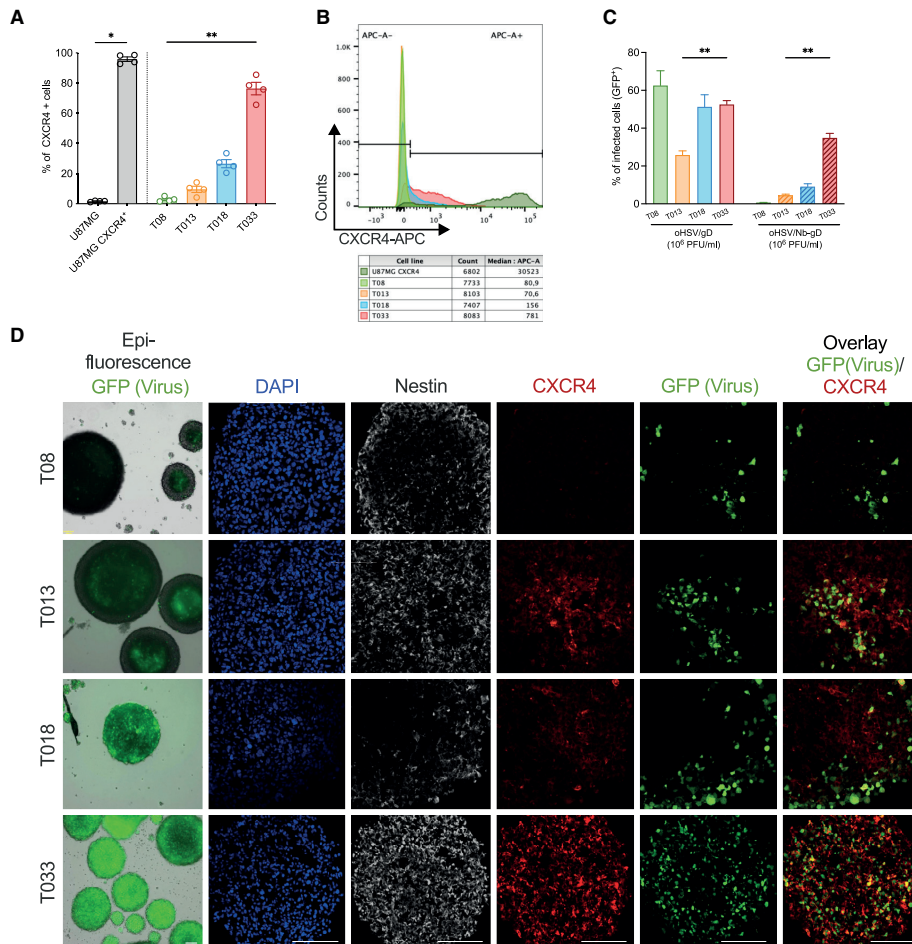


Figure 3. Efficacy of the oHSV retargeting in patient-derived GSCs

(A) Patient-derived GSCs (T08, T013, T018, and T033), U87MG, or U87MG CXCR4⁺ cells were cultured as tumorospheres and further dissociated for flow cytometry quantification of the percentage of cells expressing CXCR4 (APC⁺) at the cell membrane. Bars represent the means \pm SEM of four independent experiments. Statistical significance was determined by Kruskal-Wallis (primary cells, $^{**}p < 0.01$) or Mann-Whitney (U87MG cells, $^{*}p < 0.05$) test. (B) Overlaid histograms of a representative analysis allowing the comparison between endogenous and ectopic CXCR4 expression. Stemness features (expression of SOX2, POU3F3, and SALL2) analyzed by qRT-PCR are depicted in Figure S4. (C) Tumorospheres cultured in 24-well plates were infected with oHSV/gD or oHSV/Nb-gD (10^6 PFUs/mL). Forty-eight hours post-infection, cells were dissociated and the EGFP fluorescence was analyzed by flow cytometry. Bars represent the means \pm SEM of three independent experiments. Statistical significance was determined by ordinary two-way ANOVA with Bonferroni's multiple comparisons of means ($^{**}p < 0.01$). Raw data (overlaid histograms) representative of one experiment are shown in Figure S5. (D) Tumorospheres cultures in 24-well plates and infected for 48 h by oHSV/Nb-gD (10^6 PFUs/mL) were either analyzed by epifluorescence for EGFP detection (left panels) or fixed for immunostaining of nestin (white) or CXCR4 (red) and GFP detection (green). Nuclei were labeled with DAPI (blue). Images were recorded with a NIKON A1R confocal microscope. Scale bars represent 100 μ m. See also Figure S6 for real-time EGFP quantification and images of T033 tumorospheres infected with oHSV/gD or oHSV/Nb-gD at a higher titer (10^7 PFUs/mL).

all primary cell lines were infected by the non-retargeted virus, its efficacy greatly varied, with T013 being significantly less infected than the other cell lines.

In parallel, tumorospheres were infected with oHSV/Nb-gD (10^6 PFUs/mL) for immunostainings. Forty-eight hours post-infection, epifluorescence observation of oHSV-infected tumorospheres

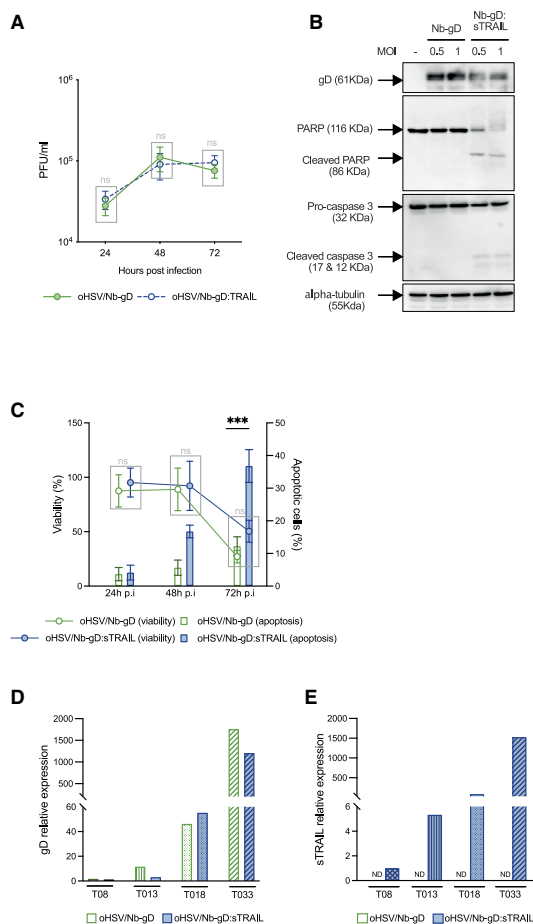


Figure 4. Efficacy of the oHSV arming

(A) The replication efficacy of the non-armed (oHSV/Nb-gD) and sTRAIL-armed (oHSV/Nb-gD:sTRAIL) oncolytic viruses was evaluated with a growth curve assay. U87MG CXCR4⁺ cells were infected at a MOI of 1, and supernatant was harvested 24, 48, and 72 h post-infection and used for titration as previously described.⁴⁹ The number of foci was calculated based on Incucyte S3 imaging. Bars represent the means \pm SEM (PFUs/mL) of three independent experiments. The lack of statistical difference is confirmed by unpaired t test analysis. (B) PARP and caspase 3 cleavage was evaluated by western blot analysis on total cell extracts from U87MG CXCR4⁺ cells infected for 18 h by oHSV/Nb-gD or oHSV/Nb-gD:sTRAIL (MOI: 0.5 or 1). gD and α -tubulin detection were used as infection or loading control, respectively. (C) Apoptosis was measured at different time points by flow cytometry using annexin V/DAPI labeling of U87MG CXCR4⁺ cells infected by oHSV/Nb-gD or oHSV/Nb-gD:sTRAIL (MOI: 5). The percentage of apoptotic cells corresponds to early (annexin V⁺/DAPI⁻) and late apoptotic (annexin V⁺/DAPI⁺) cells. Percentages of apoptotic cells upon infection at other MOI (1, 5, and 10) are shown in Figure S7. In parallel, cells were incubated with resazurin to evaluate the viability upon oHSV infection. Bars (percentage of apoptotic cells) and dots (percentage of viability) represent the means \pm SEM of three independent experiments. Statistical signifi-

cance was determined by ordinary two-way ANOVA with Bonferroni's multiple comparisons of means (**p < 0.001). (D and E) Patient-derived GSCs (T08, T013, T018, and T033) were cultured as tumorospheres in 24-well plates and infected with oHSV/Nb-gD or oHSV/Nb-gD:sTRAIL (10^6 PFUs/mL). gD and sTRAIL relative expression was analyzed 48 hpi by qRT-PCR as illustrated by a representative experiment. gD (D) and sTRAIL (E) mRNA level in oHSV/Nb-gD:sTRAIL-infected T08 are considered as the baseline (ND, not detected).

In vitro evaluation of the efficacy of the sTRAIL arming

oHSV/Nb-gD, shown to be efficiently retargeted and to specifically infect CXCR4⁺ cells, was further armed with the gene coding for sTRAIL under the control of the nestin promoter to trigger apoptosis upon viral infection. First, we showed that the armed and non-armed oHSVs replicated with the same efficacy in Vero CXCR4⁺ (data not shown) or U87MG CXCR4⁺ cells (Figure 4A), demonstrating that the arming does not impair oHSV replication. The efficacy of sTRAIL to trigger the apoptosis pathway was analyzed either by western blotting or using an annexin V/DAPI assay, while the viability was evaluated by measuring the cellular metabolism with resazurin. The expression of sTRAIL upon infection of U87MG CXCR4⁺ by oHSV/Nb-gD:sTRAIL led to the cleavage of PARP and caspase 3, while no cleavage was observed upon oHSV/Nb-gD infection (Figure 4B). The annexin V/DAPI assay further confirmed apoptosis in oHSV-infected U87MG CXCR4⁺ cells. sTRAIL-induced apoptosis was detectable 48 hpi and reached significance only 72 hpi, with an average of 36% of apoptotic cells upon oHSV/Nb-gD:sTRAIL infection compared with 12% upon oHSV/Nb-gD infection (Figure 4C). At 72 hpi, the percentage of apoptotic cells upon oHSV/Nb-gD:sTRAIL infection increased according to the MOI, which was not the case with the non-armed oHSV (Figure S7). Interestingly, the viability of the cells infected by oHSV/Nb-gD or oHSV/Nb-gD:sTRAIL measured 24, 48, or 72 hpi was not statistically different (Figure 4C).

When used to infect patient-derived GSC tumorospheres, oHSV/Nb-gD:sTRAIL led to the expression of gD and sTRAIL as measured by qRT-PCR, and this expression was significantly higher in T033 tumorospheres (Figures 4D and 4E).

Evaluation of the therapeutic efficacy of oHSV/Nb-gD and oHSV/Nb-gD:sTRAIL using an orthotopic xenograft GBM model

The capacity of oHSV/Nb-gD and oHSV/Nb-gD:sTRAIL to impact tumor growth was evaluated *in vivo* using an orthotopic xenograft

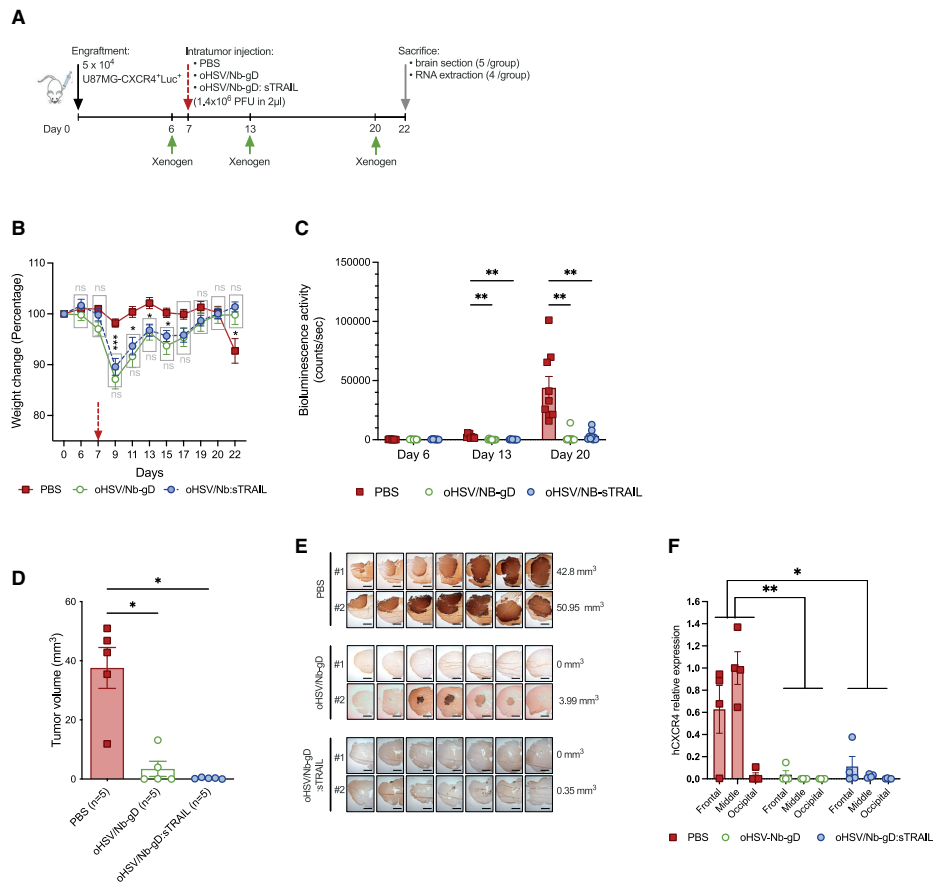


Figure 5. In vivo efficacy of oHSV/Nb-gD and oHSV/Nb-gD:sTRAIL

(A) Schematic representation of the experimental settings. Nude mice were engrafted with U87MG CXCR4⁺Luc⁺ cells and virus or PBS was injected in the tumor on day 7. Mice were regularly weighed, and for each mouse, the weight change is expressed as a percentage to the weight on day 0, considered as equal to 100%. (C) Bioluminescence activity was recorded with Xenogen IVIS 50 on day 6, 13, and 20 after engraftment. See also Figure S9 for bioluminescence imaging. (B) and (C) represent the means \pm SEM (n = 9 in each group). Statistical significance was determined by two-way ANOVA with Tukey's multiple comparisons of means (*p < 0.05; **p < 0.01; ***p < 0.001). (D–F) On day 22, brain from five mice were sectioned for immunostaining of human vimentin and the measurement of the tumor volume by 3D reconstruction (D) Data represent the means \pm SEM. Statistical significance was determined by Kruskal-Wallis test (*p < 0.05). Representative pictures of serial sections of two mice/group as well as the estimated volume of the corresponding tumor are shown in (E). In parallel, brain from the four other mice were divided into three parts (frontal, middle, and occipital), which were frozen and treated independently for RNA extraction and qRT-PCR analysis of hCXCR4 expression (F). For each sample, PBS-treated mice (middle sample) are considered as the baseline. Bars represent the means \pm SEM. Statistical significance was determined by two-way ANOVA with Tukey's multiple comparisons of means with a single pooled variance (*p < 0.05; **p < 0.01).

GBM mouse model. A first experiment was set up with engraftment of 5×10^4 U87MG CXCR4⁺Luc⁺ into the right striatum under stereotactic control (Figure S8A). PBS or oHSVs (1.4×10^6 PFUs in 2 μ L) were injected within the tumor on day 16. Weekly bioluminescence analysis revealed a very rapid tumor growth in all groups, even beyond oHSV intratumoral injection, although tumor growth appeared slightly reduced in oHSV/Nb-gD- or oHSV/Nb-gD:sTRAIL-

treated mice compared with PBS-treated mice (Figure S8B). From day 19 on, PBS-treated mice health status rapidly evolved toward a critical point that justified sacrifice on day 24 (Figure S8C). Although not conclusive, these results paved the way for the design of another experiment, in which PBS or oHSVs (1.4×10^6 PFUs in 2 μ L) were injected on day 7 after engraftment of 5×10^4 U87MG CXCR4⁺Luc⁺ GBM cells (Figure 5A). Body weight was monitored

every 2nd day, and bioluminescence recording was performed weekly to evaluate the tumor size evolution. On day 22, mice were anesthetized and either perfused with saline solution only (for RNA extraction from brain tissue) or followed by paraformaldehyde to allow immunostaining analyses. Contrary to oHSV-treated mice which temporarily lost weight just after virus infection but showed a continuous weight gain until the end of the experiment, PBS-treated mice displayed a clear weight loss from day 20 on (Figure 5B). On day 6, the tumor size appeared homogeneous among groups, with no significant difference in the bioluminescent signal (Figures 5C and S9A). On day 13, bioluminescence in PBS-treated mice dramatically increased up to day 20, whereas the signal in oHSV-treated mice remained similar to day 6 or even decreased, becoming even undetectable in some mice (Figure 5C). All mice were sacrificed on day 22, and brains were harvested for either anti-human vimentin immunohistochemical staining and tumor size measurement (five mice/group) or RNA extraction and qRT-PCR analyses (four mice/group). The size of the tumor, calculated by measuring the area positive for human vimentin on serial sections and 3D volume reconstruction, clearly showed a significant impact of both oHSV/Nb-gD and oHSV/Nb-gD:sTRAIL treatment, even if no significant difference was observed between the two viruses (Figures 5D and 5E). For RNA extraction, right hemispheres, in which the cells were engrafted, were divided into three parts (frontal, middle, and occipital). Human CXCR4 expression, reflecting the presence of implanted human CXCR4⁺ GBM cells, was evaluated in each block individually and expressed as the relative expression to the level of expression in the middle part of PBS-treated mice brains (Figure 5F). Overall, human CXCR4 expression was significantly decreased in oHSV-treated mice compared with PBS-treated mice. In both oHSV-treated groups, differences in the level of expression of hCXCR4 were observed between the three blocks, with a higher abundance of human transcripts detected in samples corresponding to the frontal and middle samples, covering the initial site of engraftment. These results were confirmed by qRT-PCR for human nestin and TBP (data not shown) and corroborated bioluminescence analyses that showed some signal, although quite low in oHSV-treated mice (Figure S9A). At the end of the experiment (15 days after virus injection), we were unable to detect gD or sTRAIL neither by immunohistochemistry nor by qRT-PCR (data not shown).

To verify whether, *in vivo*, oHSVs effectively replicate in tumor cells and sTRAIL is expressed, this experiment was repeated with the same settings, but mice were sacrificed 2 days after virus injection. Right hemispheres were divided into three parts (frontal, middle, and occipital), and total RNA was extracted from the brain tissue. gD and sTRAIL relative expression measured by qRT-PCR demonstrated the presence of gD transcripts in brains injected with oHSV/Nb-gD and oHSV/Nb-gD:sTRAIL, while sTRAIL transcripts were detected only in the oHSV/Nb-gD:sTRAIL group (Figures S9B and S9C).

Finally, a survival assay was set up with similar experimental settings (Figure 6A). U87MG CXCR4⁺Luc⁺ cells were injected under stereotactic control. All mice developed tumors (Figure S10A) and viral sus-

pension, or PBS was injected within the tumor on day 7. Body weight was monitored every 2nd day, and mice were sacrificed when showing a significant weight loss or severe clinical signs. From day 19, all PBS-treated mice continuously lost weight, while oHSV-treated mice started to lose weight only on day 29, with the mice still alive 35 days after infection continuing to gain weight (Figure S10B). Again, tumor size appeared similar in all groups just before (day 5) virus injection (Figures 6B and S10A). However, one week after the intratumoral injection (day 13), bioluminescence signal in oHSV-treated mice was significantly reduced compared with the PBS group. In these oHSV-injected tumors, bioluminescence was very low and even undetectable in four of six and three of five mice in oHSV/Nb-gD and oHSV/Nb-gD:sTRAIL, respectively (Figures 6B and S10A). However, no significant difference was observed between oHSV/Nb-gD and oHSV/Nb-gD:sTRAIL-treated mice (Figure 6B). Importantly, while all PBS-treated mice died between day 21 and 27, the oHSV-treated mice death was significantly delayed, with the first deaths observed on day 31 (Figure 6C). At day 61, one of six oHSV/Nb-gD- and two of five oHSV/Nb-gD:sTRAIL-treated mice were still alive.

Taken together, all these results show that oHSV/Nb-gD and oHSV/Nb-gD:sTRAIL are suited for intratumoral injection in GBM orthotopic models and exert a potent oncolytic activity *in vivo*.

DISCUSSION

GBM remains the most aggressive form of adult brain cancer, associated with a dismal prognosis. Therapeutic failure and high recurrence rate endorse the need for novel, alternative, or add-on approaches to improve the standard-of-care therapy. GBM exhibits a wide cellular diversity, with malignant cells being highly heterogeneous in terms of molecular profile, phenotype, tumorigenic potential, and resistance to treatment. Such heterogeneity is largely accountable for tumor recurrence.

GSCs display stemness features, appear more resistant to radio- and chemotherapies, and are endowed with increased tumorigenicity.⁵⁰ Targeting GSCs thus appears as an opportunity for new therapeutic approaches. A wide variety of therapeutic strategies aiming to target GSCs have been evaluated in preclinical models and are being clinically translated.²⁶ However, considering the biological complexity and phenotypic plasticity of those cells, the main hurdle is to target GSCs without impairing normal tissue. In the perspective of eradicating peculiar GBM cell entities, such as GSCs, highly specific and targeted strategies should be considered.

Oncolytic virotherapy has been proposed as a promising avenue for GBM therapy, and herpesviruses offer numerous opportunities for tailored design and targeting strategies. oHSVs are the first viruses approved by the U.S. Food and Drug Administration (FDA) for virotherapy. Their mechanism of cell entry is well documented⁵¹ and can be modified to restrict oHSV entry into cells that specifically express a receptor of interest at their surface. oHSV retargeting requires the replacement of the viral glycoprotein domain important for their interaction with either the heparan sulfate or the natural receptors

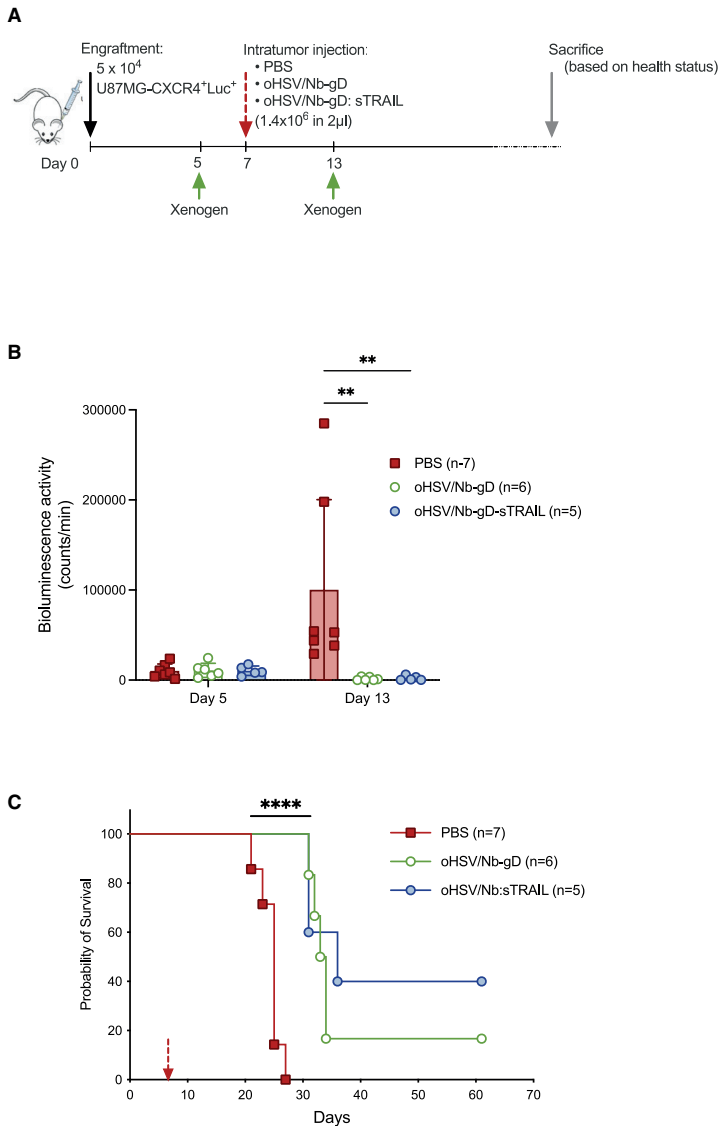


Figure 6. Survival assay upon oHSV/Nb-gD or oHSV/Nb-gD:sTRAIL treatment

(A) Schematic representation of the survival assay experimental settings. (B) Bioluminescence activity of nude mice engrafted with 5×10^4 U87MG CXCR4 Luc⁺ cells was recorded with Xenogen IVIS 50 on day 5 (2 days before treatment) and 13 (6 days after treatment). Bars represent the means \pm SEM. Statistical significance was determined by two-way ANOVA with Tukey's multiple comparisons of means. (** $p < 0.01$). See also Figure S10B for bioluminescence imaging. (C) Probability of survival of mice treated with PBS ($n = 7$), oHSV/Nb-gD ($n = 6$), or oHSV/Nb-gD:sTRAIL ($n = 5$). The red arrow indicates the day of treatment (day 7). Statistical significance was determined by log rank (Mantel-Cox) test (**** $p < 0.0001$). See also Figure S10A for weight follow-up.

In this study, GBM has been chosen as a model to evaluate the nanobody-based oHSV retargeting. As a proof of principle, we considered to genetically engineer an oHSV whose gD is modified by the insertion of a nanobody able to recognize hCXCR4, a chemokine receptor expressed on several GBM cell subtypes, including GSCs. CXCR4 has been associated with cancer cell proliferation, tumorigenesis, and migration, and its expression correlates with a poor prognosis.⁵² In addition, we have previously shown CXCR4⁺ cells as able to move away from the tumor core and specifically invade the subventricular zones,²¹ and targeting of CXCR4 therefore appears as an encouraging approach. The CXCR4-retargeted oHSV described in this paper (namely oHSV/Nb-gD) has been engineered from an attenuated backbone (Δ ICP34.5, Δ ICP6, and Δ ICP47), whose safety in GBM treatment has been largely documented.⁴¹ Other oHSVs retargeted to the epidermal growth factor receptor (EGFR), the human tyrosine kinase receptor erbB-2 (hHER2), the interleukin-13 receptor, the epithelial cell adhesion molecule (EPCAM), or the urokinase plasminogen activator receptor; all described to be overexpressed in cancer tissues have been constructed and characterized.^{31–36} Contrarily to the oHSVs described in this paper, all these retargeted viruses were engineered in a non-attenuated HSV background, inducing a higher level of viral replication. However, their safety only relies on the tight control of their entry into cancer cells and consequently requires an absence or a very low expression of the target of interest on healthy cells. Similarly, the CXCR4-retargeted oHSVs entry depends on the capacity of the virus to specifically interact with a receptor, but its attenuated character limits its

by a ligand specific for a protein of interest. Single-chain antibodies (scFv), cytokines, or specific ligands have been described for their efficacy to retarget oHSV.^{31–35} In our study, we describe oHSV retargeting using a nanobody. Nanobodies correspond to the single heavy variable domain of camelid antibodies. They can be quite easily obtained by screening either immune or artificial libraries characterized by a huge sequence diversity and thereby constitute an interesting tool for oHSV customization and specific targeting.

replication in non-cancer cells, improving its safety. We show that the CXCR4-retargeted virus (oHSV/Nb-gD) can specifically infect in a CXCR4-dependent manner, not only U87MG CXCR4⁺ but also patient-derived GSCs, despite a much lower CXCR4 endogenous expression. *In vitro*, when armed with a secreted form of TRAIL (oHSV/Nb-gD:sTRAIL), this virus is able to trigger apoptosis. The replication of these oncolytic viruses in cells transduced with CXCR4 is not impaired by the retargeting or the arming. Importantly, when inoculated at high titers (10⁷ PFUs/mL) on primary GBM cells expressing a high level of endogenous CXCR4 (T033), both the retargeted and the non-retargeted viruses show the same kinetics and the same efficacy of infection.

When used *in vivo* in an orthotopic xenograft model of GBM, in which U87MG CXCR4⁺ cells were engrafted, both sTRAIL-armed and non-armed oHSVs were able to limit the tumor progression and to significantly improve mice survival. Even though sTRAIL triggers apoptosis *in vitro*, its impact in the xenograft model seems to be limited. Contrarily to the sTRAIL-armed oHSV previously described in the literature and whose expression is driven by the HSV immediate-early promoter IE4/5,^{37,40} sTRAIL expression in oHSV/Nb-gD:sTRAIL is driven by the nestin promoter. Although nestin is overexpressed in most GBM tumors,²⁶ it might not be activated at the same level in all GBM cells and hence be too restrictive for an optimal expression of sTRAIL. Moreover, *in vitro*, the percentage of apoptotic cells as measured by flow cytometry does not reflect the strong impact of oHSV infection on U87MG viability (Figure 4C). The oncolysis mediated by the virus itself may hide the sTRAIL-induced apoptosis when high MOI are used.^{37,40} The efficacy of the arming should be further evaluated *in vivo* in the xenograft model after engraftment of patient-derived GSCs. If needed, a stronger promoter should be considered to drive sTRAIL expression. U87MG CXCR4⁺ cells engrafted in the xenograft model have a very rapid growth kinetics. Such a rapid growth can hamper the total elimination of the tumor after a single virus injection and could explain the regrowth observed in some mice. In this context, it would be worth evaluating the impact of repeated injections or of continuous delivery of the virus thanks to a mini-osmotic pump system.⁵³ In addition, the role of the tumor microenvironment and especially of the innate immune response should not be underestimated. oHSV virotherapy has been shown to rapidly activate natural killer (NK) cells that diminish the virotherapy efficacy,⁵⁴ while adenovirus virotherapy has been shown to induce a phenotypic shift of macrophages from pro-tumoral M2-like toward the anti-tumoral and pro-inflammatory M1-like phenotype.⁵⁵ A deeper characterization of the tumor microenvironment upon virotherapy will provide important information that might help to improve the treatment.

An important issue that must be carefully studied when targeting tumor cells is the fact that healthy cells might express the protein of interest and thus be infected by the oncolytic virus. Although in our study oHSVs are attenuated, this issue must be taken into consideration. CXCR4 is mainly expressed in the bone marrow or lymphoid

tissues and poorly expressed in the brain (<https://www.proteinatlas.org/ENSG00000121966-CXCR4>). Taking into consideration that the oHSV is injected within the tumor, CXCR4 expression on non-tumoral cells in the vicinity of the tumor must, however, be considered. Based on publicly available patient-derived transcriptomic data, CXCR4 is expressed in malignant cells, in endothelial cells within the tumor, and on tumor-associated macrophages (TAMs) and tumor-infiltrating lymphocytes (TILs).⁵⁶ The capacity of the CXCR4-retargeted virus to infect and potentially destroy these cells, especially endothelial cells and M2-like macrophages, would certainly be of interest; still, the benefit and risk balance has to be assessed very carefully. Unfortunately, the anti-hCXCR4 nanobody used in this study does not recognize the murine CXCR4, which limits the questions that could be addressed in the human GBM xenograft model. We are currently screening a nanobody library to identify nanobodies that recognize both the human and murine CXCR4 receptor. Such nanobodies would allow not only to address important issues, such as the undesired targeting of healthy cells, but also to evaluate the importance of the immune response and particularly of the adaptive immune response, this latest requiring a syngeneic GBM murine model.

Altogether, the results described in this proof of principle study show that the retargeting of oHSVs by the insertion of a nanobody appears highly encouraging and constitutes an interesting approach for the targeting of GBM cell subsets, e.g., GSCs, expressing specific proteins of interest. Our data support the idea that a set of nanobodies specific for diverse GSCs markers may be used to customize oHSVs that could be exploited as an add-on to complement the current standard-of-care therapeutic approaches.

MATERIAL AND METHODS

Cell lines

Vero cells (ATCC; no. CCL-81) and human glioblastoma U87MG (ATCC; no. HTB-14) cells were maintained in Dulbecco's modified Eagle medium (DMEM) (Biowest, VWR International, Leuven, Belgium) supplemented with 10% fetal bovine serum (FBS). J1.1-2 cells are HSV-1-resistant baby hamster kidney cells lacking both HVEM and nectin-1, two natural HSV-1 receptors. J/A and J/C cells are J1.1 transduced with HVEM and nectin-1, respectively (kind gift of Prof. G. Campadelli-Fiume [University of Bologna, Italy]). They were cultured with DMEM supplemented with 5% of FBS. J/A and J/C cells were treated with 400 µg/mL of G418 (Invivogen, Belgium). Vero CXCR4⁺ and U87MG CXCR4⁺ obtained by transduction of a lentivirus (Viral Vector platform, University of Liège) were treated with 20 ng/mL and 10 ng/mL of blasticidin (Invivogen, Belgium), respectively. Primary GBM primary cultures (T08, T013, T018, and T033) were established from freshly resected human GBM tissue obtained from GBM patients. They were cultured as tumorspheres in stem cell medium (DMEM/F-12 with GlutaMAX [Gibco, Fisher Scientific, Belgium] supplemented with B27 [1/50] without vitamin A [Gibco, Fisher Scientific, Belgium], 1% penicillin-streptomycin [Biowest, VWR International, Leuven, Belgium], 1 µg/mL of heparin [no. 7692.1; Carl Roth, Belgium], human EGF [20 ng/mL; BioLegend, Amsterdam, The Netherlands], and βFGF [20 ng/mL; BioLegend, Amsterdam, The Netherlands]).

Table 1. Primers used for qRT-PCR

	Forward	Reverse
HSV-1 gD	5'-GCCCCGCTGGAACACTACTATG-3'	5'-TTATCTTCACGAGCCGAGG-3'
sTRAIL	5'-CATCGAGAACGAGATCGCCC-3'	5'-TGTGTTGCTTCTCTCTGGT-3'
SOX2	5'-AGTCTCCAAGCGAGAAAAA-3'	5'-TTTCACGTTTGCAACTGTCC-3'
POU3F2	5'-CTGACGATCTCCACGCACTA-3'	5'-GGCAGAAAGCTGTCCAAGTC-3'
SALL2	5'-ACTCCTCTGGGGTGACCTTT-3'	5'-GGAGTGGTAGTGGAGGTGGA-3'
18S	5'-AACTTTCGATGGTAGTCGCCG-3'	5'-CCTTGGATGTGGTAGCCGTTT-3'
hTBP	5'-ACAGCCTGCCACCTTACG-3'	5'-TGCATAAGGCATCATTGGACTA-3'

Construction of recombinant oHSVs

Recombinant viruses were engineered in fHsvQuik-1 BAC containing an attenuated strain F HSV-1 ($\Delta\gamma34.5$, $\Delta\text{UL}39$, GFP⁺; kind gift from A. Chiocca from the University of Pittsburgh, USA). Recombinants were obtained by the two-step Red recombination technique “en passant.”⁵⁷ ICP47 deletion was done as described by Todo et al.⁵⁸ The detargeting of gD from its natural receptors was performed according to Uchida et al.⁴³ For retargeting, we inserted a patented sequence coding for a nanobody against human CXCR4 receptor (CXCR4-NB; WO2016156570A1) in the gD coding sequence. The “arming” sequence containing a soluble form of TRAIL (sTRAIL)⁴⁵ under the nestin promoter was inserted before the ICP6 promoter as shown in Figure 1. A double mutation (D285N and A549T) was inserted within gB to compensate the loss of infectivity generally observed upon gD retargeting.⁴⁴ CXCR4⁺ Vero cells were plated in 6-well plate at 40% confluence and transfected with 3 μg of BAC using JETPEI (Polyplus, Illkirch, France). Viral replication was detected 48 h after transfection by the visualization of fluorescent foci. Virus stocks were produced and concentrated as previously described.⁵⁹ Briefly, cells were infected at low MOI (0.005) and cultured for 4 to 5 days at 33°C. The day before the experiment, cells were treated with 0.45 M of NaCl and 100 $\mu\text{g}/\text{mL}$ of dextran sulfate. Supernatant was collected and centrifuged at 2,200 g for 10 min at 4°C and then filtered with 0.8- μm filter to discard cell debris. Then, viral particles were ultracentrifuged at 47,850g at 4°C using Beckman SW27 rotor. Centrifuged virus was resuspended in PBS with 10% glycerol, aliquoted, and stored at -80°C . Plaque assay in Vero CXCR4⁺ was used to titrate the virus and determine the amount of PFUs/mL.⁴⁹

Viral growth assay

U87MG CXCR4⁺ or Vero CXCR4⁺ cells were seeded in a 12-well plate and infected with oHSV/gD, oHSV/Nb-gD, or oHSV/Nb-gD:sTRAIL at a MOI of 1 for 24, 48, or 72 h. Supernatant was then harvested, and titer (PFUs/mL) was determined by plaque assay as previously described.⁴⁹ The number of foci was calculated based on Incucyte S3 imaging.

Entry assay

J1.1–2, J/A, and J/C cells were seeded in a 24-well plate the day before infection. Cells were infected with a MOI of 1, 0.1, and 0.01. After 48 h, cells were fixed with 4% paraformaldehyde and

washed with PBS. Images were collected with the Incucyte S3 (Sartorius).

qRT-PCR

Total RNA was isolated using the RNA isolation Nucleospin kit (Macherey-Nagel) according to the manufacturer’s protocol. Five hundred nanograms of RNA was reverse transcribed using RevertAid H Minus First Strand cDNA Synthesis Kit (Thermo Scientific) with random primers (for gD or sTRAIL transcripts detection) or oligo-dT primers (for stemness markers transcripts detection). TBP or 18S were used as controls. qRT-PCR reaction samples were prepared as follows: 4 μL of the diluted cDNA (2.5 ng in total for gD and sTRAIL or 10 ng in total for stemness markers) were mixed with 5 μL of SYBR green (TAKYON, Eurogentec, Liege, Belgium) and 0.2 μM of each primer in a final volume of 10 μL . Primers used for transcripts detection are described in Table 1. Quantitative real-time PCR was done using the Roche LightCycler 480 (3 min at 95°C of activation; 45 cycles: denaturation 95°C, 3 s; hybridization and elongation 60°C, 25 s).

Flow cytometry

For CXCR4 detection by flow cytometry, cells were plated in 6-well plate 2 days before analysis or cultured as tumorspheres. Tumorspheres and cells cultured as monolayers were washed with PBS and dissociated by incubating the cells for 10 min at 37°C with Accutase (Biowest, Nuaille, France). Dissociated cells were centrifuged at 350g for 5 min at 4°C and washed with flow cytometry buffer (PBS with BSA 1%, EDTA 1 mM, and ADE 0.1%). Five microliters of antigen-presenting cell (APC)-conjugated anti-CXCR4 antibody (BioLegend, Amsterdam, the Netherlands) were added to 1×10^5 cells in 100 μL of flow cytometry buffer (dilution 1/20) and kept at 4°C for 1 h in the dark. Cells were washed by adding 1 mL of flow buffer and centrifuged at 400g for 4 min at 4°C. After a second wash, cells were resuspended in 200 μL of flow buffer and directly analyzed with the FACS CANTO II (BD Biosciences). Data were analyzed with FlowJo software.

Annexin/DAPI assay

For annexin V/DAPI apoptosis assay, 92,000 cells were seeded in a 12-well plate and infected with a MOI of 1, 5, or 10 for 72 h. Cells were collected and resuspended in 140 μL of 1X Binding Buffer (ref. 556,454; BD Pharmingen). Ten microliters of DAPI (Invitrogen;

1:100) and 5 μ L of annexin V-PE (ref. AB 2869071; BD Biosciences) were added, and cells were incubated for 15 min at room temperature (RT) in the dark. Finally, 200 μ L of 1X Binding Buffer was added and samples were directly analyzed with the FACS FORTRESSA (BD Biosciences). Data were analyzed with FlowJo software.

Viability assay

U87MG and U87MG CXCR4⁺ cells were plated in a 12-well plate and infected with the different viruses at a MOI of 5. Measure of viability was done at 24, 48, and 72 hpi by evaluating the metabolic activity using a resazurin assay. At each time point, media were removed and replaced by 500 μ L of resazurin (20% [v/v] in DMEM-10% FBS), and cells were further incubated for 4 h at 37°C. Metabolized media were transferred into a 96-well flat-bottom black plate and read (λ ex = 535 nm; λ em = 595 nm) using the multi-mode microplate reader (FilterMax F5). Results are expressed as a percentage of the control.

Real-time measure of the GFP fluorescence

U87MG and U87MG CXCR4⁺ cells were plated in a 24-well flat bottom plate (46,000 cells/well). After 24 h of monolayer culture, cells were infected with oHSV/gD or oHSV/Nb-gD (MOI: 0.1) and incubated in the Incucyte S3 for real-time analyses of the mean EGFP fluorescence intensity with the whole well module (magnification 4 \times).

Patient-derived GSCs were seeded in 96-well round bottom plate (100,000 cells/well) in stem cell medium. Twenty-four hours after seeding, tumorospheres were infected with oHSV/gD or oHSV/Nb-gD (10⁴ PFUs/well) and incubated in the Incucyte S5 for a real-time analysis of the mean EGFP fluorescence intensity with the organoid module (magnification 4 \times).

Immunofluorescence staining on tumorospheres

Tumorospheres were infected with 10⁶ PFUs/mL. Forty-eight hours post-infection, cells were washed and fixed with 4% paraformaldehyde for 20 min and incubated overnight with 20% PBS-sucrose before being embedded with colored OCT (Neg-50). Spheroids were cut into 5- μ m-thick cryosections (Microm HM 560, Thermo Scientific) and placed onto SuperFrost slides (Thermo Scientific). Sections were permeabilized with 0.3% Triton X-100 PBS solution for 10 min, and unspecific binding sites were blocked with 5% BSA for 30 min. Tumorospheres sections were incubated overnight at 4°C with primary antibodies diluted in 5% BSA (rabbit anti-CXCR4 [ref. AB124824; Abcam; 1:200]; mouse anti-*nestin* [ref. sc-23927; Santa Cruz; 1:250]). After two washes, slides were incubated for 1 h at RT in the dark with secondary antibodies (goat anti-mouse Alexa Fluor 633 and goat anti-rabbit Alexa Fluor 568; 1:500). Nuclei were stained by incubation with Hoechst for 10 min at 1:50,000. Finally, Mowiol (Sigma) was added, and sections were covered by a coverslip. Images were recorded with Nikon A1R confocal microscope. Figures were composed and examined with ImageJ software.

Western blot assay

Cells were lysed with radioimmunoprecipitation assay (RIPA)-modified buffer (50 mM of Tris-HCl, 150 mM of NaCl, 1 mM of EDTA, 1% NP40, and 0.25% of DOC). Eighty micrograms of proteins were loaded on a 6% (for PARP and gD detection) or 12% (for caspase 3 and α -tubulin detection) SDS-acrylamide gel. After electrophoresis, proteins were transferred on a polyvinylidene fluoride (PVDF) membrane (GE Healthcare) according to standard protocols. Mouse anti-gD was used to determine viral infection level (ref. sc-21719; Santa Cruz; 1:1,000), and rabbit anti-PARP (ref. 9532; Cell Signaling; 1:1,000) and mouse anti-caspase 3 (CC3) (ref. ALX-804-305; Enzo, Life Sciences, Brussels, Belgium; 1:1,000) were used to detect the activation of the apoptotic pathway. Mouse anti- α -tubulin (ref. T6199; Sigma, 1:2,000) was used as loading control. Horseradish peroxidase (HRP)-conjugated anti-rabbit-immunoglobulin G (IgG) (ref. 7074; Cell Signaling) and HRP-conjugated anti-mouse-IgG (ref. 7076; Cell Signaling) were used as secondary antibodies. Signals were revealed using enhanced chemiluminescence (ECL) and imaged with LAS4000 charge-coupled device (CCD) camera (GE Healthcare).

In vivo experiments

Adult 6 weeks female immunodeficient Crl:NU-Foxn1nu mice (Charles River Laboratories, Brussels, Belgium) were used for xenograft experiments. The athymic nude mice were housed in sterilized, filter-topped cages at the Animal Facility at the University of Liège, and all experiments were performed as previously approved by the Animal Ethical Committee of the University of Liège, in accordance with the Declaration of Helsinki and following the guidelines of the Belgium Ministry of Agriculture in agreement with European Commission Laboratory Animal Care and Use Regulation. Intrastriatal grafts were performed following the previously described procedures.⁶⁰ Briefly, 50,000 U87MG CXCR4⁺Luc⁺ cells resuspended in 2 μ L of PBS were injected into the right striatum of mice previously anesthetized with an intraperitoneal injection of a Rompun (Sedativum 2%; Bayer, Brussels, Belgium) and Ketalar (ketamine 50 mg/mL, Pfizer, Brussels, Belgium) solution (V/V) prepared just before injection. Injection was performed according to stereotactic coordinates (0.5 mm anterior and 2.5 mm lateral from the bregma and at a depth of 3 mm), allowing a precise and reproducible injection site. Later, oncolytic viruses resuspended in 2 μ L of PBS were injected, under similar anesthesia, within the tumor using the same stereotactic coordinates. Mice health status was evaluated daily, and mice were weighed regularly.

Bioluminescence activity

Immunodeficient nude mice bearing intracranial U87MG CXCR4⁺Luc⁺ xenografts were injected intraperitoneally with beetle luciferin potassium salt (ref. E1605; Promega; 150 mg/kg). Under anesthesia using 2.5% isoflurane, mice were imaged with a camera-based bioluminescence imaging system (Xenogen IVIS 50; exposure time 1 min, 15 min after intraperitoneal injection). Regions of interest were defined manually, and images were processed using Living Image and IgorPro Software (v.2.60.1). Raw data were expressed as total counts/s or total counts/min.

Brain tissue processing and tumor volume measurement

Mice were euthanized with intraperitoneal (i.p.) injection of Euthazol Vet (140 mg/kg) and intracardiac perfusion of ice-cold saline solution, followed by paraformaldehyde 4% in PBS (for histology). Brains were extracted, placed in sucrose 30% for tissue cryopreservation, and sectioned into 14- μ m-thick serial sections using a cryostat. Tumor volume analysis was performed by immunohistochemistry for human vimentin detection (mouse anti-human vimentin; MAB3400; Merck; 1:200) with PolyviewPlus HRP-DAB kit (Enzo Life Sciences, Brussels, Belgium). Tumor was delineated based on anti-vimentin positivity. Ten to twelve serial brain sections were analyzed using the Mercator software (ExploraNova, La Rochelle, France). 3D reconstitution and extrapolation of tumor volume were performed using Map3D software.

Statistical analysis

All statistical analyses were performed using GraphPad Prism 9. Data are displayed as mean \pm SEM. Depending on the experiments, paired t test, Kruskal-Wallis, or two-way ANOVAs were performed as indicated in the figure legends. Statistical significance of survival assay was analyzed by log rank (Mantel-Cox) test.

DATA AND AVAILABILITY

All raw data are available upon request.

SUPPLEMENTAL INFORMATION

Supplemental information can be found online at <https://doi.org/10.1016/j.omto.2022.06.002>.

ACKNOWLEDGMENTS

J.S.G. and P.D. are, respectively, a PhD student and a PhD funded by the TELEVIE-FNRS; M.D. is a Research Fellow of the FNRS-Belgium; and A.L. is Clinical Post-doctoral Researcher of the FNRS-Belgium. This work was supported by grants from the National Fund for Scientific Research (FNRS, Télévie); the Special Funds of the University of Liège; the Leon Fredericq Foundation, Liège, Belgium; and the Neurological Foundation of New Zealand. The authors would like to thank Prof. A. Chiocca (University of Pittsburgh, USA) for fHsvQuik-1 BAC, Prof. G. Campadelli-Fiume (University of Bologna, Italy) for J1.1-2, J/A and J/C cells, A. Deward (GIGA, Université de Liège) for the graphical abstract and all the members of the GIGA Viral Vector, Imaging and Flow Cytometry, and Genomics platforms and animal facilities for valuable technical support.

AUTHOR CONTRIBUTIONS

Conception of the project, C.S.-D.; funding acquisition, B.R. and C.S.-D.; design of the experiments, J.S.G., V.N., A.L., N.C., M.L., and C.S.-D.; experiments, J.S.G., D.I., M.D., and P.D.; technical assistance, C.L., T.A., and B.B.; writing, C.S.-D. and J.S.G.; reviewing, P.D., V.N., B.R., A.L., M.L., and N.C.

DECLARATION OF INTERESTS

The authors declare no competing interests.

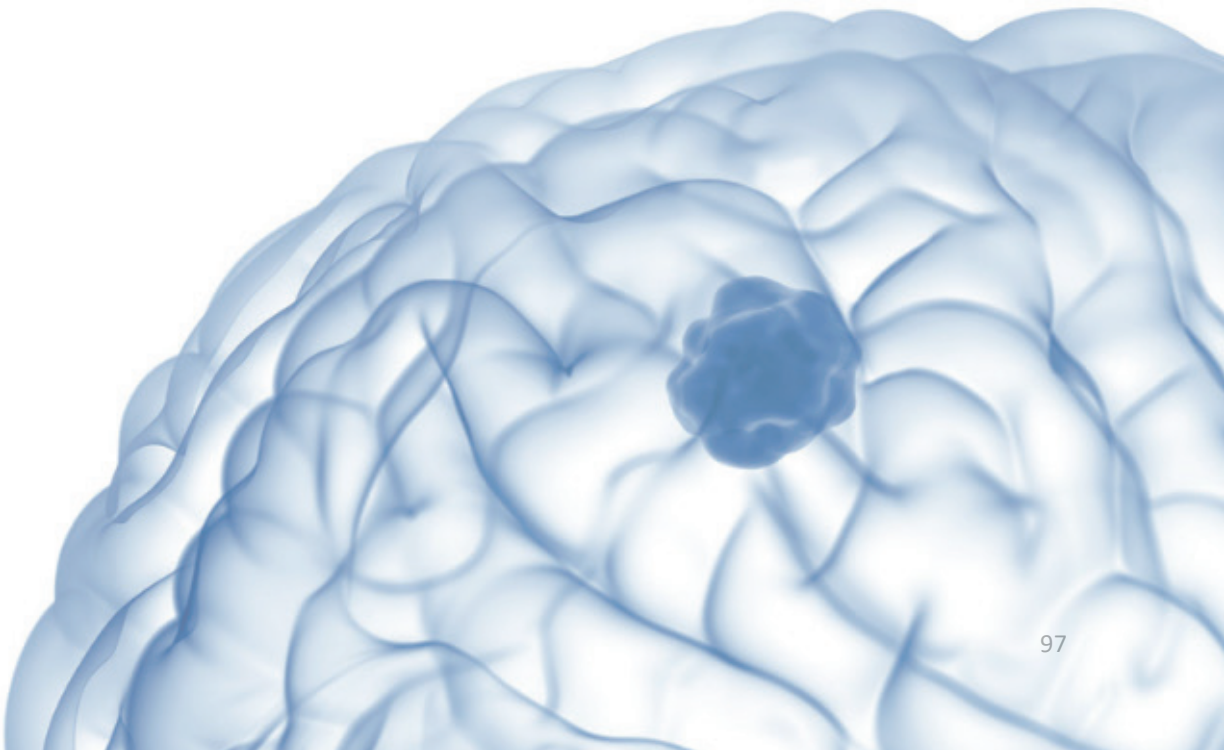
REFERENCES

- Feng, Y., Broder, C.C., Kennedy, P.E., and Berger, E.A. (1996). HIV-1 entry cofactor: functional cDNA cloning of a seven-transmembrane, G protein-coupled receptor. *Science* 272, 872–877. <https://doi.org/10.1126/science.272.5263.872>.
- Alimohammadi, M., Rahimi, A., Faramarzi, F., Alizadeh-Navaei, R., and Rafiei, A. (2021). Overexpression of chemokine receptor CXCR4 predicts lymph node metastatic risk in patients with melanoma: a systematic review and meta-analysis. *Cytokine* 148, 155691. <https://doi.org/10.1016/j.cyto.2021.155691>.
- Salmaggi, A., Gelati, M., Pollo, B., Marras, C., Silvani, A., Balestrini, M.R., Eoli, M., Fariselli, L., Broggi, G., and Boiardi, A. (2005). CXCL12 expression is predictive of a shorter time to tumor progression in low-grade glioma: a single-institution study in 50 patients. *J. Neurooncol.* 74, 287–293. <https://doi.org/10.1007/s11060-004-7327-y>.
- Katsumoto, K., and Kume, S. (2013). The role of CXCL12-CXCR4 signaling pathway in pancreatic development. *Theranostics* 3, 11–17. <https://doi.org/10.7150/thno.4806>.
- Gagliardi, F., Narayanan, A., Reni, M., Franzin, A., Mazza, E., Boari, N., Bailo, M., Zordan, P., and Mortini, P. (2014). The role of CXCR4 in highly malignant human gliomas biology: current knowledge and future directions. *Glia* 62, 1015–1023. <https://doi.org/10.1002/glia.22669>.
- Santagata, S., Ieranò, C., Trotta, A.M., Capilungo, A., Auletta, F., Guardascione, G., and Scala, S. (2021). CXCR4 and CXCR7 signaling pathways: a focus on the cross-talk between cancer cells and tumor microenvironment. *Front. Oncol.* 11, 591386. <https://doi.org/10.3389/fonc.2021.591386>.
- Gagner, J.P., Sarfraz, Y., Ortenzi, V., Alotaibi, F.M., Chiriboga, L.A., Tayyib, A.T., Douglas, G.J., Chevalier, E., Romagnoli, B., Tuffin, G., et al. (2017). Multifaceted C-X-C chemokine receptor 4 (CXCR4) inhibition interferes with anti-vascular endothelial growth factor therapy-induced glioma dissemination. *Am. J. Pathol.* 187, 2080–2094. <https://doi.org/10.1016/j.ajpath.2017.04.020>.
- Gatti, M., Pattarozzi, A., Bajetto, A., Würth, R., Daga, A., Fiaschi, P., Zona, G., Florio, T., and Barbieri, F. (2013). Inhibition of CXCL12/CXCR4 autocrine/paracrine loop reduces viability of human glioblastoma stem-like cells affecting self-renewal activity. *Toxicology* 314, 209–220. <https://doi.org/10.1016/j.tox.2013.10.003>.
- Mercurio, L., Ajmone-Cat, M.A., Cecchetti, S., Ricci, A., Bozzuto, G., Molinari, A., Manni, I., Pollo, B., Scala, S., Carpinelli, G., and Minghetti, L. (2016). Targeting CXCR4 by a selective peptide antagonist modulates tumor microenvironment and microglia reactivity in a human glioblastoma model. *J. Exp. Clin. Cancer Res.* 35, 55. <https://doi.org/10.1186/s13046-016-0326-y>.
- Gil, M., Seshadri, M., Komorowski, M.P., Abrams, S.I., and Kozbor, D. (2013). Targeting CXCL12/CXCR4 signaling with oncolytic virotherapy disrupts tumor vasculature and inhibits breast cancer metastases. *Proc. Natl. Acad. Sci. U S A* 110, E1291–E1300. <https://doi.org/10.1073/pnas.1220580110>.
- Scala, S. (2015). Molecular pathways: targeting the CXCR4-CXCL12 Axis—Untapped potential in the tumor microenvironment. *Clin. Cancer Res.* 21, 4278–4285. <https://doi.org/10.1158/1078-0432.ccr-14-0914>.
- Kioi, M., Vogel, H., Schultz, G., Hoffman, R.M., Harsh, G.R., and Brown, J.M. (2010). Inhibition of vasculogenesis, but not angiogenesis, prevents the recurrence of glioblastoma after irradiation in mice. *J. Clin. Invest.* 120, 694–705. <https://doi.org/10.1172/jci40283>.
- Lee, C.C., Lai, J.H., Hueng, D.Y., Ma, H.I., Chung, Y.C., Sun, Y.Y., Tsai, Y.J., Wu, W.B., and Chen, C.L. (2013). Disrupting the CXCL12/CXCR4 axis disturbs the characteristics of glioblastoma stem-like cells of rat RG2 glioblastoma. *Cancer Cell Int.* 13, 85. <https://doi.org/10.1186/1475-2867-13-85>.
- Ostrom, Q.T., Gittleman, H., Truitt, G., Boscia, A., Kruchko, C., and Barnholtz-Sloan, J.S. (2018). CBTRUS statistical report: primary brain and other central nervous system tumors diagnosed in the United States in 2011–2015. *Neuro. Oncol.* 20, 1–86. <https://doi.org/10.1093/neuonc/now131>.
- Stupp, R., Taillibert, S., Kanner, A., Read, W., Steinberg, D.M., Lhermitte, B., Toms, S., Idhah, A., Ahluwalia, M.S., Fink, K., et al. (2017). Effect of tumor-treating fields plus maintenance temozolomide vs maintenance temozolomide alone on survival in patients with glioblastoma: a randomized clinical trial. *JAMA* 318, 2306. <https://doi.org/10.1001/jama.2017.18718>.

16. Lara-Velazquez, M., Al-Kharboosh, R., Jeanneret, S., Vazquez-Ramos, C., Mahato, D., Tavanaiepour, D., Rahmthulla, G., and Quinones-Hinojosa, A. (2017). Advances in brain tumor surgery for glioblastoma in adults. *Brain Sci.* *7*, 166. <https://doi.org/10.3390/brainsci7120166>.
17. Singh, S.K., Hawkins, C., Clarke, I.D., Squire, J.A., Bayani, J., Hide, T., Henkelman, R.M., Cusimano, M.D., and Dirks, P.B. (2004). Identification of human brain tumour initiating cells. *Nature* *432*, 396–401. <https://doi.org/10.1038/nature03128>.
18. Galli, R., Binda, E., Orfanelli, U., Cipelletti, B., Gritti, A., De Vitis, S., Fiocco, R., Foroni, C., Dimeco, F., and Vescovi, A. (2004). Isolation and characterization of tumorigenic, stem-like neural precursors from human glioblastoma. *Cancer Res.* *64*, 7011–7021. <https://doi.org/10.1158/0008-5472.can-04-1364>.
19. Chen, R., Nishimura, M.C., Bumbaca, S.M., Kharbanda, S., Forrest, W.F., Kasman, I.M., Greve, J.M., Soriano, R.H., Gilmour, L.L., Rivers, C.S., et al. (2010). A hierarchy of self-renewing tumor-initiating cell types in glioblastoma. *Cancer Cell* *17*, 362–375. <https://doi.org/10.1016/j.ccr.2009.12.049>.
20. Singh, S.K., Clarke, I.D., Terasaki, M., Bonn, V.E., Hawkins, C., Squire, J., and Dirks, P.B. (2003). Identification of a cancer stem cell in human brain tumors. *Cancer Res.* *63*, 5821–5828.
21. Goffart, N., Kroonen, J., Di Valentin, E., Dedobbeleer, M., Denne, A., Martinev, P., and Rogister, B. (2015). Adult mouse subventricular zones stimulate glioblastoma stem cells specific invasion through CXCL12/CXCR4 signaling. *Neuro. Oncol.* *17*, 81–94. <https://doi.org/10.1093/neuonc/nou144>.
22. Goffart, N., Lombard, A., Lallemand, F., Kroonen, J., Nassen, J., Di Valentin, E., Berendsen, S., Dedobbeleer, M., Willems, E., Robe, P., et al. (2017). CXCL12 mediates glioblastoma resistance to radiotherapy in the subventricular zone. *Neuro. Oncol.* *19*, 66–77. <https://doi.org/10.1093/neuonc/now136>.
23. Dedobbeleer, M., Willems, E., Lambert, J., Lombard, A., Digregorio, M., Lumapat, P.N., Di Valentin, E., Freeman, S., Goffart, N., Scholtes, F., and Rogister, B. (2020). MKP1 phosphatase is recruited by CXCL12 in glioblastoma cells and plays a role in DNA strand breaks repair. *Carcinogenesis* *41*, 417–429. <https://doi.org/10.1093/carcin/bgz151>.
24. Cheray, M., Bégaud, G., Deluche, E., Nivet, A., Battu, S., Lalloué, F., et al. (2017). Cancer stem-like cells in glioblastoma. In *Glioblastoma, Chapter 4*, S. De Vleeschouwer, ed (Codon Publications), pp. 59–71.
25. Lombard, A., Digregorio, M., Delcamp, C., Rogister, B., Piette, C., and Coppieters, N. (2020). The subventricular zone, a hideout for adult and pediatric high-grade glioma stem cells. *Front. Oncol.* *10*, 614930. <https://doi.org/10.3389/fonc.2020.614930>.
26. Tang, X., Zuo, C., Fang, P., Liu, G., Qiu, Y., Huang, Y., and Tang, R. (2021). Targeting glioblastoma stem cells: a review on biomarkers, signal pathways and targeted therapy. *Front. Oncol.* *11*, 701291. <https://doi.org/10.3389/fonc.2021.701291>.
27. Fountzilias, C., Patel, S., and Mahalingam, D. (2017). Review: oncolytic virotherapy, updates and future directions. *Oncotarget* *8*, 102617–102639. <https://doi.org/10.18632/oncotarget.18309>.
28. Miyauchi, J.T., and Tsirka, S.E. (2018). Advances in immunotherapeutic research for glioma therapy. *J. Neurol.* *265*, 741–756. <https://doi.org/10.1007/s00415-017-8695-5>.
29. Friedman, G.K., Langford, C.P., Coleman, J.M., Cassady, K.A., Parker, J.N., Markert, J.M., and Yancey Gillespie, G. (2009). Engineered herpes simplex viruses efficiently infect and kill CD133+ human glioma xenograft cells that express CD111. *J. Neuro. Oncol.* *95*, 199–209. <https://doi.org/10.1007/s11060-009-9926-0>.
30. Rueger, M.A., Winkler, A., Miletic, H., Kaestle, C., Richter, R., Schneider, G., Hilker, R., Heneka, M.T., Ernestus, R.I., Hampl, J.A., et al. (2005). Variability in infectivity of primary cell cultures of human brain tumors with HSV-1 amplicon vectors. *Gene Ther.* *12*, 588–596. <https://doi.org/10.1038/sj.gt.3302462>.
31. Menotti, L., Nicoletti, G., Gatta, V., Croci, S., Landuzzi, L., De Giovanni, C., Nanni, P., Lollini, P.-L., and Campadelli-Fiume, G. (2009). Inhibition of human tumor growth in mice by an oncolytic herpes simplex virus designed to target solely HER-2-positive cells. *Proc. Natl. Acad. Sci. U S A* *106*, 9039–9044. <https://doi.org/10.1073/pnas.0812268106>.
32. Kamiyama, H., Zhou, G., and Roizman, B. (2006). Herpes simplex virus 1 recombinant virions exhibiting the amino terminal fragment of urokinase-type plasminogen activator can enter cells via the cognate receptor. *Gene Ther.* *13*, 621–629. <https://doi.org/10.1038/sj.gt.3302685>.
33. Zhou, G., and Roizman, B. (2006). Construction and properties of a herpes simplex virus 1 designed to enter cells solely via the IL-13 α 2 receptor. *Proc. Natl. Acad. Sci. U S A* *103*, 5508–5513. <https://doi.org/10.1073/pnas.0601258103>.
34. Grandi, P., Fernandez, J., Szentirmai, O., Carter, R., Gianni, D., Sena-Esteves, M., and Breakefield, X.O. (2010). Targeting HSV-1 virions for specific binding to epidermal growth factor receptor-vIII-bearing tumor cells. *Cancer Gene Ther.* *17*, 655–663. <https://doi.org/10.1038/cgt.2010.22>.
35. Shibata, T., Uchida, H., Shiroyama, T., Okubo, Y., Suzuki, T., Ikeda, H., Yamaguchi, M., Miyagawa, Y., Fukuhara, T., Cohen, J.B., et al. (2016). Development of an oncolytic HSV vector fully retargeted specifically to cellular EpCAM for virus entry and cell-to-cell spread. *Gene Ther.* *23*, 479–488. <https://doi.org/10.1038/gt.2016.17>.
36. Alessandrini, F., Menotti, L., Avitabile, E., Appolloni, I., Ceresa, D., Marubbi, D., Campadelli-Fiume, G., and Malatesta, P. (2019). Eradication of glioblastoma by immuno-virotherapy with a retargeted oncolytic HSV in a preclinical model. *Oncogene* *38*, 4467–4479. <https://doi.org/10.1038/s41388-019-0737-2>.
37. Jahan, N., Lee, J.M., Shah, K., and Wakimoto, H. (2017). Therapeutic targeting of chemoresistant and recurrent glioblastoma stem cells with a proapoptotic variant of oncolytic herpes simplex virus. *Int. J. Cancer* *141*, 1671–1681. <https://doi.org/10.1002/ijc.30811>.
38. Kim, M.-H., Billiar, T.R., and Seol, D.-W. (2004). The secretable form of trimeric TRAIL, a potent inducer of apoptosis. *Biochem. Biophys. Res. Commun.* *321*, 930–935. <https://doi.org/10.1016/j.bbrc.2004.07.046>.
39. Kock, N., Kasmieh, R., Weissledery, R., and Shah, K. (2007). Tumor therapy mediated by lentiviral expression of shBcl-2 and S-TRAIL. *Neoplasia* *9*, 435–442. <https://doi.org/10.1593/neo.07223>.
40. Tamura, K., Wakimoto, H., Agarwal, A.S., Rabkin, S.D., Bhere, D., Martuza, R.L., Kuroda, T., Kasmieh, R., and Shah, K. (2013). Multimechanistic tumor targeted oncolytic virus overcomes resistance in brain tumors. *Mol. Ther.* *21*, 68–77. <https://doi.org/10.1038/mt.2012.175>.
41. Wakimoto, H., Kesari, S., Farrell, C.J., Curry, W.T., Zaupa, C., Aghi, M., Kuroda, T., Stemmer-Rachamimov, A., Shah, K., Liu, T.C., et al. (2009). Human glioblastoma-derived cancer stem cells: establishment of invasive glioma models and treatment with oncolytic herpes simplex virus vectors. *Cancer Res.* *69*, 3472–3481. <https://doi.org/10.1158/0008-5472.can-08-3886>.
42. WO2016156570A1 - Bispecific CXCR4-CD4 polypeptides with potent anti-HIV activity (<https://patents.google.com/patent/WO2016156570A1/en?qoq=WO2016156570>) Google Patents 2016.
43. Uchida, H., Marzulli, M., Nakano, K., Goins, W.F., Chan, J., Hong, C.-S., Mazzacurati, L., Yoo, J.Y., Haseley, A., Nakashima, H., et al. (2013). Effective treatment of an orthotopic xenograft model of human glioblastoma using an EGFR-retargeted oncolytic herpes simplex virus. *Mol. Ther.* *21*, 561–569. <https://doi.org/10.1038/mt.2012.211>.
44. Uchida, H., Chan, J., Goins, W.F., Grandi, P., Kumagai, I., Cohen, J.B., and Glorioso, J.C. (2010). A double mutation in glycoprotein gB compensates for ineffective gD-dependent initiation of herpes simplex virus type 1 infection. *J. Virol.* *84*, 12200–12209. <https://doi.org/10.1128/jvi.01633-10>.
45. Shah, K., Tung, C.H., Yang, K., Weissleder, R., and Breakefield, X.O. (2004). Inducible release of TRAIL fusion proteins from a proapoptotic form for tumor therapy. *Cancer Res.* *64*, 3236–3242. <https://doi.org/10.1158/0008-5472.can-03-3516>.
46. Cocchi, F., Menotti, L., Mirandola, P., Lopez, M., and Campadelli-Fiume, G. (1998). The ectodomain of a novel member of the Immunoglobulin subfamily related to the poliovirus receptor has the attributes of a bona fide receptor for herpes simplex virus types 1 and 2 in human cells. *J. Virol.* *72*, 9992–10002. <https://doi.org/10.1128/jvi.72.12.9992-10002.1998>.
47. Uchida, H., Shah, W.A., Ozuor, A., Frampton, A.R., Goins, W.F., Grandi, P., Cohen, J.B., Glorioso, J.C., and Glorioso, J.C. (2009). Generation of herpesvirus entry mediator (HVEM)-Restricted herpes simplex virus type 1 mutant viruses: resistance of HVEM-expressing cells and identification of mutations that rescue nectin-1 recognition. *J. Virol.* *83*, 2951–2961. <https://doi.org/10.1128/jvi.01449-08>.
48. Frampton, A.R., Stolz, D.B., Uchida, H., Goins, W.F., Cohen, J.B., and Glorioso, J.C. (2007). Equine herpesvirus 1 enters cells by two different pathways, and infection requires the activation of the cellular kinase ROCK1. *J. Virol.* *81*, 10879–10889. <https://doi.org/10.1128/jvi.00504-07>.

49. Marconi, P., and Manservigi, R. (2014). Herpes simplex virus growth, preparation, and assay. *Methods Mol. Biol.* *1144*, 19–29. https://doi.org/10.1007/978-1-4939-0428-0_2.
50. Lathia, J.D., Mack, S.C., Mulkearns-Hubert, E.E., Valentim, C.L.L., and Rich, J.N. (2015). Cancer stem cells in glioblastoma. *Genes Dev.* *29*, 1203–1217. <https://doi.org/10.1101/gad.261982.115>.
51. Connolly, S.A., Jardtetzky, T.S., and Longnecker, R. (2021). The structural basis of herpesvirus entry. *Nat. Rev. Microbiol.* *19*, 110–121. <https://doi.org/10.1038/s41579-020-00448-w>.
52. Bian, X.w., Yang, S.x., Chen, J.h., Ping, Y.f., Zhou, X.d., Wang, Q.l., Jiang, X.f., Gong, W., Xiao, H.l., Du, L.l., et al. (2007). Preferential expression of chemokine receptor CXCR4 by highly malignant human gliomas and its association with poor patient survival. *Neurosurgery* *61*, 570–579. <https://doi.org/10.1227/01.neu.0000290905.53685.a2>.
53. Tang, C., and Guo, W. (2021). Implantation of a mini-osmotic pump plus stereotactical injection of retrovirus to study newborn neuron development in adult mouse hippocampus. *STAR Protoc.* *2*, 100374. <https://doi.org/10.1016/j.xpro.2021.100374>.
54. Alvarez-Breckenridge, C.A., Yu, J., Price, R., Wojton, J., Pradarelli, J., Mao, H., Wei, M., Wang, Y., He, S., Hardcastle, J., et al. (2012). NK cells impede glioblastoma virotherapy through Nkp30 and Nkp46 natural cytotoxicity receptors. *Nat. Med.* *18*, 1827–1834. <https://doi.org/10.1038/nm.3013>.
55. Van Den Bossche, W.B.L., Kleijn, A., Teunissen, C.E., Voerman, J.S.A., Teodosio, C., Noske, D.P., Van Dongen, J.J.M., Dirven, C.M.F., and Lamfers, M.L.M. (2018). Oncolytic virotherapy in glioblastoma patients induces a tumor macrophage phenotypic shift leading to an altered glioblastoma microenvironment. *Neuro. Oncol.* *20*, 1494–1504. <https://doi.org/10.1093/neuonc/nyy082>.
56. Isci, D., D'uonolo, G., Wantz, M., Rogister, B., Lombard, A., Chevigné, A., Szpakowska, M., and Neirinckx, V. (2021). Patient-oriented perspective on chemokine receptor expression and function in glioma. *Cancers* *14*, 130. <https://doi.org/10.3390/cancers14010130>.
57. Tischer, B.K., Kaufer, B.B., Sommer, M., Wussow, F., Arvin, A.M., and Osterrieder, N. (2007). A self-excisable infectious bacterial artificial chromosome clone of varicella-zoster virus allows analysis of the essential tegument protein encoded by ORF9. *J. Virol.* *81*, 13200–13208. <https://doi.org/10.1128/jvi.01148-07>.
58. Todo, T., Martuza, R.L., Rabkin, S.D., and Johnson, P.A. (2001). Oncolytic herpes simplex virus vector with enhanced MHC class I presentation and tumor cell killing. *Proc. Natl. Acad. Sci. U S A* *98*, 6396–6401. <https://doi.org/10.1073/pnas.101136398>.
59. Goins, W.F., Huang, S., Hall, B., Marzulli, M., Cohen, J.B., and Glorioso, J.C. (2020). Engineering HSV-1 vectors for gene therapy. In *Herpes Simplex Virus: Methods and Protocols*, Methods Mol. Biol. R.J. Diefenbach and C. Fraefel, eds. (Springer Science), p. 2060. Chapter 4.
60. Kroonen, J., Nassen, J., Boulanger, Y.G., Provenzano, F., Capraro, V., Bours, V., Martin, D., Deprez, M., Robe, P., and Rogister, B. (2011). Human glioblastoma-initiating cells invade specifically the subventricular zones and olfactory bulbs of mice after striatal injection. *Int. J. Cancer* *129*, 574–585. <https://doi.org/10.1002/ijc.25709>.

PART 6: CONCLUSION AND PERSPECTIVES



PART 6: CONCLUSION AND PERSPECTIVES

1. ACKR3 and GBM Biology

The main project of my thesis aimed to study chemokine-chemokine receptors dialog in GBM, with a particular emphasis on the ACKR3 receptor, to better understand their expression and roles in disease progression.

To provide a patient-oriented perspective on the expression and function of chemokine receptors in GBM, we conducted an initial *in silico* analysis. This study highlighted the importance of chemokine receptor CXCR4 which was predominantly overexpressed in GBM samples and played a crucial role in angiogenesis, cell invasion and treatment resistance. The ACKR3 receptor was also found to be significantly expressed in GBM samples, particularly in the regions with microvascular proliferation. ACKR3-expressing cells were mainly identified as astrocytic cells, neoplastic cells, and vascular cells. In the second *in silico* study, we included the study of chemokines to analyze chemokine-receptor interactions in GBM. We noticed that, although tumor cells were the more abundant in the TME, they were not involved in intercellular interactions based on chemokines and their receptors. In other words, the chemokine/chemokine receptor dialog appears to mainly concern immune and inflammatory cells in the GBM TME (e.g. T lymphocytes and/or myeloid cells).

The results of this thesis strongly suggest that, although the ACKR3 receptor is expressed in GBM tissue, its role seems less central than that of CXCR4. Our experimental analyzes indeed show that ACKR3 expression in resected tumors is mainly observed in TME cells, including monocytes, lymphocytes and NK cells, rather than in tumor cells themselves. Additionally, our results suggest that the CXCL12/ACKR3 signaling axis may not be as crucial for GBM as other identified axes, such as CCL5/CCR1 and CXCL16/CXCR6. Considering these results, it would be relevant to redirect research towards the CCL5/CCR1 and CXCL16/CXCR6 signaling axes, which appear to play a more significant role in GBM immunity. A more in-depth exploration of these axes could open new therapeutic avenues. Regarding ACKR3,

although its direct role in GBM tumor cells appears at least so far limited, its expression in TME immune cells suggests that it may be interesting to better understand its potential role in the GBM TME.

In conclusion, this thesis provided new insights into the expression and role of chemokine receptors in GBM. Although the ACKR3 receptor is not a major player in GBM tumor cells, its potential role in the TME and in the CXCL12/CXCR4 signaling modulation deserves special attention. These discoveries open new perspectives for the development of targeted therapies and for a better understanding of the interactions between tumor cells and the immune system in GBM.

- **Experimental strengths and limitations of the project**

Research particularly in the field of GBM is evolving at a sustained pace, requiring constant adaptation of experimental methods and models. At the time, our laboratory had chosen to focus on the study of the CXCR4 receptor within tumor cells themselves, an approach that was in line with the knowledge and advances available at that time. In line with this research, we decided to adopt a similar approach to study the ACKR3 receptor. However, GBM research has evolved considerably, and it is now impossible to conceive of studying GBM cells without considering the TME, which plays a major role in tumor progression.

During my years in the laboratory, I contributed to generating a bank of patient-derived GBM stem-like cell (GSC) models, an important step forward in understanding GBM and consolidating the results obtained with GBM lines. Previously, *in vivo* experiments were mostly performed with U87, the human GBM cell line. Although these cells are still widely used due to their ease of manipulation, they have notable limitations as a model for GBM research. Indeed, U87 cells do not faithfully produce the complexity and diversity of human GBM, forming often after xenografting experiments, massive and homogeneous tumors that do not fully reflect reality. I have played a key role in establishing xenograft models using patient-derived GBM cells. Unlike U87, these patient-derived GSCs form tumors with a slow development time but are much more

representative of the biological characteristics of GBM. These tumors are not only more invasive, but they also better reflect the complexity and clinical challenges associated with GBM, thus providing a more accurate model to study GBM. Finally, such a collection of in-house GSC cultures is a key asset for our laboratory and already has offered a lot of opportunities for sharing material and starting collaborations.

- **Perspectives – New models and approaches**

Despite their usefulness and being considered a better model compared to cell lines, patient-derived GSCs have also limitations. Indeed, these models, although they offer a more faithful representation of GBM, fail to fully reproduce the complexity of the TME. In addition, these experiments are mostly conducted in immunodeficient mouse models, which again means that tumors are developed in models lacking a fully functional immune system. Again, this lack of an immune system is a weakness, limiting the ability of the models to reflect real immunological interactions. It therefore becomes necessary to continue to develop more sophisticated models such as the generation of organoids or other more complex models capable of recapitulating not only intra- and inter-tumoral heterogeneity but also the tissue architecture that best reflects the reality observed in the patient.

Currently, we have started to generate organoids from patient tumors, based on the work of Jacobs et al. 2020³¹⁴. Immunofluorescence experiments were performed to characterize the cell types composing these organoids, revealing the presence of cells positive for the markers GFAP, Iba1, KI67, Sox2, CD31 and Nestin. It would be particularly interesting to analyze their immune cell composition, with the aim of deepening our understanding of the complexity of the TME. Ideally, these organoids would be generated directly from patient biopsies and then immediately grafted into the brain of nude mice, without long culture period. This would allow us to work with a more advanced model, which would more faithfully reproduce the TME of GBM. However, although this approach is promising, it presents significant logistical challenges. To implement it, it is necessary to have nude mice available every time a patient undergoes resection surgery, which is complicated by the fact that surgeries are rarely planned in advance. Carrying out such experiments would therefore be

CONCLUSION AND PERSPECTIVES

difficult, given that we do not have an animal facility for breeding nude mice so far. Finally, humanized mice could represent an interesting alternative to this approach although it is important to note that the cost of these models is particularly high, so is the difficulty in their establishment. Their use would allow the integration of a human immune system, thus offering an even more faithful model to study the TME of GBM.

Furthermore, our results, corroborated by numerous studies, show that ACKR3 is highly expressed not only by the cerebral vasculature but also by astrocytic cells; this opens the way to new research perspectives, including the study of the impact of endothelial cells by establishing co-cultures with cells derived from GBM patients. Innovative advances have recently emerged in the field of models used to study GBM. For example, one team developed a vascularized tumoroid model to study TME signals related to angiogenesis in GBM. This model consists of GBM spheroids and endothelial cells (HUVECs), embedded in a fibrin gel containing dermal fibroblasts. Although it does not recreate the BBB, the model is sophisticated enough to reproduce features of angiogenesis³¹⁵. More recently, another team designed 3D scaffolds mimicking the brain microvasculature to explore the response of co-cultured GBM cells and endothelial cells to proton radiation. This 3D GBM model constitutes a valuable tool for *in vitro* studies³¹⁶. In parallel, another team created a 3D model of perivascular niche using hydrogel, umbilical vein endothelial cells and GBM cells. After 14 days of culture, these researchers observed changes in HUVEC networks, differentiation of GBM cells and an increase in the concentration of certain chemokines such as CXCL12 and TGFb³¹⁷.

It would also be relevant to generate co-cultures between astrocytes and GBM cells to better understand the interaction between these cells and to identify the precise role of ACKR3 in this context. Stanke's team developed an innovative co-culture protocol to study the effects of astrocyte contact on GBM using layer-by-layer assembly and microvasculature-guided patterning. This model could be used in our research to study changes in the molecular biology of GBM due to astrocyte contact³¹⁸. Yang et al. explored how tumor-associated astrocytes influence treatment resistance in GBM. These researchers co-cultured eGFP+/Luc GBM cells with immortalized astrocytes

(TNC-1) and treated these cells with TMZ and analyzed cell viability by quantifying luciferase expression. The results showed that astrocytes significantly increased the survival of GBM cells after TMZ treatment³¹⁹. Better yet, a team designed a heterotypic 3D spheroid model integrating GBM cells with astrocytes and endothelial cells to better simulate the cellular components of the TME and study their impact on the expression of stem cell markers. The researchers highlighted an increase in the expression of stem cell markers³²⁰.

In conclusion, all these new methods represent major advances in the modeling of the GBM TME. By combining innovative approaches, such as co-culture models, multicellular spheroid models, tumor organoid models, we can reproduce in laboratory more faithfully the complete architecture of the molecular biology of the TME. These innovations will not only allow us to better understand the interactions between tumor cells and stromal or endothelial cells but also to simulate with greater precision the physiological conditions present *in vivo*.

2. AAV project

This second part of my thesis is conceptually linked to the first part. Indeed, we conclude from the part that the TME could play an essential role in the tumor development and in the case, of the GBM, in the tumor relapses. In this second part of my thesis, we set up a method to analyze in detail the influence of the specific brain area: the sub-ventricular zone or SVZ. In the AAV project, we have indeed developed an innovative technique to specifically target GBM cells that have invaded the subventricular zones. This method not only allowed us to validate our previous work, which showed that these GBM cells were able to migrate from the tumor mass to the SVZ, but also confirmed what we had so far only hypothesized: **migrating cells do not remain indefinitely in the SVZ**. Indeed, after nesting in this neurogenic zone, they seem to quickly leave the SVZ to return to the tumor mass. This observation is particularly interesting because it suggests a dynamic cycle between the tumor mainly established in the striatum and the SVZ. It seems that tumor cells could use the SVZ as a “temporary refuge” to overcome harmful therapeutic effects like radiotherapy or

chemotherapy or to become more aggressive before reintegrating the tumor. This mechanism could play an important role in the survival and radioresistance of tumor cells as well as the formation of recurrences.

However, as with the ACKR3 project, it remains crucial to validate these findings using the new AAV targeting method. Previous research in our laboratory had already demonstrated that SVZ-nested cells were particularly resistant to radiotherapy compared to their counterparts remaining in the tumor mass and that they actively participated in the recurrence. Now, using this new targeting method, we can confirm and consolidate these results with increased precision.

- **Perspectives**

This model opens fascinating perspectives to deepen our understanding of cellular dynamics within brain tumors, regarding eGFP+ cells that have migrated to the SVZ and dsRED+ cells that remained at the injection site or which have invaded other parts of the central nervous system. The opportunity to compare these two distinct cell populations in detail is invaluable and would allow us to identify tumor cell modification(s) induced by the SVZ-microenvironment. By conducting transcriptomic and proteomic analyses, we could precisely determine how eGFP+ have been modified and moreover, if those cells play a crucial role in the tumor recurrence process. These cells could also be specifically isolated by a fluorescence cell-sorting approach and then be characterized *in vitro*, to assess their proliferative, invasive and migratory character in comparison to red cells. One example based on the previous results described by the host laboratory is to confirm whether and understand how these cells, after migrating to the SVZ, have a better capacity to repair their DNA compared to dsRED+ cells that remained in the main tumor. Geno-transcriptomic and functional analyses could reveal key differences in how these cells respond to cellular damage.

We could also consider grafting T033 LRLG cells into mouse models, allowing the formation of a tumor that contacts the ventricles, followed by the injection of an AAV

CONCLUSION AND PERSPECTIVES

targeting cells that have migrated into the SVZ. After resection surgery to remove the main tumor mass, we could evaluate the ability of eGFP+ tumor cells to regenerate a post-surgery tumor. To push the experiment even further, mice could also be subjected to a radiation protocol combined with TMZ treatment, thus simulating current therapy conditions. This approach would allow us to observe whether cells that have encountered the SVZ show resistance to treatments, compared to dsRED+ cells.

In conclusion, such a study could provide important information on the role of migrating cells in tumor recurrence and open the door to therapeutic strategies based once again on the AAV method. By specifically targeting these residual cells after standard treatment combining resection and radiochemotherapy, we could consider inducing their cell death by integrating a pro-apoptotic gene into the AAV vector. This approach could offer an innovative method to improve clinical outcomes by reducing the risk of GBM recurrence.

REFERENCES

1. Ostrom, Q. T. *et al.* CBTRUS Statistical Report: Primary Brain and Other Central Nervous System Tumors Diagnosed in the United States in 2016-2020. *Neuro Oncol* **25**, IV1–IV99 (2023).
2. Modrek, A. S., Bayin, N. S. & Placantonakis, D. G. Brain stem cells as the cell of origin in glioma. *World J Stem Cells* **6**, 43 (2014).
3. Louis, D. N. *et al.* The 2007 WHO Classification of Tumours of the Central Nervous System. *Acta Neuropathol* **114**, 97 (2007).
4. Perry, A. & Wesseling, P. Histologic classification of gliomas. *Handb Clin Neurol* **134**, 71–95 (2016).
5. Ferris, S. P., Hofmann, J. W., Solomon, D. A. & Perry, A. Characterization of gliomas: from morphology to molecules. *Virchows Archiv* **471**, 257–269 (2017).
6. Louis, D. N. *et al.* The 2016 World Health Organization Classification of Tumors of the Central Nervous System: a summary. *Acta Neuropathol* **131**, 803–820 (2016).
7. Louis, D. N. *et al.* The 2021 WHO Classification of Tumors of the Central Nervous System: a summary. *Neuro Oncol* **23**, 1231–1251 (2021).
8. Weller, M. *et al.* EANO guidelines on the diagnosis and treatment of diffuse gliomas of adulthood. *Nature Reviews Clinical Oncology* **2020 18:3** **18**, 170–186 (2020).
9. Chen, R., Smith-Cohn, M., Cohen, A. L. & Colman, H. Glioma Subclassifications and Their Clinical Significance. *Neurotherapeutics* **14**, 284–297 (2017).
10. Parsons, D. W. *et al.* An Integrated Genomic Analysis of Human Glioblastoma Multiforme. *Science* **321**, 1807 (2008).
11. Yan, H. *et al.* IDH1 and IDH2 Mutations in Gliomas. *New England Journal of Medicine* **360**, 765–773 (2009).
12. Yang, H., Ye, D., Guan, K. L. & Xiong, Y. IDH1 and IDH2 Mutations in Tumorigenesis: Mechanistic Insights and Clinical Perspectives. *Clinical Cancer Research* **18**, 5562–5571 (2012).
13. Miller, J. J. *et al.* Isocitrate dehydrogenase (IDH) mutant gliomas: A Society for Neuro-Oncology (SNO) consensus review on diagnosis, management, and future directions. *Neuro Oncol* **25**, 4–25 (2023).
14. Dang, L. *et al.* Cancer-associated IDH1 mutations produce 2-hydroxyglutarate. *Nature* **462**, 739–744 (2009).
15. Turcan, S. *et al.* IDH1 mutation is sufficient to establish the glioma hypermethylator phenotype. *Nature* **483**, 479–483 (2012).
16. Haase, S. *et al.* Mutant ATRX: uncovering a new therapeutic target for glioma. *Expert Opin Ther Targets* **22**, 599 (2018).
17. Koschmann, C. *et al.* ATRX Loss Promotes Tumor Growth and Impairs Non-Homologous End Joining DNA Repair in Glioma. *Sci Transl Med* **8**, 328ra28 (2016).
18. Pekmezci, M. *et al.* Adult Infiltrating Gliomas with WHO 2016 Integrated Diagnosis: Additional Prognostic Roles of ATRX and TERT. *Acta Neuropathol* **133**, 1001 (2017).
19. Reifenberger, J. *et al.* Molecular genetic analysis of oligodendroglial tumors shows preferential allelic deletions on 19q and 1p. *Am J Pathol* **145**, 1175 (1994).
20. Cairncross, J. G. *et al.* Specific Genetic Predictors of Chemotherapeutic Response and Survival in Patients With Anaplastic Oligodendrogliomas. *JNCI: Journal of the National Cancer Institute* **90**, 1473–1479 (1998).
21. Cairncross, G. *et al.* Phase III Trial of Chemoradiotherapy for Anaplastic Oligodendroglioma: Long-Term Results of RTOG 9402. *Journal of Clinical Oncology* **31**, 337 (2013).
22. Van Den Bent, M. J. *et al.* Adjuvant procarbazine, lomustine, and vincristine improves progression-free survival but not overall survival in newly diagnosed anaplastic oligodendrogliomas and oligoastrocytomas: A randomized European Organisation for Research and Treatment of Cancer phase III trial. *Journal of Clinical Oncology* **24**, 2715–2722 (2006).
23. Lv, L. *et al.* Effects of 1p/19q Codeletion on Immune Phenotype in Low Grade Glioma. *Front Cell Neurosci* **15**, 704344 (2021).
24. Yuile, A. *et al.* CDKN2A/B Homozygous Deletions in Astrocytomas: A Literature Review. *Curr Issues Mol Biol* **45**, 5276–5292 (2023).
25. Eckel-Passow, J. E. *et al.* Glioma Groups Based on 1p/19q, IDH, and

- TERT Promoter Mutations in Tumors . *New England Journal of Medicine* **372**, 2499–2508 (2015).
26. Killela, P. J. *et al.* TERT promoter mutations occur frequently in gliomas and a subset of tumors derived from cells with low rates of self-renewal. *Proc Natl Acad Sci U S A* **110**, 6021–6026 (2013).
 27. Arita, H. *et al.* A combination of TERT promoter mutation and MGMT methylation status predicts clinically relevant subgroups of newly diagnosed glioblastomas. *Acta Neuropathol Commun* **4**, 79 (2016).
 28. Stichel, D. *et al.* Distribution of EGFR amplification, combined chromosome 7 gain and chromosome 10 loss, and TERT promoter mutation in brain tumors and their potential for the reclassification of IDHwt astrocytoma to glioblastoma. *Acta Neuropathol* **136**, 793–803 (2018).
 29. An, Z., Aksoy, O., Zheng, T., Fan, Q. W. & Weiss, W. A. Epidermal growth factor receptor (EGFR) and EGFRvIII in glioblastoma (GBM): signaling pathways and targeted therapies. *Oncogene* **37**, 1561 (2018).
 30. Iurlaro, R. *et al.* A Novel EGFRvIII T-Cell Bispecific Antibody for the Treatment of Glioblastoma. *Mol Cancer Ther* **21**, 1499–1509 (2022).
 31. Rutkowska, A. *et al.* Immunohistochemical detection of EGFRvIII in glioblastoma – Anti-EGFRvIII antibody validation for diagnostic and CAR-T purposes. *Biochem Biophys Res Commun* **685**, 149133 (2023).
 32. Yang, J., Yan, J. & Liu, B. Targeting EGFRvIII for glioblastoma multiforme. *Cancer Lett* **403**, 224–230 (2017).
 33. Keller, S. & Schmidt, M. H. H. EGFR and EGFRvIII Promote Angiogenesis and Cell Invasion in Glioblastoma: Combination Therapies for an Effective Treatment. *Int J Mol Sci* **18**, (2017).
 34. Brat, D. J. *et al.* cIMPACT-NOW Update 3: Recommended diagnostic criteria for “Diffuse astrocytic glioma, IDH-wildtype, with molecular features of glioblastoma, WHO grade IV”. *Acta Neuropathol* **136**, 805 (2018).
 35. Wijnenga, M. M. J. *et al.* Molecular and clinical heterogeneity of adult diffuse low-grade IDH wild-type gliomas: assessment of TERT promoter mutation and chromosome 7 and 10 copy number status allows superior prognostic stratification. *Acta Neuropathol* **134**, 957–959 (2017).
 36. Del Mar Inda, M. *et al.* Chromosomal abnormalities in human glioblastomas: gain in chromosome 7p correlating with loss in chromosome 10q. *Mol Carcinog* **36**, 6–14 (2003).
 37. Pinson, H. *et al.* Epidemiology and survival of adult-type diffuse glioma in Belgium during the molecular era. *Neuro Oncol* **26**, 191–202 (2024).
 38. Wen, P. Y. *et al.* Glioblastoma in adults: a Society for Neuro-Oncology (SNO) and European Society of Neuro-Oncology (EANO) consensus review on current management and future directions. *Neuro Oncol* **22**, 1073–1113 (2020).
 39. Ohgaki, H. Epidemiology of brain tumors. *Methods in Molecular Biology* vol. 472 323–342 Preprint at https://doi.org/10.1007/978-1-60327-492-0_14 (2009).
 40. Braganza, M. Z. *et al.* Ionizing radiation and the risk of brain and central nervous system tumors: a systematic review. *Neuro Oncol* **14**, 1316–1324 (2012).
 41. Ostrom, Q. T. *et al.* Risk factors for childhood and adult primary brain tumors. *Neuro Oncol* **21**, 1357 (2019).
 42. Ostrom, Q. T. *et al.* The epidemiology of glioma in adults: a ‘state of the science’ review. *Neuro Oncol* **16**, 896–913 (2014).
 43. Amirian, E. S. *et al.* Approaching a Scientific Consensus on the Association between Allergies and Glioma Risk: A Report from the Glioma International Case-Control Study. *Cancer Epidemiol Biomarkers Prev* **25**, 282 (2016).
 44. Wang, G. *et al.* Evidence from a large-scale meta-analysis indicates eczema reduces the incidence of glioma. *Oncotarget* **7**, 62598–62606 (2016).
 45. Susan Amirian, E. *et al.* Aspirin, NSAIDs, and glioma risk: Original data from the glioma international case-control study and a meta-analysis. *Cancer Epidemiology Biomarkers and Prevention* **28**, 555–562 (2019).
 46. Cote, D. J. & Ostrom, Q. T. Epidemiology and Etiology of Glioblastoma. 3–19 (2021) doi:10.1007/978-3-030-69170-7_1.
 47. McKinnon, C., Nandhabalan, M., Murray, S. A. & Plaha, P. Glioblastoma:

- clinical presentation, diagnosis, and management. *BMJ* **374**, (2021).
48. Guo, X. *et al.* Histological and molecular glioblastoma, IDH-wildtype: a real-world landscape using the 2021 WHO classification of central nervous system tumors. *Front Oncol* **13**, 1200815 (2023).
 49. Wirsching, H. G. & Weller, M. Glioblastoma. *Malignant Brain Tumors: State-of-the-Art Treatment* 265–288 (2016) doi:10.1007/978-3-319-49864-5_18/TABLES/1.
 50. Gilard, V. *et al.* Diagnosis and management of glioblastoma: A comprehensive perspective. *J Pers Med* **11**, 258 (2021).
 51. Weller, M. *et al.* EANO guidelines on the diagnosis and treatment of diffuse gliomas of adulthood. *Nat Rev Clin Oncol* **18**, 170–186 (2021).
 52. Antonelli, M. & Poliani, P. L. Adult type diffuse gliomas in the new 2021 WHO Classification. *Pathologica - Journal of the Italian Society of Anatomic Pathology and Diagnostic Cytopathology* **114**, 397–409 (2022).
 53. McKinnon, C., Nandhabalan, M., Murray, S. A. & Plaha, P. Glioblastoma: clinical presentation, diagnosis, and management. *BMJ* **374**, (2021).
 54. Watts, C. & Sanai, N. Surgical approaches for the gliomas. *Handb Clin Neurol* **134**, 51–69 (2016).
 55. Stummer, W. *et al.* In vitro and in vivo porphyrin accumulation by C6 glioma cells after exposure to 5-aminolevulinic acid. *J Photochem Photobiol B* **45**, 160–169 (1998).
 56. McCracken, D. J. *et al.* Turning on the light for brain tumor surgery: A 5-aminolevulinic acid story. *Neuro Oncol* **24**, S52–S61 (2022).
 57. Stummer, W. *et al.* Fluorescence-guided surgery with 5-aminolevulinic acid for resection of malignant glioma: a randomised controlled multicentre phase III trial. *Lancet Oncol* **7**, 392–401 (2006).
 58. Coburger, J., Hagel, V., Wirtz, C. R. & König, R. Surgery for Glioblastoma: Impact of the Combined Use of 5-Aminolevulinic Acid and Intraoperative MRI on Extent of Resection and Survival. *PLoS One* **10**, (2015).
 59. Mirza, A. B. *et al.* 5-Aminolevulinic acid-guided resection improves the overall survival of patients with glioblastoma—a comparative cohort study of 343 patients. *Neurooncol Adv* **3**, 1–11 (2021).
 60. Stupp, R. *et al.* Radiotherapy plus Concomitant and Adjuvant Temozolomide for Glioblastoma. *New England Journal of Medicine* **352**, 987–996 (2005).
 61. Newlands, E. S., Stevens, M. F. G., Wedge, S. R., Wheelhouse, R. T. & Brock, C. Temozolomide: a review of its discovery, chemical properties, pre-clinical development and clinical trials. *Cancer Treat Rev* **23**, 35–61 (1997).
 62. Hegi, M. E. *et al.* MGMT Gene Silencing and Benefit from Temozolomide in Glioblastoma. *New England Journal of Medicine* **352**, 997–1003 (2005).
 63. Stupp, R. *et al.* Effects of radiotherapy with concomitant and adjuvant temozolomide versus radiotherapy alone on survival in glioblastoma in a randomised phase III study: 5-year analysis of the EORTC-NCIC trial. *Lancet Oncol* **10**, 459–466 (2009).
 64. Van Breemen, M. S. M. *et al.* Efficacy of anti-epileptic drugs in patients with gliomas and seizures. *J Neurol* **256**, 1519–1526 (2009).
 65. Hottinger, A. F., Pacheco, P. & Stupp, R. Tumor treating fields: a novel treatment modality and its use in brain tumors. *Neuro Oncol* **18**, 1338–1349 (2016).
 66. Stupp, R. *et al.* NovoTTF-100A versus physician's choice chemotherapy in recurrent glioblastoma: a randomised phase III trial of a novel treatment modality. *Eur J Cancer* **48**, 2192–2202 (2012).
 67. Stupp, R. *et al.* Maintenance Therapy With Tumor-Treating Fields Plus Temozolomide vs Temozolomide Alone for Glioblastoma: A Randomized Clinical Trial. *JAMA* **314**, 2535–2543 (2015).
 68. Gilbert, M. R. *et al.* A randomized trial of bevacizumab for newly diagnosed glioblastoma. *N Engl J Med* **370**, 699–708 (2014).
 69. Chinot, O. L. *et al.* Bevacizumab plus radiotherapy-temozolomide for newly diagnosed glioblastoma. *N Engl J Med* **370**, 709–722 (2014).
 70. Behling, F. *et al.* Frequency of BRAF V600E mutations in 969 central nervous system neoplasms. *Diagn Pathol* **11**, (2016).
 71. Kaley, T. *et al.* BRAF Inhibition in BRAFV600-Mutant Gliomas: Results

- From the VE-BASKET Study. *Journal of Clinical Oncology* **36**, 3477 (2018).
72. Campos, B., Olsen, L. R., Urup, T. & Poulsen, H. S. A comprehensive profile of recurrent glioblastoma. *Oncogene* **2016 35:45 35**, 5819–5825 (2016).
 73. Rapp, M. *et al.* Recurrence Pattern Analysis of Primary Glioblastoma. *World Neurosurg* **103**, 733–740 (2017).
 74. Brandes, A. A. *et al.* Recurrence pattern after temozolomide concomitant with and adjuvant to radiotherapy in newly diagnosed patients with glioblastoma: Correlation with MGMT promoter methylation status. *Journal of Clinical Oncology* **27**, 1275–1279 (2009).
 75. Neilsen, B. K. *et al.* Comprehensive genetic alteration profiling in primary and recurrent glioblastoma. *J Neurooncol* **142**, 111–118 (2019).
 76. Li, C. *et al.* Characterizing tumor invasiveness of glioblastoma using multiparametric magnetic resonance imaging. *J Neurosurg* **132**, 1465–1472 (2019).
 77. Cuddapah, V. A., Robel, S., Watkins, S. & Sontheimer, H. A neurocentric perspective on glioma invasion. *Nat Rev Neurosci* **15**, 455 (2014).
 78. Venkataramani, V. *et al.* Glioblastoma hijacks neuronal mechanisms for brain invasion. *Cell* **185**, 2899-2917.e31 (2022).
 79. Abbott, N. J. Blood–brain barrier structure and function and the challenges for CNS drug delivery. *Journal of Inherited Metabolic Disease* **2013 36:3 36**, 437–449 (2013).
 80. Arvanitis, C. D., Ferraro, G. B. & Jain, R. K. The blood–brain barrier and blood–tumour barrier in brain tumours and metastases. *Nature Reviews Cancer* **2019 20:1 20**, 26–41 (2019).
 81. Steeg, P. S. The blood–tumour barrier in cancer biology and therapy. *Nature Reviews Clinical Oncology* **2021 18:11 18**, 696–714 (2021).
 82. Hardee, M. E. & Zagzag, D. Mechanisms of Glioma-Associated Neovascularization. *Am J Pathol* **181**, 1126 (2012).
 83. Van Tellingen, O. *et al.* Overcoming the blood-brain tumor barrier for effective glioblastoma treatment. *Drug Resist Updat* **19**, 1–12 (2015).
 84. Sonabend, A. M. *et al.* Repeated blood–brain barrier opening with an implantable ultrasound device for delivery of albumin-bound paclitaxel in patients with recurrent glioblastoma: a phase 1 trial. *Lancet Oncol* **24**, 509–522 (2023).
 85. Carpentier, A. *et al.* Repeated blood–brain barrier opening with a nine-emitter implantable ultrasound device in combination with carboplatin in recurrent glioblastoma: a phase I/II clinical trial. *Nature Communications* **2024 15:1 15**, 1–12 (2024).
 86. Lathia, J. D., Mack, S. C., Mulkearns-Hubert, E. E., Valentim, C. L. L. & Rich, J. N. Cancer stem cells in glioblastoma. *Genes Dev* **29**, 1203 (2015).
 87. Chen, J. *et al.* A restricted cell population propagates glioblastoma growth following chemotherapy. *Nature* **488**, 522 (2012).
 88. Singh, S. K. *et al.* Identification of human brain tumour initiating cells. *Nature* **2004 432:7015 432**, 396–401 (2004).
 89. Bao, S. *et al.* Glioma stem cells promote radioresistance by preferential activation of the DNA damage response. *Nature* **2006 444:7120 444**, 756–760 (2006).
 90. Liu, G. *et al.* Analysis of gene expression and chemoresistance of CD133+ cancer stem cells in glioblastoma. *Mol Cancer* **5**, 67 (2006).
 91. Yabo, Y. A., Niclou, S. P. & Golebiewska, A. Cancer cell heterogeneity and plasticity: A paradigm shift in glioblastoma. *Neuro Oncol* **24**, 669 (2022).
 92. Rennert, R. C. *et al.* Multiple Subsets of Brain Tumor Initiating Cells Coexist in Glioblastoma. *Stem Cells* **34**, 1702–1707 (2016).
 93. Pesenti, C. *et al.* The Genetic Landscape of Human Glioblastoma and Matched Primary Cancer Stem Cells Reveals Intratumour Similarity and Intertumour Heterogeneity. *Stem Cells Int* **2019**, (2019).
 94. Piccirillo, S. G. M. *et al.* Genetic and functional diversity of propagating cells in glioblastoma. *Stem Cell Reports* **4**, 7–15 (2015).
 95. McLendon, R. *et al.* Comprehensive genomic characterization defines human glioblastoma genes and core pathways. *Nature* **2008 455:7216 455**, 1061–1068 (2008).
 96. Verhaak, R. G. W. *et al.* An integrated genomic analysis identifies clinically relevant subtypes of glioblastoma characterized by abnormalities in

- PDGFRA, IDH1, EGFR and NF1. *Cancer Cell* **17**, 98 (2010).
97. Patel, A. P. *et al.* Single-cell RNA-seq highlights intratumoral heterogeneity in primary glioblastoma. *Science* **344**, 1396 (2014).
 98. Neftel, C. *et al.* An integrative model of cellular states, plasticity and genetics for glioblastoma. *Cell* **178**, 835 (2019).
 99. Dirkse, A. *et al.* Stem cell-associated heterogeneity in Glioblastoma results from intrinsic tumor plasticity shaped by the microenvironment. *Nature Communications* **2019 10:1** **10**, 1–16 (2019).
 100. Yabo, Y. A., Niclou, S. P. & Golebiewska, A. Cancer cell heterogeneity and plasticity: A paradigm shift in glioblastoma. *Neuro Oncol* **24**, 669 (2022).
 101. Sharma, P., Aaroe, A., Liang, J. & Puduvalli, V. K. Tumor microenvironment in glioblastoma: Current and emerging concepts. *Neurooncol Adv* **5**, (2023).
 102. Yuan, Z. *et al.* Extracellular matrix remodeling in tumor progression and immune escape: from mechanisms to treatments. *Molecular Cancer* **2023 22:1** **22**, 1–42 (2023).
 103. Wei, R., Zhou, J., Bui, B. & Liu, X. Glioma actively orchestrate a self-advantageous extracellular matrix to promote recurrence and progression. *BMC Cancer* **24**, 1–11 (2024).
 104. Brassart-Pasco, S. *et al.* Tumor Microenvironment: Extracellular Matrix Alterations Influence Tumor Progression. *Front Oncol* **10**, 527415 (2020).
 105. Galbo, P. M. *et al.* Functional Contribution of Cancer-Associated Fibroblasts in Glioblastoma. *bioRxiv* **2022.04.07.487495** (2022) doi:10.1101/2022.04.07.487495.
 106. Zhang, Q. *et al.* Cancer-associated fibroblasts-induced remodeling of tumor immune microenvironment via Jagged1 in glioma. *Cell Signal* **115**, 111016 (2024).
 107. Hussain, S. F. *et al.* The role of human glioma-infiltrating microglia/macrophages in mediating antitumor immune responses. *Neuro Oncol* **8**, 261–279 (2006).
 108. Gielen, P. R. *et al.* Elevated levels of polymorphonuclear myeloid-derived suppressor cells in patients with glioblastoma highly express S100A8/9 and arginase and suppress T cell function. *Neuro Oncol* **18**, 1253 (2016).
 109. Alban, T. J. *et al.* Global immune fingerprinting in glioblastoma patient peripheral blood reveals immune-suppression signatures associated with prognosis. *JCI Insight* **3**, (2018).
 110. Müller, S. *et al.* Single-cell profiling of human gliomas reveals macrophage ontogeny as a basis for regional differences in macrophage activation in the tumor microenvironment. *Genome Biol* **18**, (2017).
 111. Maddison, K. *et al.* Low tumour-infiltrating lymphocyte density in primary and recurrent glioblastoma. *Oncotarget* **12**, 2177–2187 (2021).
 112. Jackson, C. M., Choi, J. & Lim, M. Mechanisms of immunotherapy resistance: lessons from glioblastoma. *Nature Immunology* **2019 20:9** **20**, 1100–1109 (2019).
 113. Woroniecka, K. *et al.* T Cell Exhaustion Signatures Vary with Tumor Type and are Severe in Glioblastoma. *Clin Cancer Res* **24**, 4175 (2018).
 114. Martinez-Lage, M. *et al.* Immune landscapes associated with different glioblastoma molecular subtypes. *Acta Neuropathol Commun* **7**, (2019).
 115. White, K. *et al.* Identification, validation and biological characterisation of novel glioblastoma tumour microenvironment subtypes: implications for precision immunotherapy. *Annals of Oncology* **34**, 300–314 (2023).
 116. Zhou, S. *et al.* Reprogramming systemic and local immune function to empower immunotherapy against glioblastoma. *Nature Communications* **2023 14:1** **14**, 1–20 (2023).
 117. Sampson, J. H., Gunn, M. D., Fecci, P. E. & Ashley, D. M. Brain immunology and immunotherapy in brain tumours. *Nat Rev Cancer* **20**, 12 (2020).
 118. Lim, M., Xia, Y., Bettgowda, C. & Weller, M. Current state of immunotherapy for glioblastoma. *Nat Rev Clin Oncol* **15**, 422–442 (2018).
 119. Wen, P. Y. *et al.* A Randomized Double-Blind Placebo-Controlled Phase II Trial of Dendritic Cell Vaccine ICT-107 in Newly Diagnosed Patients with Glioblastoma. *Clin Cancer Res* **25**, 5799–5807 (2019).
 120. Chiocca, E. A. *et al.* Regulatable interleukin-12 gene therapy in patients

- with recurrent high-grade glioma: Results of a phase 1 trial. *Sci Transl Med* **11**, (2019).
121. Lang, F. F. *et al.* Phase I Study of DNX-2401 (Delta-24-RGD) Oncolytic Adenovirus: Replication and Immunotherapeutic Effects in Recurrent Malignant Glioma. *Journal of Clinical Oncology* **36**, 1419 (2018).
 122. Weller, M. *et al.* Rindopepimut with temozolomide for patients with newly diagnosed, EGFRvIII-expressing glioblastoma (ACT IV): a randomised, double-blind, international phase 3 trial. *Lancet Oncol* **18**, 1373–1385 (2017).
 123. Liau, L. M. *et al.* First results on survival from a large Phase 3 clinical trial of an autologous dendritic cell vaccine in newly diagnosed glioblastoma. *J Transl Med* **16**, 1 (2018).
 124. Desjardins, A. *et al.* Recurrent Glioblastoma Treated with Recombinant Poliovirus. *N Engl J Med* **379**, 150 (2018).
 125. Zhang, Y. *et al.* Safety and efficacy of B7-H3 targeting CAR-T cell therapy for patients with recurrent GBM. https://doi.org/10.1200/JCO.2024.42.16_suppl.2062 **42**, 2062–2062 (2024).
 126. Bagley, S. J. *et al.* Repeated peripheral infusions of anti-EGFRvIII CAR T cells in combination with pembrolizumab show no efficacy in glioblastoma: a phase 1 trial. *Nature Cancer* **2024** 5:3 **5**, 517–531 (2024).
 127. Choi, B. D. *et al.* Intraventricular CARv3-TEAM-E T Cells in Recurrent Glioblastoma. *New England Journal of Medicine* **390**, 1290–1298 (2024).
 128. Bagley, S. J. *et al.* Intrathecal bivalent CAR T cells targeting EGFR and IL13R α 2 in recurrent glioblastoma: phase 1 trial interim results. *Nature Medicine* **2024** 30:5 **30**, 1320–1329 (2024).
 129. O'Rourke, D. M. *et al.* A single dose of peripherally infused EGFRvIII-directed CAR T cells mediates antigen loss and induces adaptive resistance in patients with recurrent glioblastoma. *Sci Transl Med* **9**, (2017).
 130. Toker, J. *et al.* Clinical Importance of the lncRNA NEAT1 in Cancer Patients Treated with Immune Checkpoint Inhibitors. *Clin Cancer Res* **29**, 2226–2238 (2023).
 131. Nayak, L. *et al.* Randomized Phase II and Biomarker Study of Pembrolizumab plus Bevacizumab versus Pembrolizumab Alone for Patients with Recurrent Glioblastoma. *Clin Cancer Res* **27**, 1048–1057 (2021).
 132. Omuro, A. *et al.* Radiotherapy combined with nivolumab or temozolomide for newly diagnosed glioblastoma with unmethylated MGMT promoter: An international randomized phase III trial. *Neuro Oncol* **25**, 123–134 (2023).
 133. Reardon, D. A. *et al.* Effect of Nivolumab vs Bevacizumab in Patients With Recurrent Glioblastoma: The CheckMate 143 Phase 3 Randomized Clinical Trial. *JAMA Oncol* **6**, 1003–1010 (2020).
 134. Kaplan, A. R. & Glazer, P. M. Impact of hypoxia on DNA repair and genome integrity. *Mutagenesis* **35**, 61 (2020).
 135. Domènech, M., Hernández, A., Plaja, A., Martínez-balibrea, E. & Balaña, C. Hypoxia: The Cornerstone of Glioblastoma. *Int J Mol Sci* **22**, 22 (2021).
 136. Jing, X. *et al.* Role of hypoxia in cancer therapy by regulating the tumor microenvironment. *Mol Cancer* **18**, (2019).
 137. Doetsch, F., García-Verdugo, J. M. & Alvarez-Buylla, A. Cellular Composition and Three-Dimensional Organization of the Subventricular Germinal Zone in the Adult Mammalian Brain. *The Journal of Neuroscience* **17**, 5046 (1997).
 138. Doetsch, F., Caille, I., Lim, D. A., Garcia-Verdugo, J. M. & Alvarez-Buylla, A. Subventricular zone astrocytes are neural stem cells in the adult mammalian brain. *Cell* **97**, 703–716 (1999).
 139. Quiñones-Hinojosa, A. *et al.* Cellular composition and cytoarchitecture of the adult human subventricular zone: A niche of neural stem cells. *Journal of Comparative Neurology* **494**, 415–434 (2006).
 140. Adeberg, S. *et al.* Glioblastoma recurrence patterns after radiation therapy with regard to the subventricular zone. *Int J Radiat Oncol Biol Phys* **90**, 886–893 (2014).
 141. Jafri, N. F., Clarke, J. L., Weinberg, V., Barani, I. J. & Cha, S. Relationship of glioblastoma multiforme to the subventricular zone is associated with survival. *Neuro Oncol* **15**, 91 (2013).
 142. Mistry, A. M. *et al.* Decreased Survival in Glioblastomas is Specific to Contact with

- the Ventricular-Subventricular Zone, not Subgranular Zone or Corpus Callosum. *J Neurooncol* **132**, 341 (2017).
143. Chen, L. *et al.* Increased Subventricular Zone Radiation Dose Correlates With Survival in Glioblastoma Patients After Gross Total Resection. *Int J Radiat Oncol Biol Phys* **86**, 616 (2013).
 144. Kroonen, J. *et al.* Human glioblastoma-initiating cells invade specifically the subventricular zones and olfactory bulbs of mice after striatal injection. *Int J Cancer* **129**, 574–585 (2011).
 145. Goffart, N. *et al.* Adult mouse subventricular zones stimulate glioblastoma stem cells specific invasion through CXCL12/CXCR4 signaling. *Neuro Oncol* **17**, 81 (2015).
 146. Goffart, N. *et al.* CXCL12 mediates glioblastoma resistance to radiotherapy in the subventricular zone. *Neuro Oncol* **19**, 66–77 (2017).
 147. Willems, E. *et al.* Aurora A plays a dual role in migration and survival of human glioblastoma cells according to the CXCL12 concentration. *Oncogene* **38**, 73 (2019).
 148. Dedobbeleer, M. *et al.* MKP1 phosphatase is recruited by CXCL12 in glioblastoma cells and plays a role in DNA strand breaks repair. *Carcinogenesis* **41**, 417–429 (2020).
 149. Zlotnik, A. & Yoshie, O. The Chemokine Superfamily Revisited. *Immunity* **36**, 705 (2012).
 150. Chen, K. *et al.* Chemokines in homeostasis and diseases. *Cell Mol Immunol* **15**, 324 (2018).
 151. Mantovani, A., Bonecchi, R. & Locati, M. Tuning inflammation and immunity by chemokine sequestration: decoys and more. *Nature Reviews Immunology* **6**:12, 907–918 (2006).
 152. Blanchet, X., Langer, M., Weber, C., Koenen, R. & von Hundelshausen, P. Touch of Chemokines. *Front Immunol* **3**, (2012).
 153. Pierce, K. L., Premont, R. T. & Lefkowitz, R. J. Seven-transmembrane receptors. *Nature Reviews Molecular Cell Biology* **2002** 3:9, 639–650 (2002).
 154. Kenakin, T. Theoretical Aspects of GPCR-Ligand Complex Pharmacology. *Chem Rev* **117**, 4–20 (2017).
 155. Wettschureck, N. & Offermanns, S. Mammalian G proteins and their cell type specific functions. *Physiol Rev* **85**, 1159–1204 (2005).
 156. Smith, J. S. & Rajagopal, S. The β -Arrestins: Multifunctional Regulators of G Protein-coupled Receptors. *J Biol Chem* **291**, 8969–8977 (2016).
 157. Lefkowitz, R. J. & Shenoy, S. K. Transduction of receptor signals by β -arrestins. *Science (1979)* **308**, 512–517 (2005).
 158. DeWire, S. M., Ahn, S., Lefkowitz, R. J. & Shenoy, S. K. Beta-arrestins and cell signaling. *Annu Rev Physiol* **69**, 483–510 (2007).
 159. Hanson, J. & Chevigné, A. GPCRs in immunity: Atypical receptors and novel concepts. *Biochem Pharmacol* **114**, 1–2 (2016).
 160. Hughes, C. E. & Nibbs, R. J. B. A guide to chemokines and their receptors. *FEBS J* **285**, 2944 (2018).
 161. Feng, Y., Broder, C. C., Kennedy, P. E. & Berger, E. A. HIV-1 Entry Cofactor: Functional cDNA Cloning of a Seven-Transmembrane, G Protein-Coupled Receptor. *Science (1979)* **272**, 872–877 (1996).
 162. Sugiyama, T., Kohara, H., Noda, M. & Nagasawa, T. Maintenance of the hematopoietic stem cell pool by CXCL12-CXCR4 chemokine signaling in bone marrow stromal cell niches. *Immunity* **25**, 977–988 (2006).
 163. Salcedo, R. & Oppenheim, J. J. Role of chemokines in angiogenesis: CXCL12/SDF-1 and CXCR4 interaction, a key regulator of endothelial cell responses. *Microcirculation* **10**, 359–370 (2003).
 164. Cui, L. *et al.* Stromal cell-derived factor-1 and its receptor CXCR4 in adult neurogenesis after cerebral ischemia. *Restor Neurol Neurosci* **31**, 239–251 (2013).
 165. Tachibana, K. *et al.* The chemokine receptor CXCR4 is essential for vascularization of the gastrointestinal tract. *Nature* **393**, 591–594 (1998).
 166. Gatti, M. *et al.* Inhibition of CXCL12/CXCR4 autocrine/paracrine loop reduces viability of human glioblastoma stem-like cells affecting self-renewal activity. *Toxicology* **314**, 209–220 (2013).
 167. Panneerselvam, J. *et al.* IL-24 inhibits lung cancer cell migration and invasion by disrupting the SDF-1/CXCR4 signaling axis. *PLoS One* **10**, (2015).
 168. Raschioni, C. *et al.* CXCR4/CXCL12 signaling and protumor macrophages in

- primary tumors and sentinel lymph nodes are involved in luminal B breast cancer progression. *Dis Markers* **2018**, (2018).
169. Zheng, F., Zhang, Z., Flamini, V., Jiang, W. G. & Cui, Y. The Axis of CXCR4/SDF-1 Plays a Role in Colon Cancer Cell Adhesion Through Regulation of the AKT and IGF1R Signalling Pathways. *Anticancer Res* **37**, 4361–4369 (2017).
 170. Guo, Q. *et al.* CXCL12-CXCR4 Axis Promotes Proliferation, Migration, Invasion, and Metastasis of Ovarian Cancer. *Oncol Res* **22**, 247 (2015).
 171. Mercurio, L. *et al.* Targeting CXCR4 by a selective peptide antagonist modulates tumor microenvironment and microglia reactivity in a human glioblastoma model. *J Exp Clin Cancer Res* **35**, (2016).
 172. Gagner, J. P. *et al.* Multifaceted C-X-C Chemokine Receptor 4 (CXCR4) Inhibition Interferes with Anti-Vascular Endothelial Growth Factor Therapy-Induced Glioma Dissemination. *Am J Pathol* **187**, 2080 (2017).
 173. Bachelier, F. *et al.* New nomenclature for atypical chemokine receptors. *Nat Immunol* **15**, 207–208 (2014).
 174. Heesen, M. *et al.* Cloning and chromosomal mapping of an orphan chemokine receptor: Mouse RDC1. *Immunogenetics* **47**, 364–370 (1998).
 175. Balabanian, K. *et al.* The chemokine SDF-1/CXCL12 binds to and signals through the orphan receptor RDC1 in T lymphocytes. *Journal of Biological Chemistry* **280**, 35760–35766 (2005).
 176. Burns, J. M. *et al.* A novel chemokine receptor for SDF-1 and I-TAC involved in cell survival, cell adhesion, and tumor development. *J Exp Med* **203**, 2201 (2006).
 177. Szpakowska, M. *et al.* Different contributions of chemokine N-terminal features attest to a different ligand binding mode and a bias towards activation of ACKR3/CXCR7 compared with CXCR4 and CXCR3. *Br J Pharmacol* **175**, 1419 (2018).
 178. Szpakowska, M. *et al.* Human herpesvirus 8-encoded chemokine vCCL2/vMIP-II is an agonist of the atypical chemokine receptor ACKR3/CXCR7. *Biochem Pharmacol* **114**, 14–21 (2016).
 179. Klein, K. R. *et al.* Decoy receptor CXCR7 modulates adrenomedullin-mediated cardiac and lymphatic vascular development. *Dev Cell* **30**, 528–540 (2014).
 180. Alampour-Rajabi, S. *et al.* MIF interacts with CXCR7 to promote receptor internalization, ERK1/2 and ZAP-70 signaling, and lymphocyte chemotaxis. *FASEB J* **29**, 4497–4511 (2015).
 181. Meyrath, M. *et al.* The atypical chemokine receptor ACKR3/CXCR7 is a broad-spectrum scavenger for opioid peptides. *Nature Communications* **2020 11:1** **11**, 1–16 (2020).
 182. Naumann, U. *et al.* CXCR7 Functions as a Scavenger for CXCL12 and CXCL11. *PLoS One* **5**, e9175 (2010).
 183. Ray, P. *et al.* Carboxy-terminus of CXCR7 regulates receptor localization and function. *Int J Biochem Cell Biol* **44**, 669–678 (2012).
 184. Gustavsson, M., Dyer, D. P., Zhao, C. & Handel, T. M. Kinetics of CXCL12 binding to atypical chemokine receptor 3 reveal a role for the receptor N-terminus in chemokine binding. *Sci Signal* **12**, (2019).
 185. Zabel, B. A. *et al.* Elucidation of CXCR7-Mediated Signaling Events and Inhibition of CXCR4-Mediated Tumor Cell Transendothelial Migration by CXCR7 Ligands. *The Journal of Immunology* **183**, 3204–3211 (2009).
 186. Rajagopal, S. *et al.* β -arrestin- but not G protein-mediated signaling by the “decoy” receptor CXCR7. *Proc Natl Acad Sci U S A* **107**, 628 (2010).
 187. Luker, K. E., Gupta, M., Steele, J. M., Foerster, B. R. & Luker, G. D. Imaging Ligand-Dependent Activation of CXCR7. *Neoplasia* **11**, 1022 (2009).
 188. Boldajipour, B. *et al.* Control of chemokine-guided cell migration by ligand sequestration. *Cell* **132**, 463–473 (2008).
 189. Dambly-Chaudière, C., Cubedo, N. & Ghysen, A. Control of cell migration in the development of the posterior lateral line: Antagonistic interactions between the chemokine receptors CXCR4 and CXCR7/RDC1. *BMC Dev Biol* **7**, 1–14 (2007).
 190. Levoye, A., Balabanian, K., Baleux, F., Bachelier, F. & Lagane, B. CXCR7 heterodimerizes with CXCR4 and regulates CXCL12-mediated G protein

- signaling. *Blood* **113**, 6085–6093 (2009).
191. Montpas, N. *et al.* Ligand-specific conformational transitions and intracellular transport are required for atypical chemokine receptor 3-mediated chemokine scavenging. *J Biol Chem* **293**, 893 (2018).
 192. Thelen, M. ACKR3. *Compendium of Inflammatory Diseases* 1–5 (2016) doi:10.1007/978-3-7643-8550-7_222.
 193. Thelen, M. & Thelen, S. CXCR7, CXCR4 and CXCL12: An eccentric trio? *J Neuroimmunol* **198**, 9–13 (2008).
 194. Gerrits, H. *et al.* Early postnatal lethality and cardiovascular defects in CXCR7-deficient mice. *Genesis* **46**, 235–245 (2008).
 195. Sierro, F. *et al.* Disrupted cardiac development but normal hematopoiesis in mice deficient in the second CXCL12/SDF-1 receptor, CXCR7. *Proc Natl Acad Sci U S A* **104**, 14759–14764 (2007).
 196. Wetzels-Strong, S. E., Li, M., Klein, K. R., Nishikimi, T. & Caron, K. M. Epicardial-Derived Adrenomedullin Drives Cardiac Hyperplasia During Embryogenesis. *Dev Dyn* **243**, 243 (2014).
 197. Chang, Y. *et al.* Identification of Herpesvirus-Like DNA Sequences in AIDS-Associated Kaposi's Sarcoma. *Science (1979)* **266**, 1865–1869 (1994).
 198. Szpakowska, M. & Chevigné, A. vCCL2/vMIP-II, the viral master KEYmokine. *J Leukoc Biol* **99**, 893–900 (2016).
 199. Ikeda, Y., Kumagai, H., Skach, A., Sato, M. & Yanagisawa, M. Modulation of circadian glucocorticoid oscillation through adrenal opioid-CXCR7 signaling alters emotional behavior. *Cell* **155**, 1323 (2013).
 200. Décaillot, F. M. *et al.* CXCR7/CXCR4 Heterodimer Constitutively Recruits β -Arrestin to Enhance Cell Migration. *J Biol Chem* **286**, 32188 (2011).
 201. Meyrath, M. *et al.* Proadrenomedullin N-Terminal 20 Peptides (PAMPs) Are Agonists of the Chemokine Scavenger Receptor ACKR3/CXCR7. *ACS Pharmacol Transl Sci* **4**, 813–823 (2021).
 202. Szpakowska, M. *et al.* Human herpesvirus 8-encoded chemokine vCCL2/vMIP-II is an agonist of the atypical chemokine receptor ACKR3/CXCR7. *Biochem Pharmacol* **114**, 14–21 (2016).
 203. Meyrath, M. *et al.* The atypical chemokine receptor ACKR3/CXCR7 is a broad-spectrum scavenger for opioid peptides. *Nature Communications* **2020** *11:1* **11**, 1–16 (2020).
 204. Trousse, F. *et al.* Knockdown of the CXCL12/CXCR7 chemokine pathway results in learning deficits and neural progenitor maturation impairment in mice. *Brain Behav Immun* **80**, 697–710 (2019).
 205. Wang, Y. *et al.* CXCR4 and CXCR7 have distinct functions in regulating interneuron migration. *Neuron* **69**, 61–76 (2011).
 206. Yu, S., Crawford, D., Tsuchihashi, T., Behrens, T. W. & Srivastava, D. The chemokine receptor CXCR7 functions to regulate cardiac valve remodeling. *Dev Dyn* **240**, 384–393 (2011).
 207. Sánchez-Alcañiz, J. A. *et al.* Cxcr7 controls neuronal migration by regulating chemokine responsiveness. *Neuron* **69**, 77–90 (2011).
 208. Ueland, J., Yuan, A., Marlier, A., Gallagher, A. R. & Karihaloo, A. A novel role for the chemokine receptor Cxcr4 in kidney morphogenesis: an in vitro study. *Dev Dyn* **238**, 1083–1091 (2009).
 209. Haege, S. *et al.* CXC Chemokine Receptor 7 (CXCR7) Regulates CXCR4 Protein Expression and Capillary Tuft Development in Mouse Kidney. *PLoS One* **7**, (2012).
 210. Berahovich, R. D. *et al.* Endothelial expression of CXCR7 and the regulation of systemic CXCL12 levels. *Immunology* **141**, 111–122 (2014).
 211. Cao, Z. *et al.* Targeting of the pulmonary capillary vascular niche promotes lung alveolar repair and ameliorates fibrosis. *Nat Med* **22**, 154 (2016).
 212. Konrad, F. M., Meichssner, N., Bury, A., Ngamsri, K. C. & Reutershan, J. Inhibition of SDF-1 receptors CXCR4 and CXCR7 attenuates acute pulmonary inflammation via the adenosine A2B-receptor on blood cells. *Cell Death Dis* **8**, e2832 (2017).
 213. Ngamsri, K.-C. *et al.* The Pivotal Role of CXCR7 in Stabilization of the Pulmonary Epithelial Barrier in Acute Pulmonary Inflammation. *J Immunol* **198**, 2403–2413 (2017).

214. Thelen, M. & Thelen, S. CXCR7, CXCR4 and CXCL12: An eccentric trio? *J Neuroimmunol* **198**, 9–13 (2008).
215. Calatozzolo, C. *et al.* Expression of the new CXCL12 receptor, CXCR7, in gliomas. *Cancer Biol Ther* **11**, 242–253 (2011).
216. Puchert, M. *et al.* Astrocytic expression of the CXCL12 receptor, CXCR7/ACKR3 is a hallmark of the diseased, but not developing CNS. *Molecular and Cellular Neuroscience* **85**, 105–118 (2017).
217. Infantino, S., Moepps, B. & Thelen, M. Expression and regulation of the orphan receptor RDC1 and its putative ligand in human dendritic and B cells. *J Immunol* **176**, 2197–2207 (2006).
218. Maksym, R. B. *et al.* The role of stromal-derived factor-1 — CXCR7 axis in development and cancer. *Eur J Pharmacol* **625**, 31–40 (2009).
219. Neves, M.; *et al.* The role of ACKR3 in breast, lung, and brain cancer. *Mol Pharmacol* **96**, 819–825 (2019).
220. Miao, Z. *et al.* CXCR7 (RDC1) promotes breast and lung tumor growth in vivo and is expressed on tumor-associated vasculature. *Proc Natl Acad Sci U S A* **104**, 15735–15740 (2007).
221. Wani, N. A. *et al.* C-X-C motif chemokine 12/C-X-C chemokine receptor type 7 signaling regulates breast cancer growth and metastasis by modulating the tumor microenvironment. *Breast Cancer Research* **16**, 1–17 (2014).
222. Luker, K. E. *et al.* Scavenging of CXCL12 by CXCR7 promotes tumor growth and metastasis of CXCR4-positive breast cancer cells. *Oncogene* **2012 31:45 31**, 4750–4758 (2012).
223. Hernandez, L., Magalhaes, M. A. O., Coniglio, S. J., Condeelis, J. S. & Segall, J. E. Opposing roles of CXCR4 and CXCR7 in breast cancer metastasis. *Breast Cancer Res* **13**, (2011).
224. Azad, B. B. *et al.* Targeted Imaging of the Atypical Chemokine Receptor 3 (ACKR3/CXCR7) in Human Cancer Xenografts. *J Nucl Med* **57**, 981 (2016).
225. Yu, P. F. *et al.* Downregulation of CXCL12 in mesenchymal stromal cells by TGF β promotes breast cancer metastasis. *Oncogene* **2017 36:6 36**, 840–849 (2016).
226. Tang, X. *et al.* Downregulation of CXCR7 inhibits proliferative capacity and stem cell-like properties in breast cancer stem cells. *Tumor Biology* **37**, 13425–13433 (2016).
227. Salazar, N. *et al.* The chemokine receptor CXCR7 interacts with EGFR to promote breast cancer cell proliferation. *Mol Cancer* **13**, (2014).
228. Hattermann, K. *et al.* Effects of the chemokine CXCL12 and combined internalization of its receptors CXCR4 and CXCR7 in human MCF-7 breast cancer cells. *Cell Tissue Res* **357**, 253 (2014).
229. Neves, M., Marolda, V., Mayor, F. & Penela, P. Crosstalk between CXCR4/ACKR3 and EGFR Signaling in Breast Cancer Cells. *Int J Mol Sci* **23**, 11887 (2022).
230. Liu, H. *et al.* Overexpression of CXCR7 accelerates tumor growth and metastasis of lung cancer cells. *Respir Res* **21**, 1–13 (2020).
231. Iwakiri, S. *et al.* Higher expression of chemokine receptor CXCR7 is linked to early and metastatic recurrence in pathological stage I nonsmall cell lung cancer. *Cancer* **115**, 2580–2593 (2009).
232. Franco, R. *et al.* Cxcl12-binding receptors expression in non-small cell lung cancer relates to tumoral microvascular density and cxcr4 positive circulating tumoral cells in lung draining venous blood. *European Journal of Cardio-thoracic Surgery* **41**, 368–375 (2012).
233. Wu, Y. C., Tang, S. J., Sun, G. H. & Sun, K. H. CXCR7 mediates TGF β 1-promoted EMT and tumor-initiating features in lung cancer. *Oncogene* **2016 35:16 35**, 2123–2132 (2015).
234. Puddinu, V. *et al.* ACKR3 expression on diffuse large B cell lymphoma is required for tumor spreading and tissue infiltration. *Oncotarget* **8**, 85068 (2017).
235. Antonello, P. *et al.* ACKR3 promotes CXCL12/CXCR4-mediated cell-to-cell-induced lymphoma migration through LTB4 production. *Front Immunol* **13**, (2023).
236. Deng, L. *et al.* Chemokine receptor CXCR7 is an independent prognostic biomarker in glioblastoma. *Cancer Biomark* **20**, 1–6 (2017).
237. Flüh, C., Hattermann, K., Mehdorn, H. M., Synowitz, M. & Held-Feindt, J. Differential expression of CXCR4 and CXCR7 with various stem cell markers in paired human primary and recurrent

- glioblastomas. *Int J Oncol* **48**, 1408–1416 (2016).
238. Hattermann, K. *et al.* The chemokine receptor CXCR7 is highly expressed in human glioma cells and mediates antiapoptotic effects. *Cancer Res* **70**, 3299–3308 (2010).
 239. Calatuzzolo, C. *et al.* Expression of the new CXCL12 receptor, CXCR7, in gliomas. *Cancer Biol Ther* **11**, 242–253 (2011).
 240. Walters, M. J. *et al.* Inhibition of CXCR7 extends survival following irradiation of brain tumours in mice and rats. *British Journal of Cancer* **2014** *110*:5 **110**, 1179–1188 (2014).
 241. Salazar, N. *et al.* A Chimeric Antibody against ACKR3/CXCR7 in Combination with TMZ Activates Immune Responses and Extends Survival in Mouse GBM Models. *Molecular Therapy* **26**, 1354 (2018).
 242. LIU, Y., CARSON-WALTER, E. & WALTER, K. A. Targeting Chemokine Receptor CXCR7 Inhibits Glioma Cell Proliferation and Mobility. *Anticancer Res* **35**, (2015).
 243. Esencay, M., Sarfraz, Y. & Zagzag, D. CXCR7 is induced by hypoxia and mediates glioma cell migration towards SDF-1 α . *BMC Cancer* **13**, (2013).
 244. Ceccarelli, M. *et al.* Molecular Profiling Reveals Biologically Discrete Subsets and Pathways of Progression in Diffuse Glioma. *Cell* **164**, 550–563 (2016).
 245. Bowman, R. L., Wang, Q., Carro, A., Verhaak, R. G. W. & Squatrito, M. GlioVis data portal for visualization and analysis of brain tumor expression datasets. *Neuro Oncol* **19**, 139 (2017).
 246. Puchalski, R. B. *et al.* An anatomic transcriptional atlas of human glioblastoma. *Science* **360**, 660 (2018).
 247. Darmanis, S. *et al.* Single-Cell RNA-Seq Analysis of Infiltrating Neoplastic Cells at the Migrating Front of Human Glioblastoma. *Cell Rep* **21**, 1399 (2017).
 248. Jacobs, S. M. *et al.* CXCR4 expression in glioblastoma tissue and the potential for PET imaging and treatment with [68Ga]Ga-Pentixafor ^{177}Lu -Pentixather. *Eur J Nucl Med Mol Imaging* **49**, 481–491 (2022).
 249. Giordano, F. A. *et al.* L-RNA aptamer-based CXCL12 inhibition combined with radiotherapy in newly-diagnosed glioblastoma: dose escalation of the phase I/II GLORIA trial. *Nature Communications* **2024** *15*:1 **15**, 1–14 (2024).
 250. Thomas, R. P. *et al.* Macrophage exclusion after radiation therapy (MERT): A First in Human Phase I/II Trial using a CXCR4 Inhibitor in Glioblastoma. *Clinical Cancer Research* **25**, 6948–6957 (2019).
 251. Thomas, R. P. *et al.* Macrophage Exclusion after Radiation Therapy (MERT): A First in Human Phase I/II Trial using a CXCR4 Inhibitor in Glioblastoma. *Clin Cancer Res* **25**, 6948–6957 (2019).
 252. Lee, E. Q. *et al.* Phase I and biomarker study of plerixafor and bevacizumab in recurrent high-grade glioma. *Clinical Cancer Research* **24**, 4643–4649 (2018).
 253. Mercurio, L. *et al.* Targeting CXCR4 by a selective peptide antagonist modulates tumor microenvironment and microglia reactivity in a human glioblastoma model. *Journal of Experimental and Clinical Cancer Research* **35**, 1–15 (2016).
 254. Wu, A. *et al.* Combination anti-CXCR4 and anti-PD-1 immunotherapy provides survival benefit in glioblastoma through immune cell modulation of tumor microenvironment. *J Neurooncol* **143**, 241–249 (2019).
 255. Alghamri, M. S. *et al.* Systemic delivery of an adjuvant CXCR4-CXCL12 signaling inhibitor encapsulated in synthetic protein nanoparticles for glioma immunotherapy. *ACS Nano* **16**, 8729 (2022).
 256. Liu, C. *et al.* Chemokine receptor CXCR3 promotes growth of glioma. *Carcinogenesis* **32**, 129 (2011).
 257. Pu, Y. *et al.* High expression of CXCR3 is an independent prognostic factor in glioblastoma patients that promotes an invasive phenotype. *J Neurooncol* **122**, 43–51 (2015).
 258. Boyé, K. *et al.* The role of CXCR3/LRP1 cross-talk in the invasion of primary brain tumors. *Nat Commun* **8**, (2017).
 259. Wang, G. *et al.* CXCL11-armed oncolytic adenoviruses enhance CAR-T cell therapeutic efficacy and reprogram tumor microenvironment in glioblastoma. *Molecular Therapy* **31**, 134–153 (2023).
 260. Shono, K. *et al.* Downregulation of the CCL2/CCR2 and CXCL10/CXCR3 axes contributes to antitumor effects in a

- mouse model of malignant glioma. *Scientific Reports* 2020 10:1 **10**, 1–10 (2020).
261. Zuo, M. *et al.* Glioma-associated fibroblasts promote glioblastoma resistance to temozolomide through CCL2-CCR2 paracrine signaling. *bioRxiv* 2024.03.05.581575 (2024) doi:10.1101/2024.03.05.581575.
 262. Pant, A. *et al.* CCR2 and CCR5 co-inhibition modulates immunosuppressive myeloid milieu in glioma and synergizes with anti-PD-1 therapy. *Oncoimmunology* **13**, (2024).
 263. Chia, T. Y. *et al.* The CXCL16-CXCR6 axis in glioblastoma modulates T-cell activity in a spatiotemporal context. *Front Immunol* **14**, (2024).
 264. Barthel, F. P. *et al.* Longitudinal molecular trajectories of diffuse glioma in adults. *Nature* 2019 576:7785 **576**, 112–120 (2019).
 265. Ruiz-Moreno, C. *et al.* Harmonized single-cell landscape, intercellular crosstalk and tumor architecture of glioblastoma. *bioRxiv* 2022.08.27.505439 (2022) doi:10.1101/2022.08.27.505439.
 266. Jin, S. *et al.* Inference and analysis of cell-cell communication using CellChat. *Nature Communications* 2021 12:1 **12**, 1–20 (2021).
 267. Hattermann, K., Held-Feindt, J., Ludwig, A. & Mentlein, R. The CXCL16-CXCR6 chemokine axis in glial tumors. *J Neuroimmunol* **260**, 47–54 (2013).
 268. Lepore, F. *et al.* CXCL16/CXCR6 axis drives microglia/macrophages phenotype in physiological conditions and plays a crucial role in glioma. *Front Immunol* **9**, 2750 (2018).
 269. Tian, L. *et al.* Specific targeting of glioblastoma with an oncolytic virus expressing a cetuximab-CCL5 fusion protein via innate and adaptive immunity. *Nature Cancer* 2022 3:11 **3**, 1318–1335 (2022).
 270. Berahovich, R. D., Penfold, M. E. T. & Schall, T. J. Nonspecific CXCR7 antibodies. *Immunol Lett* **133**, 112–114 (2010).
 271. Ehrlich, A. T. *et al.* Acker3-Venus knock-in mouse lights up brain vasculature. *Mol Brain* **14**, (2021).
 272. Bobkov, V. *et al.* Antibodies Targeting Chemokine Receptors CXCR4 and ACKR3. *Mol Pharmacol* **96**, 753–764 (2019).
 273. Dekkers, S. *et al.* Small Molecule Fluorescent Ligands for the Atypical Chemokine Receptor 3 (ACKR3). *ACS Med Chem Lett* **15**, 143–148 (2024).
 274. Maussang, D. *et al.* Llama-derived single variable domains (nanobodies) directed against chemokine receptor CXCR7 reduce head and neck cancer cell growth in vivo. *Journal of Biological Chemistry* **288**, 29562–29572 (2013).
 275. Salazar, N. *et al.* A Chimeric Antibody against ACKR3/CXCR7 in Combination with TMZ Activates Immune Responses and Extends Survival in Mouse GBM Models. *Molecular Therapy* **26**, 1354 (2018).
 276. Ameti, R. *et al.* Characterization of a chimeric chemokine as a specific ligand for ACKR3. *J Leukoc Biol* **104**, 391–400 (2018).
 277. Del Barrio, I. del M., Wilkins, G. C., Meeson, A., Ali, S. & Kirby, J. A. Breast Cancer: An Examination of the Potential of ACKR3 to Modify the Response of CXCR4 to CXCL12. *Int J Mol Sci* **19**, (2018).
 278. Cebo, M. *et al.* Platelet ACKR3/CXCR7 favors antiplatelet lipids over an atherothrombotic lipidome and regulates thromboinflammation. *Blood* **139**, 1722–1742 (2022).
 279. Song, B. *et al.* Stromal cell-derived factor-1 exerts opposing roles through CXCR4 and CXCR7 in angiotensin II-induced adventitial remodeling. *Biochem Biophys Res Commun* **594**, 38–45 (2022).
 280. Huynh, C. *et al.* Target engagement of the first-in-class CXCR7 antagonist ACT-1004-1239 following multiple-dose administration in mice and humans. *Biomed Pharmacother* **144**, (2021).
 281. Pouzol, L. *et al.* ACT-1004-1239, a first-in-class CXCR7 antagonist with both immunomodulatory and promyelinating effects for the treatment of inflammatory demyelinating diseases. *FASEB J* **35**, (2021).
 282. Liu, Y. *et al.* Vascular gene expression patterns are conserved in primary and metastatic brain tumors. *J Neurooncol* **99**, 13–24 (2010).
 283. Salmaggi, A. *et al.* CXCL12, CXCR4 and CXCR7 expression in brain metastases. *Cancer Biol Ther* **8**, 1608–1614 (2009).
 284. Hattermann, K. *et al.* The chemokine receptor CXCR7 is highly expressed in human glioma cells and mediates

- antiapoptotic effects. *Cancer Res* **70**, 3299–3308 (2010).
285. Bianco, A. M. *et al.* CXCR7 and CXCR4 Expressions in Infiltrative Astrocytomas and Their Interactions with HIF1 α Expression and IDH1 Mutation. *Pathol Oncol Res* **21**, 229–240 (2015).
286. Esencay, M., Sarfraz, Y. & Zagzag, D. CXCR7 is induced by hypoxia and mediates glioma cell migration towards SDF-1 α . *BMC Cancer* **13**, (2013).
287. Wang, J. *et al.* The role of CXCR7/RDC1 as a chemokine receptor for CXCL12/SDF-1 in prostate cancer. *Journal of Biological Chemistry* **283**, 4283–4294 (2008).
288. Birner, P., Tchorbanov, A., Natchev, S., Tuettner, J. & Guentchev, M. The chemokine receptor CXCR7 influences prognosis in human glioma in an IDH1-dependent manner. *J Clin Pathol* **68**, 830–834 (2015).
289. Hartmann, T. N. *et al.* A crosstalk between intracellular CXCR7 and CXCR4 involved in rapid CXCL12-triggered integrin activation but not in chemokine-triggered motility of human T lymphocytes and CD34⁺ cells. *J Leukoc Biol* **84**, 1130–1140 (2008).
290. Liu, C. C. *et al.* CXCR7 activation evokes the anti-PD-L1 antibody against glioblastoma by remodeling CXCL12-mediated immunity. *Cell Death & Disease* **2024** *15:6* **15**, 1–12 (2024).
291. Atchison, R. W., Casto, B. C. & Hammon, W. M. D. ADENOVIRUS-ASSOCIATED DEFECTIVE VIRUS PARTICLES. *Science* **149**, 754–756 (1965).
292. Srivastava, A., Lusby, E. W. & Berns, K. I. Nucleotide sequence and organization of the adeno-associated virus 2 genome. *J Virol* **45**, 555 (1983).
293. Calcedo, R. *et al.* Adeno-Associated Virus Antibody Profiles in Newborns, Children, and Adolescents. *Clin Vaccine Immunol* **18**, 1586 (2011).
294. Calcedo, R., Vandenberghe, L. H., Gao, G., Lin, J. & Wilson, J. M. Worldwide epidemiology of neutralizing antibodies to adeno-associated viruses. *J Infect Dis* **199**, 381–390 (2009).
295. Afione, S. A. *et al.* In vivo model of adeno-associated virus vector persistence and rescue. *J Virol* **70**, 3235 (1996).
296. Daya, S. & Berns, K. I. Gene Therapy Using Adeno-Associated Virus Vectors. *Clin Microbiol Rev* **21**, 583 (2008).
297. Liu, H. *et al.* Producing high-quantity and high-quality recombinant adeno-associated virus by low-cis triple transfection. *Mol Ther Methods Clin Dev* **32**, 101230 (2024).
298. Kang, L. *et al.* AAV vectors applied to the treatment of CNS disorders: Clinical status and challenges. *Journal of Controlled Release* **355**, 458–473 (2023).
299. Pietersz, K. L. *et al.* Transduction patterns in the CNS following various routes of AAV-5-mediated gene delivery. *Gene Therapy* **2020** *28:7* **28**, 435–446 (2020).
300. Daci, R. & Flotte, T. R. Delivery of Adeno-Associated Virus Vectors to the Central Nervous System for Correction of Single Gene Disorders. *International Journal of Molecular Sciences* **2024**, *Vol. 25, Page 1050* **25**, 1050 (2024).
301. Keam, S. J. Eladocagene Exuparvovec: First Approval. *Drugs* **82**, 1427–1432 (2022).
302. Maguire, A. M. *et al.* Efficacy, Safety, and Durability of Voretigene Neparvovec-rzyl in RPE65 Mutation-Associated Inherited Retinal Dystrophy: Results of Phase 1 and 3 Trials. *Ophthalmology* **126**, 1273–1285 (2019).
303. Russell, S. *et al.* Efficacy and safety of voretigene neparvovec (AAV2-hRPE65v2) in patients with RPE65-mediated inherited retinal dystrophy: a randomised, controlled, open-label, phase 3 trial. *Lancet* **390**, 849–860 (2017).
304. Blair, H. A. Onasemnogene Apeparvovec: A Review in Spinal Muscular Atrophy. *CNS Drugs* **36**, 995–1005 (2022).
305. Ommaya Reservoir - PubMed. <https://pubmed.ncbi.nlm.nih.gov/32644437/>.
306. Choi, B. D. *et al.* Systemic administration of a bispecific antibody targeting EGFRvIII successfully treats intracerebral glioma. *Proc Natl Acad Sci U S A* **110**, 270–275 (2013).
307. Bhere, D. *et al.* microRNA-7 upregulates death receptor 5 and primes resistant brain tumors to caspase-mediated apoptosis. *Neuro Oncol* **20**, 215–224 (2018).

308. Mizuno, M., Yoshida, J., Colosi, P. & Kurtzman, G. Adeno-associated virus vector containing the herpes simplex virus thymidine kinase gene causes complete regression of intracerebrally implanted human gliomas in mice, in conjunction with ganciclovir administration. *Jpn J Cancer Res* **89**, 76–80 (1998).
309. Zhong, X. *et al.* Gene delivery of apoptin-derived peptide using an adeno-associated virus vector inhibits glioma and prolongs animal survival. *Biochem Biophys Res Commun* **482**, 506–513 (2017).
310. Meijer, D. H., Maguire, C. A., Leroy, S. G. & Sena-Esteves, M. Controlling brain tumor growth via intraventricular administration of an AAV vector encoding IFN- β . *Cancer Gene Ther* **16**, 664 (2009).
311. Guhasarkar, D., Su, Q., Gao, G. & Sena-Esteves, M. Systemic AAV9-IFN β gene delivery treats highly invasive glioblastoma. *Neuro Oncol* **18**, 1508–1518 (2016).
312. Hicks, M. J. *et al.* Genetic modification of neurons to express bevacizumab for local anti-angiogenesis treatment of glioblastoma. *Cancer Gene Ther* **22**, 1–8 (2015).
313. Yanamandra, N. *et al.* Recombinant adeno-associated virus (rAAV) expressing TFPI-2 inhibits invasion, angiogenesis and tumor growth in a human glioblastoma cell line. *Int J Cancer* **115**, 998–1005 (2005).
314. Jacob, F. *et al.* A Patient-Derived Glioblastoma Organoid Model and Biobank Recapitulates Inter- and Intra-tumoral Heterogeneity. *Cell* **180**, 188 (2020).
315. Tatla, A. S., Justin, A. W., Watts, C. & Markaki, A. E. A vascularized tumoroid model for human glioblastoma angiogenesis. *Scientific Reports* **2021 11:1 11**, 1–9 (2021).
316. Akolawala, Q. *et al.* Micro-Vessels-Like 3D Scaffolds for Studying the Proton Radiobiology of Glioblastoma-Endothelial Cells Co-Culture Models. *Adv Healthc Mater* **13**, (2024).
317. Hatlen, R. R. & Rajagopalan, P. Investigating Trans-differentiation of Glioblastoma Cells in an In Vitro 3D Model of the Perivascular Niche. *ACS Biomater Sci Eng* **9**, 3445–3461 (2023).
318. Stanke, K. M. & Kidambi, S. Direct-Contact Co-culture of Astrocytes and Glioblastoma Cells Patterned Using Polyelectrolyte Multilayer Templates. *J Vis Exp* **2022**, (2022).
319. Yang, N. *et al.* A co-culture model with brain tumor-specific bioluminescence demonstrates astrocyte-induced drug resistance in glioblastoma. *J Transl Med* **12**, (2014).
320. Nakod, P. S., Kim, Y. & Rao, S. S. The Impact of Astrocytes and Endothelial Cells on Glioblastoma Stemness Marker Expression in Multicellular Spheroids. *Cell Mol Bioeng* **14**, 639–651 (2021).